Mechanisms of 7,8-dihydroneopterin protection of macrophages from cytotoxicity

A thesis submitted in partial fulfilment
of the requirements for the degree of

Doctor of Philosophy
in Biochemistry

School of Biological Sciences
University of Canterbury
New Zealand

Anastasia Shchepetkina

2013

Contents

List of Figures **ix**

List of Tables **xv**

Acknowledgements **xvii**

Abstract **xix**

Abbreviations **xxi**

1 Introduction **1**

1.1 Overview and research question 1

1.2 Macrophages, oxLDL and 7,8-NP in atherosclerosis 2

1.3 Atherosclerotic lesion development: from onset to maturity 4

1.3.1 Oxidative modification of LDL *in vivo* and *in vitro* 8

1.4 Macrophage and oxLDL: recognition and interaction 10

1.4.1 Role of scavenger receptors in atherosclerosis 11

1.4.2 The role of CD36 in oxLDL uptake by macrophages 12

1.5 Macrophage cell death processes mediated by oxLDL 16

1.5.1 Types of cell death 16

1.5.2 OxLDL–mediated cellular death in the literature 18

1.6 Oxidative stress in macrophage–oxLDL 19

1.6.1 Reactive oxygen species 19

1.6.2 Macrophage NADPH oxidase 20

1.6.3 Mitochondrion 22

1.6.4 ROS–mediated damage to cells 23

1.6.5 Cellular defence against oxidative stress 24

1.7 7,8-Dihydroneopterin: origins, biochemistry and role in atherosclerosis 25

1.7.1 7,8-NP production . . . 26
1.7.2 Clinical utility . . . 27
1.7.3 Biochemistry and potential physiological roles of 7,8-NP . . . 29
1.8 Research programme . . . 34

2 Materials & methods **37**
2.1 Reagents, media and buffers . . . 37
2.1.1 Reagents . . . 37
2.1.2 Media . . . 39
2.1.3 General solutions and buffers . . . 40
2.2 Cell culture technique . . . 40
2.2.1 Aseptic practice . . . 40
2.2.2 Cell culture medium and experimental conditions . . . 41
2.2.3 Preparation of human serum for macrophage cell culture . . . 42
2.2.4 Preparation of foetal bovine serum for U937 cell culture . . . 42
2.2.5 Cell culture of human monocyte-derived macrophage cells . . . 43
2.2.6 Culture of U937 cells . . . 45
2.3 Isolation and oxidation of low-density lipoprotein . . . 46
2.3.1 Collection and preparation of donor plasma . . . 46
2.3.2 Lipoprotein isolation by gradient centrifugation . . . 46
2.3.3 LDL concentration . . . 47
2.3.4 Determination of LDL concentration . . . 47
2.3.5 Preparation of oxidised LDL . . . 48
2.4 Biochemical analysis . . . 49
2.4.1 Determination of protein concentration . . . 49
2.4.2 Cell viability assays . . . 49
2.4.3 HPLC methods . . . 51
2.5 Western blot technique . . . 56
2.5.1 Solutions for Western blot . . . 56
2.5.2 Antibodies . . . 57
2.5.3 Sample preparation . . . 57
2.5.4 SDS-polyacrylamide gel electrophoresis . . . 58
2.5.5 Immunoblotting and visualisation . . . 58
2.6 Fluorescent microscopy . . . 60
2.6.1 Dihydroethidium probe . . . 60
2.6.2 Sample preparation and processing . . . 60
2.7 Flow cytometry . . . 61

2.8 Polymerase chain reaction 62
2.8.1 RNA isolation and purification 62
2.8.2 cDNA synthesis 62
2.8.3 Real-time quantitative PCR 63
2.8.4 Agarose gel electrophoresis 64
2.9 Statistical analysis 64

3 OxLDL toxicity to human monocyte–derived macrophages 67
3.1 Introduction 67
3.2 Results 69
3.2.1 OxLDL–induced cytotoxicity to HMDM is concentration and time dependant 69
3.2.2 Oxidative stress and damage is an early event in oxLDL toxicity 73
3.2.3 When does HMDM cell become committed to cell death? . . . 77
3.3 Discussion: Oxidative stress as intracellular mechanism of toxicity . . 83
3.4 Summary 87

4 Antioxidant capacity of 7,8-dihydroneopterin 89
4.1 Introduction 89
4.2 Results 92
4.2.1 7,8-NP protects HMDM cells treated with oxLDL in a concentration and time dependant fashion 92
4.2.2 7,8-NP concentration and availability in cell culture 95
4.2.3 7,8-NP alleviates oxLDL–mediated stress in HMDM 104
4.2.4 7,8-NP is oxidised to neopterin in the HMDM cells treated with oxLDL 106
4.2.5 Does NOX play a role in oxLDL toxicity to HMDM cells? . . 113
4.3 Discussion 123
4.3.1 7,8-NP–mediated protection of HMDM from oxLDL 123
4.3.2 Antioxidant activity of 7,8-NP 123
4.3.3 Intracellular levels of 7,8-NP 131
4.4 Summary 135

5 Effect of 7,8-dihydroneopterin on oxLDL uptake by macrophages 137
5.1 Introduction 137
5.2 Results 139
5.2.1 Measuring oxLDL uptake in macrophages with 7-ketocholesterol 139

5.2.2 7,8-NP reduces intracellular oxLDL uptake in HMDM cells . . 144
5.2.3 7,8-NP reduces the expression of CD36 scavenger receptor protein in HMDM 147
5.2.4 7,8-NP reduces the mRNA expression of CD36 in HMDM cells 151
5.2.5 Significance of 7,8-NP–mediated CD36 down–regulation 153
5.2.6 7,8-NP–mediated reduction of intracellular 7KC is serum dependant 165
5.3 Discussion 167
5.3.1 7,8-NP down-regulates the levels of oxLDL in HMDM cells . . 167
5.3.2 CD36 down-regulation by 7,8-NP: levels and significance . . . 169
5.4 Summary 174

6 HMDM cell culture method development and troubleshooting 177
6.1 Introduction 177
6.2 Culture of human monocyte–derived macrophages 178
6.2.1 Effect of GM-CSF and overall HMDM culture success 178
6.2.2 Culture plate trial 182
6.2.3 Effect of human serum on HMDM development and growth . 186
6.3 Utility of U937 cells as a model of 7,8-NP–mediated oxLDL uptake regulation 190
6.4 Extracellular experimental factors contributing to toxicity 193
6.4.1 Extracellular serum is a factor in oxLDL toxicity 193
6.4.2 Cell density is a factor in oxLDL toxicity 200
6.5 HMDM cell resistance to oxLDL toxicity 205
6.5.1 Defining HMDM cell resistance to oxLDL 205
6.5.2 LDL oxidation is not a factor in the HMDM cell resistance . . 207
6.5.3 Delayed oxidative damage 209
6.6 Discussion 220
6.6.1 HMDM cell culture 220
6.6.2 Utility of U937 cells as a model of 7,8-NP–mediated oxLDL uptake regulation 221
6.6.3 Extracellular factors 222
6.6.4 HMDM cell *resilience* not resistance to oxLDL 229
6.7 Summary 231

7 General discussion, conclusions and future work **233**

7.1 Mechanisms of 7,8-NP–mediated protection: ROS scavenging vs. oxLDL processing 233

7.2 Source and types of ROS during oxLDL toxicity to HMDM cells . . . 237

7.3 The effect of 7,8-NP on oxLDL processing: potential for cholesterol ester efflux regulation 238

7.4 Conclusion 239

Bibliography **241**

Appendix A **255**

Appendix B **269**

List of Figures

1.1 Six stages of atherosclerotic lesion formation 6
1.2 Cholesteryl ester metabolism in cells 15
1.3 Reactive oxygen species 21
1.4 Schematic representation of NADPH oxidase complex before and after activation 22
1.5 7,8-NP biosynthesis and metabolism pathway 27
1.6 7,8-NP oxidation 30

2.1 Monocyte isolation: typical preparation 44
2.2 LDL isolation: typical preparation 47
2.3 Typical HPLC chromatograms after Pterin assay 53

3.1 OxLDL causes concentration dependant HMDM cell viability loss after 24 hours 71
3.2 Time course of oxLDL–mediated HMDM cell viability loss 72
3.3 OxLDL triggers intracellular ROS release by HMDM cells 74
3.4 OxLDL leads to concentration dependent intracellular GSH loss in HMDM 76
3.5 Time course of intracellular GSH recovery by HMDM upon oxLDL removal 78
3.6 HMDM continues to lose cellular viability when oxLDL is removed . . 79
3.7 HMDM cells significantly recover intracellular GSH upon oxLDL removal: effect of concentration 81
3.8 HMDM cells do not recover viability upon oxLDL removal: effect of concentration 82

4.1 7,8-NP protects HMDM cells from oxLDL–mediated cell viability loss in a concentration dependent manner 93

4.2 Time course of 7,8-NP–mediated protection of HMDM cells from oxLDL–induced cytotoxicity . . . 94
4.3 Time course of extracellular pterin concentration when incubated with HMDM cells . . . 96
4.4 Time course of 7,8-NP accumulation of exogenously added 7,8-NP in HMDM cells . . . 97
4.5 Intracellular pterin concentration in HMDM after 7,8-NP addition . . 99
4.6 Intracellular baseline pterin concentration in cultured HMDM 100
4.7 Endogenous neopterin production by HMDM cells in response to toxic levels of oxLDL . . . 102
4.8 Endogenous neopterin production by HMDM in response to sub-toxic level of oxLDL . . . 103
4.9 7,8-NP inhibits the oxLDL–driven elevation of intracellular ROS . . . 105
4.10 7,8-NP is oxidised to neopterin in HMDM cells treated with oxLDL . 107
4.11 Intracellular total pterin level is elevated in oxLDL–treated HMDM cells 110
4.12 Intracellular 7,8-NP level is slightly altered by the presence of oxLDL with HMDM cells . . . 111
4.13 Extracellular neopterin and total pterin after oxLDL treatment of 7,8-NP loaded HMDM cells . . . 112
4.14 Apocynin partially inhibits 7,8-NP oxidation to neopterin in oxLDL-treated HMDM cells . . . 114
4.15 Apocynin is not toxic to HMDM cells . . . 115
4.16 Apocynin does not protect HMDM cells against oxLDL (MTT) . . . 116
4.17 Annexin V and PI quadrant identification on flow cytometer output . 118
4.18 Apocynin at 200 μM does not protect HMDM cells against oxLDL (Annexin V and PI) . . . 119
4.19 Apocynin at a range of concentrations does not protect HMDM cells against oxLDL (Annexin V and PI) . . . 121

5.1 Intracellular 7-ketocholesterol (7KC) accumulation in HMDM cells exposed to oxLDL . . . 141
5.2 7KC levels in human sera used in cell culture . . . 142
5.3 Serum lipoproteins are the primary source of 7KC in culture medium 143
5.4 Time course of intracellular 7KC accumulation in HMDM cells exposed to oxLDL in the presence and absence of 7,8-NP . . . 145
5.5 7,8-NP mediates reduction of intracellular total 7KC in HMDM cells exposed to oxLDL . . . 146

5.6 7,8-NP reduces the expression of 100 kDa band of CD36 protein in HMDM in a concentration–dependent manner 148
5.7 Time course of 7,8-NP–mediated down-regulation of CD36 protein . . 149
5.8 Effect of 7,8-NP degradation products, D-neopterin and 7,8-dihydroxanthopterin on the level of CD36 150
5.9 7,8-NP reduces the CD36 mRNA expression in HMDM cells 152
5.10 CD36 and 7,8-NP levels are differentially distributed across the length of atherosclerotic plaque A 155
5.11 CD36 and 7,8-NP levels are differentially distributed across the length of atherosclerotic plaque B 157
5.12 Experiment diagram 159
5.13 CD36 recovery after 7,8-NP pre-treatment does not occur until after 6 hours 160
5.14 Pre-treatment with 7,8-NP to down-regulate CD36 does not protect HMDM cells from oxLDL-induced cell death 161
5.15 Pre-treatment with 7,8-NP leads to a small increase of intracellular GSH after subsequent exposure of HMDM to oxLDL 163
5.16 Pre-treatment with 7,8-NP does not affect free or total 7KC uptake in HMDM exposed to oxLDL for 6 hours 164
5.17 7,8-NP mediates the reduction of intracellular total 7KC in HMDM cells exposed to oxLDL only in the presence of extracellular serum . . 166

6.1 Effect of GM-CSF on HMDM cell number 180
6.2 Percentage of successful macrophage development in culture 181
6.3 Effect of plate type on HMDM cell growth 183
6.4 Determination of monocyte seeding density for HMDM cell growth in 48 well plate 185
6.5 Effect of sera on HMDM cell development 187
6.6 Effect of sera on GM-CSF–differentiated HMDM cell growth 188
6.7 Heat–inactivation of human serum does not alter HMDM growth in culture 189
6.8 Effect of 7,8-NP on the CD36 protein expression in U937 cells 191
6.9 7,8-NP has no effect on the intracellular 7KC uptake by the oxLDL–exposed U937 cells 192
6.10 Effect of experimental protocol on oxLDL toxicity to HMDM 194
6.11 Extracellular serum inhibits oxLDL–mediated HMDM toxicity in a concentration–dependent manner 196

6.12 Extracellular protein inhibits oxLDL–mediated HMDM toxicity in a concentration–dependent manner . . . 198
6.13 Effect of extracellular protein (added as BSA or as human serum) on oxLDL uptake by HMDM cells . . . 199
6.14 Effect of cell number on oxLDL–mediated U937 cell viability loss . . . 201
6.15 Effect of cell number on oxLDL–mediated HMDM cell viability loss, continued . . . 203
6.16 Resistance of HMDM to toxic concentration of oxLDL at a range of serum concentrations in the incubation medium . . . 206
6.17 Lipoprotein gel electrophoresis . . . 208
6.18 Differential oxLDL–mediated toxicity to HMDM preparations . . . 211
6.19 DHE measurement of resistant and susceptible oxLDL–treated HMDM cells . . . 213
6.20 Differential oxLDL-mediated intracellular ROS flux in HMDM preparations . . . 213
6.21 Differential oxLDL-mediated intracellular ROS flux in HMDM preparations, percentage shift into high DHE-fluorescence gate . . . 214
6.22 Cell viability after 24 vs. 48 hour incubation of HMDM cells with oxLDL 215
6.23 Time-course of intracellular GSH in "resistant" HMDM cells in response to oxLDL treatment . . . 216
6.24 Viability and GSH loss in "resistant" HMDM cells at 24 and 48 hours after oxLDL treatment. Experiment 1 . . . 218
6.25 Viability and GSH loss in "resistant" HMDM cells at 24 and 48 hours after oxLDL treatment. Experiment 2 . . . 219

A.1 Comparison of MTT and resazurin (*PrestoBlue*™) reduction assays in determining HMDM cell density . . . 256
A.2 Comparison of MTT and resazurin (*PrestoBlue*™) reduction assays in determining HMDM cell viability after oxLDL treatment . . . 257
A.3 HMDM cell morphology before and after *Accutase*™ treatment . . . 259
A.4 *Accutase*™ treatment of HMDM removes the majority of cells . . . 260
A.5 Efficiency of *Accutase*™–facilitated detachment of HMDM cells . . . 260
A.6 *Accutase*™ is not toxic to HMDM cells up to 3 hours after treatment 261
A.7 HMDM cells re-attach effectively after *Accutase*™–facilitated removal 262
A.8 Primer product size verification . . . 264
A.9 RT-qPCR standard curve of CD36, HPRT and β-actin primer amplification . . . 266

A.10 Typical RT-qPCR amplification curve of CD36, HPRT and β-actin primers 267

List of Tables

1.1 Morphological features of cells undergoing apoptosis and necrosis . . 17

2.3 List of antibodies used 57
2.4 qPCR thermal profile 64

6.1 OxLDL toxicity to HMDM cells and experimental conditions in the published literature 228

A.1 List of PCR primers tested 263

Acknowledgements

This thesis had been a long journey filled with hard (at times!) work and rewarding (at times!) results. Many roads were taken, many paths abandoned, yet during the times of both elation and doubt, fellowship and expert advice made all the difference between success and failure. I'd like to take this opportunity to thank the people that have come into my life during the years of study and research. Thank you for your support, shared knowledge and experience, time and effort that you've put into helping me do the work, write it up and gain valuable skills along the way. No words can express how much I've learned from you and how grateful I am!

No man is an island and I was not an exception. This work would not have been possible without the following people and resources. A continuous flow of macrophage cultures was ensured by the supply of blood collected by NZ Blood Service from the haemochromatosis patients at Riccarton branch. LDL supply was provided by plasma donors and nurses at the University of Canterbury. It is an honour to be entrusted with these donations. I would also like to acknowledge University of Canterbury for providing a doctoral scholarship for me and excellent research facilities for this project.

Importantly, I thank my supervisory team, Steven Gieseg, Ashley Garrill and Barry Hock for their guidance and unyielding support during the course of my PhD. I am also hugely indebted to the members of the Free Radical Biochemistry Laboratory, both past and present, for their expertise, friendship and helpful conversations. A team at Martin Kennedy's lab in Otago Medical School in Christchurch deserves a hearty mention for their assistance with mRNA experiments. Sally McCormick and Biochemistry Department at Otago University in Dunedin were very kind to allow me to use their ultracentrifuge after the Canterbury earthquakes. I'd also like to acknowledge Jack van Berkel from Kaikoura field station who hosted me for a month at the start of my write-up; this was incredibly valuable.

I owe big thanks to my postgraduate and other friends, especially: Mailee Stanbury, Jason Cambridge, Dayo Osinubi, Raj Janmale, Hanadi Katouah, Tina Yang, Nick Kirkland, Hannah Pebble, Sally Wischart, Agnetha Korevaar, Geoff Rogers, Claudia Segbold and many, many more, who were there with me and for me during different stages of my short research career. Huge thanks to Agnetha and Mailee for wonderful friendship and exquisitely decorated birthday muffins. I must also mention Campus Church – these guys have been amazing at feeding me spiritually and supporting me in the world by the fellowship of many wonderful Christians. Also, a huge thanks to my family – mom, dad, aunt Elena and my beloved grandparents - I did it for you!

Ultimately, I give thanks to the LORD for setting me onto this path and sustaining me along the way.

P.S.: Note for future students.
Remember that "devil is in the detail" – know your methodology, understand your assumptions and pay attention to the literature, both recent and old. Evaluate the difficult experiments according to the "time spent/value added" rule and remember that although research is hard, with perseverance and God's help you'll get through to the other side! Good luck and may God bless you.

Abstract

γ-Interferon stimulates human macrophages to produce 7,8-dihydroneopterin (7,8-NP). 7,8-NP and its oxidation product neopterin are excellent inflammatory markers for a variety of chronic conditions, including atherosclerosis. The biological significance of 7,8-NP in atherosclerosis is not fully understood, but 7,8-NP has been shown to protect macrophage cells from oxidised low density lipoprotein (oxLDL). Cellular accumulation of oxLDL–derived lipids and oxLDL–induced cytotoxicity are major drivers of atherosclerotic plaque progression.

This thesis investigated the mechanisms of 7,8-NP–mediated protection against oxLDL–induced damage to macrophage cells. The research assessed the relative contribution of the previously identified antioxidant capacity of 7,8-NP and its ability to down-regulate oxLDL uptake. OxLDL cytotoxicity was characterised by high intracellular oxidative stress within the first 12 hours of exposure, which was critical to oxLDL toxicity. Exogenously added 7,8-NP effectively scavenged the intracellular oxidants generated in response to oxLDL, shown by the oxidation of 7,8-NP to neopterin. The ability of 7,8-NP to alleviate oxidative stress during the critical time-frame of acute toxicity was the primary mechanism of protection. 7,8-NP was also found to down-regulate the levels of intracellular oxysterol esters in oxLDL–treated macrophages. This decrease was associated with the reduction of CD36 scavenger receptor protein and mRNA expression. The late onset of these processes in the second half of the 24 hour incubation highlighted their potential role in foam cell formation. Research indicated that 7,8-NP may play a role in the reverse cholesterol transport in these cholesterol ester-loaded cells. The CD36 down-regulation by 7,8-NP did not protect macrophages from acute oxLDL cytotoxicity.

This research reveals novel detail about the mechanism of 7,8-NP protection of macrophages from cytotoxic effects of oxLDL. It is suggested that 7,8-NP may protect macrophage cells in the atherosclerotic plaques by scavenging ROS produced during acute cytotoxicity and alleviate oxysterol ester accumulation, thus stabilising macrophage cells during chronic oxLDL exposure.

LIST OF TABLES

Abbreviations

α-TocH α-tocopherol.

β–MEtOH β–mercaptoethanol.

2-OH-HE 2-OH-hydroxyethidium.

7,8-DXP 7,8-dihydroxanthopterin.

7,8-NP 7,8-dihydroneopterin.

7KC 7-ketocholesterol.

AAPH 2,2'-azobis-2-methyl-propanimidamide, dihydrochloride.

ACAT acyl coenzymeA: cholesterol acyltransferase.

acLDL acetylated LDL.

ACN acetonitrile.

$AmPO_4$ ammonium phosphate.

ANOVA analysis of variance.

apoE apolipoprotein E.

ATP adenosine triphosphate.

AU absorbance unit.

BCA bicincronic acid.

BHT butylated hydroxytoluene.

BSA bovine serum albumin.

CD36 CD36.

cDNA cyclic DNA.

Cl^- chloride ion.

CNT concentrative nucleoside transporter.

CPDA-1 citrate-phophate-dextrose-adenine.

$CuCl_2$ copper chloride.

CVD cardiovascular disease.

DEPC diethyl-pyro-carbonate.

DHE dihydroethidium.

DIC differential interference contrast.

DMSO dimethyl sulfoxide.

DNA diribonucleic acid.

DOPA L-3,4-dihydroxyphenylalanine.

E^+ ethidium.

EC endothelial cell.

EDTA ethylene-diamine-tetra-acetic acid.

EGTA ethylene glycol-bis(2-aminoethylether)-N,N,N,N-tetraacetic acid.

ENT equilibrative nucleoside transporter.

ETC electron transport chain.

FAD flavin adenine dinucleotide.

FC free cholesterol.

GAPDH glyceradehyde-3-phosphate dehydrogenase.

GCH-I GTP cyclohydrolase-I.

GM-CSF granulocyte macrophage colony stimulating factor.

GPx glutathione peroxidase.

GSH glutathione.

GTP guanosine-5'-triphosphate.

H_2O_2 hydrogen peroxide.

HCl hydrochloric acid.

HDL high-density lipoprotein.

HIHS heat–inactivated human serum.

HMDM human monocyte-derived macrophage.

$HO^{\bullet -}$ hydroxyl radical.

HOCl hypochlorus acid.

HPLC high performance liquid chromatography.

HRP hydrogen peroxidase.

HS human serum.

ICAM-1 intercellular adhesion molecule-1.

IFN-γ interferon-γ.

IMC integrated modulation contrast.

iNOS inducible nitric oxide synthase.

IPA isopropyl alcohol.

JNK c-Jun-N-terminal kinase.

KCl potassium chloride.

$KHCO_3$ potassium bicarbonate.

KOH potassium hydroxide.

LACE lysosomal acid cholesterol esterase.

LDL low-density lipoprotein.

LPS lipopolysaccharide.

lymphoprep Lymphoprep®.

MAPK mitogen–activated protein kinase.

MBB 1H,7H-pyrazolo(1,2-ŏ3B1)pyrazole-1,7-dione, 3-(bromomethyl)-2,5,6-trimethyl-.

$MgCl_2$ magnesium chloride.

MPO myeloperoxidase.

MTT 3-[4,5-dimethylthiazol-2-yl]-2,5-diphenyl-tetrazolium bromide.

NaCl sodium chloride.

NADH nicotinamide adenine dinucleotide.

NADPH nicotinamide adenine dinucleotide phosphate.

NaH_2PO_4 sodium dihydrogen orthophosphate.

$NaHCO_3$ sodium bicarbonate.

NaOH sodium hydroxide.

NC nitrocellulose.

NF-κB nuclear factor kappa B.

NH_4Cl ammonium chloride.

NOX NADPH oxidase.

$O_2^{\bullet -}$ superoxide anion radical.

$ONOO^-$ peroxynitrite.

oxLDL oxidized low-density lipoprotein.

PBMC polymorphonuclear blood monocytic cells.

PBS phosphate buffered saline.

PDA photodiode array.

PI propidium iodide.

PKC protein kinase C.

PMA phorbol-12-myristate-13-acetate.

PPAR-γ peroxisome proliferator activator receptor-γ.

PS phosphatidyl serine.

PTS 6-pyruvoyl-tetrahydropterin synthase.

PUFA polyunsaturated fatty acid.

RCT reverse cholesterol transport.

REM relative electrophoretic mobility.

RM repeated measures.

RNA ribonucleic acid.

RNS reactive nitrogen species.

ROS reactive oxygen species.

RPMI-1640 Roswell Park Memorial Institute 1640 complete medium.

RT reverse transcriptase enzyme.

SD standard deviation.

SDS sodium dodecyl sulphate.

SEM standard error of the mean.

SIP sample introduction probe.

SMC smooth muscle cell.

SOD superoxide dismutase.

SR sepiapterin reductase.

TBARS thiobarbituric acid reactive substances.

TBS tris-buffered saline.

TCA trichloroacetic acid.

TM transition metal.

TNB 5-nitro-2-thiobenzoic acid.

TNF-α tumour necrosis factor-α.

U937 U937 monocyte-like cell line.

VCAM-1 vascular cell adhesion molecule-1.

VLDL very low-density lipoprotein.

1

Introduction

1.1 Overview and research question

Oxidative stress and inflammatory cell death are the core pathologies in many chronic diseases, including cardiovascular disease (CVD). CVD manifests as angina, stroke and myocardial infarction and is one of the leading causes of morbidity and mortality worldwide (Roger *et al.*, 2011). CVD is caused by the occlusion of the blood flow as a consequence of atheroslerosis (Naghavi *et al.*, 2003). Atherosclerosis, or vascular wall hardening, is characterised by lipid and cellular deposition in the arterial walls (Lusis, 2000). It is thought to be driven by the death of inflammatory cells recruited to the atherosclerotic site (Libby, 2002).

One of the key interactions during atherosclerosis is the death of macrophage cells in response to oxidatively modified low-density lipoprotein (LDL) (oxLDL), the main cholesterol carrier in the circulation (Moore & Tabas, 2011). Macrophages participate in the clearance of damaged host molecules (Fox & Rossi, 2010), which include oxLDL. OxLDL is toxic to cells, possesses pro-inflammatory properties and is abundant inside developing atherosclerotic lesions (Berliner & Heinecke, 1996; Steinberg & Witztum, 2010; Ylä-Herttuala *et al.*, 1989). Many studies have investigated the oxLDL–induced toxicity to macrophage cells, yet certain aspects of the process are not completely understood (Hessler *et al.*, 1983; Hodis *et al.*, 1994; Wintergerst *et al.*, 2000). The initial interaction and subsequent uptake of oxLDL by macrophages is facilitated by the cell surface receptors for oxLDL, called scavenger receptors. CD36 is the scavenger receptor most commonly associated with oxLDL–induced cytotoxicity and cell death (Collot-Teixeira *et al.*, 2007). OxLDL binding to CD36 triggers a signalling cascade that results in the production of reactive oxygen species (ROS) and

oxidative stress (Park *et al.*, 2009). This also affects the intracellular redox balance, which leads to the oxidative modification of key cellular enzymes, followed by changes in the cell metabolism and, ultimately, by cell death (Katouah, 2012; Sukhanov *et al.*, 2006).

The macrophage cells rely on a large pool of intracellular ROS-dismutating enzymes and small antioxidant molecules like glutathione (Gotoh *et al.*, 1993; Pietarinen-Runtti *et al.*, 2000) to withstand oxLDL–induced oxidative stress. Moreover, macrophages are known to release extracellular reduced thiols (Gmünder *et al.*, 1990) and a reduced pyrimidine 7,8-dihydroneopterin (7,8-NP) (Werner *et al.*, 1989). 7,8-NP is a redox sensitive molecule which has been shown to protect macrophage cells from oxLDL-induced cell death (Baird *et al.*, 2005; Gieseg *et al.*, 2010a).

7,8-NP and its oxidised counterpart, neopterin, have been linked to the atherosclerotic burden in cardiovascular disease. Both compounds had been detected in atherosclerotic plaques (Gieseg *et al.*, 2009) and neopterin was identified as a possible independent predictor of atherosclerosis complications (Ray *et al.*, 2007; Sugioka *et al.*, 2010). This suggests a plausible connection between oxLDL–induced cell death and 7,8-NP/neopterin availability (Gieseg *et al.*, 2009). Indeed, a number of studies have shown that 7,8-NP protects cells of myelocytic origin from the cytotoxic effects of oxLDL (Baird *et al.*, 2005; Gieseg *et al.*, 2001b, 2010a). The aim of this research is to establish the mechanism of this protection. Previous studies suggested that the protective effect of 7,8-NP on oxLDL–treated cells could be due to its ability to neutralise oxidants (Baird *et al.*, 2005; Gieseg *et al.*, 2001b). Recently, however, 7,8-NP has also been reported to reduce the uptake of oxLDL by macrophages (Gieseg *et al.*, 2010a). This thesis will investigate how the two capacities of 7,8-NP may contribute to its protective effect on human monocyte-derived macrophage (HMDM) cells treated with oxLDL.

1.2 Macrophages, oxLDL and 7,8-NP in atherosclerosis

Atherosclerosis is characterised by the hardening, occlusion and vascular modification of the arterial wall as a result of lipid deposition, immune cell recruitment and cellular death (Ross, 1999). The development of atherosclerotic lesions (also known as plaques) is thought to involve lipid deposition below the arterial endothelium and

the recruitment of inflammatory cells such as macrophages (Hansson & Hermansson, 2011; Libby, 2002; Packard & Libby, 2008; Ross, 1999).

Macrophage

Macrophage infiltration has been shown to contribute to all stages of atherosclerotic lesion development, from the early arterial wall thickening (Nakashima *et al.*, 2008) to the extensively remodelled, rupture-prone advanced plaque (Shaikh *et al.*, 2012). Moreover, mouse models with deficient monocyte-macrophage attracting mechanisms display significantly reduced lipid deposition in the arterial wall (Gu *et al.*, 1998; Potteaux *et al.*, 2011; Smith *et al.*, 1995). Many histological studies also report that macrophage markers co-stain with the lipid-rich areas of the plaque core, suggesting a relationship between the two (Ball *et al.*, 1995; Shaikh *et al.*, 2012).

Macrophages are involved in both innate and adaptive immunity and ensure an adequate response to stimuli in host defence (Fox & Rossi, 2010). This response includes the clearance of pathogens, damaged host cells and large molecules, as well as the production of molecules that are used in host defence (Fox & Rossi, 2010). Macrophage activation and the associated oxidative stress are common to a large number of chronic diseases, in addition to atherosclerosis. These include rheumatoid arthritis, inflammatory bowel disease, multiple sclerosis and obesity (Boyle, 2005; Fox & Rossi, 2010; Haider *et al.*, 2011; Nathan, 2008; Weisberg, 2003). Therefore, although this thesis focuses on macrophage cell death in response to oxLDL as implicated in atherosclerosis (Moore & Tabas, 2011), parts of this work could be applied to a wider range of inflammatory conditions.

Oxidised LDL

The lipoprotein pool is an important source of lipids in the circulation and within the atherosclerotic plaques. Low density lipoprotein, in particular, has been linked to atherosclerosis (Lusis, 2000; Steinberg & Witztum, 2010). The majority of mouse models of this disease are based on the apolipoprotein E and/or LDL-receptor deficient genetic background, suggesting a direct link between low density lipoprotein homeostasis and atherosclerosis (reviewed in Jawień *et al.* (2004)). LDL can undergo oxidative modification which renders it cytotoxic to the cells in the vasculature, including macrophages. The resulting oxLDL is a pro-inflammatory stimulus that induces the proliferation and spreading of macrophages and triggers oxidative stress

(Berliner & Heinecke, 1996; Glass & Witztum, 2001). OxLDL had been shown to contribute to macrophage death *in vitro* and was suggested to do so within atherosclerotic plaque (Ball *et al.*, 1995; Li *et al.*, 1998; Reid & Mitchinson, 1993).

7,8-Dihydroneopterin

7,8-Dihydroneopterin (7,8-NP) is associated with the process of atherosclerosis due to its origin within the activated human macrophage (Huber *et al.*, 1984). Both 7,8-NP and its oxidation product neopterin have been detected in atherosclerotic plaques (Gieseg *et al.*, 2008) and appear to be associated with acute CVD events (Ray *et al.*, 2007; Weiss *et al.*, 1994). A recent meta-analysis by Sugioka *et al.* (2010) suggested that neopterin is an important biomarker of plaque instability in both coronary and carotid atherosclerotic lesions. The role of 7,8-NP in atherosclerosis may be related to its macrophage origin and antioxidant properties. *In vitro*, 7,8-NP has been shown to interfere with LDL oxidation (Firth *et al.*, 2008a; Gieseg *et al.*, 1995; Greilberger *et al.*, 2004), ROS-mediated reactions (Dántola *et al.*, 2008a; Oettl *et al.*, 1997, 2004a) and cellular death induced by free radical species and oxLDL (Baird *et al.*, 2005; Duggan *et al.*, 2002). Therefore, 7,8-NP may mediate significant protection against inflammatory oxidative stress and thus protect macrophages trapped in the vicinity of oxidised LDL inside the atherosclerotic plaque.

1.3 Atherosclerotic lesion development: from onset to maturity

Atherosclerotic plaque classification

The atherosclerotic plaque development is a complicated process that can span a lifetime of an individual. Six stages of atherosclerotic plaque progression have been characterised according to lesion complexity (Ross, 1995). Type I and II plaques are often found in adolescents. These plaques manifest as the initial thickening of an arterial wall and a fatty streak, caused by the monocyte infiltration and the presence of what is believed to be plasma–derived lipid in the intimal layer of the vascular wall (fig. 1.1) (Ross, 1986; Stary *et al.*, 1995; Steinberg *et al.*, 1989). Continued expansion of the lipid and cell–enriched region and cellular death in this area produce type III lesions. These feature what appears as small extracellular pools of lipid on a histology sample (Stary *et al.*, 1995). The next stages of atherosclerosis are characterised by the development of extensive lipid–rich area devoid of cells. This is located deep within

the intimal layer of the artery and is referred to as the "necrotic core" region (1.1). In type IV lesions, the tissue that separates the "core" from the lumen is relatively thin, whereas in type V plaques it constitutes a thick fibrous structure, known as the "cap". Mature type VI atherosclerotic lesions are referred to as atheromas and are often more complex, containing regions of calcium deposits, ulceration and arteriogenesis with signs of vascular remodelling (Ross, 1986; Stary *et al.*, 1995; Steinberg *et al.*, 1989).

Plaque initiation hypotheses

At least three hypotheses have been proposed to explain the events that lead up to the formation of the arterial thickening and fatty streak (reviewed in Stocker & Keaney (2004)). The early response-to-injury hypothesis was developed by Ross (1986). He suggested that the perturbation of vascular homeostasis is the initial step in the disease (Ross, 1986). Endothelial injury frequently triggers compensating responses that upset the vascular homeostasis. The causes associated with endothelial injury are: non-laminar and oscillatory shear stress at the arterial bifurcation, local infection of the vascular wall and myeloperoxidase activity associated with phagocytes (Malek *et al.*, 1999). The disturbed endothelium produces leukocyte adhesion molecules (intercellular adhesion molecule-1 (ICAM-1), vascular cell adhesion molecule-1 (VCAM-1)) (Khan & Sefton, 2010). It also loses the ability to vaso-regulate becoming more permeable to atherogenic lipoproteins circulating in the blood (Malek *et al.*, 1999). The immune cells that are recruited to the site of injury release cytokines that promote and propagate the inflammatory response (Wick *et al.*, 2004). Monocytes are recruited to the arterial wall, being attracted by the cytokine stimuli. They then differentiate into macrophages and take up the infiltrated low density lipoprotein, forming lipid-laden cells (Lusis, 2000).

The response-to-retention hypothesis developed by Williams & Tabas (1998) suggests that atherogenesis is initiated by lipoprotein retention inside the arterial wall. The LDL aggregates in the intimal layer of the vascular wall and is taken up by the recruited macrophages. These develop into the lipid-laden "foam" cells, named so after their "foamy" appearance under the microscope.

The oxidative modification hypothesis also states that LDL traverses the sub-endothelial space and is retained for longer than the usual period of time in the atherosclerosis-prone sites (reviewed in Steinberg *et al.* (1989) and Stocker & Keaney (2004)). During

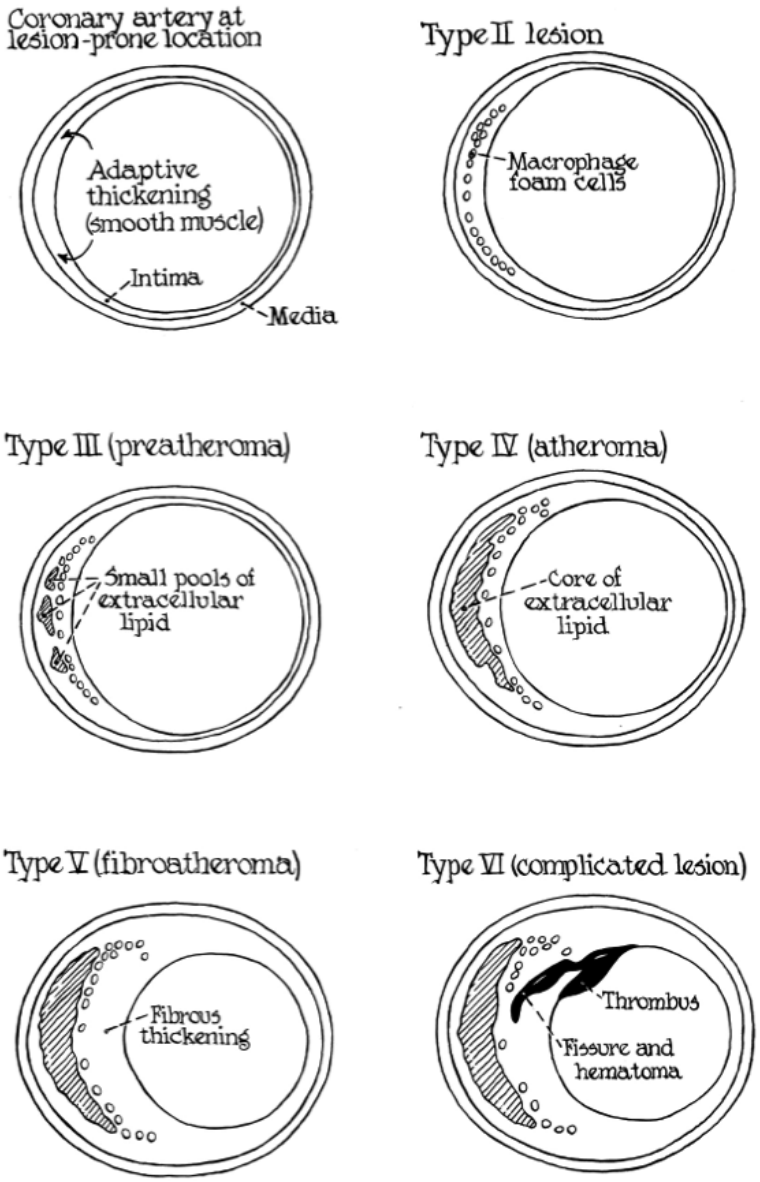

Figure 1.1: Six stages of atherosclerotic coronary lesion formation: cross-sectional drawing.

The progression of atherosclerosis is depicted from the earliest Type I and II stages to the most advanced Type VI stage, culminating in plaque rupture and associated thrombosis. Identical morphologies may be found in other lesion-prone parts of the coronary and many other arteries. From (Stary *et al.*, 1995).

this time it undergoes oxidative modification, which renders it a high-uptake molecule for residing and recruited cells in the vascular wall, enhancing foam cell formation.

The dual nature of atherosclerosis

Atherosclerosis is recognised for its binary nature, with both lipid imbalance and chronic inflammation playing a part in the pathology (Libby, 2002).
It has long been considered a lipid storage disease due to multiple lines of evidence (Ross, 1986; Stocker & Keaney, 2004). Firstly, LDL – one of the major lipid and cholesterol carriers in the blood – constitutes both a risk factor and a mechanism of atheroslerosis development (Lusis, 2000). An increased low to high density lipoprotein (LDL/HDL) ratio in the blood is indicative of potential for the development of atherosclerotic complications (National Cholesterol Education Program NCEP Expert Panel on Detection & of High Blood Cholesterol in Adults Adult Treatment Panel III, 2002). The modified LDL is pro-atherogenic and can directly contribute to atherosclerotic plaque growth. It displays pro-inflammatory properties, inhibiting macrophage migration (Park *et al.*, 2009; Quinn *et al.*, 1987) and inducing proliferation (Gordon *et al.*, 1990) of the cells found in the atherosclerotic plaque. It is also toxic to a variety of cells, directly contributing to the growth of the plaque core region (Salvayre *et al.*, 2002). The second line of evidence is the success of the so called "lipid-lowering" statin therapy in the primary and secondary prevention of CVD complications in "at risk" populations (de Lorenzo *et al.*, 2006; Edwards & Moore, 2003; Taylor *et al.*, 2011). The third line of evidence comes from animal models of atherosclerosis. Mouse and rabbit models, bred to study the disease, develop atherosclerosis only when fed a high cholesterol diet (Dornas *et al.*, 2010; Jawień *et al.*, 2004; Nakashima *et al.*, 1994). They also show a positive response to the lipid–lowering therapies (Aikawa *et al.*, 2002).

While being sensitive to lipid imbalance, the atherosclerotic plaques also present features of a chronic inflammatory disease (Pearson *et al.*, 2003; Wick *et al.*, 2004). Moreover, inflammatory cell infiltration is observed at all stages of atherosclerotic plaque development, from fatty streak to advanced atheroma (Moore & Tabas, 2011; Nakashima *et al.*, 2008; Shaikh *et al.*, 2012). Coincidentally, a large proportion of biochemical markers used in the clinical diagnosis and prognosis of atherosclerosis indicate immune system activation. An example of this is acute response C-reactive protein

Advancement of the atherosclerotic lesion: macrophage cell death

While in the early fatty streaks the cellular component is primarily derived from smooth muscle cells (SMCs), more advanced atherosclerotic plaques contain higher

proportion of macrophage cells (Gown *et al.*, 1986; Katsuda *et al.*, 1992; Kockx *et al.*, 1998). As the plaque develops, undifferentiated monocytes infiltrate the lesion attracted by a suite of cytokines produced by activated T cells and other cells (Ross, 1993). Monocytes are also attracted by oxLDL, as opposed to macrophages in which migration is inhibited by the oxLDL (Quinn *et al.*, 1987). Monocyte adhesion to the vascular endothelium is facilitated by the cell adhesion molecules ICAM-1 and VCAM-1, the expression of which is also induced by oxLDL (Amberger *et al.*, 1997). Penetrated monocytes differentiate into macrophages upon exposure to various growth factors released by other cells within the plaque. Meanwhile, the continued accumulation of modified LDL within the atherosclerotic lesion leads to an increased uptake by the resident macrophages (professional phagocytes). This drives the "foam" cell formation and culminates in cellular death (Stary *et al.*, 1992; Steinberg, 2009). From type III onwards, the plaques feature an extensive area of extracellular lipid, known as the "necrotic core" region of an atherosclerotic plaque. This is believed to develop through the cellular death processes within the plaque (Seimon & Tabas, 2009).

Many reviewers suggest that macrophage cell death induced by oxidised lipids is one of the key drivers of atherosclerotic plaque advancement (Ball *et al.*, 1995; Bjorkerud & Bjorkerud, 1996b; Boyle, 2005). This hypothesis is based on the following observations. Firstly, there is strong evidence that atherosclerotic lesions, in both humans and rabbits, contain oxidatively modified LDL constituents (Li *et al.*, 2006; Waddington *et al.*, 2003; Ylä-Herttuala *et al.*, 1989). Secondly, the oxidised lipid–rich regions on histological samples of advanced atherosclerotic plaques co-localise with the macrophage cell epitopes (Ball *et al.*, 1995; Waldo *et al.*, 2008). Thirdly, these regions are also characterised by extensive cellular death (Hegyi *et al.*, 1996; Isner *et al.*, 1995; Kockx *et al.*, 1998; Martinet *et al.*, 2011). The combined evidence points towards oxLDL–mediated macrophage cell death as a distinctive feature of the advanced atherosclerotic plaque. Indeed, this hypothesis is supported by the numerous *in vitro* studies showing oxLDL cytotoxicity to macrophages (Asmis & Wintergerst, 1998; Gieseg *et al.*, 2010a; Hardwick *et al.*, 1996; Wintergerst *et al.*, 2000).

1.3.1 Oxidative modification of LDL *in vivo* and *in vitro*

Lesion–modified LDL and *in vitro* oxidised LDL share many physical and chemical properties, which are significantly different from the plasma LDL. These include: increased negative charge resulting in higher electrophoretic mobility; increased density;

increased free cholesterol content; altered phospholipid fraction; and an increased proportion of oxidised lipids (Ylä-Herttuala *et al.*, 1989). Most lipid oxidation markers observed in atherosclerotic plaques are common to *in vitro* produced oxLDL. Oxysterols (advanced products of cholesterol oxidation) and thiobarbituric acid reactive substances (TBARS) (a product of polyunsaturated fatty acid (PUFA) oxidation) have been found within atherosclerotic lesions and on Cu-oxLDL (Brown *et al.*, 1997; Carpenter *et al.*, 1995; Waddington *et al.*, 2003). Numerous products of protein oxidation such as carbonyls, protein-bound L-3,4-dihydroxyphenylalanine (DOPA), dityrosine and chloramines, some of which are common to both Cu- and HOCl-oxLDL were also detected in atherosclerotic plaques (Fu *et al.*, 1998).

The biological properties were also similar. For example, the lesion LDL was internalised through the scavenger receptors; it produced a greater stimulation of cholesterol esterification, and was degraded more rapidly by macrophages (Ylä-Herttuala *et al.*, 1989). When added to murine cell line and human cultured macrophages, plaque gruel was phagocytosed, followed by progressive cellular death (Li *et al.*, 2006). Another group demonstrated that the gruel induced peroxidation in microsomes (Smith *et al.*, 1992). Atheromatous ceroid, an insoluble polymer of oxidised lipid and protein that contains abundant carbonyls/aldehydes, was found to be even more cytotoxic than oxLDL (Li *et al.*, 2006).

The exact nature of the LDL modification has been difficult to identify. To reproduce some of the natural heterogeneity, multiple *in vitro* oxidation mechanisms have been tested and characterised (Aviram *et al.*, 1996; Berliner & Heinecke, 1996; Jürgens *et al.*, 1987). Furthermore, non-oxidative modifications of LDL such as aggregation, acetylation, glycosylation and immunocomplexing, have also been extensively used in research (Al Gadban *et al.*, 2010; Levitan *et al.*, 2010). It is likely that *in vivo*, researchers are presented with a heterogeneous population of oxLDL molecules oxidised to various degrees and displaying various types of oxidative modifications. This work focuses on the so-called "heavily" oxidised LDL, produced by the Cu^{2+}–mediated oxidation of LDL at 37 °C for 24 hours. Such oxLDL is rich in TBARS and oxysterols (Gerry *et al.*, 2008). Since these markers of lipid and cholesterol oxidation had been detected in plaques and plaque gruel, the assumption that heavily oxidised LDL resembles its *in vivo* counterpart is supported by experimental evidence (Carpenter *et al.*, 1995; Gerry *et al.*, 2008; Shchepetkina, 2008).

Copper-mediated oxidation is often used to generate a high uptake oxLDL *in vitro*. This reasonably well–controlled, well–characterised and replicable system yields oxLDL with extensive fragmentation of apoB-100 (protein moiety on LDL) and the formation of large quantities of oxysterols and some protein hydroperoxides (Esterbauer *et al.*, 1990). Extensive peroxidation of polyunsaturated fatty acids and decomposition of lipid hydroperoxides into aldehyde fragmentation products is also observed (Gieseg & Esterbauer, 1994). This study used an adaptation of the method developed by Gerry *et al.* (2008).

1.4 Macrophage and oxLDL: recognition and interaction

Early studies of endothelial cells co-incubated with LDL indicated that it could be oxidatively modified in the presence of cells (Henriksen *et al.*, 1979; Hessler *et al.*, 1979). The oxidative modification of the LDL molecule facilitated the formation of macrophage "foam" cells (Henriksen *et al.*, 1983) with subsequent cell death. These observations led to the development of the oxidative hypothesis of atherosclerosis. The theory was founded partly on the fact that cultured monocytes/macrophages internalise oxLDL much more rapidly than native LDL (Ho *et al.*, 1976). Specific receptors on macrophages (and other vascular wall cells: SMC and, to an extent, endothelial cell (EC)) bind oxLDL with high affinity (Boullier *et al.*, 2001). These are not down-regulated by the increasing intracellular cholesterol levels and thus allow cholesteryl ester accumulation to the point of foam cell formation (Ho *et al.*, 1976). Effectively, oxLDL contents (oxidised apoB-100 and oxidised phospholipids) are the structural features recognised by the immune system as foreign ligands (Steinberg, 2009).

The second part of the oxidative hypothesis of atherosclerosis rests on the fact that oxLDL elicits a detrimental effect on cellular viability. This is believed to be mediated via multiple oxidised moieties on oxLDL. Attempts have been made to link oxysterols, ox-phospholipids and oxidised protein with the cytotoxicity exerted by the oxLDL molecule (Larsson *et al.*, 2006; Salvayre *et al.*, 2002). The majority of these studies, however, have investigated only the effect of a specific ligand in isolation, upon direct binding or internalisation by the cell. This approach is problematic as a toxic component incorporated within another ligand (for example, an oxysterol within the oxLDL particle) will interact with the cell differently from how an oxysterol added

directly to the cell medium will. This concept was illustrated by Rutherford & Gieseg (2012) who showed that the incorporation of 7-ketocholesterol (7KC) into acetylated LDL particles completely aborted its cytotoxicity. Thus, many of the aforementioned studies may be of little relevance until our understanding of the intracellular trafficking of the complex oxLDL molecule is increased to a point where we can state in what form these individual moieties are indeed present within the cell, and exert a specific function. This work will, therefore, focus on the holistic effect of the oxLDL and the resulting cellular response.

The following sections will outline the mechanisms of macrophage cell death in response to oxLDL by giving a brief overview of the recognition, binding, uptake, processing and cellular response to oxidised LDL. Special attention will be paid to the redox processes within the macrophage.

1.4.1 Role of scavenger receptors in atherosclerosis

OxLDL is initially recognised by macrophage scavenger receptors (SRs), a family of cellular transmembrane proteins that are implicated in the recognition and clearance of foreign bodies and apoptotic cells (Ashraf & Gupta, 2011). A number of SR classes with a large sequence variation have been identified to date (Ashraf & Gupta, 2011). Only a select few of those, however, have been shown to contribute significantly to oxLDL uptake by macrophages (reviewed in Moore (2006)). The most abundant evidence exists for the following receptors: class A scavenger receptor A (SR-A) (Kodama *et al.*, 1988), class B scavenger receptors SR-BI and CD36 (de Villiers & Smart, 1999; Endemann *et al.*, 1993), class D scavenger receptor CD68 (which has been implicated in endosomal utilisation of oxLDL and acLDL (Ramprasad *et al.*, 1996; Zeibig *et al.*, 2011) and class E scavenger receptor, lectin-like oxidised low–density lipoprotein receptor-1 (LOX-1) (Boullier *et al.*, 2001; Yoshida *et al.*, 1998). In addition, some of the toll-like receptors (TLRs), a family of pattern recognition receptors implicated in host defense against bacterial pathogens, were recently shown to facilitate lipid uptake and foam cell formation (Keyel *et al.*, 2012; Miller *et al.*, 2009).

While the relative contribution of each of the aforementioned receptors to oxLDL uptake by macrophage *in vivo* is unknown, experimental evidence supports an important role for both SR-A and CD36 in the pathogenesis of atherosclerosis (Boullier *et al.*, 2001). Specifically, mice deficient in SR-A or CD36 on a pro-atherosclerotic

background (apolipoprotein E deficiency coupled with a so-called Western diet) exhibit a significant reduction in atherosclerotic lesion development (Febbraio *et al.*, 2000; Suzuki *et al.*, 1997). The monocytes/macrophages derived from these murine models displayed a significantly decreased uptake of oxLDL. Another mouse model deficient in both SR-A and CD36 showed a 70 to 90% decrease in the uptake of oxLDL (Kunjathoor *et al.*, 2002). In contrast, the effect of combined CD36 and SR-A knockout on the atherosclerotic lesion area in mice in the Kuchibhotla *et al.* (2008) study was not additive. Yet another study had observed no reduction of the lesion or "foam" cell formation in a similar $CD36^{-}$ SRA^{-} mice but the lesions did not progress to an advanced state (Manning-Tobin *et al.*, 2008). Thus, while the involvement of SR-A and CD36 scavenger receptors in the pathogenesis of atherosclerosis is undisputed, it is likely to be multi-factorial.

Evidence from the previous studies for SR-A–specific contribution to the development of atherosclerotic lesions in animals or oxLDL uptake *in vitro* is not in absolute agreement. Kuchibhotla *et al.* (2008) did not detect any significant difference in the size of atherosclerotic lesion in SR-A–null male mice, while a CD36-null background was protective irrespective of gender. Terpstra *et al.* (1997) showed that the macrophages of SR-A knockout mice internalised significantly less acetylated LDL (acLDL) than the wild type, but the trend was much less marked for oxLDL uptake. The degree of and conditions for SR-A involvement in macrophage cell death are also unclear. While some authors have reported a necessary SR-A engagement in the initiation of apoptosis (DeVries-Seimon *et al.*, 2005), others showed that although the SR-A route accounted for half of the oxLDL uptake, this receptor was not involved in oxLDL–mediated apoptosis of HMDM cells (Wintergerst *et al.*, 2000). Based on this evidence, a number of reviewers have suggested that SR-A–mediated uptake may be more important for the acetylated/aggregated LDL than oxidised LDL (de Villiers & Smart, 1999; Gough *et al.*, 1999).

1.4.2 The role of CD36 in oxLDL uptake by macrophages

The evidence for CD36 involvement in atherosclerotic plaque development is more substantial and extensive than that of the SR-A, potentially due to its ubiquity of expression (Febbraio *et al.*, 2001). While the expression of SR-A is restricted to macrophages, CD36 is also expressed in adipocytes, microvascular endothelium, platelets, erythroid precursors, and smooth muscle cells, where it facilitates oxLDL uptake (Moore, 2006; Ricciarelli *et al.*, 2000). CD36 plays a role in platelet adhesion

(Asch *et al.*, 1987), fatty acid transport in adipose tissue (Abumrad *et al.*, 1998) and the clearance of apoptotic cells by macrophages (Ren *et al.*, 1995; Rigotti *et al.*, 1995). In addition, a soluble form of the CD36 receptor with a role in metabolic syndrome and atherosclerosis has recently been identified (Handberg *et al.*, 2006; Koonen *et al.*, 2011).

Binding

CD36 is an 88 kDa glycoprotein which traverses the membrane twice, and comprises a heavily glycosylated extracellular loop with 2 short intracellular tails. The extracellular portion of the protein contains motifs that are able to recognise and bind oxidised moieties on oxLDL. Specifically, suggestions have been made that it recognises oxidised lysine residues on the apo B-100 and oxidised phospholipids in the lipid fraction (Bird *et al.*, 1999; Boullier *et al.*, 2001; Silverstein *et al.*, 2010; Steinbrecher, 1999). Interestingly, CD36 binding of apoptotic bodies has also been proposed to proceed through the binding of modified cellular phospholipid membrane (Boullier *et al.*, 2001). It is known that monocytes almost lack CD36 (and a number of other receptors) and that CD36 expression is enhanced upon the maturation into macrophages (Alessio *et al.*, 1996; Nakagawa *et al.*, 1998).

In atherosclerosis, CD36 has been proposed to contribute to the development of lesions through the pro-atherogenic and pro-inflammatory properties of CD36–mediated macrophage–oxLDL interaction (reviewed in Moore (2006); Silverstein *et al.* (2010); Steinbrecher (1999)). OxLDL binding to CD36 activates the cells to produce and release pro-inflammatory cytokines and ROS (Boyle, 2005). The signalling pathways have been extensively reviewed in Silverstein *et al.* (2010), but, briefly, CD36 can associate with Src kinases (Lyn, Fyn) and MAP-kinase kinase family member MEKK2 via its intracellular "tail" domains. Src kinase activation leads to phosphorylation of mitogen–activated protein kinase (MAPK) family members p38 and c-Jun-N-terminal kinase (JNK). The effect of this activation may be cellular death, inflammatory gene expression, adhesion, and migration. The latter modulates cytoskeletal dynamics which leads to trapping of macrophages in plaques (Park *et al.*, 2009).

Regulation of CD36 expression

Receptor–facilitated uptake of oxidised LDL is not regulated by the same mechanism as that of native LDL, where the LDL-receptor is feedback down-regulated by the intracellular cholesterol content (Heinecke *et al.*, 1993; Hoff & O'Neil, 1988; Steinberg

& Witztum, 2010). In contrast, the ligand(s) that bind(s) to the CD36 have been demonstrated to up-regulate this receptor. Acetylated LDL, and oxidised LDL cause an increase in the levels of CD36 mRNA and protein in monocytes, macrophages, macrophage-like cells and SMCs (Han *et al.*, 1997; Munteanu *et al.*, 2006; Nakagawa *et al.*, 1998; Ricciarelli *et al.*, 2000). The regulatory mechanism proceeds via the nuclear hormone receptor peroxisome proliferator activator receptor-γ (PPAR-γ), which, once activated by a lipid-like ligand, drives the transcriptional activation of CD36 expression (Munteanu *et al.*, 2006; Tontonoz *et al.*, 1998). Cholesteryl ester hydroperoxides on oxLDL have been proposed to drive this activation (Jedidi *et al.*, 2006). In addition, little evidence exists with respect to the feedback regulation of the uptake by the processes and/or products governing the oxLDL internalisation or breakdown.

OxLDL uptake and processing

The intracellular processes that control the internalisation and trafficking of oxLDL components are fairly well understood. It is thought that the receptors congregate in coated pits/lipid rafts of plasma membrane, called caveolae (Patel & Insel, 2009). Upon oxLDL binding to receptors, the plasma membrane in such regions is pulled inward to form a vesicle that encapsulates oxLDL (Collins *et al.*, 2009). This vesicle merges with the endosome and lysosome where the oxLDL is then targeted for degradation and/or esterification (Jerome & Yancey, 2003; Wang *et al.*, 2005). Normally, the intracellular concentration of unmodified LDL cholesterol is maintained via the mechanism presented in fig. 1.2 . Cholesteryl esters within the LDL particle are hydrolysed either by acidic cholesteryl ester hydrolase in the endosome (Wang *et al.*, 2005) or lysosomal acid cholesterol esterase (LACE) in the lysosome (Jerome & Yancey, 2003), which seem to be the same enzyme EC 3.1.1.13 (Sando & Rosenbaum, 1985). Free cholesterol is trafficked out of the lysosome for membrane synthesis or efflux. Any excess free cholesterol is directed to the endoplasmic reticulum where it is re-esterified by the enzyme acyl coenzymeA: cholesterol acyltransferase (ACAT). The esterified cholesterol is stored in the cytoplasmic inclusions and can be hydrolysed when necessary by a neutral cholesterol esterase (Jerome & Yancey, 2003; Sekiya *et al.*, 2011; Yvan-Charvet *et al.*, 2010). Cholesterol efflux onto high-density lipoprotein (HDL) apo-A1 is facilitated via adenosine triphosphate (ATP)–binding cassette transporters ATP binding cassette A1 (ABCA1) and ATP binding cassette G1 (ABCG1) (Yvan-Charvet *et al.*, 2010). SR-BI receptor has also been shown to mediate cholesterol efflux (Chroni *et al.*, 2005). LDL modification, however, have

been shown to reduce the rate of its degradation and efflux from the macrophage (Hoff *et al.*, 1993). In addition, certain oxysterols (7KC) have been shown to inhibit the action of cholesterol transporters (Jessup & Kritharides, 2000; Jessup *et al.*, 2002). Thus, not only is oxLDL taken up in higher amount than LDL, but its efflux is reduced, facilitating the formation of lipid-rich foam cells.

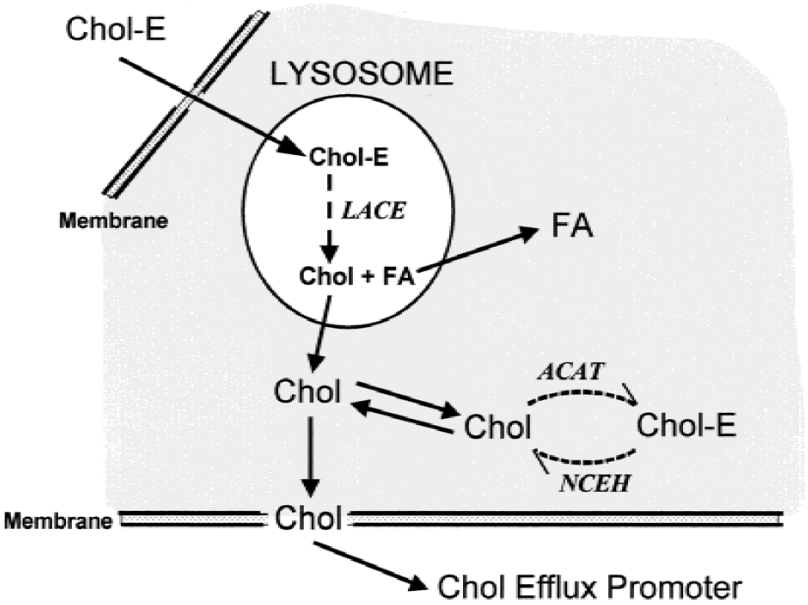

Figure 1.2: Cholesteryl ester metabolism in cells.
Intracellular cholesterol processing mechanism (from Jerome & Yancey (2003)) Cholesteryl esters within the LDL particle are hydrolysed by LACE and free cholesterol is trafficked out of the lysosome for membrane synthesis or efflux. Any excess free cholesterol is directed to the endoplasmic reticulum where it is re-esterified by the enzyme ACAT. The esterified cholesterol is stored in the cytoplasmic inclusions and can be hydrolysed when necessary by a neutral cholesterol esterase (Jerome & Yancey, 2003; Sekiya *et al.*, 2011; Yvan-Charvet *et al.*, 2010). Cholesterol efflux onto HDL Apo-A1 is facilitated via ATP–binding cassette transporters ABCA1 and ABCG1.

CD36 and macrophage cell death

It is highly probable that CD36–facilitated uptake, processing and accumulation of oxLDL is controlled by multiple cellular processes, because the results of CD36 binding or signaling inhibition studies vary significantly. While Rahaman *et al.* (2006) observed a 70-80% inhibition of foam cell formation in macrophages of CD36–null mice, Nozaki *et al.* (1995) reported up to 40% inhibition of oxLDL uptake in the CD36-null human macrophages and Wintergerst *et al.* (2000) saw no effect of CD36

ligand inhibition on oxLDL uptake by macrophages. In contrast to uptake, the evidence for CD36 involvement in oxLDL–induced cellular death is more discreet. For example, sequestration of CD36 with an antibody blocked ROS production and cell death in SMCs and macrophages (Higashi *et al.*, 2005; Park *et al.*, 2009; Wintergerst *et al.*, 2000). This has been further confirmed by Wintergerst *et al.* (2000) who observed that CD36-negative macrophage cells did not undergo apoptosis.

1.5 Macrophage cell death processes mediated by oxLDL

High concentrations of oxLDL exhibit a cytotoxic effect on macrophages, endothelial and smooth muscle cells *in vitro*. This suggests that oxLDL may promote the formation of atherosclerotic plaques by inducing damage to the arterial tissue (Galle *et al.*, 2006; Hsieh *et al.*, 2001; Wintergerst *et al.*, 2000). Macrophage cell death in response to oxLDL is central to the growth of the plaque necrotic core. Hence, the mechanisms of oxLDL–induced macrophage cell death *in vivo* and *in vitro* have been the subject of extensive research since the end of 1970's. The signaling cascades and intracellular processes that lead to cell death are diverse, but a few common features can be identified.

1.5.1 Types of cell death

The complexity of the cellular response to oxLDL makes it difficult to ascribe a particular pathway to the process of cell viability loss. The two widely recognised types of cellular death, apoptosis and necrosis, have both been implicated in oxLDL–induced macrophage cell death (Boullier *et al.*, 2001; Martinet *et al.*, 2011). Apoptosis is the physiological process (that can become pathological) of programmed cellular self-destruction (Edinger & Thompson, 2004; Krysko *et al.*, 2008). The process involves a tightly controlled series of events, the execution of which is powered by ATP (Edinger & Thompson, 2004; Krysko *et al.*, 2008) (for a non-oxLDL related review of apoptosis: Ashkenazi & Dixit (1998)). Conversely, necrosis is a pathological process of unrestrained cell death, which has been described as a "bioenergetic catastrophe" (Edinger & Thompson, 2004). Necrotic death results in a pro-inflammatory response from the surrounding cells . The key features of the two pathways are presented in the table 1.1 (Salvayre *et al.*, 2002). The main distinguishing property between the two is the availability of cellular energy in the form of ATP and nicotinamide

adenine dinucleotide phosphate (NADPH) (Edinger & Thompson, 2004; Skulachev, 2006). The features of cell death pathways are of particular interest since they are often employed in the cell death detection assays.

Apoptosis proceeds if the apoptotic machinery is in place and could be activated,

Table 1.1: Morphological features of cells undergoing apoptosis and necrosis from Salvayre *et al.* (2002) and Fiers *et al.* (1999).

	Apoptosis	**Necrosis**
Cell volume	decreased	increased
Cytoplasmic appearance	electron dense[a]	normal[a]
Plasma membrane integrity	intact	defective
trypan blue permeability	non-permeant[b]	permeant[b]
propidium permeability	non-permeant[c]	permeant[c]
morphology	blebbing[a,b]	
phosphatidyl serine exposure	yes	no/sometimes
Mitochondrial appearance	densification[a]	swelling, rupture[a]
Nuclear morphology	fragmented[b]	normal[b]
chromatin appearance	condensed[a]	loose[a]
nuclear membrane presence	absent[a]	present[a]
Cell fragmentation	apoptotic bodies[a,b]	debris[a,b]
Caspase activation	yes/sometimes	no
Cytochrome c release	yes	no

[a]Electron microscopy [b]Optical microscopy [c]Fluorescence microscopy

i.e. the energy (ATP and NADPH) is sufficient to ensure that the damaged cell is packaged and removed cleanly (Skulachev, 2006). If, on the other hand, the apoptotic processes fail to activate and/or the cellular energy is insufficient to complete the apoptotic liquidation, the cell undergoes "secondary" necrosis. This can happen in the circumstances of excessive intracellular damage or damage to key metabolic enzymes (Katouah, 2012).

The two best described alternative cell death pathways are "programmed necrosis" and autophagy (Edinger & Thompson, 2004). The concept of programmed necrosis is sometimes considered a separate cell death mechanism (Han *et al.*, 2011). It manifests as a necrosis–like cell death pathway but is triggered by a set of signaling

cues. However, because the net result of the "necrotic" signaling is also ATP depletion, it is incorporated into the aforementioned definition of necrosis (Han *et al.*, 2011). Autophagy has been described as a self-sacrificing mechanism with the cell degrading its own constituents for energy production under nutrient stress conditions or as a suicide (Edinger & Thompson, 2004; Mihalache & Simon, 2012). It had been associated with oxLDL-induced endoplasmic reticulum stress and lysosomal oxLDL degradation, a more chronic type of cellular death (as discussed below) (Muller *et al.*, 2010; Ouimet *et al.*, 2011). In fact, all of these cellular death processes have been named in association with oxLDL-induced cellular death and atherosclerosis (Boullier *et al.*, 2001; De Meyer & Martinet, 2009; Martinet *et al.*, 2011; Verheye *et al.*, 2007).

1.5.2 OxLDL–mediated cellular death in the literature

In vitro, the cytotoxicity of oxLDL can be measured experimentally by the loss of various cell viability markers, including: 3-[4,5-dimethylthiazol-2-yl]-2,5-diphenyl-tetrazolium bromide (MTT) reduction (Gieseg *et al.*, 2009); trypan blue exclusion (Baird *et al.*, 2005); the release of lactate dehydrogenase (Carpenter *et al.*, 2003); radioactive adenine (Wang *et al.*, 2006); or detection of the classical apoptosis/necrosis features like DNA fragmentation (propidium iodide (PI) binding) and phosphatidyl serine (PS) exposure (Annexin V binding) (Muller *et al.*, 2001). Some of these markers have been observed within complex plaques (Bjorkerud & Bjorkerud, 1996b; Isner *et al.*, 1995; Kockx *et al.*, 1998). The reported cytotoxicity of oxLDL *in vitro* varies considerably between different laboratories. The experimental protocols are very diverse with respect to the range of oxLDL concentrations (25 to 3000 μg per mL LDL) and incubation times (4-48 hours), as well as the measured cytotoxicity outcomes (Asmis *et al.*, 2005; Gieseg *et al.*, 2009; Kinscherf *et al.*, 1998). The cytotoxicity outcome may depend on the oxLDL preparation, type of cells, or possibly, experimental conditions. This topic will be addressed in more detail in Chapter 3.

The type of cellular death (apoptosis vs. necrosis) in response to oxLDL may also be subject to inter-cellular variations, as highlighted by a comparative study of THP-1 and U937 monocyte-like cell lines (Baird *et al.*, 2004). Baird *et al.* (2004) found that THP-1 underwent a caspase–mediated apoptosis characterised by a relatively slow loss of intracellular glutathione, whereas U937 cells displayed no caspase activation combined with rapid glutathione (GSH) loss and lack of phosphatidyl serine (PS) externalisation characteristic of necrosis. In HMDM cells, both caspase–dependent

(Wintergerst *et al.*, 2000) and independent cell death have been reported (Asmis & Begley, 2003; Gieseg *et al.*, 2010a). With the current experimental setting in the Gieseg laboratory, HMDM cells were observed to undergo caspase-3 independent necrosis and a rapid loss of glutathione (Gieseg *et al.*, 2010a).

1.6 Oxidative stress in macrophage–oxLDL

The key feature of oxLDL cytotoxicity to all cell types is the generation of intracellular ROS. In a large proportion of cell types, the production of ROS plays a significant role in the cellular death process. Oxidative stress, or the prevalence of ROS production over the cellular antioxidant defence, can originate from multiple sources in oxLDL-treated macrophages: phagocytic NADPH oxidase (NOX), mitochondrial and lysosomal destabilisation and endoplasmic reticulum stress (Moore & Tabas, 2011). The key role of oxLDL–induced ROS production in atherosclerotic cell death is supported by the studies of compounds with a free radical-neutralising ability. Probucol, probucol analogs and vitamin E have been shown to inhibit cell death *in vitro* and the progression of atherosclerosis in the animal models, thus suggesting that ROS is important to the disease pathology (Steinberg, 2009). A water soluble antioxidant 7,8-NP was also shown to inhibit cellular death in U937 cells from a variety of sources of oxidative stress, including oxLDL (Baird *et al.*, 2005; Gieseg *et al.*, 2001b).

1.6.1 Reactive oxygen species

Reactive oxygen species are involved in both signaling and oxidative stress, and thus have the capacity to be both beneficial and detrimental to cells (Carmody & Cotter, 2001). The biological effects of ROS range from cell activation to proliferation, survival to apoptosis. These are mediated by multiple signaling pathways, including MAPK kinases, Akt, nuclear factor kappa B (NF-κB), caspases and calcium (Carmody & Cotter, 2001; Dröge, 2001). OxLDL has been shown to induce intracellular ROS production in all vascular cell types examined (Salvayre *et al.*, 2002). The role of ROS in oxLDL-mediated cytotoxicity has been reported to proceed both through the activation of the caspase cascade, causing apoptosis (Baird *et al.*, 2004); and without caspase-3 activation through oxidative inactivation of metabolic enzyme, glyceradehyde-3-phosphate dehydrogenase (GAPDH) causing necrosis (Gieseg *et al.*, 2010a).

A large proportion of oxidative damage in biological systems is done via free radicals. Free radical is a reactive chemical species that contains one or more unpaired electrons and is capable of independent existence (Stocker & Keaney, 2004). Free radicals can be extremely damaging to biological molecules due to their ability to initiate a self-propagating chain reaction, where for each initial radical many more are generated (Buettner, 1993; Halliwell & Whiteman, 2004). Of the four different types of free radical species: oxygen, nitrogen, carbon and sulphur–centered free radicals, oxygen–centered radicals (ROS) are the most abundant during the cellular response to oxLDL (Dröge, 2001; Valko *et al.*, 2007). Superoxide anion radical ($O_2^{\bullet-}$) is the main source of ROS in the cell (Dröge, 2001; Valko *et al.*, 2007). It serves as a precursor to a range of other ROS (fig. 1.3) (Buettner, 1993; Stocker & Keaney, 2004). The $O_2^{\bullet-}$ gives rise to hydrogen peroxide (H_2O_2), hydroxyl radical ($HO^{\bullet-}$) and hypochlorus acid (HOCl) as well as participating in the formation of reactive nitrogen intermediates (Beckman & Koppenol, 1996; Dröge, 2001; Valko *et al.*, 2007). Hydroxyl radicals are highly reactive but short-lived, attacking a wide range of molecules in the immediate vicinity of the site of origin (Buettner, 1993). This type of free radical can be formed from $O_2^{\bullet-}$ and H_2O_2 *via* the Haber-Weiss reaction or *via* the Fenton interaction of H_2O_2 with copper or iron ions (Kehrer, 2000; Morel & Barouki, 1999). These reactions are biologically significant as the substrates can be found within cells and tissues and can easily interact. H_2O_2 can also serve as substrate for myeloperoxidase (MPO) enzyme thus leading to the formation of hypochlorous acid, which had been implicated in many pathophysiological conditions, including atherosclerosis (Klebanoff, 2005; Podrez *et al.*, 2000).

1.6.2 Macrophage NADPH oxidase

Macrophage phagocytic NADPH oxidase (NOX) is one of the main immediate sources of superoxide radicals upon cellular activation by a ligand, such as oxLDL (Bedard & Krause, 2007). The NADPH oxidase complex exists as a cluster of membrane-bound subunits and associated cytoplasmic soluble subunits that donate an electron from NADPH to molecular oxygen (O_2) which produces superoxide ($O_2^{\bullet-}$) (Bedard & Krause, 2007). Superoxide can then be enzymatically dismutated into H_2O_2 by superoxide dismutases and further to or $HO^{\bullet-}$ by Fenton reaction (Matés *et al.*, 1999). This initiates a respiratory burst which is a key step in the immune defence against bacterial and fungal pathogens (Bedard & Krause, 2007) and, it seems, during the oxLDL binding (Park *et al.*, 2009).

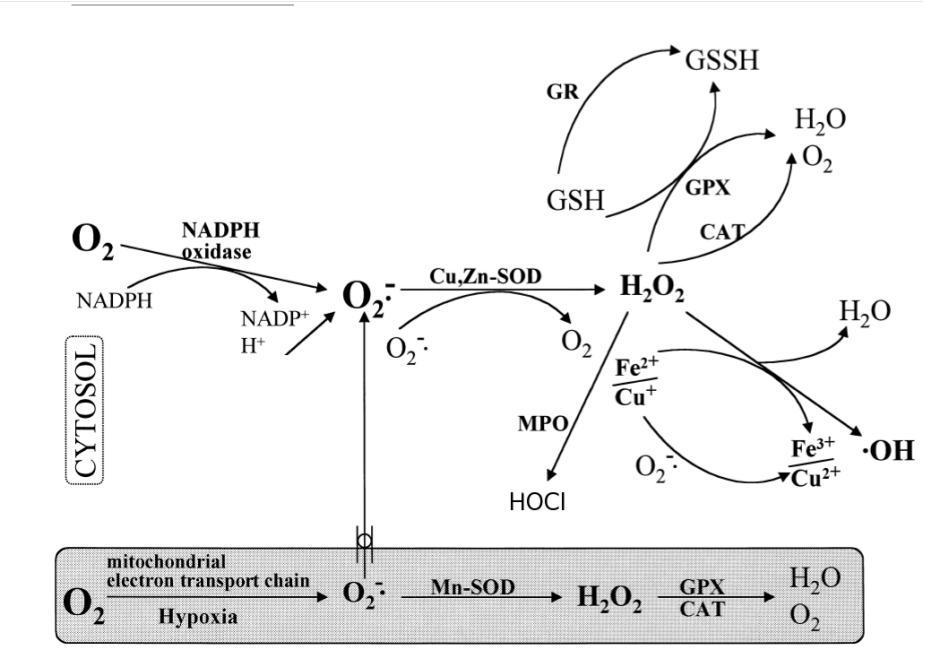

Figure 1.3: Reactive oxygen species.
Molecular oxygen undergoes successive reductions which yield the superoxide radical anion ($O_2^{\bullet-}$), hydrogen peroxide (H_2O_2), hypochlorite (HOCl) and hydroxyl radical ($HO^{\bullet-}$). Antioxidant systems act as ROS scavengers to maintain the intracellular redox status.SODs dismutate superoxide into oxygen and hydrogen peroxide and catalase neutralises hydrogen peroxide into oxygen and water. Glutathione peroxidase (GPx) acts like catalase on various peroxide compounds, including H_2O_2. The catalytic cycle of glutathione peroxidase involves the oxidation of GSH. GSSG can be reduced back to GSH by glutathione reductase. Adapted from Matés *et al.* (1999)

In its resting state the NADPH complex consists of the cytosolic and plasma membrane–integrated components (fig. 1.4). The membrane-bound $gp91^{phox}$ (primary active component) and $p22^{phox}$ are collectively referred to as cytochrome b558 (Groemping & Rittinger, 2005). The smaller $p22^{phox}$ protein has an SH3 binding domain, suggesting that it is a docking site for the soluble cytosolic components of NOX, $p40^{phox}$, $p47^{phox}$ and $p67^{phox}$ (Groemping & Rittinger, 2005).
A variety of stimuli may lead to the activation of NOX and superoxide production. With respect to oxLDL binding, CD36 and TLR4 were identified to cause a NOX-dependant oxidative flux (Bae *et al.*, 2009; Park *et al.*, 2009). Receptor activation upon ligand binding initiates a cytosolic signaling cascade that culminates with the release of Ca^{2+} from the ER and the activation of the protein kinase C (PKC) (Bedard & Krause, 2007). PKC, in turn, phosphorylates $p47^{phox}$ which results in its translocation and binding to the $p22^{phox}$ on the membrane. Other stimuli activate several

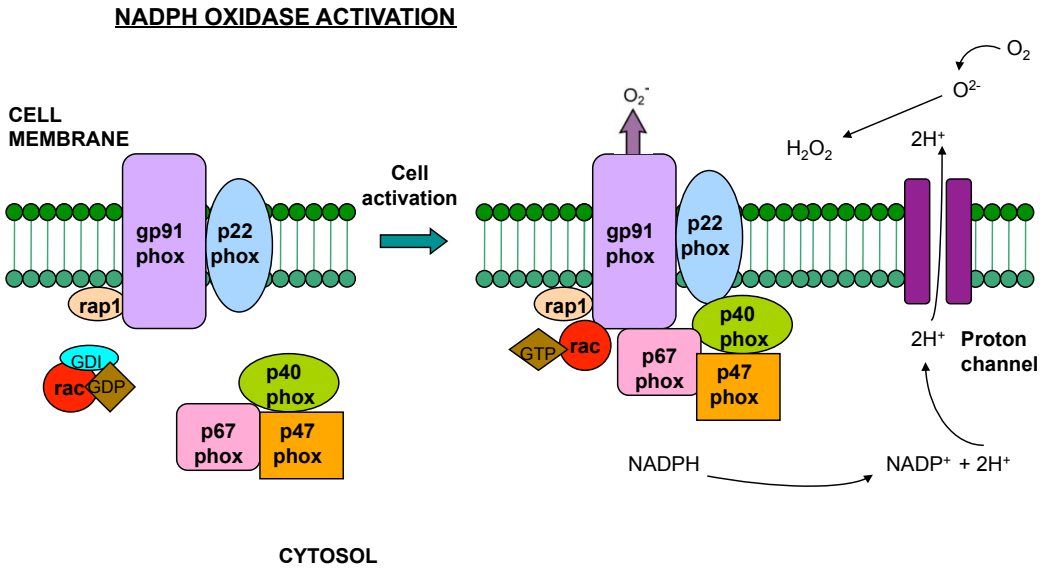

Figure 1.4: NADPH oxidase components and activation.
The transmembrane portion of a phagocytic NADPH oxidase consists of $p22^{phox}$ and $gp91^{phox}$ which constitute the smaller and larger chain of the cytochrome-b558, respectively. The cytosolic part of the complex is comprised of two $p67^{phox}$ and $p47^{phox}$ subunits, accessory protein $p40^{phox}$ and a Rac-GTP binding protein The cytosolic subunits translocate to the cell membrane upon cell activation to form the active NADPH oxidase complex which generates superoxide radical. Adapted from Assari (2006).

other kinases (e.g. Akt, c-Src, MAPK) which can also phosphorylate $p47^{phox}$ (Bedard & Krause, 2007). OxLDL has been proposed to activate NOX through CD36 binding in SMCs as well (Sukhanov *et al.*, 2006). In Sukhanov *et al.* (2006), ROS production after oxLDL treatment caused the loss of the glycolytic enzyme glyceraldehyde-3-phosphate dehydrogenase (GAPDH). This curbed the cellular ATP stores and led to subsequent necrosis (Sukhanov *et al.*, 2006). The loss of GAPDH was prevented by various antioxidants and NADPH oxidase inhibitor. Anti-CD36 antibodies also blocked ROS production and GAPDH loss suggesting that activation of NADPH oxidase was triggered by oxLDL binding to CD36 (Sukhanov *et al.*, 2006).

1.6.3 Mitochondrion

Mitochondrion is another source of ROS (Turrens, 2003). The uncoupling of the electron transport chain can occur as a result of mitochondrial damage or destabilisation. It leads to the transfer of electrons onto molecular oxygen to yield the superoxide radical (Morel & Barouki, 1999). Under normal circumstances, this superoxide is quickly

dismutated by a suite of antioxidant enzymes into hydrogen peroxide, followed by water and hydrogen (Turrens, 2003). In contrast, under conditions of high oxidative stress or redox imbalance, the ROS are not dismutated fully and can, therefore, react with proteins and membranes, inflicting damage (Valko *et al.*, 2007). This damage can perpetuate further uncoupling of the electron transport chain, leading to energy loss, release of cytochrome c into the cytoplasm and the formation of the mitochondrial transition pore, which constitutes a part of apoptotic shut-down process (Madamanchi & Runge, 2007).

The role of mitochondrion has been discussed in relation to oxLDL-induced cellular death. Reports of both the involvement and relative redundancy of the mitochondrial ROS in macrophage death have been made (Amit, 2008; Asmis & Begley, 2003; Ryan *et al.*, 2003). Previous study in the Gieseg laboratory by Amit (2008) indicated that during acute cellular death inflicted by the oxLDL damage, mitochondrial involvement was minor (as shown by limited cytochrome c release into the cytosol). Ryan *et al.* (2003) also showed that the ROS production from the mitochondria in response to the oxLDL oxysterol 7-ketocholesterol was relatively modest, causing only a small yet significant reduction in cellular glutathione. Asmis & Begley (2003), however, reported that oxLDL–mediated decrease in mitochondrial membrane potential contributed to macrophage lysis.

1.6.4 ROS–mediated damage to cells

Gieseg *et al.* (2010b) proposed that in macrophage cells which express high levels of NOX or NOX–activating receptor(s), oxLDL–induced ROS production and release overtakes the slower mitochondrial destabilisation and caspase–dependent cell death. It is likely that in phagocytic cells such as macrophages, the magnitude of oxidative stress produced in response to the binding and internalisation of oxLDL is the distinguishing parameter between apoptotic and necrotic cell death. During high cellular ROS production and/or reduced intracellular antioxidant defence (e.g. glutathione or ascorbate), the cellular ATP-producing and apoptotic machineries will become oxidised (Gieseg *et al.*, 2010a,b). This will result in a failure of apoptosis and lead to secondary necrosis. The most prominent feature of this hypothesis is the magnitude and rapidness of the oxidative stress. This model has been demonstrated experimentally by Troyano *et al.* (2003), who showed that during intensified H_2O_2–mediated oxidative stress, cell death by apoptosis was switched to necrosis.

Associated with the magnitude of the oxidative stress is the timing of ROS release. Presumably, a longer (chronic) time-frame due to a slower activation of cytotoxic mechanisms would allow for a more controlled shut-down of the cellular processes and liquidation of the cell *via* apoptosis. Importantly, during the conditions of slow sub-toxic ROS release, cellular compensatory mechanisms, like the up-regulation of GSH or superoxide dismutase (SOD) enzymes allow sufficient time for the antioxidant capacity of the cell to increase and deactivate ROS (Sagara *et al.*, 1998). It is also possible that during the chronic oxLDL-induced cell death ROS does not play the primary cytotoxic role and other responses like mitochondrial and lysosomal destabilisation, as well as ER stress, become the ultimate causes of cellular death. However, in the conditions of acute toxicity, cellular antioxidant defense like GSH and other dismutating enzymes become overwhelmed and damaged beyond repair, leading to the oxidation of the key cellular enzymes and uncontrolled necrotic death.

1.6.5 Cellular defence against oxidative stress

Cellular antioxidant defence system plays a very important role in maintaining the redox balance and combating oxidative stress. In macrophages these defences include antioxidant enzymes that catalyse the conversion of reactive species into benign molecules (such as catalase, superoxide dismutase, superoxide reductase and peroxidise enzymes) and low molecular weight molecules that scavenge oxidants (such as GSH, ascorbate, α-tocopherol and urate) (Stocker & Keaney, 2004). Another defence mechanism involves sequestration of pro-oxidants such as transition metal ions by proteins (for example, transferrins, metalloproteins and albumin) and repair systems that repair oxidised compounds or remove the damaged proteins (such as thioredoxin, methionine sulphoxide reductase and ubiquitination) (Stocker & Keaney, 2004). GSH in the cytoplasm plays an important role in the ROS–induced cellular death. Reduced GSH/oxidised GSSG ratio is the primary redox sensor of the cell and an important defense machanism against oxidant flux (Dröge, 2001; Valko *et al.*, 2007). This was observed by Yang *et al.* (2012) in HMDM treated with HOCl, where the cellular death followed the loss of GSH. The role of intracellular GSH in the oxLDL–mediated macrophage death has also been well documented. The loss of cellular GSH through various inhibitors or derivatising agents increased the cells' sensitivity to oxLDL cytotoxicity while up-regulation of GSH had been shown to decrease toxicity (Bea, 2003; Cho *et al.*, 1999; Gotoh *et al.*, 1993; Shen & Sevanian, 2001).

1.6.5.1 Protective role of the extracellular environment

There is some evidence that the extracellular environment at atherosclerotic sites plays a protective role against the oxLDL–induced cellular damage and death (Gieseg *et al.*, 2009). Human serum has been described as the source of a variety of ROS scavenging molecules and enzymes (Stocker & Keaney, 2004). The small antioxidant molecules in human serum like uric acid, GSH and bilirubin compete with the cellular protein for oxidising power of the released ROS and any other source of oxidative stress. Serum albumin has been proposed as an antioxidant "sink" (Roche *et al.*, 2008). Serum HDL could contribute to the efflux of oxLDL from cells (Zanotti *et al.*, 2012) as well as having some direct antioxidant effect *via* an HDL-associated paraoxonase enzyme (Graham *et al.*, 1997). The composition of extracellular environment in the atherosclerotic plaque is unclear. It is evident from the published studies that the atherosclerotic plaques contain both oxidised and reduced forms of α-tocopherol (α-TocH), ascorbate, albumin and other molecules (Carpenter *et al.*, 1995; Gieseg *et al.*, 2009; Shchepetkina, 2008). Generally, the inclusion of serum into the incubation mix varies in the published reports (Asmis & Wintergerst, 1998; Harris *et al.*, 2006; Terasaka *et al.*, 2007), which makes it difficult to compare the experimental results. Although the standardisation of laboratory procedures is not a viable option for a variety of reasons, consistent reporting of the methodology is necessary for a successful comparison. This issue will be further discussed in chapter 6.

1.7 7,8-Dihydroneopterin: origins, biochemistry and role in atherosclerosis

7,8-Dihydroneopterin is the product of the inflammatory activation of human macrophage cells. As mentioned earlier, many studies have used 7,8-NP and, especially, its oxidised counterpart neopterin, as markers of macrophage activation and oxidative stress in chronic and acute inflammatory diseases (Berdowska & Zwirska-Korczala, 2001; Firth *et al.*, 2008b; Sucher *et al.*, 2010). Due to the link between neopterin and atherosclerotic plaque instability (Adachi *et al.*, 2007), it is of both scientific and clinical interest to unravel the mechanisms of 7,8-NP–mediated action during the macrophage–oxLDL interaction in the context of CVD.

1.7.1 7,8-NP production

7,8-dihydroneopterin is synthesised by the truncated biopterin pathway of primate and human cells of myelocytic lineage, i.e. monocytes/macrophages, dendritic cells, monocyte-like cell lines; and, to a lesser extent, fibroblasts, endothelial cells and kidney cells (Andert *et al.*, 1992; Henderson *et al.*, 1991; Weiss *et al.*, 1999; Werner *et al.*, 1989, 1991; Werner-Felmayer *et al.*, 1990, 1993, 1995; Wirleitner *et al.*, 2002). Two enzymes are involved in the process, GTP cyclohydrolase-I (GCH-I) and a "non-specific" phosphatase, the description of which probably reflects the ubiquity of the performed reaction (Fuchs *et al.*, 2009). In the first step of the 7,8-NP biosynthesis, GCH-I converts guanosine-5'-triphosphate (GTP) into dihydroneopterin triphosphate (fig. 1.5) (Walter *et al.*, 2001).

During normal biopterin synthesis, the next step would be the elimination of inorganic triphosphate by the enzyme 6-pyruvoyl-tetrahydropterin synthase (PTS), followed by the processing into tetrahydrobiopterin by sepiapterin reductase (SR) (Walter *et al.*, 2001). Interestingly, this pathway is altered in human and primate cells of myelocytic origin. These cells lack a PTS activity due to the alternative splicing of the PTS mRNA (Leitner *et al.*, 2003). Thus, in the absence of functional PTS protein, dihydroneopterin triphosphate accumulates and gives rise to 7,8-NP after a phosphatase-mediated cleavage (Leitner *et al.*, 2003). Neopterin is a product of 7,8-NP oxidation and the reactions that yield neopterin will be discussed in the next section.
The major stimulant for 7,8-NP production is an inflammatory cytokine interferon-γ (IFN-γ). IFN-γ is released from Th1 and natural killer cells during innate and adaptive immune responses (Huber *et al.*, 1984; Schoedon *et al.*, 1986). Thus, 7,8-NP production reflects a multi-cellular cooperation between immuno-competent cells. To date, only IFN-γ has been shown to significantly induce the activity of GCH-I enzyme and, therefore, 7,8-NP production (Henderson *et al.*, 1991; Huber *et al.*, 1984). With the exception of tumour necrosis factor-α (TNF-α) and bacterial lipopolysaccharide (LPS) which have been shown to synergistically enhance IFN-γ–induced neopterin production, IFN-γ remains indispensable for this process in cell culture (Henderson *et al.*, 1991; Weiss *et al.*, 1999). *In vivo*, however, the elevated serum neopterin levels have been found in the absence of functional IFN-γ (Sghiri *et al.*, 2005). Elevated neopterin levels were found in the plasma of patients with a rare condition - the syndrome of Mendelian susceptibility to mycobacterial disease, which is characterised by deeply impaired or absent IFN-γ signaling (Sghiri *et al.*, 2005). Sghiri

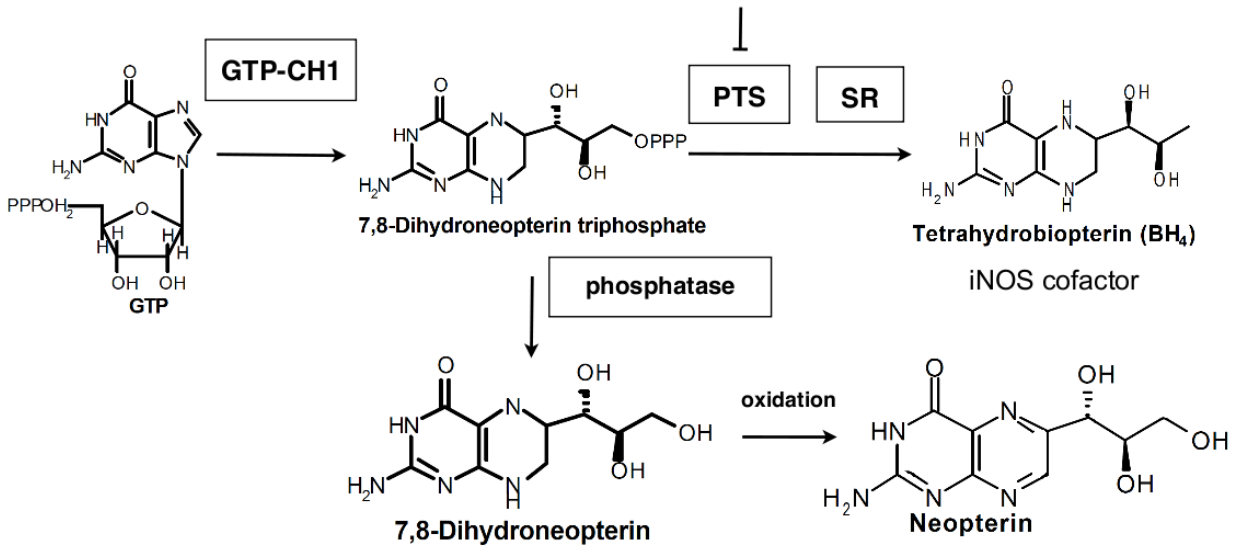

Figure 1.5: 7,8-NP biosynthesis and metabolism pathway
During 7,8-NP synthesis in human macrophages, GTP cyclohydrolase-1 (GTP-CH1) converts GTP into 7,8-dihydroneopterin triphosphate, which accumulates due to deficient 6-pyruvoyl-tetrahydropterin synthase (PTS) enzyme. Subsequently, phosphate groups are removed by phosphatase to 7,8-dihydroneopterin which could be oxidised to neopterin. Adopted from Fuchs *et al.* (2009) and Leitner *et al.* (2003).

et al. (2005) suggested that other stimuli apart from IFN-γ induced neopterin synthesis *in vivo*. Therefore, it remains to be seen whether stimuli other than IFN-γ or disease-associated ligands like bacterial LPS are able to induce 7,8-NP production.

1.7.2 Clinical utility

Neopterin is routinely used as a marker of adverse immune system activation in the screening of donor blood in Austria due to its stability and ease of detection (Hönlinger *et al.*, 2008; Murr *et al.*, 2005). A stable ratio of 7,8-NP to neopterin for arterial blood (2:1) and for venous blood (3:1) have been reported *in vivo*, which makes both compounds useful markers of inflammatory cell activation (Fuchs *et al.*, 1989; Weiss *et al.*, 1992). Clinical studies have demonstrated a strong correlation between neopterin levels in body fluids and the severity, progression, and outcome of infectious and inflammatory diseases. The literature suggests that high neopterin concentration in serum and urine is a reliable indicator of the severity of viral (including HIV-1), bacterial, protozoic, parasitic and fungal infections (reviewed in Berdowska & Zwirska-Korczala (2001); Fuchs *et al.* (2009); Hoffmann *et al.* (2003); Sucher *et al.* (2010)). For example, Denz *et al.* (1990) concluded that neopterin could prove to be a

useful parameter for distinguishing between viral and bacterial origins of infection (in combination with other markers). The authors noted that the patients with bacterial infections had significantly lower urinary neopterin concentrations than patients with viral pneumonia, although it rose after 5 days of illness (Denz *et al.*, 1990). In contrast to the bacterial infection, neopterin became elevated before the specific antibodies were formed during viral infections, serving as a distinguishing parameter in diagnosis (Denz *et al.*, 1990). Correlations between neopterin levels and the state of disease were also reported for rheumatoid arthritis, insulin-dependent diabetes mellitus, systemic lupus erythematosus, multiple sclerosis, coeliac disease, cancer and rheumatic fever (Hoffmann *et al.*, 2003; Reibnegger *et al.*, 1991). Potentially, an improved understanding of the biological role(s) of 7,8-NP will aid in the interpretation of the clinical results of the blood screening in the context of the multiple aforementioned pathologies.

The normal baseline level for neopterin in healthy subjects is 5.2 ± 2.7 nM in blood and 100-200 μmol/mol creatinine in urine (Wachter *et al.*, 1989) or 6.7 ± 1.5 nM in blood (Murr *et al.*, 2005). For 7,8-NP the reported normal measurements vary between ∼5.8 nM (Flavall *et al.*, 2008) and ∼18 nM (Genet, 2011). However, these levels are significantly elevated during disease. Weiss *et al.* (1992) reported 15-25 nmol/L of total neopterin in cancer patients with 7,8-NP concentration being twice as high as neopterin concentration. Weiss *et al.* (1992) reported that highly elevated leveld of neopterin (109-1679 nmol/L) post mortem; these varied depending on the site of sampling. Flavall *et al.* (2008) reported an average of approximately 40 nM total neopterin in the plasma of septicaemia patients and approximately 68 nmol/L was observed in the plasma of coronary heart disease patients undergoing angioplasy (Genet, 2011).

Elevation of neopterin levels during cardiovascular disease probably reflects the Th1-type immune response activation. A comprehensive review by Fuchs *et al.* (2009) addresses many underlying mechanisms and the prognostic utility of neopterin as a marker of acute CVD progression. Briefly, neopterin levels in plasma have been reported to correlate with the progression of cerebrovascular and peripheral artery atherosclerosis, carotid artery atherosclerosis, coronary atheromatous disease and its complications, such as acute coronary syndrome, and acute myocardial infarction (Fuchs *et al.*, 2009). Moreover, two large studies by Ray *et al.* (2007) and Kaski *et al.* (2008) identified the prognostic value of neopterin as an independent predictor

of adverse cardiac events.

It is likely that in disease, neopterin and its reduced form 7,8-NP in the circulation originate and diffuse out from the sites of inflammation as proposed by (Firth *et al.*, 2008b). Firth *et al.* (2008b) detected neopterin levels in pus of septicemia patients up to 100 times higher than those reported in plasma (1.28 μM vs. 10 nM). Furthermore, Gieseg *et al.* (2008) observed 2.2 nmoles neopterin per gram of tissue in some sections of an atherosclerotic plaque (2.2 μM if 1 g = 1 mL). Given such high availability inside the inflammatory sites, neopterin and 7,8-NP are likely to not only serve as a potential laboratory marker for an IFN-γ–mediated immune response, but they are also likely to exert biochemical and physiological functions in the course of host-defense interactions. These functions are of significant clinical and scientific interest.

1.7.3 Biochemistry and potential physiological roles of 7,8-NP

7,8-Dihydroneopterin (IUPAC: 2-amino-6-[(1S,2R)-1,2,3-trihydroxypropyl]-7,8- dihydropteridin-4(3H)-one) is an aromatic heterocyclic pteridine that has reducing properties. It is structurally related to the flavins (flavin-adenine dinucleotide (FAD), flavin mononucleotide (FMN)), to nicotinamide dinucleotides (NAD, NADP), acetyl coenzyme A, biotin and many other pyrimidine-containing enzyme cofactors and biologically active molecules. 7,8-NP can be readily oxidised by a range of electrophiles to form either neopterin or 7,8-dihydroxanthopterin (7,8-DXP) (fig. 1.6). Neopterin is produced by the oxidation of the 7,8-NP pterin moiety by hypochlorous acid and acidic iodide. While the HOCl–mediated reaction is a physiological one, the 7,8-NP oxidation by acidic iodide has been used in the laboratory, enabling the detection of the compound (Widner *et al.*, 2000). Recently, a reaction of 7,8-NP with $^1O_2$ (singlet oxygen), that also produces neopterin has been characterised (Dántola *et al.*, 2007).

It is generally believed that 7,8-DXP is the product of 7,8-NP oxidation by oxygen–centered radicals (Widner *et al.*, 2000). 7,8-DXP is formed when 7,8-NP is exposed to oxygen in the air, or to H_2O_2, which abstracts the side chain (Dántola *et al.*, 2008a,b). 7,8-DXP dismutates to form xanthopterin at a relatively slow rate (Dántola *et al.*, 2008b). During oxidative stress, this reaction is likely to prevail over the neopterin-generation processes unless the oxidative stress is driven by HOCl. Unfortunately, the

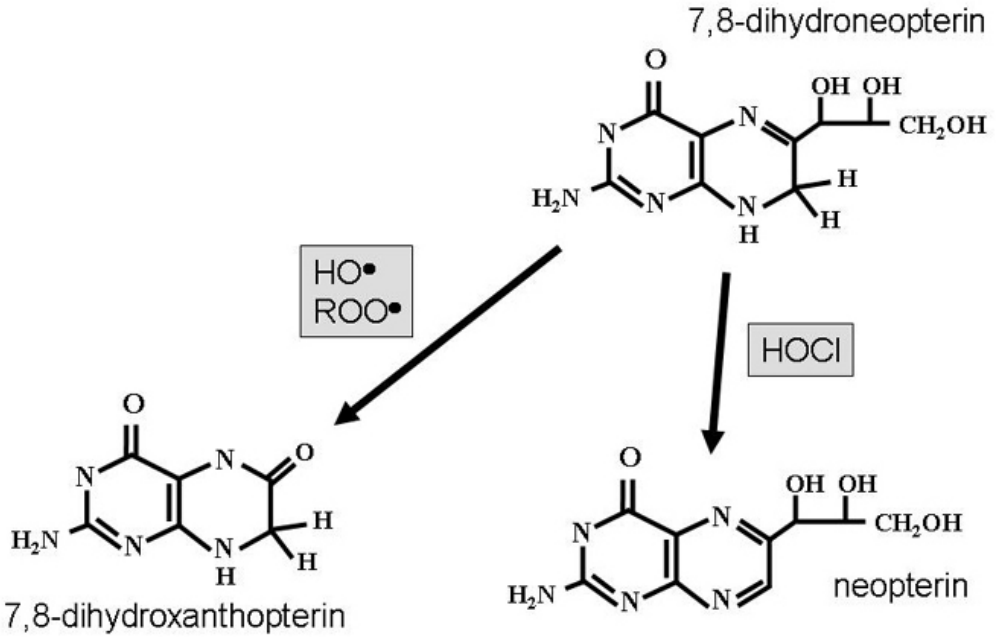

Figure 1.6: 7,8-NP oxidation
7,8-NP is oxidised to neopterin by the action of HOCl and to 7,8-dihydroxanthopterin by the action of peroxyl and hydroxyl radicals. Figure adopted from (Gieseg *et al.*, 2009).

clinical utility of 7,8-DXP for *in vivo* analysis of 7,8-NP oxidation is limited. In addition to the slow dismutation rate which would be difficult to predict in a complex system, xanthopterin is not exclusive to the 7,8-NP oxidation. Xanthopterin is an important oxidation product of other biologically important biopterins: dihydrobiopterin and dihydrofolic acid and thus would not solely reflect monocyte/macrophage immune activation (Vásquez-Vivar, 2009).

In contrast, neopterin is a good marker of immune system activation because it is derived only from 7,8-NP or dihydroneopterin triphosphate (Fuchs *et al.*, 2009), is stable in body fluids and has a relatively long half–life (90 min) that is only dependant on urinary excretion (Fuchs *et al.*, 1989). These properties make NP a good diagnistic tool for a variety of pathological conditions (reviewed in Berdowska & Zwirska-Korczala (2001), Fuchs *et al.* (2009) and Sucher *et al.* (2010)).

Known antioxidant properties of 7,8-NP

Reduced pterins, including 7,8-NP are known for their antioxidant properties (Rezk *et al.*, 2003). 7,8-NP has been shown to act as a weak scavenger of superoxide (rate constant 10^3 $M^{-1}s^{-1}$) and a strong scavenger of peroxyl radicals (10^7 $M^{-1}s^{-1}$) generated by 2,2'-azobis-2-methyl-propanimidamide, dihydrochloride (AAPH) (Oettl *et al.*, 1997, 2004a). 7,8-NP also reacts with hydrogen peroxide and chloramine-T (Weiss *et al.*, 1993). In addition, 7,8-NP inhibited peroxinitrite–driven reaction with a spin probe and the nitration of tyrosine (Oettl *et al.*, 2004a). These chemical properties of 7,8-NP are relevant in a biological context as discussed below.

7,8-NP is a very efficient inhibitor of AAPH–mediated oxidation of biological molecules as its reaction rate with peroxyl radical approaches the rate of diffusion, as demonstrated in a number of studies (Duggan *et al.*, 2001; Gieseg *et al.*, 1995, 2001a). 7,8-NP was shown to inhibit oxidation of linoleate by AAPH and diene formation on LDL during AAPH– and copper–mediated oxidation and α-tochopherol loss in LDL (Gieseg *et al.*, 1995). During the course of the reaction, the authors observed a formation of a neopterin-like fluorescent compound, along with conjugated diene formation (Gieseg *et al.*, 1995). 7,8-NP has also been shown to protect bovine serum albumin (BSA) from AAPH–mediated oxidation. The results of this study suggested the scavenging of the primary radical (Duggan *et al.*, 2001).

Another study by Gieseg *et al.* (2001a) found a reduction in erythrocyte haemolysis caused by HOCl, H_2O_2 and AAPH treatments. The degree of protection varied from complete protection in the presence of AAPH, to about 40% in the presence of H_2O_2 (Gieseg *et al.*, 2001a). 7,8-NP reacted directly with the three oxidants, forming neopterin in the reaction with HOCl and, predominantly, 7,8-DXP in the reactions with AAPH and H_2O_2 (<5% NP formed). The authors also reported 7,8-NP–mediated protection against the lipid hydroperoxide formation and protein oxidation (Gieseg *et al.*, 2001a). Further studies confirmed the ability of 7,8-NP to inhibit/slow down protein hydroxide formation and lipid peroxide formation on LDL, mediated by HMDM and THP-1 cells (Firth *et al.*, 2008a). In these conditions, (the presence of LDL and cells) 7,8-NP was oxidised primarily to 7,8-DXP. In summary, this literature suggests that 7,8-NP may act as an antioxidant *in vivo*, conveying protection against reactive oxygen species.

Effect of 7,8-NP on cell viability and survival

Over the years, the Gieseg laboratory has performed a number of studies aimed at assessing whether 7,8-NP antioxidant capacity is maintained in a more complex cellular system. It had been demonstrated that protein and thiol oxidation in U937 cells exposed to the peroxyl radical generator AAPH were also inhibited by 7,8-NP (Duggan *et al.*, 2002). This process was studied further to reveal that 7,8-NP inhibited the cytotoxic effect of oxLDL on U937 cell line by protecting the intracellular GSH, which was lost in response to oxLDL (Baird *et al.*, 2005). The lack of effect of 7,8-NP supplementation on oxLDL-mediated GSH loss or cytotoxicity to THP-1 was, thus, unclear but may relate to the mode of oxidative stress that each of the cell lines experiences upon oxLDL treatment, as suggested by the disparity in the GSH loss kinetics (Baird *et al.*, 2005).

While these experiments confirmed the protective effect of 7,8-NP, another set of studies found 7,8-NP to be pro-apoptotic. At high concentrations and/or in other cell lines 7,8-NP has been found to induce apoptotic cell death. Schobersberger *et al.* (1996) reported that 100 μM of both 7,8-NP and neopterin induced 17% and 13% apoptosis in rat alveolar epithelial cell line L2. At 5 mM (but not at 1 mM) 7,8-NP also caused apoptosis in Jurkat T lymphocytes (Wirleitner *et al.*, 1998). This 7,8-NP-mediated cell death was significantly blocked by an antioxidant pyrrolidine dithiocarbamate, suggesting a role for a redox-sensitive signal transduction pathway (Wirleitner *et al.*, 1998). In a study by Enzinger *et al.* (2002), reduced 7,8-NP led to an increase in apoptotic cells in rat pheochromocytoma cell line PC12 at a concentration of 5 mM but no such effect was observed at 1 mM 7,8-NP or neopterin. Cells incubated with 5 mM 7,8-NP showed an activation of the MAPK and to a lesser degree JUN/SAP kinase. Antioxidants (catalase, superoxide dismutase) partially suppressed pteridine-induced apoptosis, suggesting the involvement of reactive oxygen intermediates. Speth *et al.* (2000) also advocated for ROS involvement in 7,8-NP–mediated apoptosis in astrocytes and neurons. As suggested by Wirleitner *et al.* (2001), the overproduction of radicals caused by high levels of 7,8-dihydroneopterin may be responsible for the pro-apoptotic effects observed in these cell cultures.

In contrast to the above, Bratslavska *et al.* (2007) showed that neither neopterin nor 7,8-NP had any effect on the cellular viability of Hep-2. In Gieseg's laboratory no negative effect of 7,8-NP (up to 0.3 mM) on cellular viability of human monocyte-derived macrophages, THP-1 or U937 cell lines has been observed. The described

discrepancies may be determined by the tolerance of different cell lines to perturbations of the intracellular redox balance.

Effect of neopterin on NOX activity in phagocytes

While 7,8-NP has been predominantly thought of as an antioxidant, neopterin has been shown to play a specific role in the stimulation of the phagocytic ROS–producing NADPH oxidase. A range of authors suggested and demonstrated neopterin-dependant regulation of NOX—, xanthine oxidase– and myeloperoxidase–dependent oxidative burst (Kojima *et al.*, 1992, 1993; Nathan, 1986; Oettl *et al.*, 1997; Razumovitch *et al.*, 2004). Some of these studies were performed on isolated enzymes, while others were carried out on neutrophil and macrophage cell cultures. The results varied with Oettl *et al.* (1997) showing that 20 μM neopterin almost completely inhibited the conversion of xanthine into uric acid by xanthine oxidase, while others observed only a slight reduction of the formation of superoxide radicals by xanthine/xanthine oxidase system in the presence of 370 μM of neopterin (Kojima *et al.*, 1992). Yet in the same study neopterin significantly diminished superoxide in phorbol-12-myristate-13-acetate (PMA)–stimulated macrophages (Kojima *et al.*, 1992). The latter result was further expanded with subsequent work, showing neopterin as a competitive inhibitor of PMA–stimulated superoxide production in rat macrophage (whole cell system) and in solubilised membranes (cell free system) (Kojima *et al.*, 1993).

The macrophage cell may be significantly different from other phagocytes, such as the neutrophil, in this area. Contrary to the described results, Razumovitch and co-workers observed that in neutrophils neopterin increased the formation of ROS detected by luminol chemiluminescence system (non-MPO associated) (Razumovitch *et al.*, 2004). Yet in the MPO/H_2O_2/luminol system the authors observed a sharp drop of chemiluminescence signal after the addition of neopterin. Through a series of inhibitor studies, the authors attributed this effect to the decrease in superoxide and hydrogen peroxide. In their earlier publication the authors reported that NP induced chemiluminescence in adherent and/or cells generating ROS in the presence of luminol but not lucigenin (Razumovitch *et al.*, 2003). The authors speculated that in neutrophils, neopterin is able to induce the short-term generation of singlet oxygen, hydroxyl radicals, and nitrogen oxide (II) by an NADPH-oxidase–independent mechanism, possibly MPO (Razumovitch *et al.*, 2003). A recent paper by some of the same authors investigated the influence of neopterin and 7,8-NP on MPO activity (Petukh *et al.*, 2009). Neopterin–mediated increase in the chemiluminescence of neutrophils

was confirmed, but no additional mechanistic detail was proposed (Petukh *et al.*, 2009). The only study assessing the effect of 7,8-NP on the MPO activity (Petukh *et al.*, 2009) was inconclusive, as the authors reported "inhibition" of NOX–induced ROS without controlling for the scavenger activity of 7,8-NP.

Neopterin is not just involved in the regulation of ROS–generating enzymes in phagocytic neutrophils and macrophages. A correlation of neopterin release and ROS–generating and phagocytic potential has been reported (Nathan (1986)). This may be partly dependent on neopterin's ability to enhance ROS cytotoxicity (Murr *et al.*, 1994; Weiss *et al.*, 1993) and its regulation of pro-inflammatory signaling molecules, as neopterin has been associated with NF-κB and TNF-α (Hoffmann & Schobersberger, 2004; Hoffmann *et al.*, 1996, 1998; Schroecksnadel *et al.*, 2010). Thus, the majority of the evidence described above and in the literature points towards anti-inflammatory and antioxidant properties of 7,8-NP, whereas neopterin may be implicated in the propagation of inflammatory response.

1.8 Research programme

A number of studies to date have shown that 7,8-NP protects cells of myelocytic origin from the cytotoxic effects of oxLDL, yet the mechanism(s) of this protection are poorly understood (Baird *et al.*, 2005; Gieseg *et al.*, 2001b, 2010a). While the antioxidant capacity of 7,8-NP is predicted from the available literature and the assessment of the 7,8-NP chemical structure, its inhibitory effect on the oxLDL uptake is not obvious from examining the biochemical properties of 7,8-NP. This thesis will investigate how the two capacities of 7,8-NP may contribute to its protective effect towards HMDM cells treated with oxLDL. In particular, this thesis aims to establish which of the two biological activities of 7,8-NP is the primary mechanism for this protection against acute cell death: the antioxidant or the uptake-regulatory capacity.

In order to achieve this goal, chapter 3 will establish the factors that influence the acute oxLDL–induced cytotoxicity to HMDM *in vitro*. Chapter 4 will focus on the antioxidant activity of 7,8-NP during oxLDL-mediated HMDM cell death, and will allude to the sources of the oxidative stress that contribute to the process. Finally, chapter 5 will investigate the effect and potential mechanisms of 7,8-NP on the oxLDL uptake by the HMDM. It will also evaluate the significance of this process in the con-

text of acute cell death. Chapter 6 will address problems that arose during this thesis, and will investigate the effect of cell culture factors on HMDM cell death.

2

Materials & methods

2.1 Reagents, media and buffers

2.1.1 Reagents

All reagents used were of analytical grade or better. All solutions were prepared with de-ionised water purified with Milli-Q ultrafiltration system (Millipore, Massachusetts, USA). This is referred to as nano-pure water.

β-Mercaptoethanol	Sigma Chemical Co., MO, USA
3-[4,5-Dimethylthiazol-2-yl]-2,5 -diphenyl-tetrazolium bromide (MTT)	Sigma-Aldrich Co. LLC, New Zealand
5,5'-Dithio-bis(2-nitrobenzoic acid) (DTNB)	Sigma-Aldrich Co. LLC, New Zealand
7,8-Dihydroneopterin (7,8-NP)	Schircks Laboratory, Switzerland
7,8-Dihydroxanthopterin (7,8-DXP)	Schircks Laboratory, Switzerland
Acetic acid (glacial)	Scharlau Chemie S.A., Barcelona, Spain
Acetonitrile (ACN)	J.T. Baker, NJ, USA
Agarose	AppliChem Gmbh, Germany
Ammonium chloride (NH_4Cl)	May & Baker Ltd, Dagenham, England
Ammonium phosphate dibasic ($AmPO_4$)	Sigma-Aldrich Co. LLC, New Zealand
Ascorbic acid	Sigma Chemical Co., MO, USA
Butylated hydroxytoluene (BHT)	Sigma-Aldrich Co. LLC, New Zealand

Bovine serum albumin (BSA)	Sigma-Aldrich Co. LLC, New Zealand
Bromophenol blue	Sigma-Aldrich Co. LLC, New Zealand
Chelex–100 resin	Bio-Rad Laboratories, California, USA
Ethylene-diamine-tetra-acetic acid (EDTA)	Sigma-Aldrich Co. LLC, New Zealand
Diethyl ether	BDH Lab Supplies Ltd, Poole, England
Diethyl pyrocarbonate (DEPC)	Sigma-Aldrich Co. LLC, New Zealand
Dimethyl sufloxide (DMSO)	BDH Lab Supplies Ltd, Poole, England
Dithiothreitol	Invitrogen, Life Sciences, New Zealand
Ethanol	BDH Lab Supplies Ltd, Poole, England
Glutathione (GSH), 99% reduced	Sigma-Aldrich Co. LLC, New Zealand
Glycerol	Sigma-Aldrich Co. LLC, New Zealand
Granulocyte-macrophage colony-stimulating factor (GM-CSF) as Leukine® sargamostim	Bayer Healthcare Pharma. LLC Seattle, USA
HEPES buffer	Sigma-Aldrich Co. LLC, New Zealand
Hexane, 95% pure	Ajax Chemicals, Auburn, Australia
Hydrochloric acid (HCl)	BDH Lab Supplies, Poole, England
Iodine (I)	BDH Lab Supplies Ltd, Poole, England
Isopropanol	BDH Lab Supplies Ltd, Poole, England
Lymphoprep®	Axis-Shield PoC AS, Oslo, Norway
Methanol	Merck, Darmstadt, Germany
MOPS buffer	Sigma Chemical Co., MO, USA
Neopterin	Schircks Laboratory, Switzerland
Phosphoric acid	Sigma-Aldrich Co. LLC, New Zealand
Ponceau S	Sigma Chemical Co., MO, USA
Potassium bicarbonate ($KHCO_3$)	May & Baker Ltd, Dagenham, England
Potassium chloride (KCl)	Merck, Darmstadt, Germany

Potassium hydroxide (KOH)	Merck, Darmstadt, Germany
Potassium iodide (KI)	May & Baker Ltd, Dagenham, England
Sodium bicarbonate ($NaHCO_3$)	May & Baker Ltd, Dagenham, England
Sodium chloride (NaCl)	BDH Lab Supplies Ltd, Poole, England
Sodium dihydrogen orthophosphate (NaH_2PO_4)	Merck, Darmstadt, Germany
Sodium dodecyl sulphate (SDS)	Sigma-Aldrich Co. LLC, New Zealand
Sodium hydroxide (NaOH)	Merck, Darmstadt, Germany
Sodium hypochlorite (NaOCl)	Clorogene Supplies, Petone, New Zealand
Thimerosal	Sigma Chemical Co., MO, USA
Trichloroacetic acid (TCA)	Merck, Darmstadt, Germany
Tris buffer	Roche Diagnostics Corp., Indianopolis, USA
Trizol®	Invitrogen, Life Sciences, New Zealand
Trypan blue solution (0.4%)	Sigma-Aldrich Co. LLC, New Zealand
Tween 20®	Sigma-Aldrich Co. LLC, New Zealand

2.1.2 Media

Penicillin/Streptomycin solution, 1000 U of Penicillin G & 1000 μg of Streptomycin/mL	Invitrogen, Life Technologies, New Zealand
Roswell Park Memorial Institute 1640:	
- RPMI 1640 media, with phenol red	Sigma-Aldrich Co. LLC, New Zealand
- RPMI 1640 media, without phenol red	Sigma-Aldrich Co. LLC, New Zealand

2.1.3 General solutions and buffers

Phosphate buffered saline

Phosphate buffered saline (PBS) solution contained 150 mM sodium chloride (NaCl), 10 mM sodium dihydrogen orthophosphate (NaH_2PO_4) at pH 7.4, and was prepared the following way. Fifty milliliters of 3M NaCl, 40 mL of 250 mM NaH_2PO_4, pH 7.4, was mixed with 910 mL of nano-pure water. PBS required for cell culture work was vacuum filtered through a 0.45 μm membrane (Phenomenex) and autoclaved for 15 minutes at 121 °C and 15 psi. The pH of the solution remained stable for 3 months.

7,8-Dihydroneopterin solution

A 2 mM 7,8-dihydroneopterin (7,8-NP) stock solution was prepared by dissolving 7,8-NP powder (Schircks Laboratories, Switzerland) in the appropriate medium in a 50 mL tube via a 10 minute ultrasonication. The solution was sterilised by filtration through a 0.22 μm PES® syringe filter (Membrane Solutions, USA) before being added to cells. The solution was kept on ice at all times and used within 1 hour of preparation.

Apocynin solution

Apocynin stock solution was perpared by dissolving apocynin powder (Sigma-Aldrich) in PBS to give a concentration of 1 mM before filter–sterilising it through a 0.22 μm PES® syringe filter. The solution was stored at –4 °C and used within one month.

2.2 Cell culture technique

2.2.1 Aseptic practice

All cell culture work was performed under aseptic conditions in a Class II biological safety cabinet (Clyde-Apex BH 200). All instruments and equipment were either sterile–bought plastic-ware (Falcon, Bector Dickinson & Co.; Nunc, Nalge Nunc International; Greiner, Greiner Bio-one, Neuburg, Germany) or had been sterilised by autoclaving (15 min, 121 °C, 15 psi). All media and solutions added to cells were sterilised by autoclaving or by filtration through a 0.22 μm membrane filter (Membrane Solutions, USA). The cells were kept at 37 °C in a humidified atmosphere calibrated to 5% carbon dioxide : 95% air (Sunnyo Electric Co. Ltd, Japan). All items were

sprayed with 70% ethanol (diluted in distilled water) before being placed in the Class II cabinet.

2.2.2 Cell culture medium and experimental conditions

A number of media with different chemical compositions are used for cell culture. In the present study, Roswell Park Memorial Institute 1640 complete medium (RPMI-1640) was used to culture HMDM cells and U937 monocyte-like cell line (U937). RPMI-1640 is a complex medium containing an extensive list of essential amino-acids, minerals and glucose (Freshney, 2010).

Roswell Park Memorial Institute 1640 Medium

Powdered RPMI-1640 was prepared according to the manufacturer's instructions. After the RPMI-1640 powder was dissolved in nano-pure water, sodium bicarbonate ($NaHCO_3$) was added and the pH adjusted to 7.4 by the addition of 11.4 M hydrochloric acid (HCl). The medium was sterilised by filtration through a 0.22 μm Millex®-GP_{50} filter (Sartorius AG, Goettingen, Germany) and a peristaltic pump (CP-600, Life Technologies, Maryland, USA) into sterile 500 mL bottles and stored at 4 °C.

Cell culture experimental conditions

Unless stated otherwise, all the experiments with HMDM cells were performed in RPMI-1640 with or without phenol red, supplemented with 100 U/mL penicillin, 100 μg/mL streptomycin and 10% (v/v) human serum. This solution is referred to as whole medium. Unless stated otherwise, experiments were performed in the original plates the cells were seeded into. Fresh medium was added to wells at least 30 minutes prior to the addition of other constituents to allow cells to adapt to the change of conditions.

The total volume of incubation medium during any treatment was 1 mL for HMDM cells that were grown in 12 well plates, and 0.4 mL for HMDM cells grown in 48-well plates. For comparison, surface to volume ratio in these conditions was 3.9 for 12 well and 2.5 for 48 well plates. All experiments with U937 cells were performed in 12 well suspension plates (Cellstar®), coated (unless stated otherwise) with 8 μL of 50 mg/mL bovine serum albumin (Sigma-Aldrich) followed by air-drying, in the

total experimental volume of 1 mL. The cells were counted and re-suspended in the experimental medium before an experiment.

2.2.3 Preparation of human serum for macrophage cell culture

The procedure of plasma and cell isolation from unlinked haemochromatosis patient blood was carried out under ethics approval CTY/98/07/069 granted by the Upper South (B) Regional Ethics Committee.

Unlinked (no donor identification) blood from consenting patients was collected into 450 mL "dry" bags (no anticoagulant included, Fresenius Kabi, Homburg, Germany) by the New Zealand Blood Bank (Riccarton branch, Christchurch). The blood bag was left in the vertical position in the polypropylene container at room temperature for 2 hours to allow the formation of a blood clot and then transferred to 4 °C overnight to provide sufficient time for the serum to separate from the clot.

The following day the bag was opened under aseptic conditions and the serum was collected into 50 mL centrifuge tubes using a 20 mL syringe attached to a mixing cannula. The tubes were centrifuged at 1000 *g* for 15 minutes (Heraeus Multifuge-SR, BioStrategy, New Zealand) to pellet the remaining blood erythrocytes, and the clear serum was carefully transferred to new 50 mL centrifuge tubes. If the resulting serum appeared to contain any red blood cells, the centrifugation step was repeated. Human serum was heat–inactivated at the beginning of the project, but this step was omitted after the review of the literature (Biochrom AG, 2010; Hyclone®, 1996; Leshem *et al.*, 1999) and discussions with S.P. Gieseg and B. Hock. Further investigation showed that the heat inactivation treatment had no effect on the cell growth and activity (chapter 6). Throughout the following chapters, the abbreviation HIHS is used for heat–inactivated human serum, whereas HS denotes non-heat inactivated human serum. The serum was heat inactivated in a water bath at 56 °C for 30 minutes before being cooled to 4 °C. It was then transferred to a $--20$ °C followed by a $--80$ °C freezer for long term storage. The serum was stored for up to 6 months, but generally used within 3 months from preparation.

2.2.4 Preparation of foetal bovine serum for U937 cell culture

Foetal bovine serum (Invitrogen, New Zealand) was used directly without any manipulation.

2.2.5 Cell culture of human monocyte-derived macrophage cells

Isolation of Monocytes

Unlinked blood from clinically healthy consenting haemochromatosis patients was collected into 500 ml autologous bag by the NZ Blood Service (Compoflex® containing the anticoagulant citrate-phophate-dextrose-adenine (CPDA-1)). It was kept at 4 °C for up to 18 hours before processing, although the cells were usually prepared immediately.

The monocytes were isolated using the method described by Amit (2008) and Yang (2009). The procedure involved taking a bag of whole blood, gently inverting it 10 times to distribute the cells evenly, aseptically placing into the CII cabinet and cutting it open. The blood was transferred from the bag into 50 mL centrifuge tubes and centrifuged at 1000 *g* with slow deceleration for 30 minutes at room temperature.

The centrifugation step produced a layer of erythrocytes at the bottom of the tube, topped with a white layer of leukocytes ("buffy coat") and overlaid with plasma. The leukocyte layer was removed using a mixing cannula attached to a 10 mL syringe, pooled and mixed with the equal amount of PBS by thorough inversion. The mixture was underlaid with 15 mL of Lymphoprep® (lymphoprep) using a mixing cannula attached to a 20 mL syringe. After centrifugation at room temperature at 1000 *g* for 30 minutes with slow acceleration/deceleration, a white layer of monocytes/lymphocytes was visible approximately halfway down the centrifuge tube surrounded by clear plasma and lymphoprep layers (fig. 2.1).
The top layer was aspirated, leaving 2 cm of solution above the layer of leukocytes. The cells were transferred into a new 50 mL tube by a syringe attached to a mixing cannula. The cells were thoroughly re-suspended and evenly divided between the appropriate number of tubes, each containing no more than 15 mL of solution. Each tube was topped up with PBS, inverted to mix and centrifuged at 500 *g* for 15 min. After the centrifugation, the supernatant was aspirated, cell pellets tapped to re-suspend the leukocytes and topped up with PBS. The tubes were inverted to mix and centrifuged at 500 *g* for 10 min. The procedure was performed once more, after which the cells were re-suspended in the RPMI-1640 containing pen/strep, counted on the haemocytometer, plated into 6 well suspension plates (Cellstar) at $5x10^6$ cells/mL and incubated at 37 °C at 5% CO2 for 40 hours in the absence of serum.

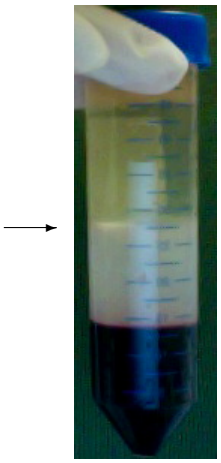

Figure 2.1: Monocyte isolation: typical preparation. Leukocytes separated from erythrocytes after the gradient centrifugation with Lymphoprep®. The arrow indicates the layer of leukocytes.

Plating and culture of HMDM cells

The cells were incubated in the absence of serum for approximately 40 hours during which time the T-cells died due to serum deprivation, the platelets attached to the surface of the plate while the monocytes remained viable in suspension (Bennett *et al.*, 1992; Yang, 2009). The well content was aspirated, pooled, centrifuged at 500 *g* for 15 min at room temperature and re-suspended in RPMI-1640, supplemented with 10% (v/v) human serum at a concentration required for seeding ($1x10^6$ and $5x10^6$) cells/mL. A pulse of granulocyte macrophage colony stimulating factor (GM-CSF) administered as Leukine® (Bayer, USA) was added to the cell suspension to drive the differentiation of monocytes into macrophages. The final GM-CSF concentration was either 25 or 50 ng/mL of cell suspension. The cells were plated (seeded) at $5x10^6$ cells/well into 12 well plates (adherent, Nunc) and $1x10^6$ cells/mL into 48 well plates (adherent, Cellstar). Information on comparative growth in different plate types and seeding densities could be found in chapter 6. RPMI-1640 containing 10% human serum was renewed every 3 to 4 days and experiments were conducted once the majority of monocytes had matured to macrophages, usually 11-16 days after the seeding of cells.

Monitoring of HMDM culture

HMDM cell morphology was examined every 3–4 days through an inverted microscope Leica DM IL (Leica Microsystems, Wetzlar, Germany), equipped with a camera and connected to the computer featuring Leica Application Suite Version 2.8.1 (Build:

1554). A satisfactory preparation of cells showed signs of differentiation, such as loss of monocytic morphology by over 10% of the well population, by the 4^{th} day after seeding. By the 7^{th}–8^{th} day the well surface was dominated by round poached-egg-like cells with a few elongated cells. At least 70% surface coverage was considered acceptable.

2.2.6 Culture of U937 cells

The U937 monocyte-like cell line was originally developed from the pleural fluid of a 37-year old man with generalised lymphoma (Sundstrom & Nilsson, 1976). The U937 cells used in this research were a gift from the Haematology Research Laboratory of the Christchurch School of Medicine, University of Otago.

To revive U937 stock after storage in liquid nitrogen, a 1 mL storage vial containing 20x10^6 cells/mL in dimethyl sulfoxide (DMSO) freezing medium was defrosted in a 37 °C water bath until almost completely thawed. This cell suspension was poured into 30 mL of RPMI-1640 and centrifuged at 500 g for 5 minutes to separate the freezing medium from the cells. The cell pellet was re-suspended in 10 mL of RPMI-1640 and initially cultured in 25 cm^3 tissue culture flask (Falcon, BD, USA).

The cells were considered fit for experimental work when the cells reached an appropriate cell density (approximately 1x10^6 cells/mL) and their division rate normalized (doubling time 92-96 hours (Sundstrom & Nilsson, 1976) followed by 20-48 hours in subsequent passages (Harris & Ralph, 1985)). The "healthy" U937 cells displayed a spherical morphology with small grain-like protrusions on the membrane (cytoplasmic granules) and without extensive clustering. The U937 cells were propagated in culture for up to 6 months (passages 15-50 were used for experiments). Cell density was maintained at 0.3-1.5x10^6 cells/mL by passaging in Cellstar® 150 cm^3 tissue culture flasks (Greiner Bio-one, Germany) every 2-4 days.

After a 6 month period a new stock of the original U937 cells was brought up to avoid any artefacts associated with prolonged cell culture, such as genetic drift and mycoplasma contamination.

2.3 Isolation and oxidation of low-density lipoprotein

2.3.1 Collection and preparation of donor plasma

Collection of blood from donors and preparation of LDL from plasma were carried out under ethics approval CTY/98/07/069 granted by the Upper South (B) Regional Ethics Committee. The blood was collected by venipuncture from consenting healthy male and female donors after an overnight fast. In total, 200 mL of blood was collected from each donor into 50 mL tubes containing 0.5 mL of 100 mg/mL ethylene-diamine-tetra-acetic acid (EDTA). The tubes were centrifuged for 20 minutes at 4 °C in a swing-out rotor at 2350 *g*. Plasma was transferred to 50 mL round bottomed centrifuge tubes and centrifuged for 30 minutes at 11,000 *g* with slow acceleration/deceleration in a fixed angle rotor to remove any remaining cells. Plasma from all donors (5-6 at a time) was pooled to minimise the inter-individual variation (Gieseg & Esterbauer (1994)). The plasma was stored in 30-32 mL aliquots at -80 °C for a maximum of 6 months.

2.3.2 Lipoprotein isolation by gradient centrifugation

The method used for LDL isolation involved creating a gradient that separated the lipoproteins during centrifugation. A modification of a single vertical spin method first reported by Chung *et al.* (1980), as described in Gieseg & Esterbauer (1994), was used in this research. Briefly, 30 mL of EDTA-plasma was thawed under running cold water and centrifuged at 2000 *g* for 10 minutes at 4 °C to remove any precipitated fibrinogen. The supernatant was decanted into a beaker, placed on ice and the plasma density was adjusted to a density of 1.3 by gradual addition of 381.6 mg of solid KBr per mL of plasma. The solution was flushed with argon, capped with parafilm and gently stirred to dissolve KBr. Eight milliliters of deoxygenated 1 mg/mL EDTA (pH 7.4) solution was added to each of the 8 ultracentrifugation tubes (OptiSeal™, Beckman Coulter, USA) before under-laying with 4 mL (or less) of KBr-plasma using a long luer-fitting needle attached to a 5 ml syringe. The tubes were transferred to Beckman Near Vertical Ti-65 rotor and centrifuged at 341,705 *g* (60,000 rpm) for 2 hours at 4 °C using slow acceleration/deceleration in Optima™ L-90K Preparative Ultracentrifuge (Beckman Coulter, Inc., Fullerton, California). A yellow band of LDL (fig. 2.2) in the density range of 1.019 g/mL to 1.063 g/mL was collected using a syringe attached to 90 °C–bent needle.

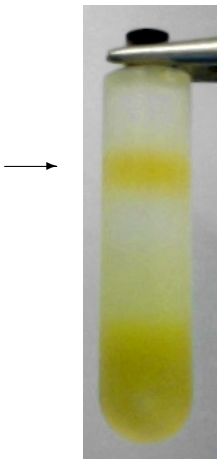

Figure 2.2: LDL isolation: typical preparation.
LDL isolation from plasma via density centrifugation. Arrow indicates the LDL band.

.

2.3.3 LDL concentration

LDL was concentrated using Amicon® Ultra-15 membrane filter tubes (Millipore, USA). Prior to use, the tubes were rinsed gently with nano-pure water and centrifuged with PBS for 2 min at 2500 g to wash. After use, the tubes were rinsed with nano-pure water, centrifuged for 2 min with nano-pure water, then for 1 min with 100% ethanol and stored in the fridge in 50% ethanol.

LDL was placed into Amicon® centrifuge tubes, topped up with PBS and centrifuged at 2500 g, fast acceleration/deceleration, at 4 °C for 30 min. The procedure was repeated three more times in order to eliminate the remaining EDTA from the LDL. The purified LDL was concentrated by centrifugation for 10-20 minutes using the same procedure. The centrifugation time varied depending on the original concentration of the LDL. It was adjusted to give a final concentration of approximately 10 mg of LDL per mL of solution (total mass), which was determined as described below.

2.3.4 Determination of LDL concentration

LDL concentration was determined as a function of total cholesterol level which was measured by an enzymatic reaction using a CHOL® kit (Roche Diagnostics, Germany).

The total cholesterol content of LDL was determined by incubating 10 μL of LDL with 1 mL of the CHOL® reagent at room temperature. After incubation for 10 min,

the absorbance was measured at 500 nm against a CHOL® reagent blank. LDL concentration was calculated from this absorbance, based on an estimate of LDL having a molecular weight of 2500 kDa and cholesterol accounting for 31.69% of the LDL particle by weight (Gieseg & Esterbauer, 1994). The value used for LDL concentration used in this thesis is in total mass rather than the mass of the apolipoprotein B-100 protein moiety as used by some other research teams (Asmis & Begley, 2003; Hardwick *et al.*, 1996). The value of total LDL mass relates to the mass apolipoprotein B-100 (protein component of the molecule) as 5:1 (Gieseg & Esterbauer, 1994).

2.3.5 Preparation of oxidised LDL

Preparation of dialysis tubing for LDL oxidation

The dry dialysis membrane tubing (Medical International Ltd, London, England) with 14.4 mm flat width and 14,000 D molecular weight cut off was pre-treated before use. The dialysis tubing was cut into 25 cm sections and boiled in a glass beaker containing 5% (w/v) $NaHCO_3$ and 1 mM EDTA for 20 minutes. The tubes were washed with nano-pure water and boiled again in a glass beaker containing nano-pure water. After 20 minutes, the tubes were washed thoroughly with nano-pure water and stored in solution of water:ethanol (50:50, v/v) at 4 °C. The tubes were rinsed thoroughly with water and PBS prior to being used for LDL oxidation.

LDL oxidation

The method for LDL oxidation was adapted from that described by Gerry *et al.* (2008). Concentrated LDL was mixed with 500 μM copper chloride ($CuCl_2$), placed into double–knotted dialysis tubing and secured with a zip clip and a knot. The dialysis tubing was placed in a bottle of 37 °C PBS also containing 500 μM $CuCl_2$. The volume of PBS was adjusted according to the amount of LDL to constitute 1L of buffer per 10 mg of LDL protein.

The loosely capped bottle containing the dialysis bag was placed on an orbital shaker (Bioline, Edwards Instrument Company, Australia) at 37 °C for 24 hours during which the yellow LDL solution turned colourless with a tinge of cloudy white. Following this, the dialysis bag was transferred into 1L of 4 °C PBS containing a quarter of a teaspoon of washed Chelex-100 resin and a magnetic flea. The solution was left stirring for 2 hours at 4 °C after which the dialysis bag was transferred to a new bottle of Chelex-containing PBS and stirred for 2 more hours. It was left overnight in the

third change of PBS–Chelex.

Approximately 20 hours after the start of dialysis, oxidized low-density lipoprotein (oxLDL) was taken out of the dialysis bag, filter-sterilised through a 0.22 μm membrane filter in the CII cabinet and stored at 4 °C. The oxLDL solution was used within one month from the time of oxidation.

2.4 Biochemical analysis

2.4.1 Determination of protein concentration

Protein concentration was determined using the bicincronic acid (BCA) protein analysis kit (Pierce, Rockford, USA). This method combines the reduction of Cu^{2+} to Cu^{+} by protein in an alkaline medium (by oxidation of peptide bonds and reducing protein groups, e.g. Cys-SH, Tyr-OH, Trp) coupled with the colorimetric detection of Cu^{+} using a reagent containing bicincronic acid.

Sample preparation: The working reagent for BCA assay was freshly prepared by mixing Reagent A (containing: sodium carbonate, sodium bicarbonate, BCA and sodium tartrate in 0.1 M sodium hydroxide) and Reagent B of the kit (4% $CuSO_4.5H_2O$) in a 50:1 ratio. Fifty microliters of diluted sample were mixed with 1 mL of working reagent and incubated at 60 °C for 30 minutes with gentle shaking. The reaction was stopped by placing samples on ice. Protein concentration was determined from the absorbance reading at 562 nm and compared to the standard curve prepared by the incubation of known concentrations of BSA (0-250 μg/mL) in 1 mL of working reagent. The absorbance is nearly linear over 20-2000 μg/mL range (Pierce Instruction manual).

2.4.2 Cell viability assays

One of the common ways to assess cytotoxicity is the loss of cellular viability following a treatment with the toxic compound (Berridge *et al.*, 1996). The reduction of MTT is widely accepted as a reliable method to measure cell number and, therefore, can be used to assess cell viability (Mosmann, 1983; Shen & Sevanian, 2001). The dehydrogenase enzymes of metabolising cells generate reducing agents such as nicotinamide adenine dinucleotide (NADH) and NADPH, which reduce yellow tetrazolium salt to purple formazan. The resulting formazan crystals can be solubilised and quantified

spectrophotometrically (Mosmann, 1983). The colour intensity provides a measure of both the number of cells and their metabolic activity.

Another widely used method is Trypan blue exclusion assay, where the cell's ability to exclude a coloured dye (trypan blue) serves as a measure of membrane integrity, and, thus, cell survival.

MTT reduction assay

MTT stock solution was prepared by dissolving the MTT powder (Sigma-Aldrich Co., St. Louis, USA) in RPMI-1640 without phenol red, to give the final concentration of 5 mg/mL. The stock solution was filter-sterilised through a 0.22 μm syringe filter and stored at –20 °C in the dark. For the cellular viability assay the stock solution was further diluted in pre-warmed RPMI-1640 without phenol red to give a 0.5 mg/mL final MTT concentration.

Sample preparation: The adherent HMDM cells were washed briefly with room temperature PBS and incubated with 0.6 mL of the MTT solution at 37 °C in the dark for approximately 30 minutes. The time varied depending on the overall metabolic activity of the control cells and plating density. The non-adherent cells were treated in RPMI-1640 without phenol red, and the 5 mg/mL MTT reagent was added directly to the treatment wells to give a final concentration of 0.5 mg/mL. The plates were incubated in the dark at 37 °C for 1 to 2 hours to allow for sufficient formazan development.
The formazan crystals were solubilised by the addition of an equal volume of 10% (w/v) sodium dodecyl sulphate (SDS) (in 0.01 M HCl) into each well and thorough mixing. The absorbance was recorded at 570 nm against a blank containing the reagents only.

PrestoBlue™ cell viability assay

PrestoBlue™ (Molecular Probes, Invitrogen, Life Technologies Inc., New Zealand) is a viability assay based on the cellular capacity to reduce a non-fluorescent compound to fluorescent resazurin. Similarly to MTT, PrestoBlue™ is reduced by the metabolically active cells, thus providing a measure of cell number and viability.

Sample preparation. The adherent HMDM cells were rinsed with warm PBS and incubated with 200 μL of 10% PrestoBlue^{TM} solution in RPMI-1640 without phenol red. The cells were incubated at 37 °C for 50-90 minutes to allow for resazurin reduction and fluorescence development. One hundred μL of the supernatant was transferred into black polystyrene microplates (Nunc), for fluorescence to be recorded. The data was collected on a POLARstar Galaxy plate reader (Alphatech Systems Ltd., Auckland, New Zealand) equipped for fluorescence detection. The settings were: 544 nm excitation and 590 nm emission wavelengths, gain: 4, number of cycles: 1, number of flashes: 20 and positioning delay: 1. Software used was FLUOstar Control.

Trypan blue exclusion assay

The suspension cells were mixed by pipetting and 100 μL was collected into a separate tube. Trypan blue dye was added at the appropriate ratio (usually 1:1 for U937 cells and 1:10 for monocytes) and the stained/unstained cells were counted using a hemocytometer.

2.4.3 HPLC methods

High performance liquid chromatography (HPLC) is an analytical technique that enables the separation and quantification of specific compounds from a complex mixture based on their chemical properties. The HPLC system used in this study (Shimadzu Corporation, Japan) consisted of LC20AD pump with on-line degasser, SIL-20AC temperature controlled autosampler, CT0-20 column oven, RF10AXL fluorescence detector and SPD-M20A photodiode array (PDA) detector. Peaks were integrated and peak areas were determined using LCsolution software (Shimadzu Corporation, Japan).

Pterin assay

Neopterin has high native fluorescence which can be used for its detection. 7,8-NP was quantified after its oxidation to the fluorescent neopterin (labelled "total neopterin") as a function of (total neopterin – neopterin). The assumption of the method is that all 7,8-NP is converted to neopterin and that only a small amount of the compound is lost during the preparation of oxidised sample (Flavall *et al.*, 2008).

HPLC set-up: The HPLC set-up was Synergi 4μ Hydro-RP 80A, 250 x 4.6 mm, 5 μm column (Phenomenex, USA) as a stationary phase; 20 mM ammonium phosphate ($AmPO_4$) with 5% acetonitrile (ACN), pH 6 in mobile phase, pumped at a flow rate of 1 mL/min. The oven was set at 35 °C. The elutant was monitored using a fluorescence detector set at 353 nm excitation and 438 nm emission wavelengths, 1.5 response, x4 gain, and medium sensitivity. Pure D-neopterin (Schircks Laboratory, Switzerland) dissolved in the mobile phase was used as a standard. Due to the difficulty in the resolution of neopterin and acetonitrile (ACN) peaks on the chromatogram, an ACN standard was also run.

Sample preparation: Adherent cells were washed with cold PBS twice, incubated with 300 μL of ice-cold acetonitrile:water (1:1) for 1 minute with the plate lid on. Cell lysate was collected by scraping and aliquoted into 1.5 mL centrifuge tubes. After sonification at 4 °C for 1 min, 10 μL of the sample were collected for protein analysis. The remainder of the sample was centrifuged at 10,300 g at 4 °C for 5 min and 50 μL of the supernatant was taken for neopterin analysis (10 μL injection volume). For the total pterin analysis, another 100 μL of the supernatant was further incubated with 20 μL of acidic iodide (5.4% I_2 : 10.8% KI in 1 M HCl) at room temperature in the dark for 15 minutes. After that, 20 μL of 0.6 M ascorbic acid was added to neutralise the excess acidic iodide. The samples were further centrifuged for 5 minutes as described above. Ten μL of supernatant were injected into the HPLC. The neopterin-containing sample was stable for at least 3 days when stored at –20 °C (Laich *et al.*, 2002).

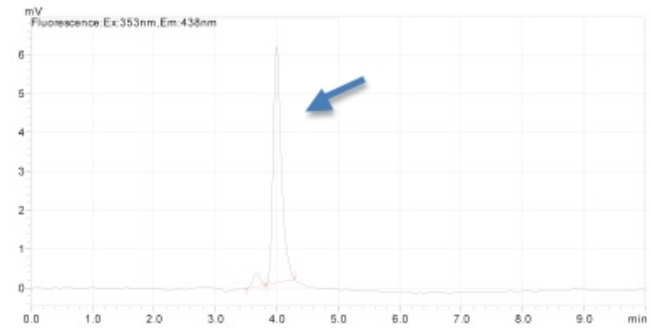

(a) 25 nM neopterin standard

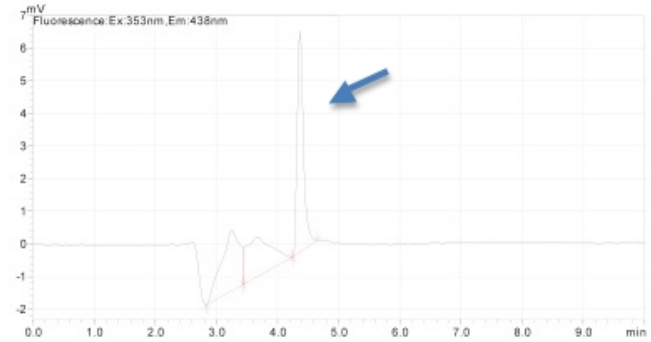

(b) 65 nM 7,8-NP oxidised to neopterin

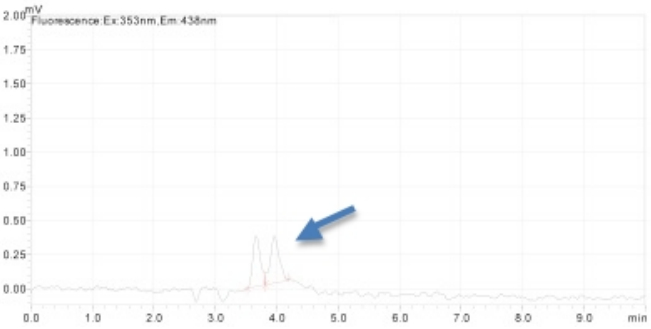

(c) Cells control neoptern

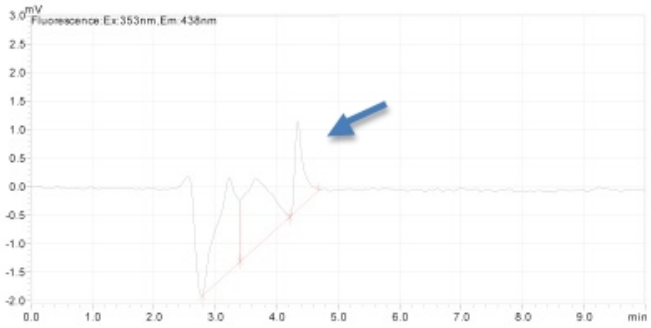

(d) Cells control oxidised

Figure 2.3: Typical HPLC chromatograms after Pterin assay.
The standards and samples were prepared as outlined in 2.4.3. The arrows indicate neopterin peak. The author is grateful to Tejraj Janmale for the images.

7-Ketocholesterol assay

Oxysterols are a product of advanced cholesterol oxidation. 7KC is an oxysterol that received significant attention in the literature due to its reported cytotoxicity (Jessup *et al.*, 2002; Vejux & Lizard, 2009). It is found in copper and AAPH-oxidised LDL and is also abundant in atherosclerotic plaques (Brown *et al.*, 1996; Garcia-Cruset *et al.*, 2001). Oxysterols absorb at a range of wavelengths; 234 nm wavelength was used in this study for 7KC. The method was adopted from Kritharides *et al.* (1993) and Brown *et al.* (1997).

Sample preparation: Adherent cells were washed twice with cold PBS and incubated with 500 μL of 0.2 M sodium hydroxide (NaOH), 0.2 mg/mL butylated hydroxytoluene (BHT) and 2 mg/mL EDTA for 8 min on ice and harvested by scraping. After a two minute sonification, 10 μL of each sample were taken for protein analysis. Three hundred μL of a sample were transferred into glass culture tubes with a screw-on cap. Protein precipitation was induced by the addition of 0.5 mL ice-cold ethanol followed by a brief vortex. Upon the addition of 5 mL of hexane, the samples were vortexed for 60 sec to allow the migration of the lipid–soluble 7KC into the hexane layer. These samples were stored at $-80\,^{\circ}$C.

On the day of the analysis, the samples were vortexed again and centrifuged at 200 g for 10 minutes at $4\,^{\circ}$C to ensure phase separation. Two millilitres of the top layer were transferred to tapered glass evaporation tubes and dried under nitrogen gas. The residue was re-solubilised in ACN:isopropyl alcohol (IPA) in the ratio 4:5 and 20 μL was injected into the HPLC.

Alkaline hydrolysis of cholesterol esters: Alkaline hydrolysis with potassium hydroxide (KOH) allows the conversion of 7KC esters into free 7KC and their detection by the same method. OxLDL and cell lysate were prepared as described above, but evaporation tubes were substituted for the glass culture tubes with a screw top. After evaporation, saponification was carried out as described by Brown *et al.* (1997). Two and a half mL of diethyl ether and 2 mL of 20% (w/v) KOH solution in methanol were added to the residue, vortexed to mix, flushed with argon and incubated on ice for 3 hours with 30 second vortex every 30 minutes. The hydrolysis was stopped by adding 2 mL of 20% (v/v) acetic acid followed by a 30 second vortex. Two and a half mL of hexane were added to the tubes, vortexed for 1 minute allowing the transfer of all hydrophobic material into the hexane-ether layer, and centrifuged at 200 g for 10

minutes at 4 °C. Eighty percent of the top layer was collected into evaporation tubes, dried under nitrogen, re-solubilised in ACN/IPA as described above and injected into the HPLC.

HPLC set-up: HPLC set-up for 7KC assay consisted of a stationary phase, Phenosphere C18, 250 x 6.60 mm, 5 μm column (Phenomenex, USA) and mobile phase, comprising acetonitrile/isopropanol/water in the ratio of 44:54:2. The column was maintained at 35 °C with a flow rate of 1 mL/min. The PDA detector was set to 190 nm starting wavelength and 370 nm end wavelength; 234nm was used for analysis. The sampling was done at 1.5625 Hz; slit width was 1.2 nm. 7KC standard (Seraloids Inc, USA) was dissolved in the mobile phase to 10 μM. The injection volume for standard and samples was 20 μL.

Reduced glutathione assay

Intracellular GSH is an important intracellular antioxidant and can be used as a marker of oxidative damage in cells (Valko *et al.*, 2007). Monobromobimane, 1H,7H-pyrazolo(1,2-ǒ3B1)pyrazole-1,7-dione, 3-(bromomethyl)-2,5,6-trimethyl- (MBB) is a cell permeable fluorescent compound that binds -SH groups, specifically that of GSH. MBB-GSH adduct can be detected by the HPLC (Cotgreave & Moldeus, 1986). Because of the tight binding between GSH and MBB, the BCA protein assay of an MBB–treated sample would yield an artificially lower protein concentration as –SH groups would be unavailable for the BCA reagent binding. Therefore, the results of the GSH assay in this thesis are presented without correction for cellular protein concentration.

Sample preparation: All procedures were carried out under minimum light conditions as MBB is light-sensitive. MBB (Fluka Analytical, Switzerland) was dissolved in ACN to a 40 mM stock solution, which could be stored in the dark at 4 °C for up to 2 weeks. Commercially available reduced GSH served as a standard. It was dissolved in PBS to 0, 5 and 10 μM on the day of the analysis. For cell lysate preparation, incubation medium was aspirated from adherent cells and 400 μL of PBS, 9 μL of 0.1 NaOH (to adjust pH to 8.0), and 10 μL of 40 mM MBB were added to each well in this order. After 20 minute incubation in the dark at room temperature, 20 μL of 100% trichloroacetic acid (TCA) was added and swirled to precipitate the protein and lyse the cells. The cell lysate was harvested by scraping and centrifuged at 13,000

g, 4 °C for 5 min. Five or ten microliters of the supernatant was injected into the HPLC.

HPLC set-up: The stationary phase consisted of Phenosphere reverse phase C-18 150x4.6 mm, 5 μm column (Phenomenex, Auckland, New Zealand) heated to 35 °C. The mobile phase, flowing at a rate of 1.5 mL/min, was set as a gradient flow. For the first 10 minutes, the mobile phase was a mixture of 10% acetonitrile and 90% of 0.25% acetic acid. The concentration of ACN was raised to 100% during the 11^{th} minute of a sample run and kept at that for the following 5 minutes. The post-run washing step started at minute 16 and was comprised of 95% of ACN and 5% of 0.25% acetic acid. The GSH–MBB adduct was detected by a fluorescence detector with the following settings: 394 nm excitation and 480 nm emission wavelengths, 1.5 response, x4 gain and medium sensitivity.

2.5 Western blot technique

2.5.1 Solutions for Western blot

Cracker buffer: To prepare the cracker buffer, 125 mM Tris-HCl, pH 6.8 (adjusted with concentrated HCl), 1% SDS (w/v), 20% glycerol (w/v) and 0.1% bromophenol blue (w/v) were mixed in nano-pure water. Prior to use, 2% (v/v) of β–mercaptoethanol (β–MEtOH) and 0.5 mM EDTA was added to 1 mL of the above solution.

Lysis Buffer: The lysis buffer consisted of 40 mM HEPES, 50 mM NaCl, 1 mM EDTA, and 1 mM ethylene glycol-bis(2-aminoethylether)-N,N,N,N-tetraacetic acid (EGTA) in nanopure water, pH 7.4 (adjusted with 5 M NaOH) and stored at 4 °C. Protease inhibitor, reconstituted and frozen to the manufacturers recommendations (ProteaseMini, Roche Diagnostics), was defrosted and added to the lysis buffer on the day of sample collection.

MOPS buffer: A 10x stock solution of MOPS was prepared with 500 mM MOPS, 500 mM Tris base, 1% SDS (w/v), and 10 mM EDTA in water with pH adjusted to 7.7. This was diluted with water to 1x concentration before use.

Transfer buffer: The transfer buffer incorporated 25 mM Tris, 200 mM glycine and 20% methanol (v/v) in water and was stored at 4 °C. The transfer buffer was re-used once.

Tris-buffered saline: Tris-buffered saline (TBS) used for nitrocellulose membrane washing, consisted of 40 mM Tris-HCl, 150 mM NaCl at pH 7.5, 0.05% Tween20 (w/v) and 0.01% thimerosal (w/v) (contains Hg, toxic) dissolved in water.

TBSM: The membrane blocking solution (TBS-milk, TBSM) was 5% (w/v) of non-fat milk powder (Anchor, New Zealand) made in TBS. It was stored at 4 °C for up to one week.

Ponceau S stain: The Ponceau S stain consisted of 0.01% Ponceau S (w/v) in 5% acetic acid (v/v).

2.5.2 Antibodies

Antibodies were stored at 4 °C and added directly to the incubation solution. A table of antibodies and concentrations used is presented (table 2.3).

Table 2.3: List of antibodies used.

Agent	Raised in	Dilution	Medium	Inc. time	Supplier	Conj.	Poly/monoclonal
CD36	rabbit	1:1,000	1% TBSM	1.5h	Novus Biologicals	-	poly, aff. purified
anti-rabbit	goat	1:2,000	2% TBSM	1h	Novus Biologicals	HRP	-
β-actin	mouse	1:7,500	1% TBSM	1	Sigma Aldrich	-	monoclonal
anti-mouse	goat	1:7,500	2% TBSM	1.5	GE Healthcare	HRP	-
CD68	rabbit	1:500	1% TBSM	1	Novus Biologicals	-	monoclonal
p47phox	mouse	1:250	2% TBSM	1.5	Santa Cruz	-	monoclonal
anti-mouse	goat	1:750	2% TBSM	1	Santa Cruz	HRP	-

2.5.3 Sample preparation

Cell lysate preparation. HMDM samples for western blot were prepared the following way. All medium was aspirated from the wells and the adherent cells were washed twice with cold PBS. Two hundred μL of ice-cold lysis buffer containing protease inhibitor was added to each well. The cells were harvested by scraping and sonified for 1 minute to ensure complete lysis.

Plaque homogenization. Atherosclerotic plaques for analysis were supplied by the Department of Surgery, Christchurch Hospital. Consent was obtained from each patient for their plaques to be included in the research prior to surgery. Ethical approval for this research has been granted by the Upper South (A) Regional Ethics Committee, approval number CTY/01/04/036.

Plaques collected during carotid endarterectomy surgery were immediately transported to the Free Radical Biochemistry Laboratory on ice, snap frozen in liquid nitrogen and stored at –80 °C. The plaques were dissected into 3-5 mm sections longitudinally starting with the leading end and proceeding in the direction of blood flow. Each section was homogenized under liquid nitrogen using pestle and mortar and mixed with 3 mL of water containing 50 μL of 100 mg/mL EDTA (pH 7.4) and 20 μL of 20 mg/mL BHT (in methanol). The protein content of the samples was determined by BCA protein assay in order to achieve equal loading of protein onto the gel.

2.5.4 SDS-polyacrylamide gel electrophoresis

The required amount of sample (based on the protein concentration, commonly up to 200 μL) was aliquoted into 1.7 mL centrifuge tubes. One mL of –20 °C acetone was added to each tube and centrifuged at 15,000 *g*, at 0 °C for 10 min. The supernatant was discarded and the tubes were left in the fume hood for the remaining acetone to evaporate. The pellet was re-suspended in the cracker buffer containing 2% β–MEtOH to the final protein concentration 0.5-1 μg protein per μL. The samples were heated in a heating block at 95 °C for 3 minutes to denature the protein. This was followed by centrifugation for 5 minutes at 20,000 *g*. Five microlitres of pre-stained molecular weight marker mix (Fermentas International Inc, Ontario, Canada) and 5-25 μL/well (depending on required protein content) of samples were loaded into the gel wells. The samples were subjected to electrophoresis on a gradient polyacrylamide gel, (4-12% Bis-Tris Gel, Invitrogen, Carslband, CA, USA) in 1x MOPS buffer. The gel was run at 200 V after the dye front eluted from the wells.

2.5.5 Immunoblotting and visualisation

After SDS-PAGE, the proteins were transferred onto an nitrocellulose (NC) membrane (Invitrogen, USA, 0.45 μm pore size) over 10 h at 70 V in a tank transfer electrophoresis unit (TE22, Hoefer, USA) containing the transfer buffer. At the end

of the transfer, the NC membrane was taken out of the transfer cassette, rinsed with nano-pure water and stained with 0.01% Ponceau S stain for 1 minute to examine the transfer efficiency. Pink protein bands were visible with Ponceau S stain.

The following procedures were performed on a rocking platform mixer (Ratex Instruments, Australia). After a quick rinse with water, the membrane was blocked using 5% TBSM for 1.5 hours. The TBSM was changed every 30 minutes. Subsequently, the membrane was probed with rabbit polyclonal affinity purified antibody raised against human CD36 (NB400-145, Novus Biologicals Inc., USA) or mouse monoclonal antibody raised against β-actin (A5316, Sigma-Aldrich Chemical Co., USA) for 1.5 hours. The primary antibody against CD36 was diluted to 1:1,000 in 1% TBSM and against β-actin to 1:7,500 in 2% TBSM. The membrane was washed 3 times for 5 minutes in TBS followed by 1 hour incubation with the secondary antibody. The secondary antibody to anti-CD36 was a goat polyclonal anti-rabbit IgG, conjugated to HRP (NB730-H, Novus Biologicals Inc., USA) 1:2,000 dilution. β-Actin secondary antibody was anti-mouse IgG Peroxidase-linked NA931 (GE Healthcare, UK) diluted to 1:7,500 in 2% TBSM. This was followed by 5 of 5 minute washes in TBS and a brief rinse with water before visualisation. The re-probing of the membrane with β-actin antibody was done after the visualisation of the first desired protein. The membranes were kept in TBS at 4 °C until re-probing. Usually, the membrane had to be stripped off the anti-CD36 antibodies before probing it for β-actin. The membrane was incubated with stripping buffer (2% SDS, 50 M Tris, 100 μM β–MEtOH, pH 6.8, heated to 50 °C on a water bath) for 20 min, followed by 5 of 5 minute washes in TBS. The membrane was then directly incubated with the primary anti-β-actin antibody without blocking.

The chemiluminescence signal corresponding to the position of the hydrogen peroxidase (HRP)-conjugated secondary antibody was detected by incubating the membrane with Supersignal West Dura Chemiluminescence (TerumoScientific, USA) substrates, which were mixed at a ratio of 1:1. According to the manufacturer's instructions, the image data was recorded 2.5 minutes after the application of the visualisation HRP solution. The images were obtained at high resolution, without filter or light, using time-lapse auto-exposure setting on a Syngene Chemigenius-2 bioimaging system (USA). Exposure times varied for different antibodies – from a few seconds for the detection of β-actin to 3.5 minutes for CD36 detection. The images were analyzed for band intensity with GeneSnap (Syngene, USA) and ImageJ64 1.42q.

2.6 Fluorescent microscopy

2.6.1 Dihydroethidium probe

Dihydroethidium (DHE) bromide is a fluorescent probe widely used to detect superoxide anion $O_2^{\bullet-}$ production within cells. The precursor compound, DHE (dissolved in DMSO) is readily taken up by cells and is retained intracellularly after cleavage by esterases. Non-fluorescent DHE is oxidised to highly fluorescent ethidium through the reaction with $O_2^{\bullet-}$ (Kobzik *et al.*, 1990; Rothe & Valet, 1990), or, according to a more recent report, to 2-OH-hydroxyethidium (2-OH-HE) (Zhao *et al.*, 2005). Originally, DHE was reported to have a low affinity for hydrogen peroxide (Benov *et al.*, 1998; Bindokas *et al.*, 1996), yet later the specificity of DHE has been questioned (Tarpey, 2004), although some reports still favour its specificity when the right product is measured (Fernandes *et al.*, 2006; Zhao *et al.*, 2005). Despite this, DHE remains an effective tool for measuring the overall intracellular reactive oxygen species' burden (Fernandes *et al.*, 2006; Kobzik *et al.*, 1990; Tarpey, 2004).

2.6.2 Sample preparation and processing

HMDM cells were seeded at a concentration of 5 x 10^6 cells per 22 x 22 mm sterile glass cover slip in a 6 well plate. At the end of the experimental incubation, the cells were washed with PBS twice, after which a coverslip was lifted off the plate with a bent hypodermic needle and transferred to a clean 6 well tissue culture plate. DHE stock in DMSO (1 mM) was dissolved in PBS just before use to a concentration of 10 μM and kept in the dark. A hundred and fifty microliters of the 10 μM DHE solution was loaded on top of coverslips and the HMDM cells were incubated in a humidified incubator for 20 minutes in the dark. Excess probe solution was washed off with PBS (twice). Forty microlitres of PBS was placed on top of the glass slide and the coverslip was carefully lowered onto the glass slide with the cells facing down.

The cells grown on coverslips and stained with fluorescent probes were examined using a Zeiss AxioImager.M1 epifluorescent microscope (Carl Zeiss (NZ) Ltd, Wellington, New Zealand), equipped for differential interference contrast (DIC). A condenser was fitted with an HBO 100 W mercury vapour lamp. The cells were viewed using 20x and 40x Plan-NEOFLUAR objectives with numeric aperture of 0.5 and 0.75 respectively. The fluorescent filter used for DHE staining was a Zeiss filter set 00 for propidium iodide (PI). The images were captured using a Zeiss AxioCam HRc CCD camera with

AxioVision Rel. 4.5 image analysis software (1300 x 1030 pixel resolution). Densiometric quantification was done with ImageJ64 1.42q software. After data collection, the images were manipulated with Gimp version 2.6 used in conjunction with XQuartz 2.1.6 application to achieve the appropriate publication standard.

2.7 Flow cytometry

Analysis of intracellular processes was carried out by flow cytometry. This technique is used for a vast number of biomedical applications of quantitative analytical nature (Shapiro, 2003). Flow cytometry often operates on the same optical measurement as the fluorescent microscope but allows high sample throughput. An Accuri C6 flow cytometer (BD Biosciences, USA) was used to measure ethidium, propidium iodide and annexin V probe fluorescence.

Sample preparation: After an experimental treatment, HMDM cells were rinsed briefly with warm PBS and incubated with 130 μL *Accutase*™ (Millipore Australia Pty., New Zealand) for 20 min in the dark at 37 °C. Accutase™ facilitates the detachment of adherent cells from the bottom of the well (Simard *et al.*, 2008). *Accutase*™ solution contained: 1 x Accutase enzymes in Dulbecco's PBS (0.2 g/L KCl, 0.2 g/L KH_2PO_4, 8 g/L NaCl, and 1.15 g/L Na_2HPO_4, containing 0.5 mM EDTA·4Na and 3 mg/L Phenol Red (Millipore product description). After a 20 minute incubation, the plate was removed from the incubator, the cells in each well were pipetted 7-10 times to dislodge the detached cells and aliquoted into 1.5 mL tubes. For DHE measurements, 10 μM DHE was added directly to *Accutase*™ and analysed after detachment using the Accuri C6. For apoptosis/necrosis measurements, the samples were prepared according to the manufacturer's instructions (ApoAlert kit, BD Bioscience, USA) after detachment with *Accutase*™.

Data on HMDM was collected using the following settings: flow rate 55 μl/min, core size 30 μm and number of events: 10,000 into the gated area. The gate contained healthy HMDM cells as well as HMDM at the early stages of cell toxicity, and was determined experimentally. The lazer settings used were: 488 nm excitation wavelength and a range of emission filters including FL1 filter (533/30 nm) for FITC and FL3 (>670 nm) for PI and DHE. All data were collected and analysed using the cFlow Plus software (BD Biosciences).

2.8 Polymerase chain reaction

2.8.1 RNA isolation and purification

Ribonucleic acid (RNA) was extracted into TRIzol (Invitrogen, Life Sciences, New Zealand) according to the manufacturer's instructions. Briefly, 200 μL of TRIzol was added to each well after the medium was aspirated. The liquid was pipetted 10 times, accompanied by the scraping of the bottom of the well with the pipette tip (RNase/DNase-free pipette tips were from Maxymum Recovery^{TM}). Three wells were combined per treatment into a single 1.5 mL tube (Axygen Scientific, Inc, Union City, CA, USA). Each tube was incubated for 5 min at room temperature and frozen at –80 °C. The sample was processed for RNA isolation and cyclic DNA (cDNA) synthesis within 7 days.

For the RNA isolation, the samples were thawed at room temperature, topped up with chloroform (0.2 mL chloroform per 0.75 mL TRIzol), vortexed for 15 seconds, incubated for 15 minutes at room temperature and centrifuged for 15 minutes at 12,000 g and 4 °C. Three quarters of the aqueous phase were transferred into a new set of tubes and topped up with isopropanol (0.5 mL per 0.75 mL TRIzol in the initial sample). The tubes were inverted to mix, incubated for 10 minutes at room temperature and centrifuged at 12,000 g for 10 minutes at 4 °C. After centrifugation, the supernatant was carefully removed and the pellet was topped up with at least 1 mL 75% ethanol in diethyl-pyro-carbonate (DEPC)–treated water and re-suspended via vortexing. The samples were centrifuged at 7,500 g for 5 min at 4 °C.

To re-dissolve the RNA, the pellet was air dried at room temperature for approximately 30 minutes, re-dissolved in 20 μL DEPC-water, heated for 10 minutes at 55 °C and assessed for absorbtion at 260 nm using the Nano Drop (ND-1000 Spectrophotometer, BioLab). The RNA suitable for further processing had an absorbance reading above 1.8 on the 260/280 ration and a reading above 1.2 at 260/230 wavelengths ratio. The latter was lower than recommended (Nockengost, 2009), but the corresponding RNA was successfully converted into cDNA that specifically amplified by PCR. An absorbance of 1 unit at 260 nm corresponds to 40 μg of RNA per mL.

2.8.2 cDNA synthesis

All components of the qScript^{TM} Flex cDNA Synthesis Kit (Quanta Biosciences), except for the reverse transcriptase enzyme (RT), were thawed, mixed thoroughly and

centrifuged before use. Two microliters of Random Oligos (from the kit) and 2 μL of Random Primers (kit) per tube were made up into a master-mix and 4 μL of this solution was aliquoted into 200 μL PCR tubes. RNA was thawed and added to the tubes to give 950-990 μg RNA per tube. Each tube was topped up with Nuclease-free water (kit) to the final volume of 15 μL. The tubes were capped, vortexed gently, centrifuged for 5 seconds, incubated for 5 minutes at 65 °C in Mastercycler epgradient S (Eppendorf, Hamburg, Germany) and snap-chilled on ice.

During this time, a master-mix of 4 μL of 5x Reaction Mix (kit) and 1 μL of RT (kit) was prepared. Five μL of that was added to each RNA-containing tube with the exception of one, which was prepared in a similar fashion but did not contain RT (no RT control). The tubes were vortexed gently, centrifuged for 5 seconds and subjected to the following incubation treatment: 80 minutes at 42 °C followed by 5 minutes at 85 °C and held at 4 °C. After the final step, cDNA concentration was measured spectrophotometrically at 260 nm (Nanodrop). The final cDNA concentration was approximately 1000 ng/μL.

2.8.3 Real-time quantitative PCR

RT qPCR master mix was prepared using the following procedure. A 10 μL qPCR reaction consisted of 1 μL dNTP, 1 μL 10x PCR reaction buffer (Invitrogen), 0.3 μL Cyto9 probe, 0.05 μL of 5 U/μL *Platinum* TaQ polymerase (Invitrogen), 1 μL cDNA, 1 μL of 5 μM forward primer, 1 μL of 5 μM reverse primer topped with nano-pure water. The reaction master mix containing everything but the cDNA and the primers was prepared, vortexed and aliquoted into individual wells of a 48 well plate (dNature, New Zealand). Each primer pair was pre-mixed before addition to the wells. Primer pair mixes and the cDNA was added to the appropriate wells individually due to the issues with dimerisation of one primer pair. The PCR plate included a no RT control and a no template (no cDNA) control. The plates were sealed, centrifuged to remove bubbles and subjected to the thermal profile outlined in table 2.4. The amplification of the appropriate PCR products was judged by the product melting temperature.

Table 2.4: qPCR thermal profile.

Step	Temperature, °C	Time
Polymerase activation	95	2 min
PCR Cycling step 1	95	30 sec
PCR Cycling step 2	57	1 min
PCR Cycling step 3	72	1 min
Melt Curve step 1	95	15 sec
Melt Curve step 2	55	15 sec
Melt Curve step 3	95	15 sec

2.8.4 Agarose gel electrophoresis

PCR products were examined by electrophoresis on 1-2% agarose gel and visualised. The gels were prepared by melting agarose (AppliChem GmbH, Germany) in 1x TBE in the microwave, cooling the agarose solution to 50-60 °C and pouring into a gel-casting tray (Easy-CastTM Electrophoresis system, Owl separation systems, Portsmouth, NH, USA). The solidified gel was covered by 1x TBE. The samples were prepared in 0.7 mL tubes containing 2 μL of amplified sample and 2 μl of Loading Dye Solution (Fermentas International Inc., Burlington, Otario, Canada) and loaded into the wells. Five microlitres of 100bp GeneRuler^{TM} DNA ladder (Fermentas) was run as a molecular weight indicator. The gel was run at 100 V until the dye front had migrated approximately three quarters of the length of the gel. The sample bands were visualised under UV light (Bio-Rad Laboratories Pty Ltd, NSW, Australia), equipped with Quantity One 4.6.1 software.

2.9 Statistical analysis

Statistical analysis was performed using GraphPad Prism Version 5.0d for Mac OS X (GraphPad Software, San Diego, California, USA). All experiments, unless otherwise stated, were performed in triplicate and each data point was replicated at least thrice within an experiment. Unless stated otherwise, the results are displayed as mean ± SEM of mean values from **(A)** single experiment and **(B)** combined mean values from three separate experiments. Where experiments were performed as a repetition of the work done previously, a single experiment is presented (for example, figures 3.4 and 4.1).

Statistical significance of the results was tested using one- and two-factor analysis of variance (ANOVA), t-test with 95% confidence interval and linear regression. Where indicated, a paired t-test or repeated measures (RM)-ANOVA (identical to randomised block design) were conducted on the replicate data from combined experiments as indicated the figure captions (Motulsky, 2007). One specific test (fig. 6.10) was performed using linear mixed model function in R (R Core Team, 2012). One-factor ANOVA was followed by Dunnetts post test, Bonferroni post test or Turkey's multiple comparison test, where appropriate. A two-tailed t-test with 95% confidence interval was used when two sets of values were compared.

For quantitative factors (time and dose) regression lines were fitted using the least squares fit. Non-linear (quadratic and segmented linear) regression was employed if the response was not linear, and was carried out using the nonlinear regression functionality in Prism5. Comparison between treatments or of two models within a treatment was performed using extra sum-of squares F test in Prism5 (α=0.05). The type of statistical test used in each experiment is indicated in the figure caption. Statistical significance is denoted by *, $p < 0.05$, **, $p < 0.01$ and ***, $p < 0.001$.

3

OxLDL toxicity to human monocyte–derived macrophages

3.1 Introduction

Macrophage cell death from oxLDL is a key event in the development of the atherosclerotic plaque (Ball *et al.*, 1995; Lusis, 2000; Moore & Tabas, 2011). Since oxLDL–mediated cytotoxicity was described by Henriksen *et al.* (1979) and Hessler *et al.* (1979), the underlying mechanisms have been investigated extensively (Steinberg & Witztum, 2010). The present study will focus on modelling an aspect of this process in cell culture.

OxLDL is toxic to human macrophages *in vitro*, with both apoptosis and necrosis implicated in cell death (Asmis & Wintergerst, 1998; Gieseg *et al.*, 2010a; Hardwick *et al.*, 1996; Wintergerst *et al.*, 2000). Amongst many mechanisms proposed to govern oxLDL cytotoxicity, oxidative stress is very prominent (Galle *et al.*, 2006; Gieseg *et al.*, 2010b; Salvayre *et al.*, 2002). Intracellular glutathione/glutathione disulfide (GSH/GSSG) acts as a buffer preventing fluctuations of redox status that may upset intracellular homeostasis and lead to cell death. OxLDL has been shown to deplete intracellular GSH, inhibit glutathione reductase, and reduce the GSH/GSSG ratio (Wang *et al.*, 2006). Depletion of intracellular GSH enhanced oxLDL toxicity, while supplementation of intracellular GSH stores substantially diminished oxLDL toxicity (Amit, 2008; Gotoh *et al.*, 1993; Kinscherf *et al.*, 1998; Wang *et al.*, 2006).

GSH loss is proposed to be the consequence of increased ROS flux triggered by oxLDL (Gieseg *et al.*, 2010a). ROS generation in response to oxLDL has been demonstrated

in all major vascular cell types: SMCs (Higashi *et al.*, 2005; Hsieh *et al.*, 2001), ECs (Cho *et al.*, 1999; Zmijewski *et al.*, 2005) and macrophages (Asmis & Begley, 2003; Bae *et al.*, 2009; Gieseg *et al.*, 2010a; Lee *et al.*, 2010; Park *et al.*, 2009). Despite this wealth of research, very few studies have concentrated on the time–dependant activity of intracellular ROS formation. Thus, the understanding of the kinetics of ROS production by macrophages in response to oxLDL is incomplete. To address this, the research presented here aims to compare and contrast the kinetics of oxLDL–mediated HMDM cell viability loss, oxidative stress and damage and establish the time-frame for irreversible cellular damage.

In this thesis the terms "toxicity" and "cytotoxicity", which could be used rather broadly (Freshney, 2010), will refer to the loss of cellular viability in response to oxLDL and the ability of oxLDL to cause that loss. The investigation will focus on mechanisms of macrophage death upon acute exposure to toxic levels of oxLDL (but not chronic exposure as may be implicated in foam cell formation (Kruth, 2001)). A 24 hour acute toxicity experimental design will be adopted in order to simplify the complexity of the system for experimental purposes. HMDM cells cultured for two weeks will be treated with a toxic LC_{50} concentration of Cu-oxLDL for 24 hours. The term LC_{50} denotes a toxic concentration of oxLDL that is required to kill 50% of cells within 24 hours (Zhang *et al.*, 2006). This chapter will define the scope and basic characteristics of the experimental setting, such as toxic concentrations of oxLDL to HMDM cells and time-dependant kinetics of toxicity. These will be used to inform experimental design in subsequent chapters. A time-course of ROS production and subsequent oxidative damage will also be investigated, as the association between kinetics of toxicity and oxLDL–triggered oxidative stress have been largely overlooked in the literature. Overall, the results obtained in this chapter will lay the foundation for subsequent work by exploring important aspects of intracellular mechanisms of oxLDL toxicity to macrophages.

3.2 Results

3.2.1 OxLDL–induced cytotoxicity to HMDM is concentration and time dependant

The acute cytotoxicity of oxLDL to macrophages was examined by incubating HMDM cells with increasing concentrations of oxLDL in the whole medium (RPMI-1640 supplemented with 10% human serum and antibiotics as described in sec. 2.2.2). The toxicity was measured by the ability of viable cells to reduce MTT to formazan via the action of cellular NADPH–converting enzymes (Mosmann, 1983). The MTT assay is routinely used to determine the overall metabolic activity or number of viable cells per well (Bjorkerud & Bjorkerud, 1996a; Mosmann, 1983). Previous work in this laboratory observed a strong correlation between MTT reduction and trypan blue exclusion assays (Amit, 2008; Baird *et al.*, 2004) and studies are currently under way to compare this to apoptosis/necrosis assays in the context of oxLDL–induced cellular death (Mohd Othman, personal communication).

OxLDL caused a concentration–dependant loss of cellular viability in HMDM cells (fig. 3.1). In a typical experiment (fig. 3.1a), oxLDL concentrations of above 1 mg/mL were significantly toxic (as determined by one-factor ANOVA with Dunnett post test). Cellular viability decreased linearly at a rate of approximately 15% per mg/mL of oxLDL. LC_{50} was 3 mg/mL, which agreed with some published HMDM cell results from this laboratory (Gieseg *et al.*, 2009), but contradicted another (Gieseg *et al.*, 2010a). Gieseg *et al.* (2010a) observed a 50% cell viability loss in response to a much lower 1 mg/mL oxLDL.

In order to provide a more robust assessment of the oxLDL toxicity to HMDM cells, a regression line was fitted to the mean values of cell viability from 14 combined experiments (fig. 3.1b). A steeper slope of 20% cell viability drop per 1 mg/mL oxLDL was observed on the combined data. Based on these results, the toxic range (LC_{50}) of oxLDL concentrations was established to be between 2 and 3 mg of oxLDL cholesterol per mL, with some variation between HMDM cell preparations from different donors.

A time–course observation of HMDM cell viability during exposure to oxLDL revealed that the majority (40%) of cell viability decline happened within the first 12 hours of incubation (fig. 3.2). The remaining 10% was lost during the following 12–24 hours of incubation. A segmented regression fitted to the 0–12 hour and 12–24

hour data confirmed that the slopes of the two parts were significantly different (fig. 3.2b). This result agreed with the observations of Katouah (2012) but differed from those of Gieseg *et al.* (2010a), where the majority of oxLDL–mediated cell viability loss was observed during the 12–24 hours. Previous experimental work by Gieseg *et al.* (2010a) suggested that rapid loss of cellular viability could be associated with oxidative damage. This mechanism was explored further.

[A]

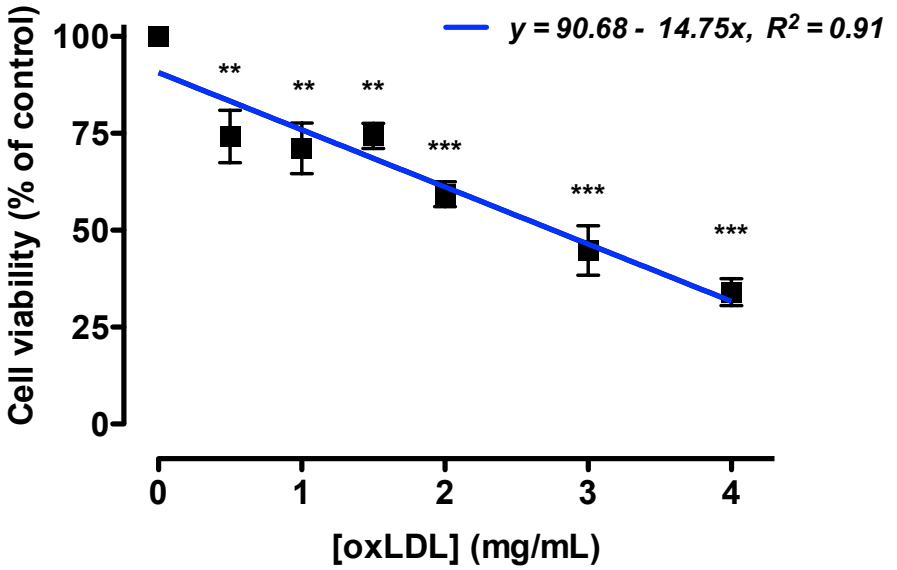

[B]

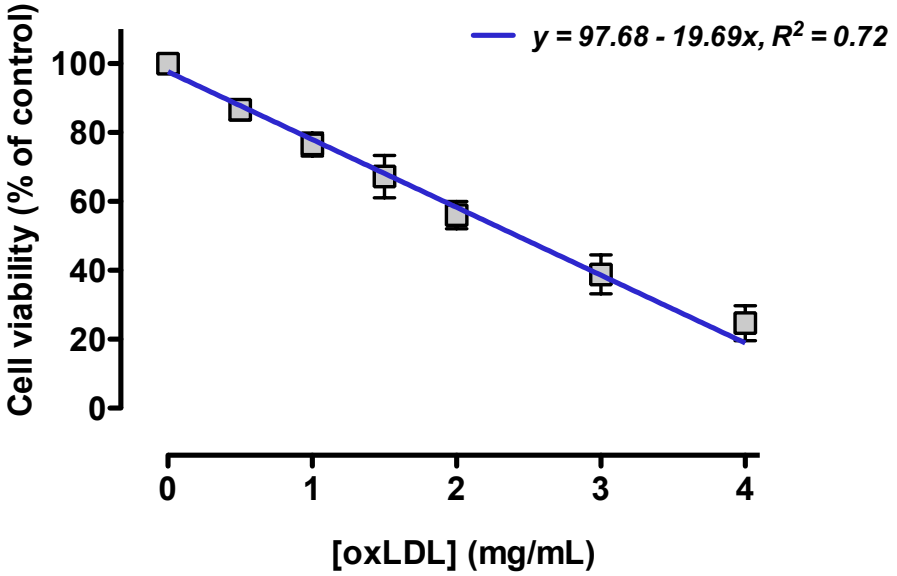

Figure 3.1: OxLDL causes concentration dependant HMDM cell viability loss after 24 hours.

HMDM cells ($5x10^6$ cells mL^{-1}) were incubated with increasing concentrations of oxLDL for 24 hours, followed by cell viability assessment (MTT reduction). The results are expressed as percentage relative to untreated control and the results are displayed as mean ± SEM of **(A)** a single experiment or **(B)** combined experimental results from n=14 experiments for [oxLDL] from 0 to 3 mg/mL and n=6 for [oxLDL]=4 mg/mL. One-way ANOVA with Dunnetts post-test was performed on the raw data for (a) and linear regression was fitted for (b). Significance is indicated from cell only control, **, $p<0.01$, ***, $p<0.001$

[A]

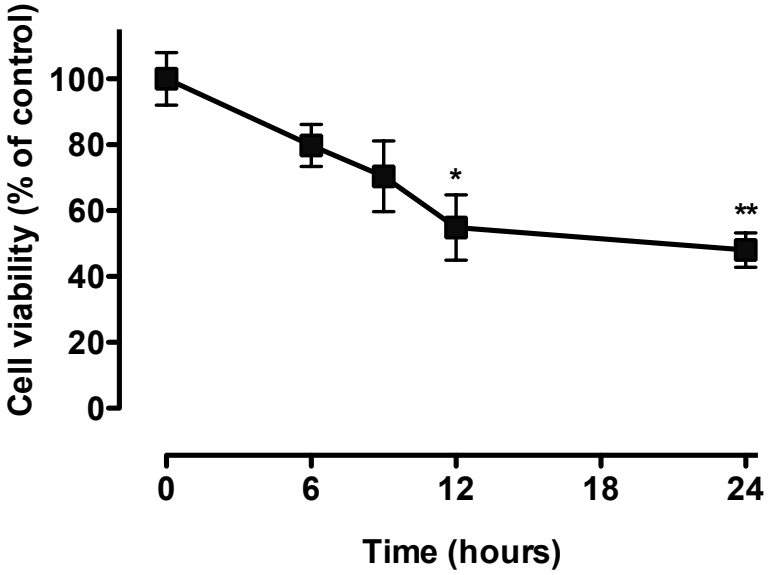

[B]

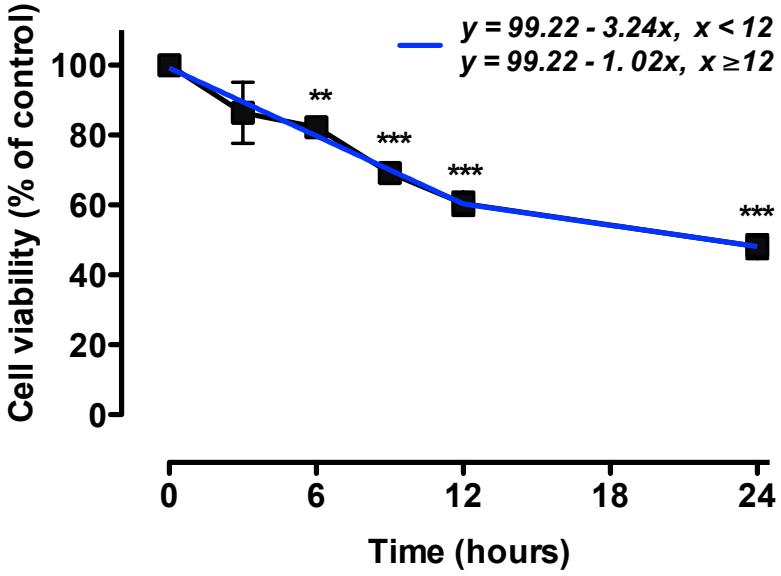

Figure 3.2: Time course of oxLDL–mediated HMDM cell viability loss. HMDM cells ($5x10^6$ cells mL^{-1}) were incubated with the LD_{50} oxLDL concentration in the whole medium for the indicated time. Cell viability was determined via MTT reduction assay and expressed as percentage relative to untreated control. Results are displayed as mean ± SEM of mean values from **(A)** a single experiment and **(B)** combined mean values from three separate experiments. Statistical analysis ((A) one-factor-ANOVA with Dunnett's post test or (B) RM–one-factor-ANOVA with Dunnett's post test compared to control) is as indicated: *, $p<0.05$, **, $p<0.01$, ***, $p<0.001$. Segmented regression was a preferred model fit over linear regression, $p=0.0015$.

3.2.2 Oxidative stress and damage is an early event in oxLDL toxicity

Intracellular ROS generation and the resulting oxidative damage were studied in HMDM cells exposed to oxLDL. ROS were detected using fluorescent products of DHE oxidation. The following experiments repeated the work by Gieseg *et al.* (2010a) but advanced further to quantify ROS flux. The DHE method (sec. 2.6.1) was used as a generic proxy for determining the the overall intracellular oxidative flux. The internalised DHE probe reacts with superoxide and a range of ROS with related chemistries to yield fluorescent ethidium and 2-OH-HE (Fernandes *et al.*, 2006; Kobzik *et al.*, 1990; Tarpey, 2004). These were detected through an epifluorescent microscope and quantified using densitometry.

Intracellular oxidative flux was an early event in the HMDM cell interaction with oxLDL, reaching a 50-70% increase in mean cellular fluorescence as early as 3 hours after the addition of oxLDL (fig. 3.3). Intracellular levels of ROS increased sharply and continuously to almost double the initial level by 12 hours, followed by a gradual decline to 3/4 of the peak value. Figure 3.3a represents a single experiment, whereas three experiments are combined in one graph on figure 3.3b. It is important to combine experimental means in order to eliminate the effects specific to individual HMDM cell preparations, even at the expense of large error bars, which represent the inter-experimental variation of absolute HMDM cell response to oxLDL (fig. 3.3b). The results confirm that HMDM cells release intracellular ROS when treated with oxLDL and that this oxidative flux is an early event in the acute toxicity setting.

[A]

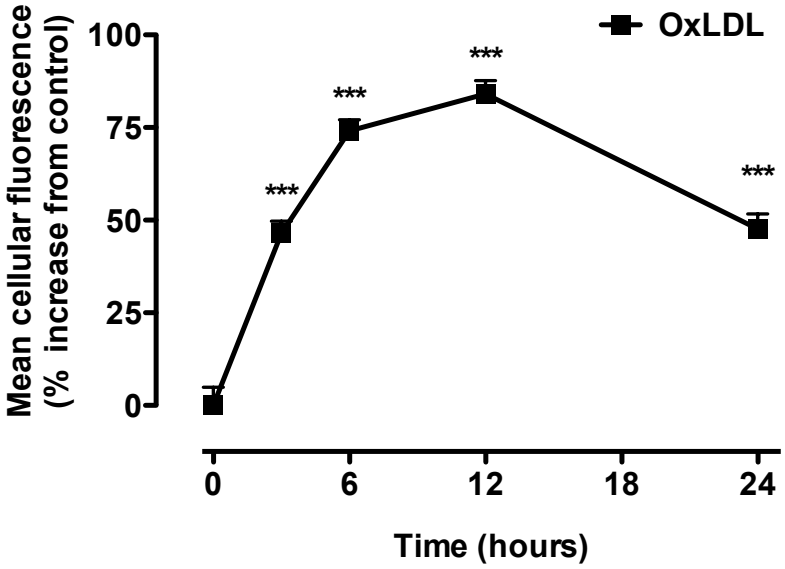

[B]

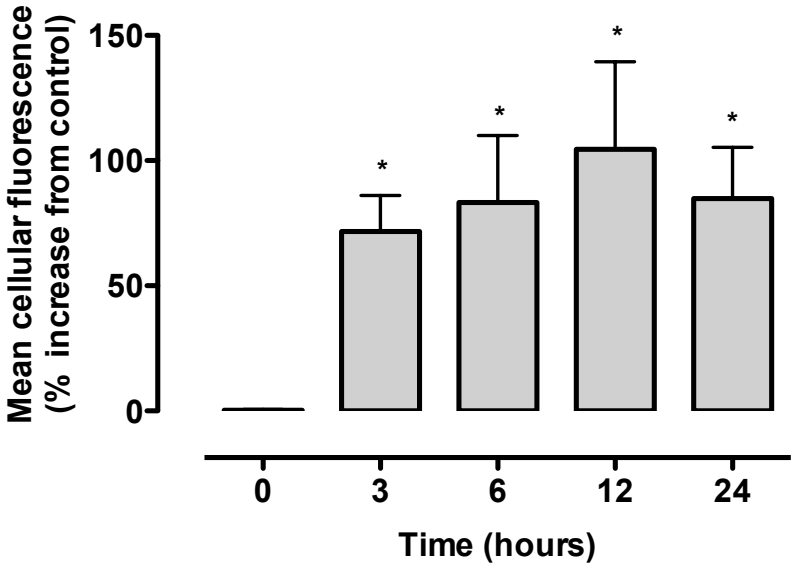

Figure 3.3: OxLDL triggers intracellular ROS release by HMDM cells. HMDM cells, cultured on coverslips ($5x10^6$ cells mL^{-1}) were incubated with 2 mg/mL oxLDL in the whole medium. Oxidant production was measured by DHE using an epifluorescent microscope at λex/λem of 500-530nm/590-620nm. Images were taken at the indicated time points and fluorescence intensity was converted into the numerical values using ImageJ64 software. Data are presented as percentage increase from the 0 hour control and shown as mean ± SEM of **(A)** duplicate measurements from a single experiment or **(B)** three separate experiments combined. Statistical significance (one-factor ANOVA performed on raw numerical data for (A) and RM-ANOVA for (B)) is indicated between the treatments at a respective time point, ***, $p<0.001$.

To confirm that ROS production and oxidative flux were damaging to the HMDM cells, the loss of intracellular GSH was assessed. Intracellular GSH is one of the primary antioxidant defence mechanisms and its decrease is an excellent marker of oxidative damage (Valko *et al.*, 2007). Previous studies in this laboratory and by other groups showed that oxLDL incubation caused an oxidative depletion of GSH (Amit, 2008; Gotoh *et al.*, 1993; Kinscherf *et al.*, 1998; Wang *et al.*, 2006). Therefore, this experiment was performed to confirm that the HMDM cells in the present study responded to oxLDL in a manner similar to the published literature. The results confirmed that toxic concentrations of oxLDL led to the loss of intracellular GSH in HMDM cells (fig. 3.4). Two milligrams per mL oxLDL caused approximately 50% GSH loss, while 3 mg/mL caused about a 70% loss (fig. 3.4a). Contrary to the results observed by Amit (2008), 0.5 and 1 mg/mL oxLDL triggered an increase in GSH, most likely due to the upregulation of GSH synthesis, as observed by Hägg *et al.* (2006). The decrease in GSH was lower after correction for cellular protein (figures 3.4 a) and b) which was most likely due to the interference of MBB-based GSH assay with bicicronic acid (BCA) assay for protein). The BCA based protein assay which was used in this study relies, in part, on the -SH thiol functional group for assessment of protein concentration. However, the same -SH functionality was utilised in GSH detection by reaction with MBB. Therefore, the protein assay performed on cellular lysates previously treated with MBB would be devoid of reactive protein–free -SH groups. Thus, GSH results were not corrected for protein, as the sample protein concentration was likely to be erroneous. This limitation of the methodology probably resulted in the over-reporting of GSH loss per cell as the results could not be corrected for cell lysis at toxic oxLDL concentrations. In addition, cells are known to upregulate GSH upon in response to oxLDL, complicating the analysis (Bea, 2003; Cho *et al.*, 1999; Shen & Sevanian, 2001).

[A]

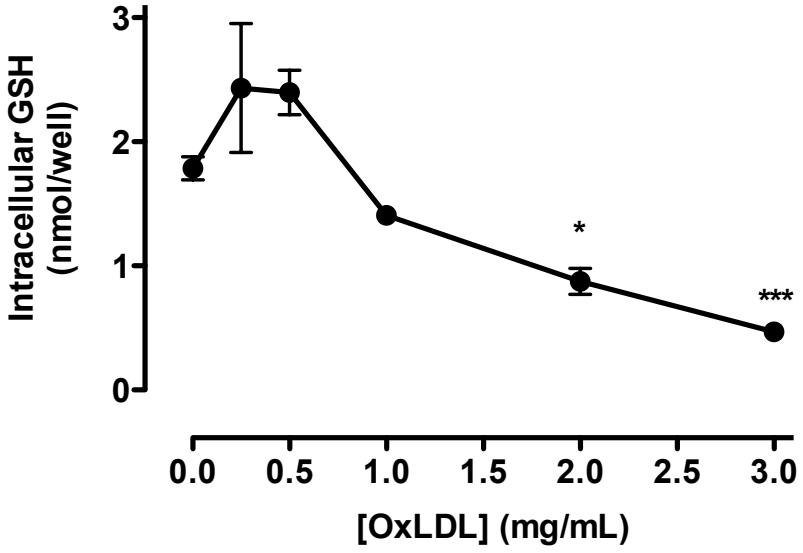

[B]

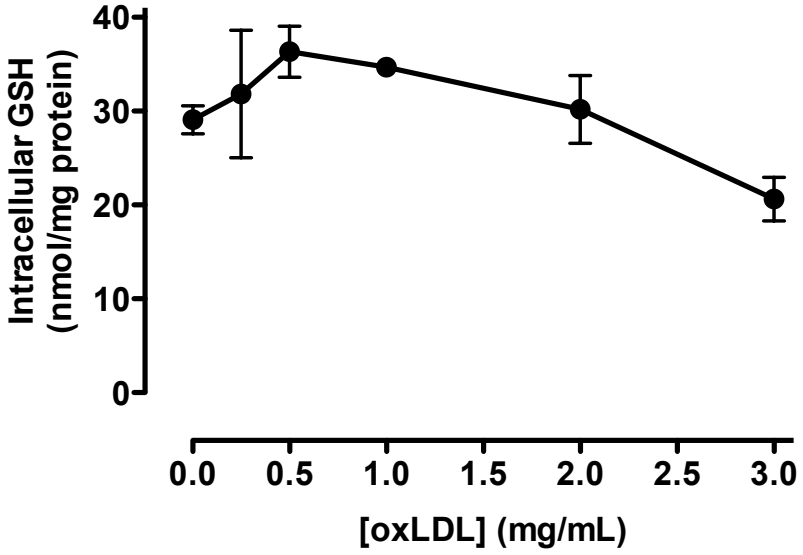

Figure 3.4: OxLDL leads to concentration dependent intracellular GSH loss in HMDM.

HMDM cells (5 x 10^6 cells mL^{-1}) were incubated with increasing oxLDL concentrations for 24 hours. Cell lysate was analyzed for reduced GSH via HPLC. Results are displayed as mean ± SEM of triplicate measurements from a single experiment **(A)** expressed uncorrected, **(B)** corrected for protein. Significance (one-way ANOVA, Dunnett's test) is indicated from 0 mg/mL oxLDL, *, $p<0.05$, ***, $p<0.001$. Average protein concentration in control was 61.4 μg/well.

3.2.3 When does HMDM cell become committed to cell death?

The results presented so far indicate that the mechanism of acute oxLDL toxicity to HMDM cells involves rapid ROS production and oxidative damage. Identifying the point at which the damage becomes irreversible is an important question in the *in vivo* situation. Since cell viability loss became significant by the 6^{th} hour of incubation (fig. 3.2b) and the rate of intracellular ROS release (corresponding to slope of the graph, greatest increase of ROS over time) was highest at 0–6 hours (fig. 3.3), 6 hours was chosen as a cut-off point to test the reversibility of damage inflicted by oxLDL on HMDM cells. The cells were treated with LC_{50} oxLDL for 6 hours, after which the medium was removed and replenished with fresh whole medium for a further 18 hours (referred to as the 6+18 hour treatment). Such experimental design enabled comparison between the "oxLDL removed" treatment (6 hours) and "oxLDL throughout" treatment (24 hours) to be made on the same time scale. Oxidative damage to GSH and cell viability loss were assessed in this experimental setting.

Within the first 6 hours of oxLDL treatment, the HMDM culture lost almost 50% of the intracellular GSH (fig. 3.5). The cells that were further incubated with oxLDL continued to lose GSH until the 9^{th} hour of incubation, after which the level of intracellular GSH had plateaued. In contrast, the 6+18 HMDM cells in which oxLDL was removed after the 6^{th} hour had recovered their intracellular GSH by the 12^{th} hour of incubation. The GSH remained at this level for the rest of the incubation period. No such recovery was observed for cellular viability. After the initial 20% viability loss in the first 6 hours, the 6+18 cells continued to lose metabolic activity (fig. 3.6). Thus, cellular metabolic activity was irreversibly affected by the 6 hour exposure to LC_{50} oxLDL. HMDM cells in the 6+18 treatment still had lower toxicity (higher cell viability) at the end of 24 hours than their counterparts which were exposed to oxLDL for the full duration (as indicated by # in fig. 3.6). This pointed towards additional processes that may have occurred in these cells. Yet the 6+18 HMDM cells were unable to regain cellular viability in a fashion similar to GSH recovery.

[A]

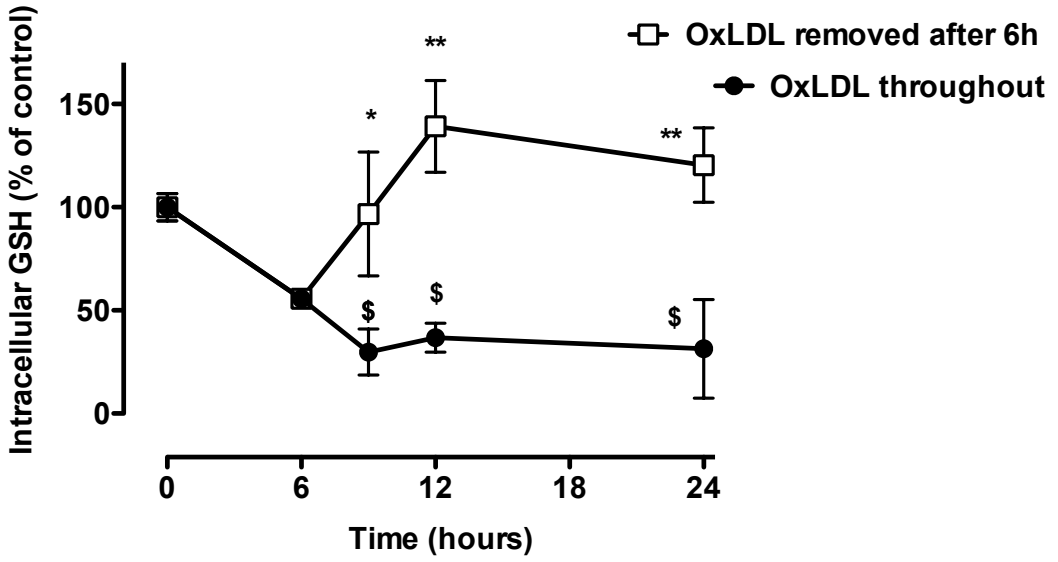

[B]

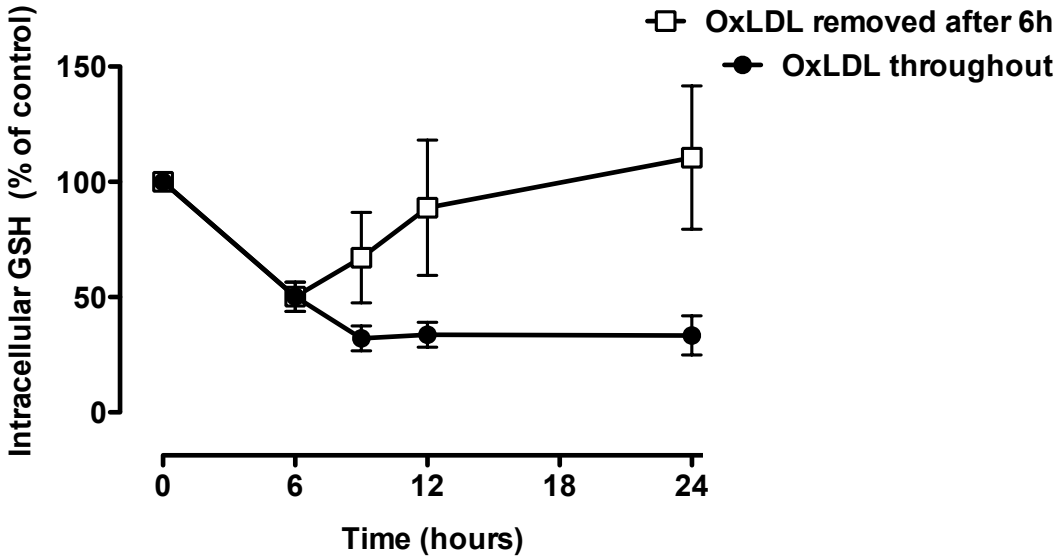

Figure 3.5: Time course of intracellular GSH recovery by HMDM upon oxLDL removal.

HMDM cells ($1x10^6$ cells mL^{-1}) in whole medium were treated with 2 mg/mL oxLDL. OxLDL was either replaced with fresh medium after 6 hours (empty rectangles) or present for the indicated time (filled circles). Cell lysates were analysed via HPLC using the MBB method and expressed as percentage of untreated control. The results are presented as mean ± SEM of mean values from **(A)** a single experiment and **(B)** combined mean values from three separate experiments. Significance is indicated: between treatments (one-factor ANOVA with Bonferroni post test of treatment pairs *, Dunnet post test comparison to control $), *,$ $p<0.05$, ** $p<0.01$. Due to the inter-batch variability in the GSH recovery, the data pairing was not effective and significance was $p=0.079$ and $p=0.165$ at 24 and 12 hour time points, respectively.

[A]

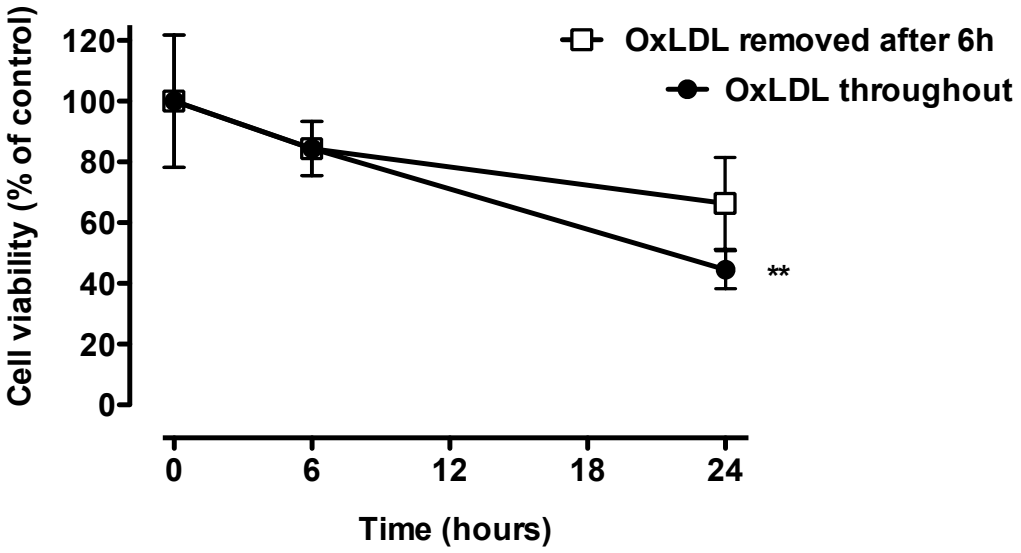

[B]

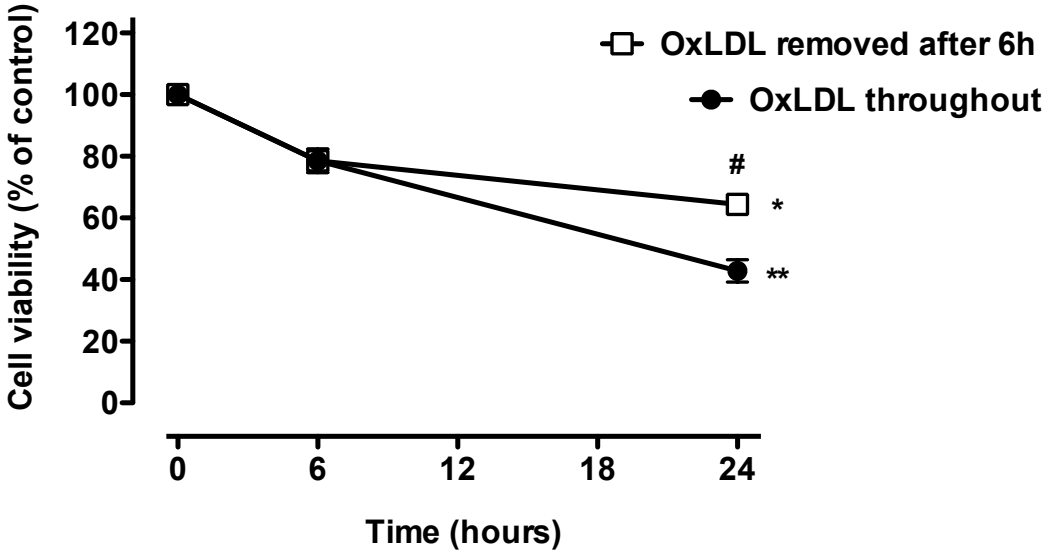

Figure 3.6: HMDM continues to lose cellular viability when oxLDL is removed.

HMDM cells ($1x10^6$ cells mL^{-1}) in whole medium were treated with 2 mg/mL oxLDL. OxLDL was either removed after 6 hours (empty rectangles) followed by the incubation in the whole medium or present for the indicated 24 hours (filled circles). Cell viability was measured by MTT reduction and expressed as percentage of 0 hour control. Results are displayed as mean ± SEM of mean values from **(A)** single experiment and **(B)** combined mean values from three separate experiments. Paired t-test (95% confidence interval) was performed on the raw data and data expressed as a percentage of control. Significant difference from 6 hour time point, *, $p<0.05$, **, $p<0.01$; between the treatments #, $p<0.05$.

Similar patterns of GSH recovery in the absence of viability recovery were observed in a concentration study. HMDM cells in the whole medium were treated with increasing concentrations of oxLDL for either 6+18 or for 24 hours, followed by GSH and cell viability measurement (figures 3.7 and 3.8, respectively). Intracellular GSH was considerably elevated in the cells exposed to oxLDL for 6 hours, compared to cells exposed for 24 hours over the whole range of oxLDL concentrations (fig. 3.7). The difference between the two treatments was higher at the sub-toxic concentrations of oxLDL (1 and 2 mg/mL) than at a toxic 3 mg/mL (fig. 3.7, filled vs. clear bars). Intracellular GSH was lower than control in the HMDM cells exposed to 3 mg/mL oxLDL for 6 hours (fig. 3.7, clear bars). This was lower compared to cells treated with 1 and 2 mg/mL oxLDL for 6 hours, which indicated that GSH recovery after 3 mg/mL was not as dramatic.

Despite GSH recovery at all oxLDL concentrations, cellular viability did not follow the same trend (fig. 3.8). Cellular metabolic capacity dropped between 2 and 3 mg/mL oxLDL for both 6+18 and 24 hour treatments and no significant difference was observed between the treatments for any of the concentrations tested.

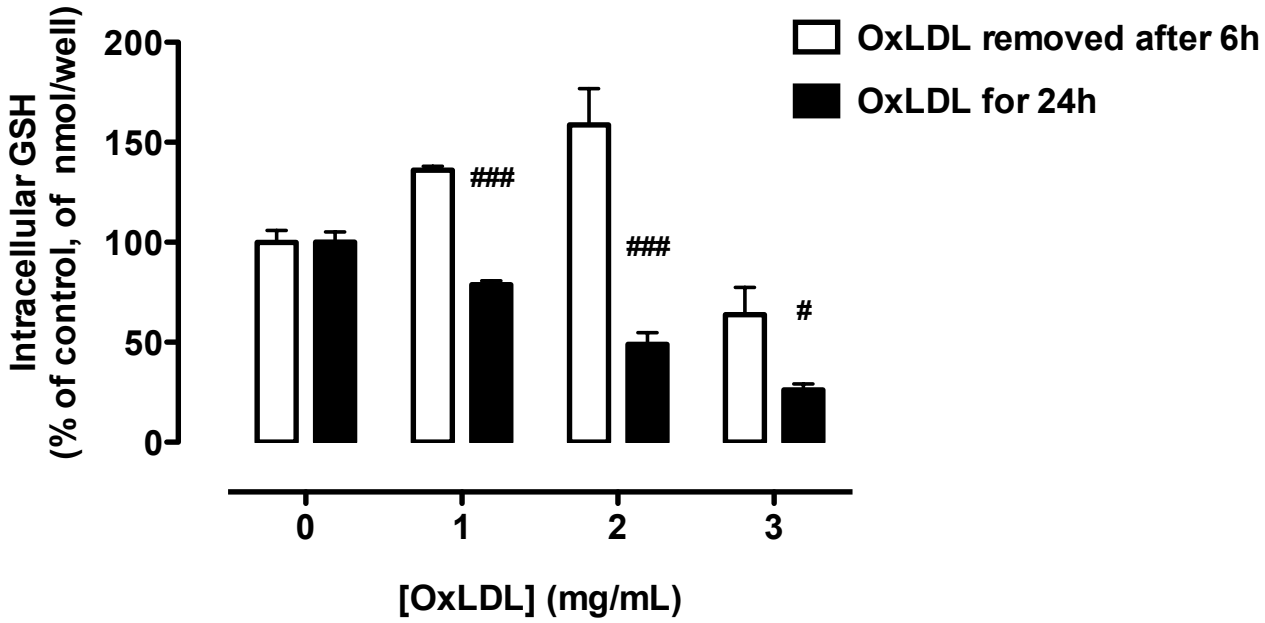

Figure 3.7: HMDM cells significantly recover intracellular GSH upon oxLDL removal: effect of concentration.

HMDM cells ($5x10^6$ cells mL^{-1}) in the whole medium were treated with varying concentrations of oxLDL for either 24 hours (filled bars) or 6 hours (empty bars) with subsequent removal of oxLDL and incubation in whole medium for another 18 hours. The intracellular GSH level was analysed at the end of the 24 hour period. Results are displayed as mean ± SEM of triplicates from a single experiment. Statistical significance (two-factor ANOVA, Dunnetts post test): time of exposure (6 vs. 24h), [oxLDL] and the interaction are all statistically significant ($p<0.001$). One-factor ANOVA with Bonferroni pairwise comparison of 6 vs. 24h was significant, #, $p<0.05$, #, $p<0.001$.

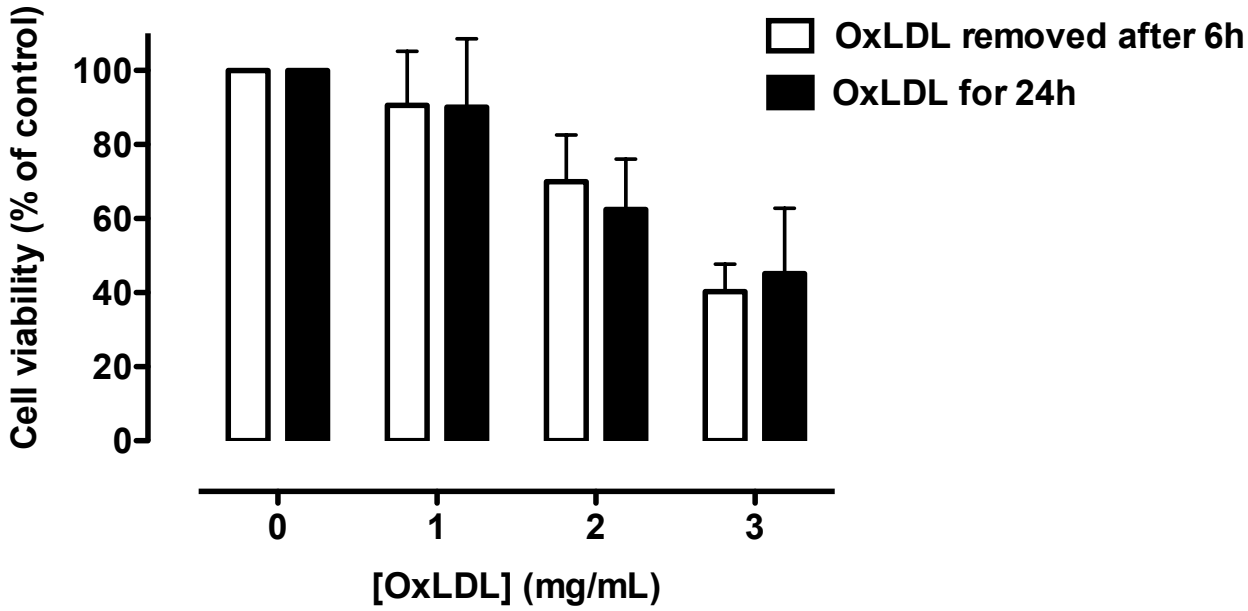

Figure 3.8: HMDM cells do not recover viability upon oxLDL removal: effect of concentration.

HMDM cells ($5x10^6$ cells mL^{-1}) in the whole medium were treated with varying concentrations of oxLDL for either 24 hours (filled bars) or 6 hours (empty bars) with subsequent removal of oxLDL and incubation in whole medium for another 18 hours. Cell viability was measured by MTT reduction and expressed as percentage of 0 hour control. Results are displayed as mean ± SEM of experimental means (n=3, except for [oxLDL]=3 mg/mL where n=2). The 24 and 6+18 hour treatments were not statistically different (one-factor ANOVA with Bonferroni post-test).

3.3 Discussion: Oxidative stress as intracellular mechanism of toxicity

OxLDL toxicity to HMDM cells

OxLDL toxicity was concentration and time dependant (figures 3.1 and 3.2), as had been observed previously (Amit, 2008; Asmis & Begley, 2003; Asmis & Wintergerst, 1998; Gieseg *et al.*, 2010a; Hardwick *et al.*, 1996). It has to be noted that the concentrations of oxLDL presented in the literature could vary by a factor of 5 depending on the unit. One hundred μg/mL oxLDL determined via protein assay equals 500 μg/mL oxLDL expressed as mg/mL of LDL cholesterol (Baird *et al.*, 2004; Gieseg *et al.*, 2009, 2010a; Katouah, 2012), as apoB protein comprises 1/5 of total LDL molecular mass (Gieseg & Esterbauer, 1994).

One hundred μg/mL of oxLDL protein caused approximately 50% cytotoxicity to HMDM according to Asmis & Begley (2003) and Hardwick *et al.* (1996) and 31% apoptosis in Asmis & Wintergerst (1998), which was considerably lower than the 10% cell viability loss observed with 500 μg/mL of oxLDL cholesterol in the present study. However, different experimental conditions were used in this than in other studies which prevented direct comparison of the results (see sec. 6.4 for detail). LC_{50} was determined to be between 2 and 3 mg/mL based on the data from multiple experiments (fig. 3.1) which was in agreement with the concentration used recently by Katouah (2012) and Gieseg *et al.* (2009).

The first significant drop of cell viability was observed after 6 hours incubation with LC_{50}, similar to the MTT results observed by Hardwick *et al.* (1996) and Katouah (2012). It continued to drop until reaching 40% at 12 hours and then another 10% in the following 12 hours, showing significantly different rates of change during the first and second half of the oxLDL treatment. The trend suggested that toxic processes within the first half of the acute oxLDL incubation had a major contribution to cell viability loss in HMDM cells. This agreed with the observation in Katouah (2012), but was different to the trend observed in Gieseg *et al.* (2010a) where the majority of toxicity took place in the second half of the incubation. However, Gieseg *et al.* (2010a) observed a 50% decrease in intracellular GSH and ROS elevation in the first 6 hours after oxLDL exposure, just like the present study (figures 3.3 and 3.5), which suggested that the intracellular processes mediated by oxLDL were similar.

3. OXLDL TOXICITY TO HUMAN MONOCYTE–DERIVED MACROPHAGES

Oxidative stress as a mediator of cell damage and death

The cause of oxLDL toxicity to cells could be the inherent properties of the oxLDL molecule, such as cytotoxic oxysterols, 4-hydroxynonenal, LOOH (Levitan *et al.*, 2010). Yet Rutherford & Gieseg (2012) showed that extrapolation from the effect of a part onto the effect of the whole may be extremely limited. 7-Ketocholesterol, which was found to be toxic when applied exogenously in solution, was not found to be toxic when presented to U937 cells more physiologically as part of acetylated LDL (Rutherford & Gieseg, 2012). This research is, therefore, focused on the cellular response to oxLDL molecule as a whole. Oxidative stress is a characteristic response to oxLDL, that has been proposed to mediate, at least in part, oxLDL toxicity (Gieseg *et al.*, 2010b).

Intracellular oxidant production in oxLDL-treated HMDM was assessed by dihydroethidium (DHE) probe. Non-fluorescent DHE is rapidly internalised and becomes oxidised to highly fluorescent ethidium and 2-OH-HE through the reaction with $O_2^{\bullet-}$ (Kobzik *et al.*, 1990; Rothe & Valet, 1990; Zhao *et al.*, 2005). As mentioned in section 2.6.1 DHE is an effective tool for measuring the overall intracellular reactive oxygen species' burden, since it is not exclusively specific for $O_2^{\bullet-}$ (Fernandes *et al.*, 2006; Kalyanaraman, 2011; Kobzik *et al.*, 1990; Tarpey, 2004).

Mean cellular fluorescence in oxLDL-treated HMDM was highly elevated compared to the control at all times, indicating substantial oxidant production in response to oxLDL. Within the first 3 hours it increased by 50-70%, reached 75-100% at 12 hours and then began declining (fig. 3.3). This pattern of a quick initial burst and fast escalation which wears off with time is that of an initial trigger → propagation cascade → sequestration type that is common to free radical reactions. Alternatively, such kinetics is similar to the phagocytic NOX activation and respiratory burst (Robinson, 2008). Such a type of oxidative flux is not obvious from the literature on the oxLDL–HMDM cell interaction. For example, the kinetics observed here were different from the steady DCFH-DA(6-carboxy-2',7'-dichlorodihydrofluorescein diacetate)–detected H_2O_2 increase in HMDM study by Asmis & Begley (2003). DHE primarily measures $O_2^{\bullet-}$, while DCFH-DA is more specific for H_2O_2. Asmis & Begley (2003) reported that oxLDL–mediated peroxide fluorescence intensity reached 300% by the 9^{th} hour, while its rate of formation appeared fairly constant. Asmis & Begley (2003), however, did not observe any DHE–reactive $O_2^{\bullet-}$. In EC cells, DCFH-DA–detectable ROS was shown to peak at 3 hours and remain constantly elevated for the duration of 24

hour incubation with oxLDL. Both H_2O_2 and Mito-SOX–detectable $O_2^{\bullet-}$ (Mito-SOX is based on DHE chemistry) were elevated in U937 cells at 5 and 4 hours post-Cu-oxLDL addition (Al Gadban *et al.*, 2010; Ermak *et al.*, 2010). In Gieseg *et al.* (2010a) we also documented that oxLDL induced a DHE–reactive oxidative stress over the first 6 hours. The present work observed and quantified the $O_2^{\bullet-}$ dominated ROS flux in HMDM cells exposed to oxLDL over time. Oxidative flux appeared to be an early event in oxLDL toxicity which agreed with some, but not all, published studies (Al Gadban *et al.*, 2010; Ermak *et al.*, 2010; Gieseg *et al.*, 2010a).

The observed discrepancy could be caused by differences in cell culture conditions or the type of cell: U937, EC and HMDM. Some of the observed discrepancy among the published studies could be explained by the different ROS probes used, which measure different types of ROS. It is difficult to interpret with certainty the combined data from multiple studies. $O_2^{\bullet-}$ is the precursor for most other cellular ROS and reactive nitrogen species (RNS), thus the lack of $O_2^{\bullet-}$ production observed by Asmis & Begley (2003) is unclear. $O_2^{\bullet-}$ dismutation by SOD yields H_2O_2. According to Beckman & Koppenol (1996), NO is the only molecule in the cell that can out-compete SOD in the reaction with $O_2^{\bullet-}$, yielding peroxynitrite ($ONOO^-$). Thus, in the excess of $O_2^{\bullet-}$ to NO, H_2O_2 will be produced. In the presence of transition metal (TM) ions, H_2O_2 could give rise to $HO^{\bullet-}$ which will react further. The rapid rate of elevation of DHE–reactive moieties could reflect the reactive oxygen/nitrogen species generation, rather than the rate of *de novo* production of $O_2^{\bullet-}$. Potential reactants that may oxidise DHE to fluorescent product are $O_2^{\bullet-}$, H_2O_2 and $ONOO^-$ (Kalyanaraman, 2011). Alternatively, the source of rapid ROS production could be NOX, which, as indicated in chapter 4, may be activated in HMDM cells upon oxLDL exposure.

The net result of this exponentially growing ROS is rapid oxidant generation and, likely, damage to cellular enzymes, membranes and structural proteins. Thus in the first 6 hours, the cellular antioxidant defence may be overwhelmed by the generated oxidants.

GSH recovery and cell viability

Oxidative flux has been suggested to precede oxidative damage, which would, in turn, precede cell viability loss if it was caused by oxidative processes (Gieseg *et al.*, 2010b;

Yang *et al.*, 2012). Glutathione is a key component of cellular defence against oxidative and nitrosative stress and an integral part of intracellular GSH/GSSG redox buffer that maintains cellular redox homeostasis (Valko *et al.*, 2007). Glutathione loss as a consequence of oxidative flux thus serves as barometer of oxidative stress, as GSH oxidation reflects oxidative damage to other cellular systems (Valko *et al.*, 2007).

OxLDL in this study caused a concentration–dependant GSH loss (fig. 3.4), which confirmed the oxidative nature of the damage inflicted by oxLDL on HMDM cells. The time of the initial ROS generation observed in this study (fig. 3.3) was paralleled by the sharp drop in glutathione level (fig. 3.5 (solid squares)), suggesting a correlation between the two. This was also previously reported by Wang *et al.* (2006) and Gieseg *et al.* (2010a). The novelty of this work lies in answering the question of whether oxidative (and other) stress that HMDM cells experience within the first 6 hours of exposure to oxLDL was sufficient to cause irreversible damage and cell death.

The results in this study showed that the initial oxidative and other processes initiated in HMDM cells upon oxLDL exposure for six hours were sufficient to irreversibly compromise cellular metabolic capacity. HMDM cells managed to restore GSH within 6 hours after oxLDL removal, while the cells incubated with oxLDL for the whole duration lost the majority of their GSH by the 9^{th} hour (fig. 3.5). Previously, Shen & Sevanian (2001) also showed that 200 μg/ml oxLDL caused a rapid depletion of intracellular GSH within 3 hours in J774 A.1 mouse macrophage cell line, followed by an adaptive increase to 175% of control by 24 hours. Cho *et al.* (1999) reported that 50 μM oxLDL up-regulated GSH synthesis in EC cells. Thus it is not surprising that removal of extracellular oxLDL after 6 hours of incubation led to an adaptive increase of intracellular GSH to levels that were higher than in control cells. Yet, when cells in both treatments were assessed for metabolic activity via MTT, the difference between treatments was very small (fig. 3.6). The cells continued to loose viability even after the removal of oxLDL after 6 hours of incubation.

The trend was repeated in a concentration study (fig. 3.7). GSH recovery after oxLDL removal was observed at all concentrations (1-3 mg/mL), albeit smaller at 3 mg/mL (fig. 3.7). All the concentrations showed a lack of cellular viability recovery. This suggests that oxLDL damage to cells caused or initiated within the first 6 hours of incubation was irreversible, irrespective of the oxLDL concentration. This theory contrasts with Gotoh *et al.* (1993) observation that THP-1 cell pre-incubation with

sub-toxic oxLDL (100 μg/mL) to up-regulate GSH had a protective effect against toxic oxLDL concentrations (400 μg/mL).

This has important implications for the understanding of the dynamics of atherosclerotic plaque. The result might suggest that macrophages infiltrating the plaque are destined for destruction when they encounter oxLDL at concentrations that cause any level of metabolic impairment, as the damage to cells will be permanent over the long term.

3.4 Summary

The results in this section confirmed that oxLDL is toxic to HMDM cells and established that under the current experimental conditions the LC_{50} of oxLDL was between 2 and 3 mg/mL. Cellular viability loss was faster in the first 12 hours of incubation (40%), followed by a more gradual loss of 10% over the remaining 12 hours. The results suggested that oxLDL induced damage to cellular metabolism and that it was higher during the first half of the incubation. This is likely to be dependant on the initial ROS generation and oxidative damage to cells. Intracellular ROS increased dramatically in the first 6 hours, peaking at 12 hours, which correlated with extensive loss of GSH by the 9^{th} hour of incubation. When extracellular oxLDL was removed from HMDM cells after 6 hours of incubation, the cellular viability failed to recover despite the recovery of intracellular glutathione. This response suggested that acute oxidative damage was irrepairable. These results imply that even a short-term exposure of macrophages to toxic levels of oxLDL within atherosclerotic plaque may compromise cellular function beyond repair thus leading to cell death and expansion of the plaque necrotic core region.

3. OXLDL TOXICITY TO HUMAN MONOCYTE–DERIVED MACROPHAGES

4

Antioxidant capacity of 7,8-dihydroneopterin

4.1 Introduction

Atherosclerotic plaques infiltrated with activated monocytes/macropages are a likely source of elevated levels of neopterin in the circulation (Firth *et al.*, 2008b; Gieseg *et al.*, 2009). Thus, it is not surprising that neopterin and its reduced counterpart 7,8-NP have been associated with atherosclerotic burden in cardiovascular disease (Fuchs *et al.*, 2009). Although serum levels of neopterin have been shown to correlate and even predict atherosclerotic complications and the disease instability (Adachi *et al.*, 2007; Ray *et al.*, 2007; Sugioka *et al.*, 2010), the biological role(s) of 7,8-NP in atherosclerosis are not well understood.

A number of studies have shown that 7,8-NP protects cells of myelocytic origin from the cytotoxic effects of oxLDL, which is one of the key drivers of atherosclerotic plaque development (Baird *et al.*, 2005; Gieseg *et al.*, 2001b, 2010a). The mechanisms for this protection are not entirely clear, but the available data suggest two plausible routes: the antioxidant capacity of 7,8-NP and 7,8-NP–mediated reduction of oxLDL uptake by macrophages (Gieseg *et al.*, 2010a). The research in this chapter will address the role of antioxidant activity of 7,8-NP in oxLDL–macrophage interaction and cellular death.

Oxidative nature of macrophage-oxLDL interaction: sources of ROS

As discussed in the previous chapter 3, oxLDL–mediated acute HMDM cell death is characterised by early oxidative stress. Therefore, antioxidant properties of 7,8-NP

will be evaluated by observing its effect on the overall intracellular oxidative burden induced by oxLDL and examining the evidence for 7,8-NP oxidation.

$O_2^{\bullet-}$ has been proposed to be the primary ROS formed after oxLDL–triggered signalling (Deng *et al.*, 2008; Gieseg *et al.*, 2010a; Park *et al.*, 2009). However, superoxide is the precursor of a suite of ROS, that are more reactive and, consequently, toxic, such as H_2O_2, $HO^{\bullet-}$, $ONOO^-$ and HOCl (fig. 1.3) (Stocker & Keaney, 2004). For example, Asmis & Begley (2003) showed that peroxide and the resulting peroxyl radicals, rather than superoxide, were the main drivers of oxLDL–induced macrophage lysis. The nature of cellular oxidants triggered by oxLDL signalling is difficult to discern as many molecular probes used to study these lack specificity. The unique nature of 7,8-NP oxidation to neopterin will be used in this work to further understanding of the identity of oxLDL–upregulated intracellular ROS. In addition, this work will offer insight into potential physiological processes that give rise to neopterin within atherosclerotic plaques.

Several enzymatic systems have been implicated in the production of cellular ROS. These include NADPH oxidases, uncoupled inducible nitric oxide synthase (iNOS), myeloperoxidase, and the enzymes of dysfunctional mitochondrial electron transport chain (ETC) (Ignarro, 2009; Podrez *et al.*, 2000; Stocker & Keaney, 2004). NOXs are of major importance because their activation and subsequent $O_2^{\bullet-}$ release seem to be triggered by the initial binding of oxLDL to macrophage receptor(s) and are, therefore, upstream of the other pathways (Park *et al.*, 2009). However, the connection between mitochondrial dysfunction and NOX is less clear as evidence for both cause-and-effect relationships exists (Wingler *et al.*, 2011; Wosniak *et al.*, 2009). Recent evidence from murine macrophage cell line J774A.1 suggests that cellular NOX–produced $O_2^{\bullet-}$ contributes to iNOS–mediated reactive nitrogen species (RNS) formation because apocynin, a NOX inhibitor, prevented both ROS and RNS formation (Muijsers *et al.*, 2000). Myeloperoxidase, too, requires $O_2^{\bullet-}$, dismutated into H_2O_2, to catalyse the formation of HOCl (Podrez *et al.*, 2000). A large body of evidence points towards NOX as the source of ROS during oxLDL-mediated cellular oxidative stress (Aviram *et al.*, 1996; Brandes *et al.*, 2010; Lee *et al.*, 2010; Sheehan *et al.*, 2011; Singh & Jialal, 2006). NOX complex assembly is activated by oxLDL binding and cellular signalling (Park *et al.*, 2009) and involves translocation and docking of cytosolic subunits to the plasma membrane–bound NOX domains (Groemping & Rittinger, 2005). To investigate the contribution of NOX–generated superoxide to the oxLDL-mediated oxidative

stress in macrophages, a NOX inhibitor, apocynin, will be used in conjunction with the assessment of intracellular oxidation of 7,8-NP. The 7,8-NP→NP oxidation chemistry will be used as a marker of oxidative processes within the cell. Apocynin is a widely used inhibitor of NOX which acts by preventing the NOX complex assembly via inhibiting $p47^{phox}$ phosphorylation and subsequent translocation to the plasma membrane (Kanegae *et al.*, 2007; Stefanska & Pawliczak, 2008; Stolk *et al.*, 1994). Apocynin had been repeatedly shown to inhibit ROS flux in different cell types including macrophages (Holland *et al.*, 1997; Stefanska & Pawliczak, 2008; Stolk *et al.*, 1994) but, to the researcher's knowledge, had not been used to investigate the effect of NOX inhibition on the secondary markers of oxidative stress, such as 7,8-NP oxidation. Neither have there been any reports on how apocynin inhibition of NOX affects cell survival of oxLDL–exposed HMDM cells. Since ROS-mediated oxidative stress is reported to play an important role in oxLDL–mediated cell death, the contribution of NOX to macrophage cell death triggered by oxLDL will be evaluated.

4.2 Results

4.2.1 7,8-NP protects HMDM cells treated with oxLDL in a concentration and time dependant fashion

7,8-Dihydroneopterin–mediated protection of HMDM cells was examined after treatment with LC_{50} of oxLDL. Two hundred μM of exogenously added 7,8-NP showed statistically significant protection (fig. 4.1). It was chosen as the working concentration for subsequent experiments, as it was also similar to the previous findings (Gieseg *et al.*, 2010a).

In order to establish a time-frame for the protective activity of 7,8-NP, a time-course study was performed. Two hundred μM of 7,8-NP provided protection of cell viability at all times over the course of 24 hours, with a statistically significant effect observed after 6 hours (fig. 4.2a). 7,8-NP inhibited oxLDL–induced cell viability loss by approximately 30%, on average, at the end of 24 hours (fig. 4.2b). Interestingly, the protection was almost complete until the 12^{th} hour of incubation (95% for 7,8-NP–treated HMDM vs. 63% for non 7,8-NP–treated HMDM), but reduced during the next 12 hours of incubation (12–24 hours).

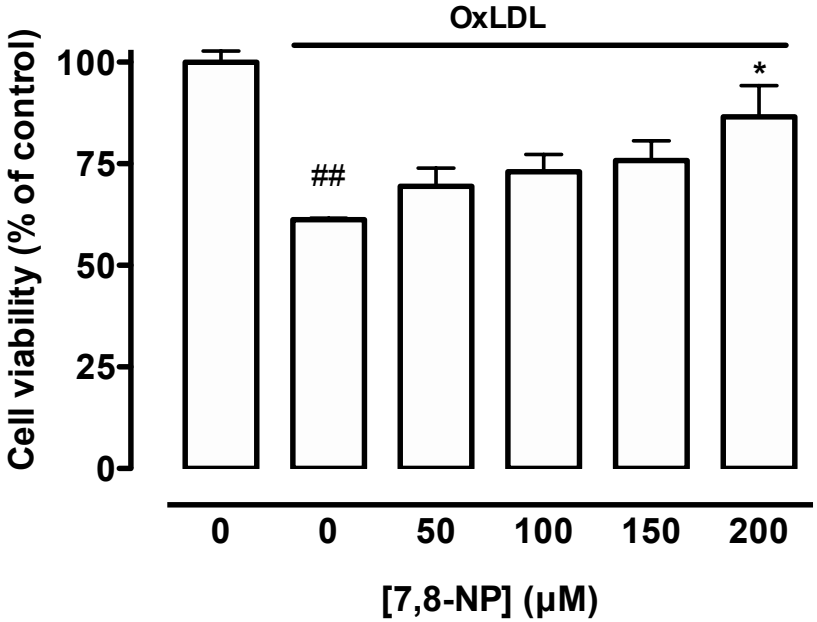

Figure 4.1: 7,8-NP protects HMDM cells from oxLDL–mediated cell viability loss in a concentration dependent manner.
HMDM cells ($5x10^6$ cells mL^{-1}) were incubated with 2 mg/mL oxLDL in the presence of increasing concentrations of 7,8-NP in the whole medium for 24 hours. Cell viability was assessed via MTT reduction assay. The data are expressed as a percentage of the untreated control. Results are displayed as mean ± SEM of triplicate measurements from a single experiment. Statistical significance (one-factor ANOVA with Dunnet's post test) is indicated as *, $p<0.05$ from 0 μM 7,8-NP in the presence of oxLDL; ##, $p<0.01$ from control in the absence of oxLDL.

[A]

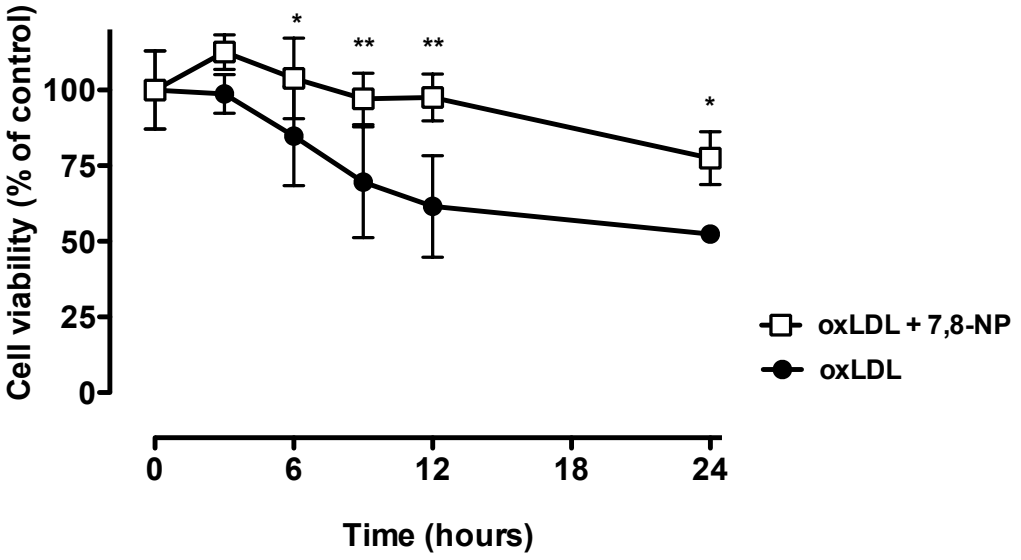

[B]

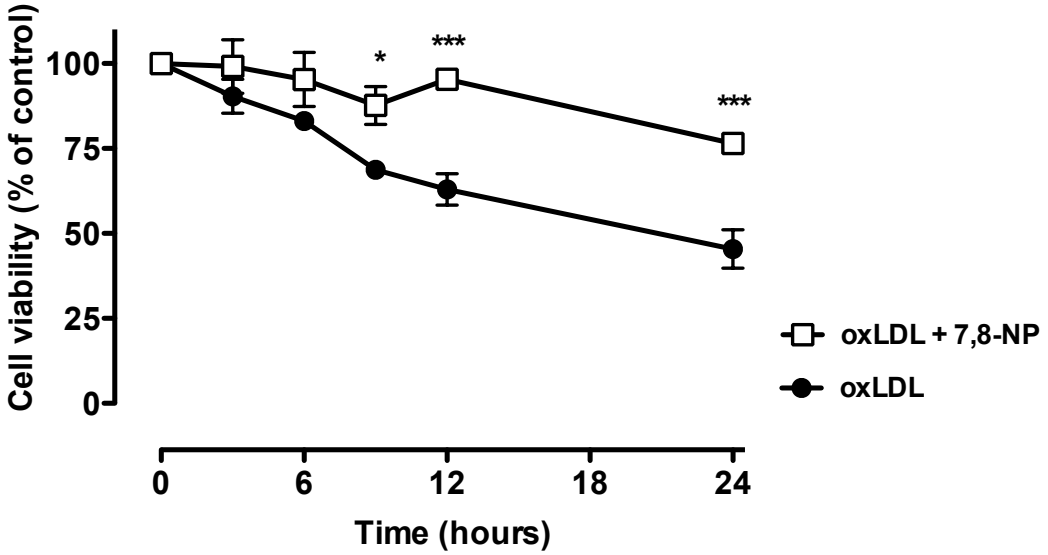

Figure 4.2: Time course of 7,8-NP–mediated protection of HMDM cells from oxLDL–induced cytotoxicity.

HMDM cells ($5x10^6$ cells mL^{-1}) were incubated with LC_{50} oxLDL either in the presence (empty square) or absence (filled circle) of 200 μM 7,8-NP in the whole medium. Cell viability was assessed at indicated times via MTT reduction and the data are expressed as a percentage relative to the untreated control. Results are displayed as mean ± SEM of mean values from **(A)** single experiment and **(B)** combined mean values from three separate experiments. Statistical analysis (one-factor-ANOVA with Bonferroni comparison between treatments at respective time points) is as indicated: *, $p<0.05$, **, $p<0.01$, ***, $p<0.001$. Regression lines fitted to the 0–12 hour data (Prism5) were different between treatments in the first 12 hours (not shown) ($p<0.001$).

4.2.2 7,8-NP concentration and availability in cell culture

7,8-NP oxidises in HMDM cell medium over 24 hours

The extracellular availability of 7,8-NP in the medium during the course of 24 hours was investigated. During the first 12 hours of incubation with HMDM cells, total pterin, the majority of which was comprised of 7,8-NP, decreased by about 10% from the starting concentration of 200 μM (fig. 4.3a). This was followed by a sharper drop to $\sim$130 μM during the following 12 hour period (12–24 hours). Interestingly, this decrease did not correspond with a reciprocal increase in neopterin concentration (fig. 4.3b), indicating that this extracellular 7,8-NP was converted to a different product, most likely 7,8-dihydroxanthopterin (Gieseg *et al.*, 2001a). Our research group has previously reported a decrease of extracellular 7,8-NP added to HMDM cell culture to 100 μM after 24 hours (Gieseg *et al.*, 2010a). The difference between the kinetics reported here and in Gieseg *et al.* (2010a) is likely due to inter-experimental variation. Control cells incubated for 24 hours in the absence of 7,8-NP showed a slight increase in extracellular total pterin and neopterin (results not displayed). The values rose from 25 to 32 nM for total pterin and from 2 to 3.7 nM for neopterin, indicating that some production and/or oxidative processes were taking place. A measurement of 10% serum supplemented RPMI-1640 returned 32.5 nM neopterin and 35 nM of total neopterin (data courtesy T. Janmale), indicating that the baseline extracellular neopterin originated from serum.

[A]

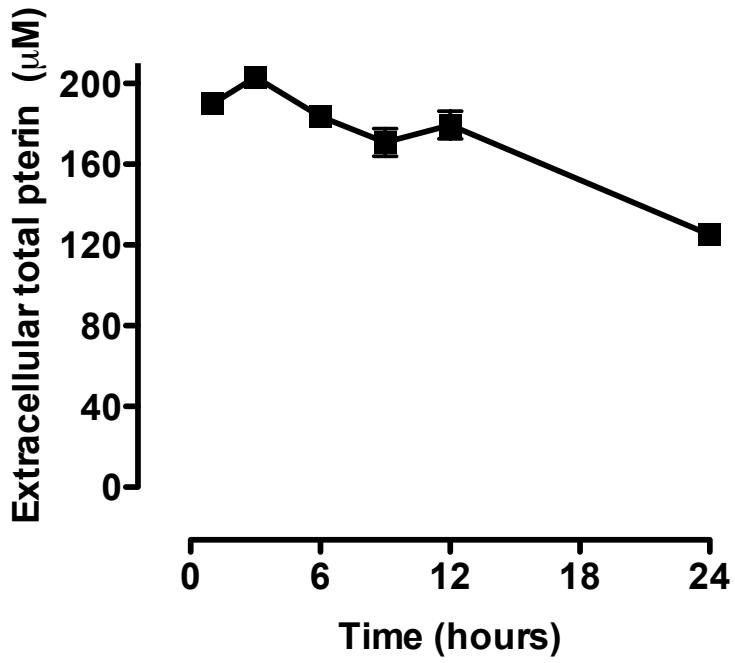

[B]

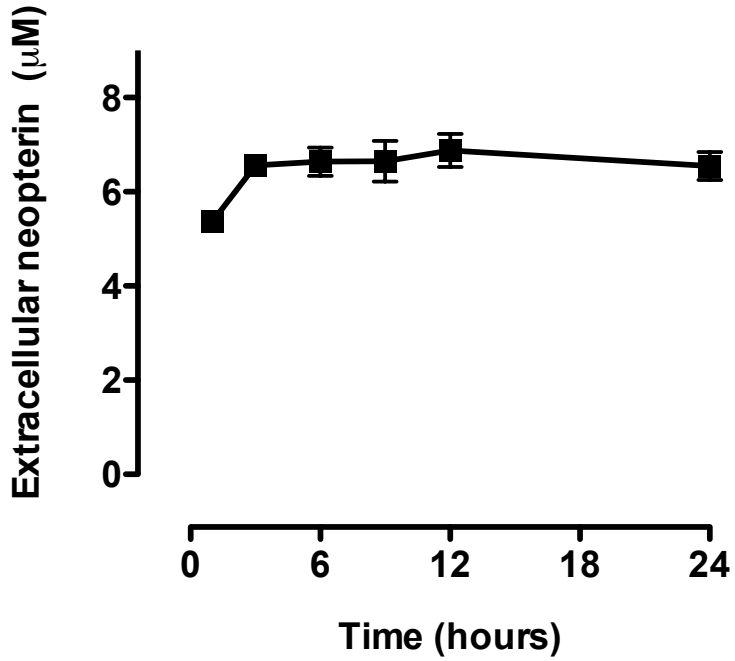

Figure 4.3: Time course of extracellular pterin concentration when incubated with HMDM cells.

HMDM cells ($5x10^6$ cells mL^{-1}) were incubated with 200 μM 7,8-NP in the whole medium. The samples of the extracellular medium were taken at the indicated times and neopterin and total neopterin were measured by HPLC. Results are displayed as mean ± SEM of triplicate measurements from a single experiment.

Measurement of effective intracellular [7,8-NP] when added exogenously

An initial hypothesis stated that 7,8-NP–mediated protection against oxLDL was associated with its intracellular action. The effective intracellular concentration of 7,8-NP was, therefore, measured after exogenous application. HMDM cells were treated with 200 μM 7,8-NP and assessed for neopterin and total neopterin (fig 4.4). The level of total intracellular neopterin, the majority of which was comprised of 7,8-NP, rose sharply in the first 1 hour of incubation and continued to rise until the 12th hour of incubation, reaching 3.1 nmol/mg cellular protein or 142 pmol/well, to then plateau. Neopterin levels remained small starting from 175 pmol/mg protein in the 1st hour reaching 286 pmol/mg protein or 6.42 pmol/well at 24 hours.

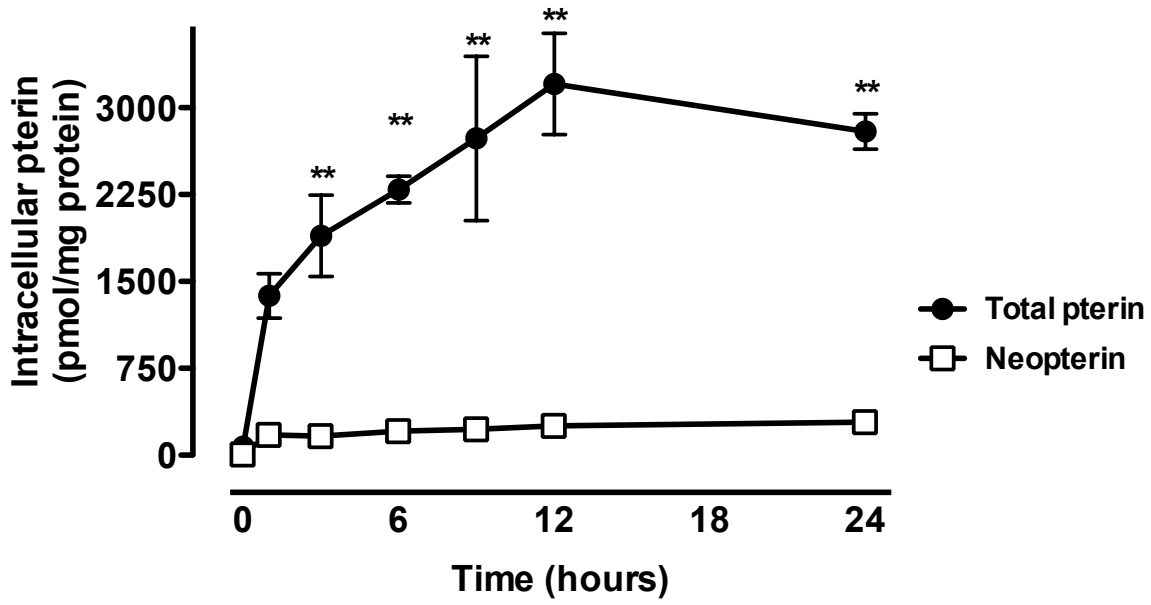

Figure 4.4: Time course of 7,8-NP accumulation of exogenously added 7,8-NP in HMDM cells.

HMDM cells (5x10^6 cells mL^{-1}) were incubated with 200 μM 7,8-NP (with a 10 minute pre-incubation prior to the collection of 0 hour sample). Cell lysates were collected at the indicated times and analysed for neopterin and total pterin via HPLC. Results are displayed as mean ± SEM of triplicate measurements from a single experiment. For reference, [total pterin]=142 pmol/well and [neopterin]=6.7 pmol/well at 12 hours; average protein content was 196 μg/well. Statistical significance (one-factor ANOVA, compared to control) is as indicated, **, $p<0.01$.

Multiple preparations of HMDM cells were tested for intracellular 7,8-NP concentration and the data were pooled to assess the variation. The intracellular neopterin and 7,8-NP concentrations varied between HMDM preparations incubated with 200 μM 7,8-NP for 24 hours (fig. 4.5). As these data were analysed retrospectively, the experiments should be treated as a pilot study. Five HMDM preparations were incubated with 200 μM 7,8-NP for 24 hours. Two out of the five experiments were performed on the HMDM cells seeded at 5x10^6 cells/mL in 12 well plates (fig. 4.5, squares). In the remaining three experiments, HMDM cells were seeded at 1x10^6 cells/mL in 48 well plates. The intracellular neopterin and 7,8-NP concentrations measured in all five experiments varied between 7 and 42 pmol/well for neopterin and between 82 and 286 for calculated 7,8-NP (fig. 4.5). Correction for cellular protein was performed in order to mitigate the difference associated with the number of HMDM cells per well in these different plate types (fig. 4.5b). Following the correction, however, the variation in concentration (between 300–2065 pmol/mg protein) of calculated 7,8-NP was still present.

An attempt was made to interpret the 7,8-NP uptake variation in the view of the baseline intracellular levels of 7,8-NP and neopterin in these HMDM cells. Yet the cells seeded at the same density demonstrated similar baseline total pterin levels: 5x10^6 cells/mL showed a $\sim$45 pmol of calculated 7,8-NP per mg protein, whereas in the cells seeded at 1x10^6 cells/mL, $\sim$80 pmol/mg protein was consistently observed (fig. 4.6). Pairwise comparison of the respective experiments in figures 4.6 and 4.5 showed that the pattern of high-low [7,8-NP] was not consistent. It thus remains to be seen whether 7,8-NP uptake is variable due to the experimental conditions or cellular physiology.

[A]

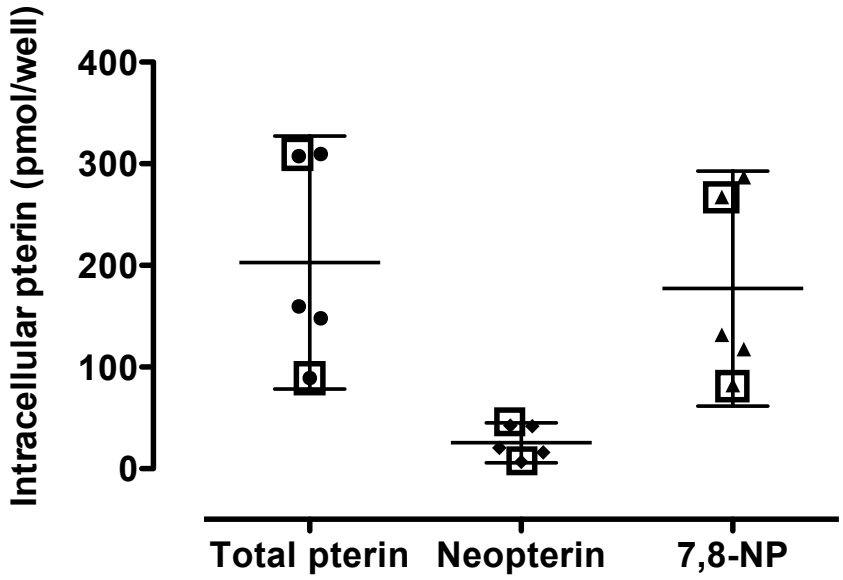

[B]

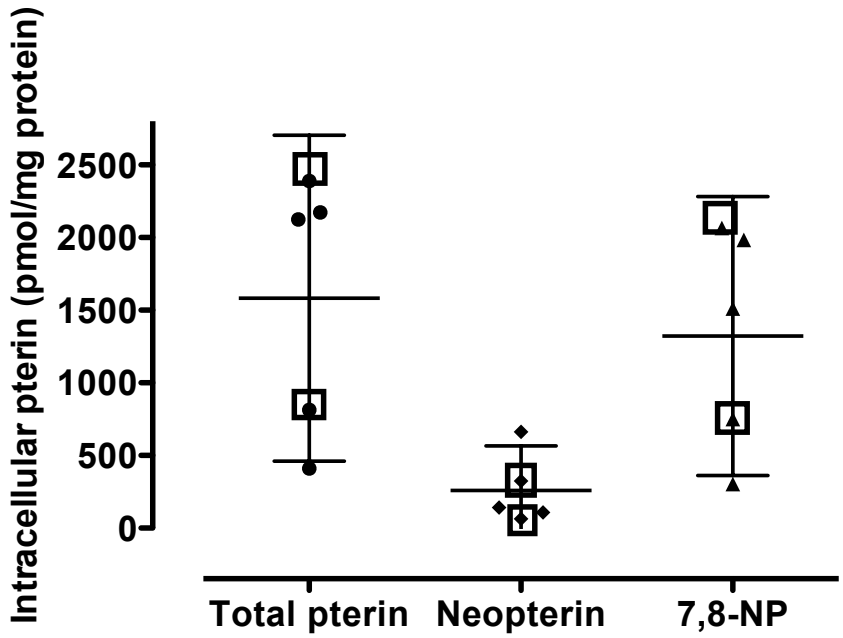

Figure 4.5: Intracellular pterin concentration in HMDM after 7,8-NP addition.

HMDM cells ($5x10^6$ cells mL^{-1} (framed) and $1x10^6$ cells mL^{-1}) were incubated with 200 μM 7,8-NP for 24 hours. Total pterin and neopterin were measured by HPLC on cell lysates, while 7,8-NP was calculated as a difference between the two measurements. Protein concentration was measured by BCA assay. The results are presented as scatter dot plot of five separate experimental measurements, each performed in triplicate. The data is mean ± 95% CI, expressed as **(A)** pmol/well and **(B)** pmol/mg protein.

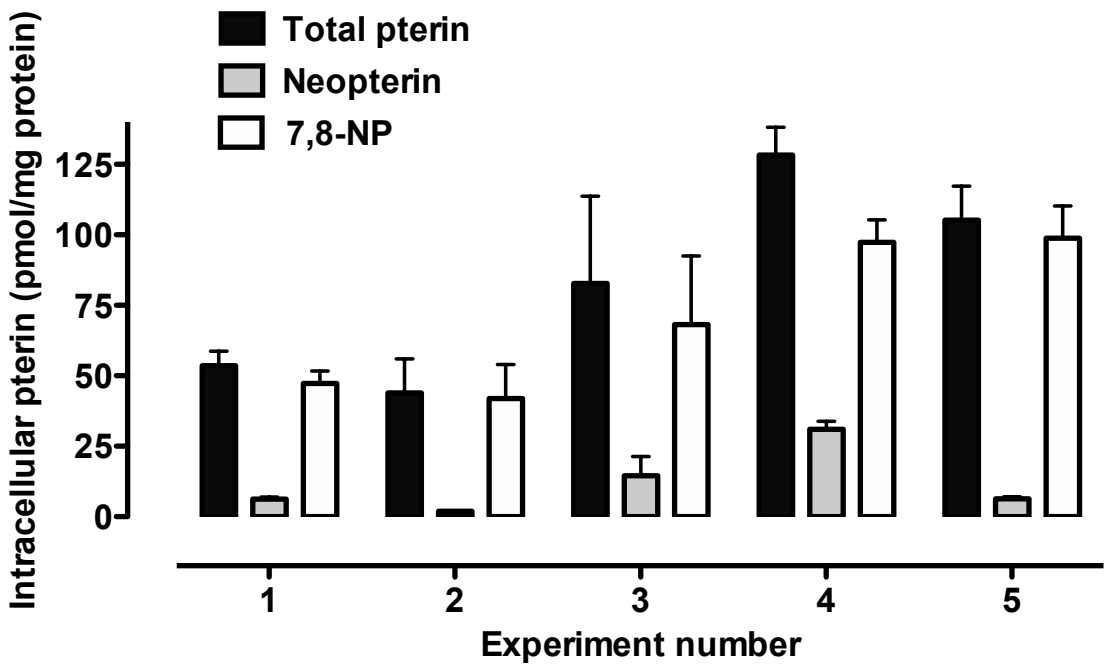

Figure 4.6: Intracellular baseline pterin concentration in cultured HMDM. HMDM cells seeded at $5x10^6$ cells mL^{-1} (experiments 1 and 2) and $1x10^6$ cells mL^{-1} (experiments 3-5) were cultured in the whole medium. Baseline levels of neopterin (grey bars) and total neopterin (black bars) were measured by HPLC, while 7,8-NP (white bars) was calculated as the difference between the two measurements. Protein concentration was measured by BCA assay. Results are presented as mean ± SEM of triplicate measurements from five separate experiments. For reference, [total pterin] ranged from 3.7 to 53.6 pmol/well, [neoptrin] from 0.24 to 12.9 pmol/well, [protein] from 32.7 to 196 μg/well Statistical analysis (two-factor ANOVA) showed that the difference between the experiments was significant, $p<0.001$

HMDM cells produce small level of pterin in response to oxLDL

To determine whether the majority of 7,8-NP during HMDM cells' incubation with oxLDL was derived from an exogenous source, the ability of oxLDL to induce 7,8-NP synthesis in HMDM cells was investigated. OxLDL elicited a small increase in total pterin of 175, 43 and 17 pmol/mg protein, in the three HMDM preparations tested (fig. 4.7). In two out of three experiments, this increase was due to an increase in 7,8-NP concentration. However, the inter-experimental variation in the pterin levels comparative to the size of the effect was too large for the result to be statistically significant.

The experiment was repeated with a sub-toxic concentration of oxLDL to discern the effect of oxLDL levels that do not cause loss of cellular protein. HMDM cells, treated with 1 mg/mL oxLDL for 24 hours in the whole medium, were assessed for neopterin and total pterin (fig. 4.8). The intracellular 7,8-NP increase was much smaller than demonstrated previously, showing a 8.6 and 2.4 pmol/mg protein increase. No difference between treatments was observed in the extracellular pterin levels (data not shown). Thus, the small level of 7,8-NP production up-regulated by oxLDL appeared to be extremely small compared to the micromolar concentration added exogenously. Consequently, the primary source of 7,8-NP during the HMDM cell experiments with oxLDL was the exogenously added 7,8-NP.

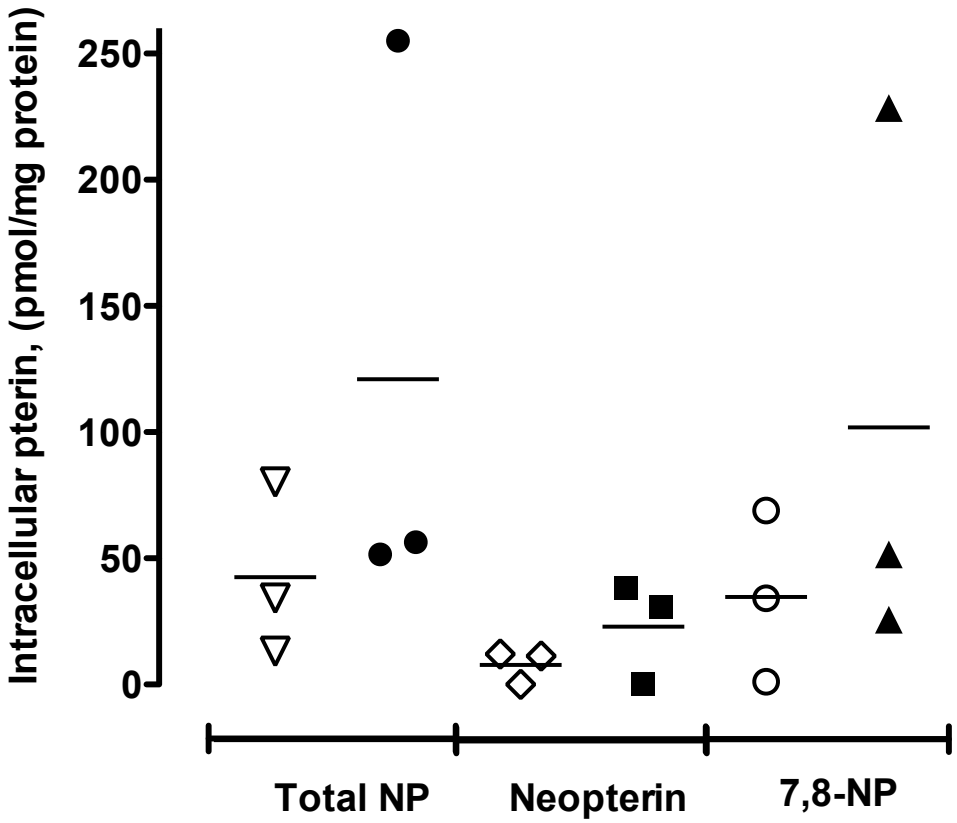

Figure 4.7: Endogenous neopterin production by HMDM cells in response to toxic levels of oxLDL.

HMDM cells ($1x10^6$ cells mL^{-1}) were incubated with (filled symbols) or without (clear symbols) 2.5 mg/mL oxLDL for 24 hours in the 2% serum-containing medium. Cell lysate was analysed for neoptein and total neopterin, and 7,8-NP was calculated as the difference between the two measurements. Data is presented as a scatter dot plot of three experiments, where each symbol represents the mean of triplicate measurements from one experiment. For each type of pterin, the change in mean values after oxLDL treatment is indicated with an arrow. Statistical analysis (two-tailed t-test on the combined data, n=3) showed no significant difference between the treatments.

[A]

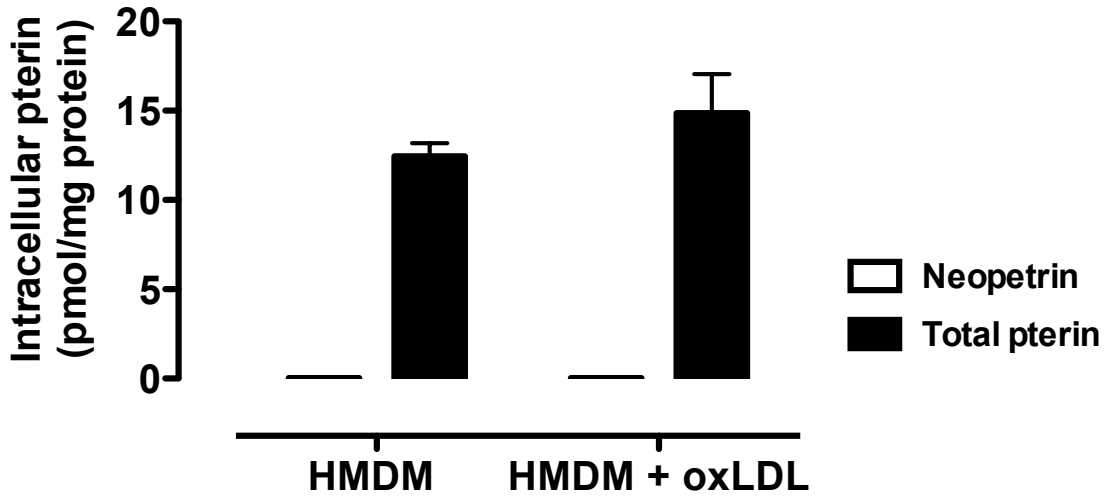

[B]

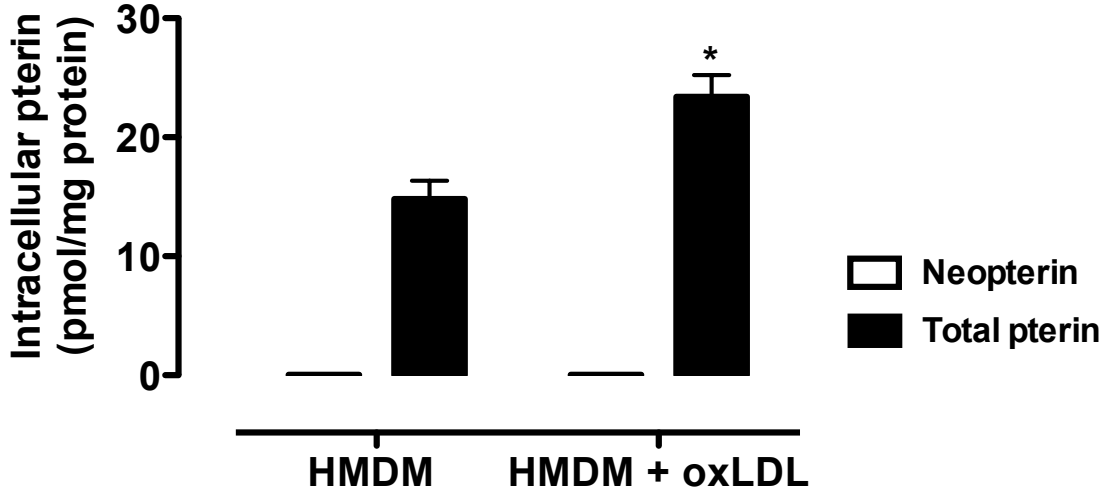

Figure 4.8: Endogenous neopterin production by HMDM in response to sub-toxic level of oxLDL.

HMDM cells ($1x10^6$ cells mL^{-1}) were incubated with 1 mg/mL oxLDL for 24 hours in the whole medium. Cell lysate was analysed for neoptein and total neopterin. Results are displayed as mean ± SEM of mean values from single experiment; **(A)** and **(B)** represent two separate experiments. No neopterin was detected. Fore reference, average cellular protein in control wells of both experiments was approximately 45 μg/well. Significance (two tailed t-test) on individual experiments is as indicated *, $p<0.05$; t-test on combined data showed no significant effect of oxLDL treatment.

4.2.3 7,8-NP alleviates oxLDL–mediated ROS stress in HMDM

The effect of 7,8-NP on the overall oxidative flux induced by oxLDL in HMDM cells was determined in order to investigate the mechanism(s) of protection. Intracellular ROS were measured with dihydroethidium (DHE) probe, as described in section 3.2.2. 7,8-NP was very effective at stopping the ROS-related increase in the probe fluorescence (fig. 4.9). The effect was, on average, most pronounced during the first 6 hours, with 7,8-NP preventing the rise in mean cellular fluorescence by approximately 50%. The capacity of 7,8-NP to scavenge/inhibit oxLDL–induced ROS decreased to about 30% in the 12^{th} hour (combined data) with a further drop by the 24^{th} hour (fig. 4.9b). The magnitude of the effect varied between the experiments, thus a single experiment is presented alongside the combined data (fig. 4.9a and b, respectively). The data suggest that 7,8-NP was highly effective at alleviating the initial oxidative stress in HMDM cells, but was not always able to sustain the low levels of ROS beyond the 12^{th} hour of incubation. The absorption/emission spectra of 7,8-NP and DHE oxidation products did not overlap.

[A]

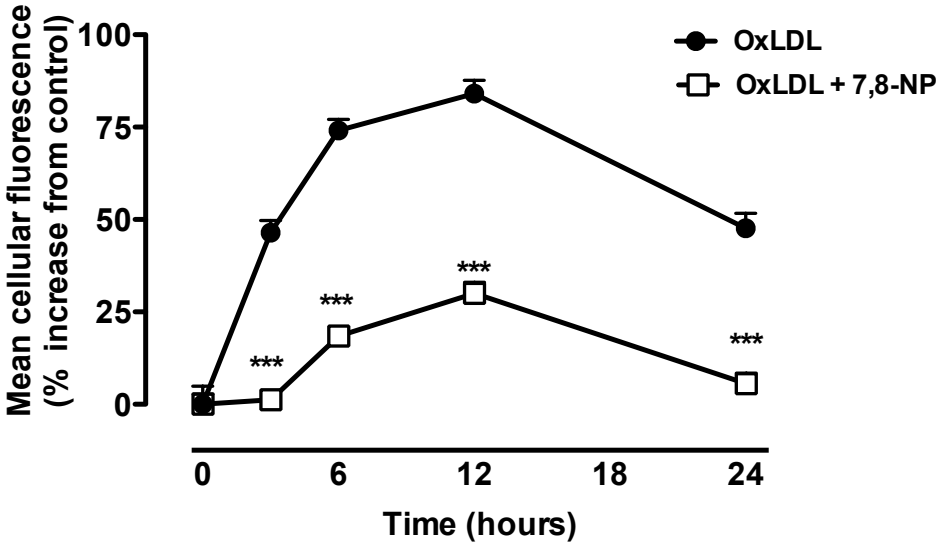

[B]

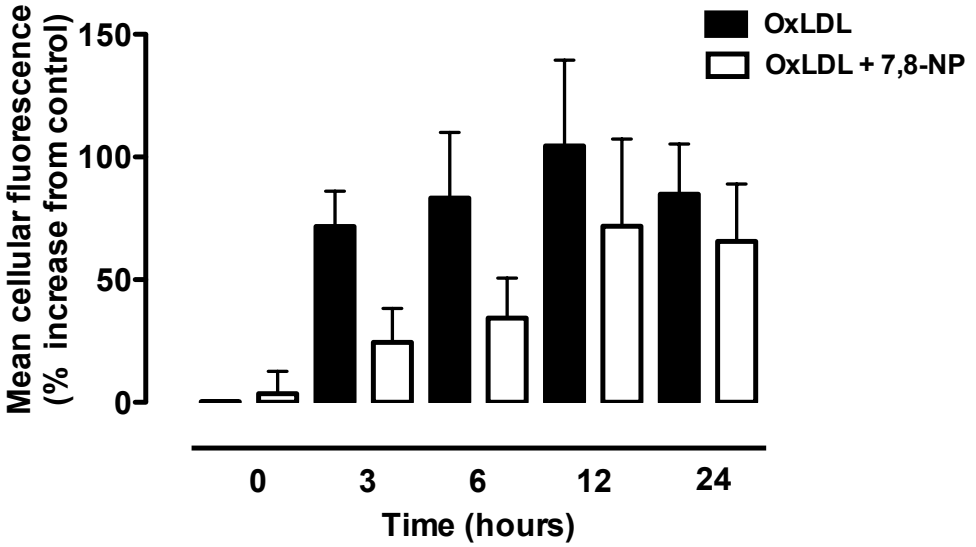

Figure 4.9: 7,8-NP inhibits the oxLDL–driven elevation of intracellular ROS. HMDM cells cultured on coverslips ($5x10^6$ cells mL^{-1}) were incubated with 2 mg/mL oxLDL in the whole medium in the presence (clear bars) or absence (filled bars) of 200 μM 7,8-NP. Oxidant production was measured by fluorescent microscopy with DHE at λex/λem of 500-530nm/590-620nm. Images were taken at the indicated times and fluorescence intensity per cell was digitised with ImageJ64. Both ± 7,8-NP data are presented as percentage increase from the respective control shown as mean ± SEM of mean values from **(A)** single experiment and **(B)** combined mean values from three separate experiments. One-factor ANOVA with Bonferroni pairwise comparison of treatments at each time point was performed on raw numerical data. Significance is indicated between the treatments at a respective time: ***, $p<0.001$.

4.2.4 7,8-NP is oxidised to neopterin in the HMDM cells treated with oxLDL

The possible mechanism for 7,8-NP–mediated decrease of the intracellular oxidative load is oxidant scavenging and/or prevention of oxidant formation. Oxidant scavenging can be tested by analysing the oxidation products of 7,8-NP: neopterin and 7,8-DXP (fig. 1.6). While direct 7,8-DXP detection was not pursued due to the difficulty of assessing picomolar levels of this compound in cells, neopterin is highly fluorescent and its levels were investigated further.

OxLDL treatment of HMDM cells pre-incubated with 200 μM 7,8-NP led to a consistent increase in intracellular neopterin, which was 2.4 times higher than the non-oxLDL control by the end of 24 hours (fig. 4.10). The rise in neopterin driven by oxLDL followed linear kinetics after the first 3 hours of incubation. The levels of neopterin reached 250 pmol/mg protein in two HMDM preparations and 1300 pmol/mg protein in another (fig. 4.10b). In contrast, neopterin level in 7,8-NP-only HMDM cells plateaued at $\sim$100 (and 600) pmol/mg protein after the first 3 hours, while 7,8-NP-free control cells did not produce any neopterin. There were notable differences between HMDM preparations in the absolute levels of neopterin, yet the trend and the magnitude were identical. Due to the toxicity of the oxLDL concentration used in this experiment, the data were corrected for protein to account for cell loss due to oxLDL toxicity.

[A]

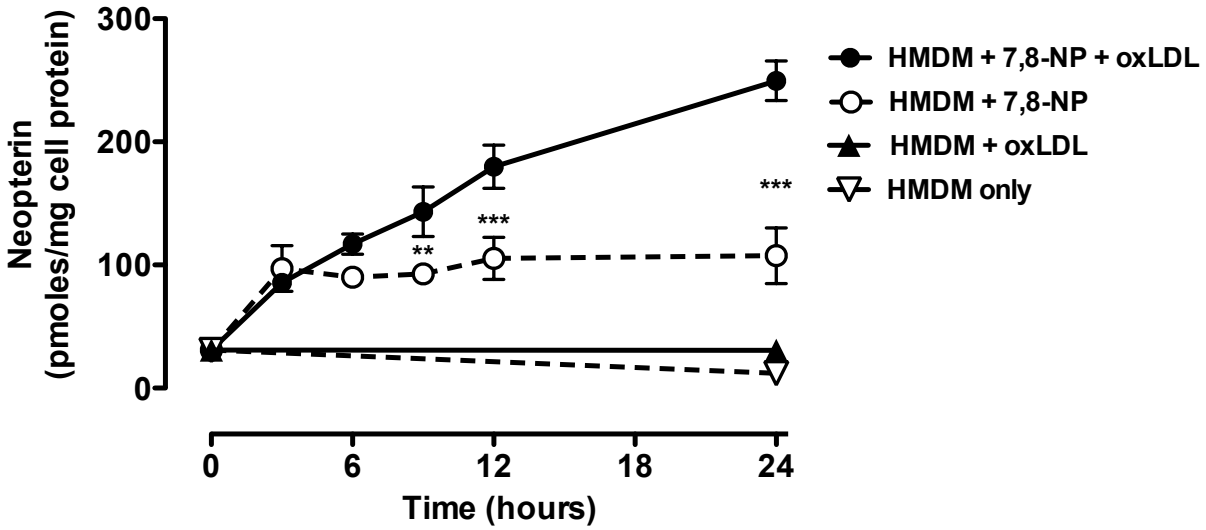

[B]

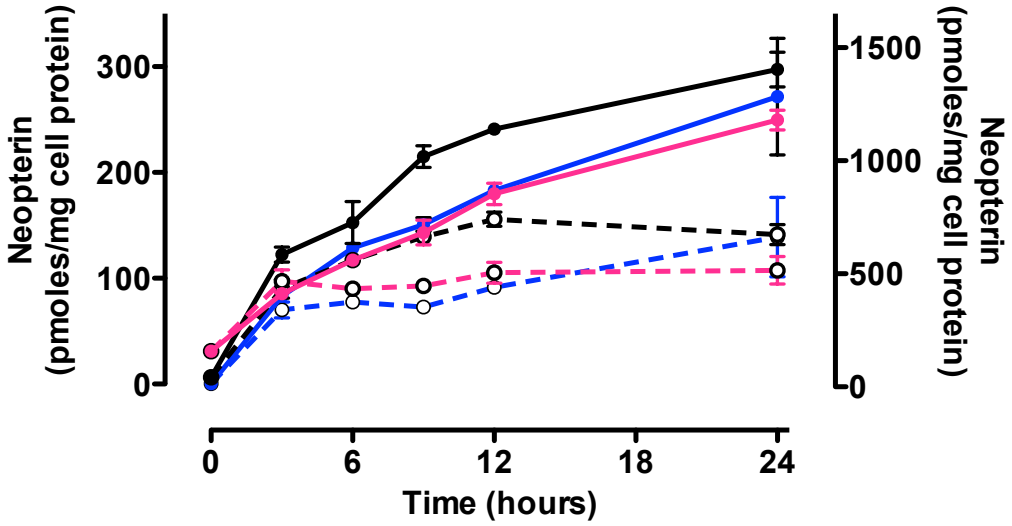

Figure 4.10: 7,8-NP is oxidised to neopterin in HMDMs treated with oxLDL. HMDM cells ($1x10^6$ cells mL^{-1}) were incubated with 200 μM 7,8-NP in the presence (solid line) or absence (dotted line) of 2.5 mg/mL oxLDL (in 2% serum). Cell lysates were collected at the indicated times and analysed for intracellular neopterin. Results are expressed as **(A)** mean ± SEM of triplicate measurements from a single experiment, **(B)** three separate experiments. **(B)** Separate experiments are colour-coded, black and pink are on the left Y-axis, blue is on the right Y-axis. For reference, [neopterin] in control cells at 24 hours ranged from 16 to 42 pmol/well. [Protein] in control cells was 32.7, 125 and 150 μg/well. Regression analysis showed significant difference between the slopes of oxLDL–treated and untreated cells **(B)**; one-factor ANOVA with Bonferroni pairwise comparison was significant as indicated in **(A)**: **, $p<0.01$, ***, $p<0.001$.

The level of remaining 7,8-NP was investigated to determine the relative magnitude of its oxidation into neopterin. Also, any difference in the remaining 7,8-NP between the treatments could be indicative of another 7,8-NP oxidation product, 7,8-DXP. The level of intracellular 7,8-NP was measured by subtracting neopterin values from the total intracellular pterin level. Total pterin and the calculated 7,8-NP levels are presented in figures 4.11 and 4.12, respectively. As above, HMDM cells were incubated with 200 μM 7,8-NP in the presence or absence of LC_{50} of oxLDL. The treatments were not statistically different from one another in total pterin or 7,8-NP[1]. However, given the size of the effect and the inter-experimental variance due to individual HMDM batch response, is likely that the test does not have sufficient power to detect a statistically significant effect of this magnitude.

OxLDL-induced oxidative stress resulted in the oxidation of 7,8-NP to neopterin which comprised 34% $\pm$ 11 (SEM) of the total intracellular pterin in HMDM cells at the end of 24 hours (figures 4.10 and 4.12). OxLDL treatment resulted in a slight elevation of the intracellular total pterin starting at 3-6 hours post-oxLDL addition (fig. 4.11). This was consistent with the onset of neopterin increase seen earlier (fig. 4.10) and continued during the remaining incubation time. Total pterin level encompasses both neopterin and 7,8-NP. Therefore, higher total pterin in oxLDL–treated cells was reflecting the increase in neopterin levels.

OxLDL caused an incremental change in the intracellular 7,8-NP level compared to the oxLDL–free control. This also commenced around 3-6 hours after the addition of oxLDL, but, contrary to the level of total pterin, this difference in 7,8-NP level between the treatments ceased by the 24^{th} hour as indicated by the fitted curves converging (fig. 4.12). Both oxLDL–treated and untreated cells showed slight decrease in intracellular total pterin concentration (due to a decrease in 7,8-NP concentration) after the first 12 hours of incubation, indicating potential oxidation to 7,8-DXP or reduced uptake of 7,8-NP.

[1]Each data set ($\pm$oxLDL) was either fitted with an individual or a shared nonlinear regression line in Prism5 as indicated (fig. 4.12a, b). The horizontal y asymptotes between the shared and individual fits were compared with extra sum of squares F test (α=0.50) to determine whether the treatments were significantly different from each other. The asymptotes were not significantly different with p=0.85 for 7,8-NP and total pterin likewise. This result was confirmed with the Bonferroni pairwise comparison of treatments at each individual time point after RM-one-factor ANOVA (n=3).

Extracellular concentrations of neopterin and total pterin were examined as well (fig. 4.13). The presence of oxLDL with HMDM led to a slightly reduced neopterin concentration in the extracellular medium (by $\sim$1 μM) and reduced total pterin concentration (by $\sim$20 μM) (fig. 4.13a and b, respectively).

[A]

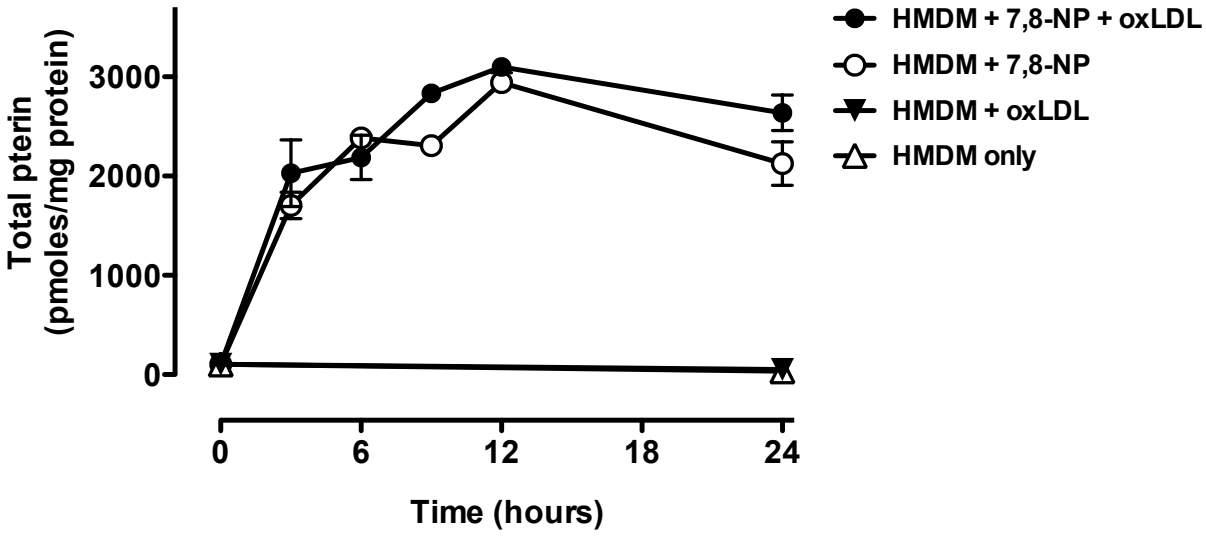

[B]

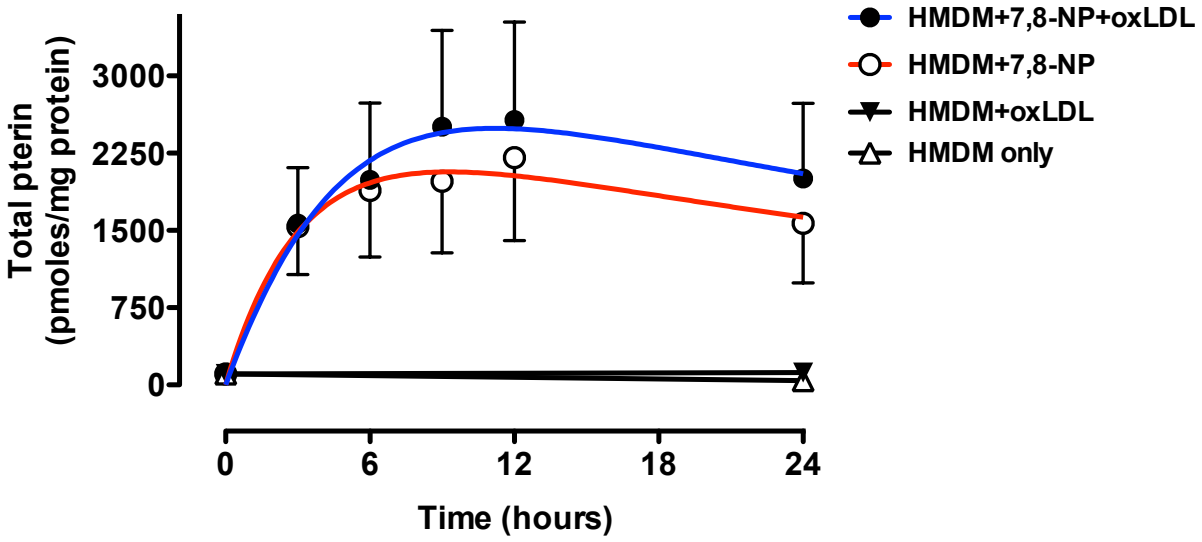

Figure 4.11: Intracellular total pterin level is elevated in oxLDL–treated HMDM cells.

HMDM cells ($1x10^6$ cells mL^{-1}) in the 2% serum-containing medium were incubated with 200 μM 7,8-NP in the presence (blue line, filled circles) or absence (red line, empty circles) of 2.5 mg/mL oxLDL. Cell lysates were collected at the indicated times and analysed for intracellular total pterin via HPLC. Protein was determined via BCA assay. For reference, [total pterin] in control cells at 12 hours ranged from 165 to 400 pmol/well. Results are displayed as mean ± SEM of mean values from **(A)** single experiment and **(B)** combined mean values from three separate experiments. Statistical analysis (on B) showed that non-linear regression fitted to data was not significantly different between the treatments.

[A]

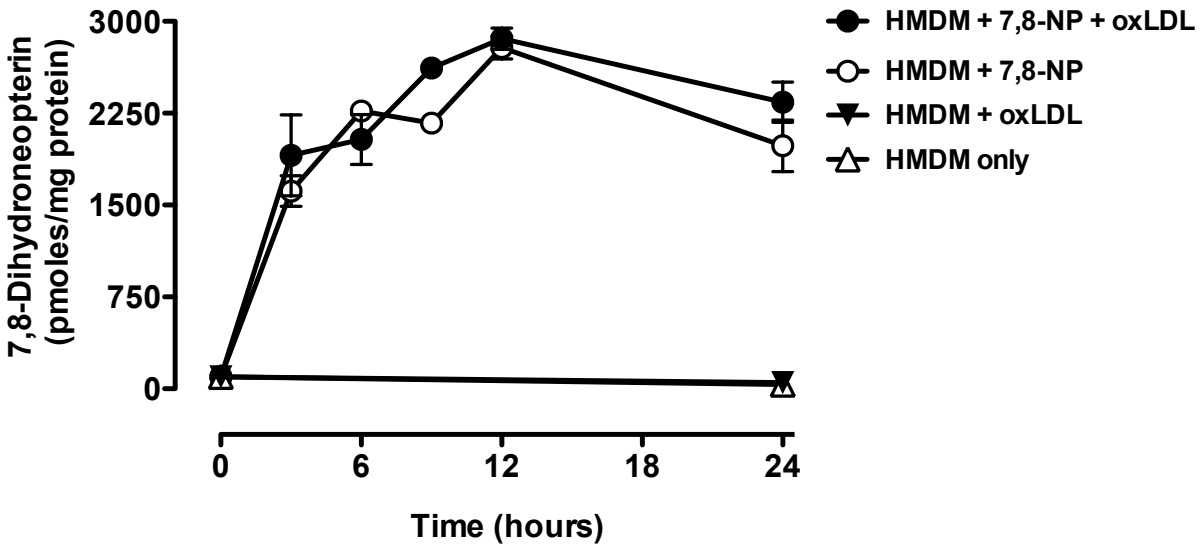

[B]

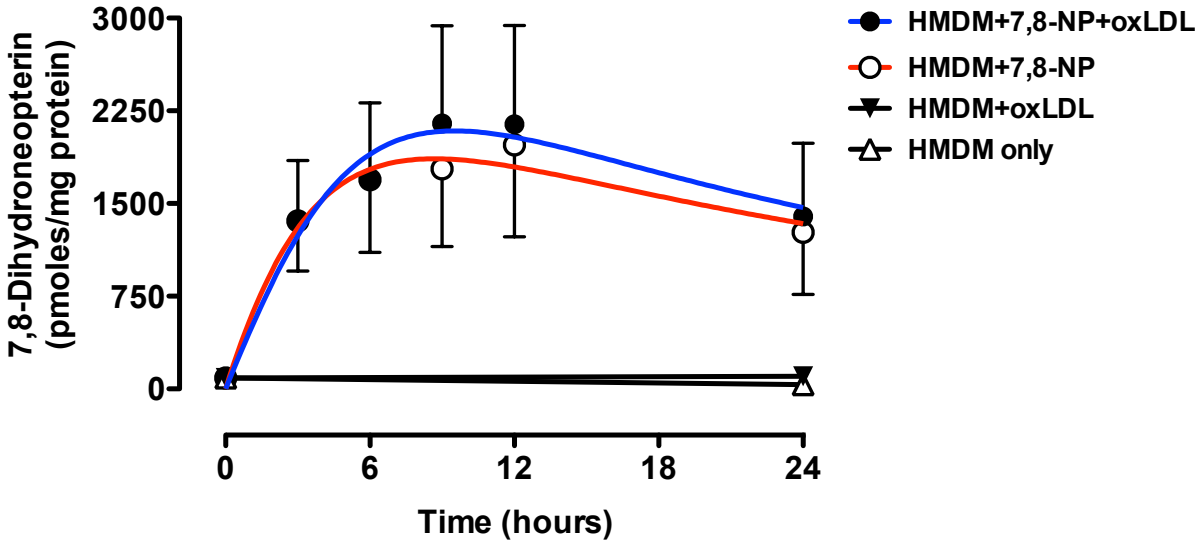

Figure 4.12: Intracellular 7,8-NP level is slightly altered by the presence of oxLDL with HMDM cells.

HMDM cells (1x10^6 cells mL^{-1}) in the 2% serum-containing medium were incubated with 200 μM 7,8-NP in the presence (blue line, filled circles) or absence (red line, empty circles) of 2.5 mg/mL oxLDL. Cell lysates were collected at the indicated times and analysed for intracellular neopterin and total pterin via HPLC, while 7,8-NP was calculated as the difference of the two. Protein was determined via BCA assay. Results are displayed as mean ± SEM of mean values from **(A)** single experiment and **(B)** combined mean values from three separate experiments. Statistical analysis (on B) showed that nonlinear regression fitted to data was not significantly different between the treatments.

[A]

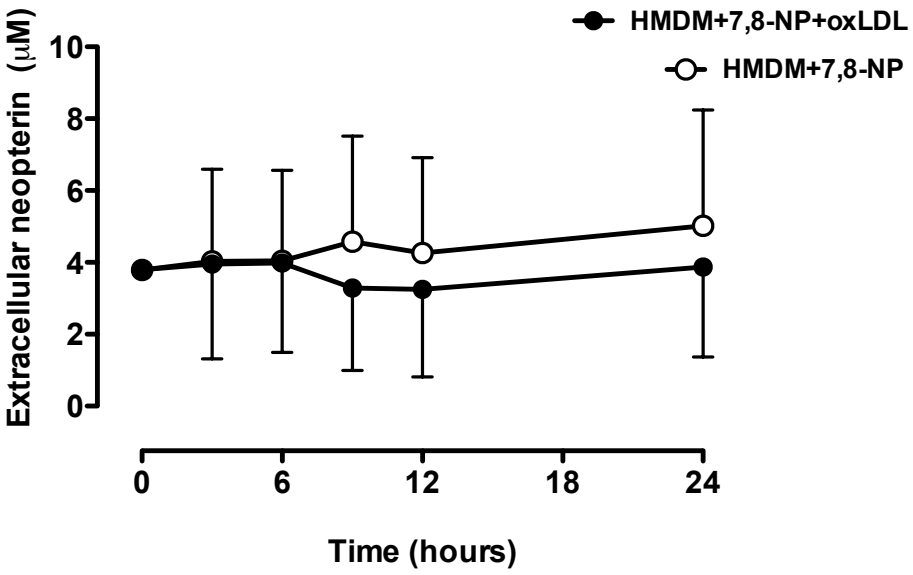

[B]

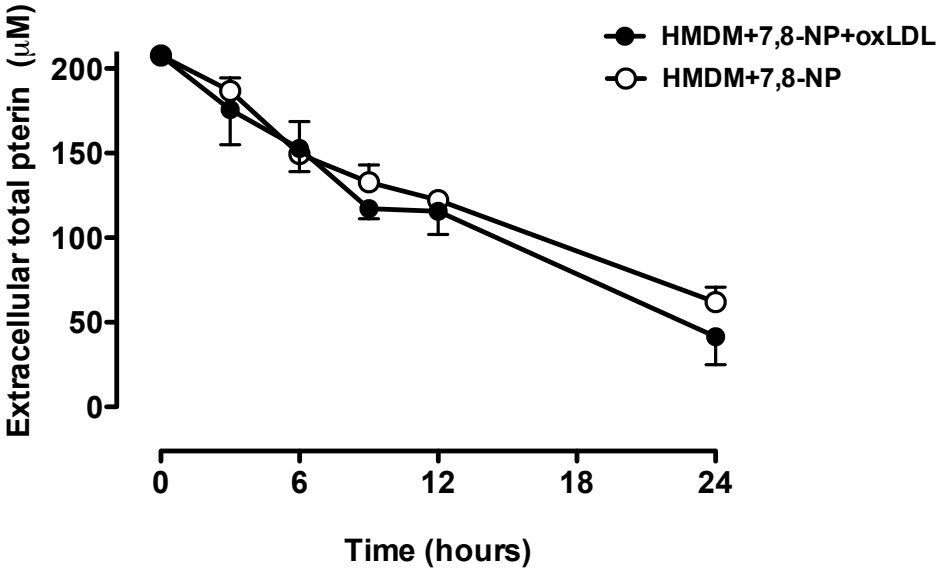

Figure 4.13: Extracellular neopterin and total pterin after oxLDL treatment of 7,8-NP loaded HMDM cells.

HMDM cells ($1x10^6$ cells mL^{-1}) in the 2% serum-containing medium were incubated with 200 μM 7,8-NP in the presence (filled circles) or absence (empty circles) of 2.5 mg/mL oxLDL. Supernatants were collected at the indicated times and analysed for neopterin and total pterin via HPLC. Results are displayed as mean ± SEM of combined mean values from three separate experiments. **(A)** neopterin and **(B)** total neopterin. Statistical analysis of regression line slopes did not reveal any difference between treatments for A or B, the difference at the 24 hour was not statistically significant (RM one factor ANOVA, Bonferroni test)

4.2.5 Does NOX play a role in oxLDL toxicity to HMDM cells?

Apocynin partially protects 7,8-NP from oxidation

In order to investigate the mechanism contributing to the oxidation of 7,8-NP and, thus, the source of oxidants, a NOX inhibitor, apocynin, was added to the cells. Apocynin was added to HMDM culture 3 hours prior to the addition of oxLDL to allow for the full inhibitory action, followed by the oxLDL treatment at the LC_{50} (2.5 or 3 mg/mL). Cellular neopterin was measured after 12 hours, as ROS production was previously shown to peak at this time point. The addition of 200 μM apocynin reduced 7,8-NP oxidation to neopterin caused by oxLDL addition by approximately 50% (fig. 4.14a, b). This did not return the average intracellular neopterin levels to the control levels of 173 pmol/mg cell protein (or 10.6 pmol/well) observed in 7,8-NP treated HMDM cells in the absence of oxLDL (fig. 4.14a).

[A]

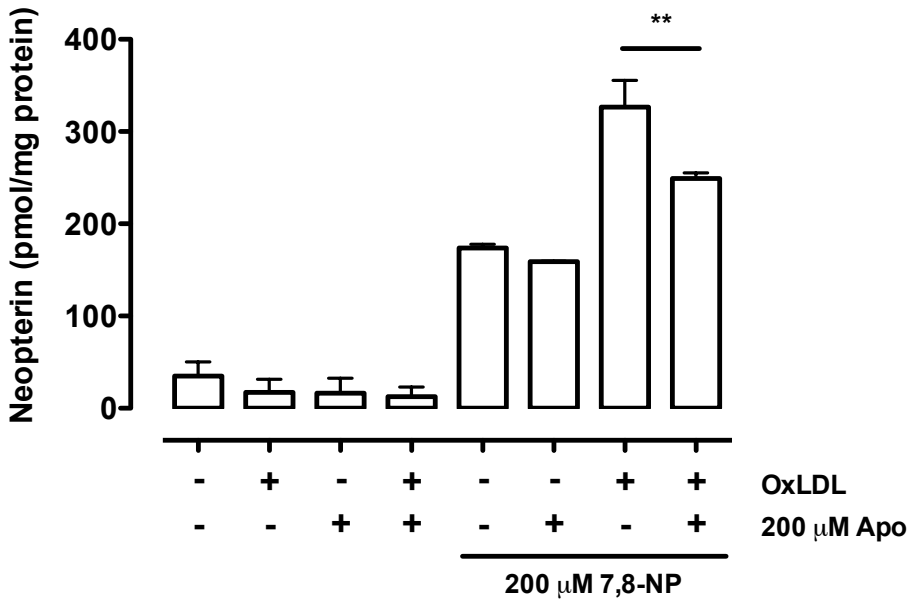

[B]

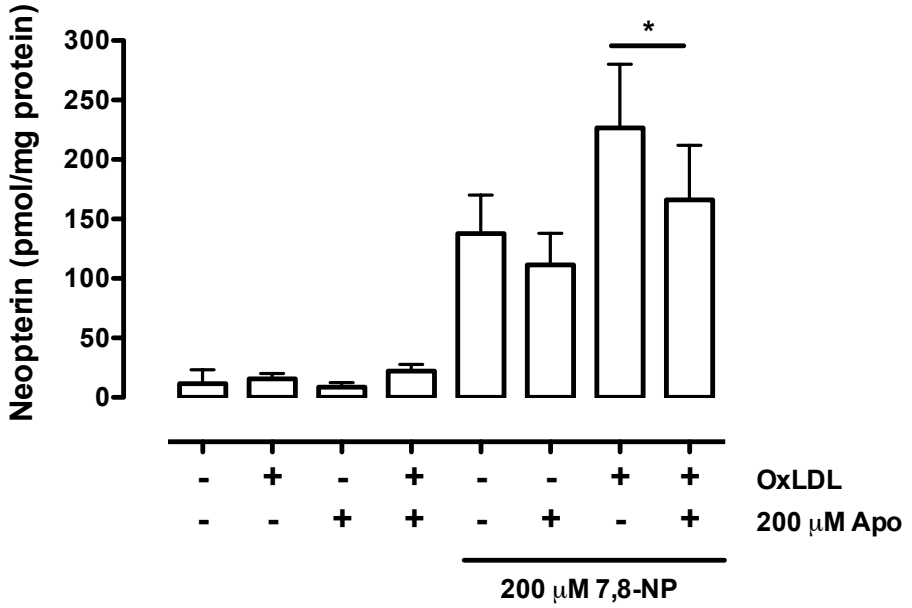

Figure 4.14: Apocynin partially inhibits 7,8-NP oxidation to neopterin in oxLDL-treated HMDM cells.

HMDM (1x10^6 cells mL^{-1}), pre-treated with 200 μM apocynin (Apo) for 3 hours, were incubated with 2.5 mg/mL oxLDL and 200 μM 7,8-NP in the presence of apocynin for a further 12 hours. Cell lysates were analysed for intracellular neopterin via HPLC. Results are displayed as mean ± SEM of mean values from **(A)** single experiment and **(B)** combined mean values from three separate experiments. For reference, average [neopterin] in 7,8-NP control cells was 6.6 pmol/well. Statistical significance ((A) one-factor ANOVA with Bonferroni pairwise comparison and (B) paired t-test) is as indicated: *, $p<0.05$; **, $p<0.01$.

Apocynin does not protect HMDM cells from oxLDL–mediated cell death

To investigate the effect of NOX–derived ROS on oxLDL–induced HMDM cell death and survival, the apocynin treatment of macrophages exposed to oxLDL was followed by a cell viability assay. Preliminary experiments showed that apocynin was not toxic to HMDM over 27 hours (fig. 4.15) at the concentrations tested of up to 300 μM. Therefore, HMDM cells were incubated with apocynin and oxLDL for 24 hours and assessed for cellular viability. Despite the observed inhibition of oxidative process in HMDM, 200 μM apocynin did not protect HMDM from oxLDL-induced cell death after 24 hours of incubation (fig. 4.16a). Lower concentrations of 50 and 100 μM apocynin did not convey any protection against oxLDL toxicity, either, as HMDM cells showed the similar levels of viability loss across the range of apocynin concentrations tested (fig.4.16b).

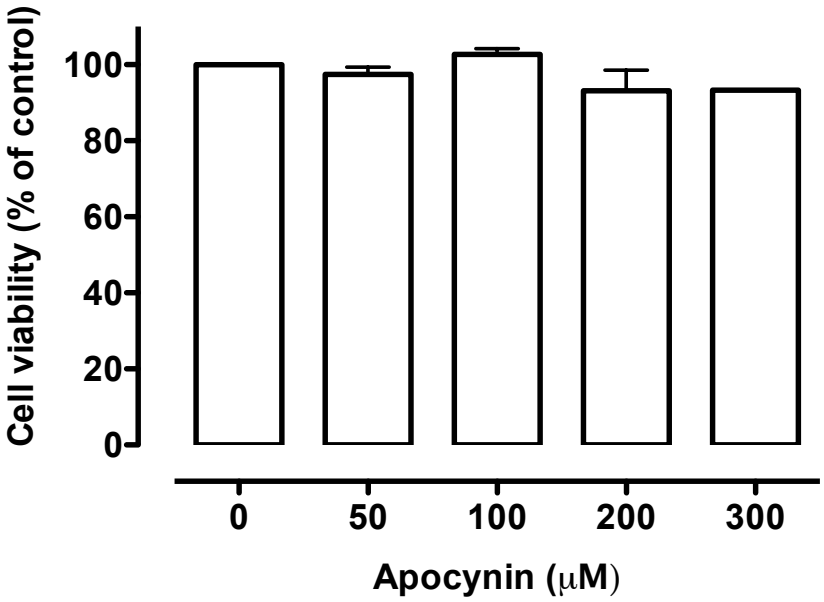

Figure 4.15: Apocynin is not toxic to HMDM cells.
HMDM ($5x10^5$ cells mL^{-1}) in the whole medium were incubated with increasing concentrations of apocynin for 27 hours. Cell viability loss was measured by MTT reduction. Results are displayed as percentage of remaining cell viability relative to untreated control, shown as mean ± SEM of experimental means from two separate experiments. Statistical analysis on raw data (one-factor ANOVA) revealed no significant differences.

[A]

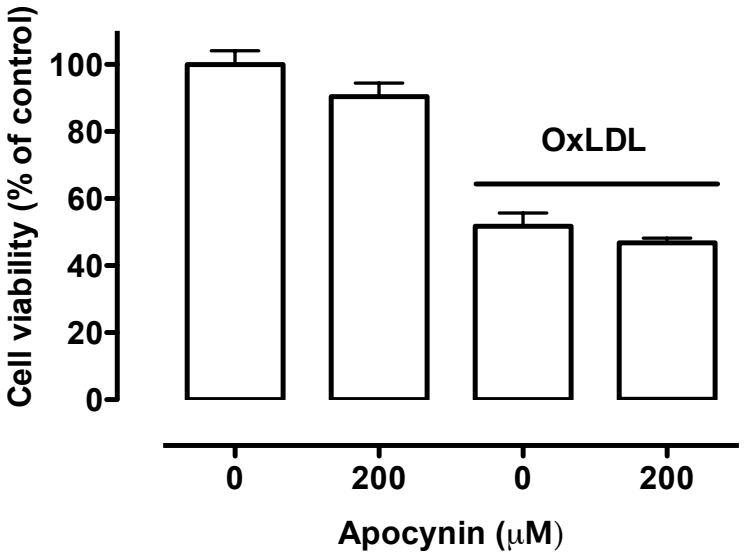

[B]

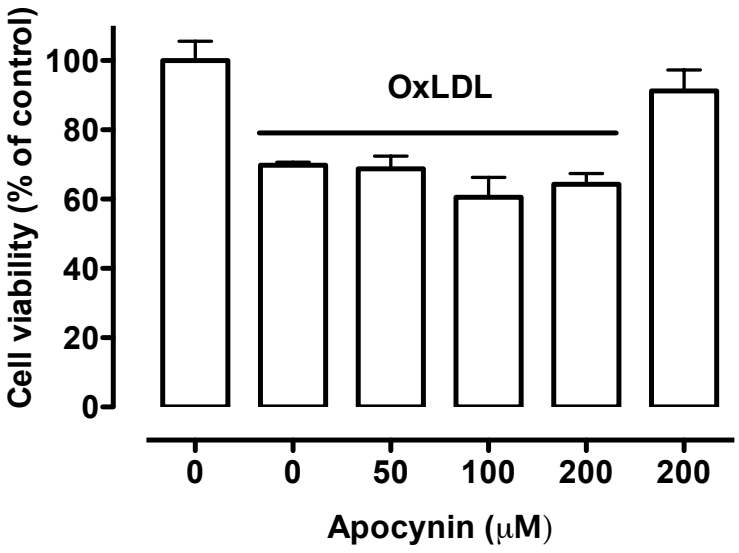

Figure 4.16: Apocynin does not protect HMDM cells against oxLDL (MTT). HMDM (1x10^5 cells mL^{-1}), pre-treated with the indicated concentrations of apocynin for 3 hours, were incubated with oxLDL in the presence of apocynin for a further 24 hours. Cell viability loss was measured by MTT reduction. Results are displayed as percentage of remaining cell viability relative to control, shown as mean ± SEM of triplicate measurements from a single experiment. **(A)** and **(B)** represent two separate experiments. ± Apocynin treatments were not statistically different (one-factor ANOVA).

Since oxidative stress in HMDM cells in response to oxLDL was an early event, the incubation time of the experiments was shortened from 24 to 15 hours. HMDM cells were treated with oxLDL for 15 instead of 24 hours and the cellular viability was assessed with an ApoAlert kit (BD). HMDM cells were harvested into Accutase™, incubated with Annexin V and propidium iodide (PI) and assessed for a shift in cellular fluorescence that corresponded to apoptosis (annexin^{+}) and necrosis (PI^{+}) by flow cytometery. The channels were compensated for spectral overlap by adjustment with single dye control cells permeabilised with 2% paraformaldehyde. Each sample output was gated based on forward/side scatter and split into annexin$^{+/-}$ and PI$^{+/-}$ quadrants (fig. 4.17). The experimental results are presented as a comparison between annexin^{+} and PI^{+} treatments (not mutually exclusive, fig. 4.18a) and a mutually exclusive separation into four quadrants (fig. 4.18b). No significant difference in the percentage of cells stained with PI or Annexin V was detected between the ± apocynin treatments in the presence of 2.5 mg/mL oxLDL (fig.4.18a). A slight re-distribution of annexin V staining was observed in the apocynin-oxLDL–treated cells (fig. 4.18b, grey and black bars), yet the difference was not statistically significant ($p>0.05$). The experiment was repeated with a range of apocynin concentrations (fig. 4.19). A slight concentration dependant reduction in the frequency of annexin^{+} cells was observed, yet the result was not statistically significant (fig. 4.19a). No statistical difference was observed in the relative quadrant frequency distribution, either. Thus, the distribution of apoptotic, necrotic and live HMDM cells after oxLDL treatment was unaffected by the presence of apocynin (fig. 4.18 and 4.19), which suggests that apocynin was not protective against oxLDL toxicity, despite its ability to reduce 7,8-NP oxidation.

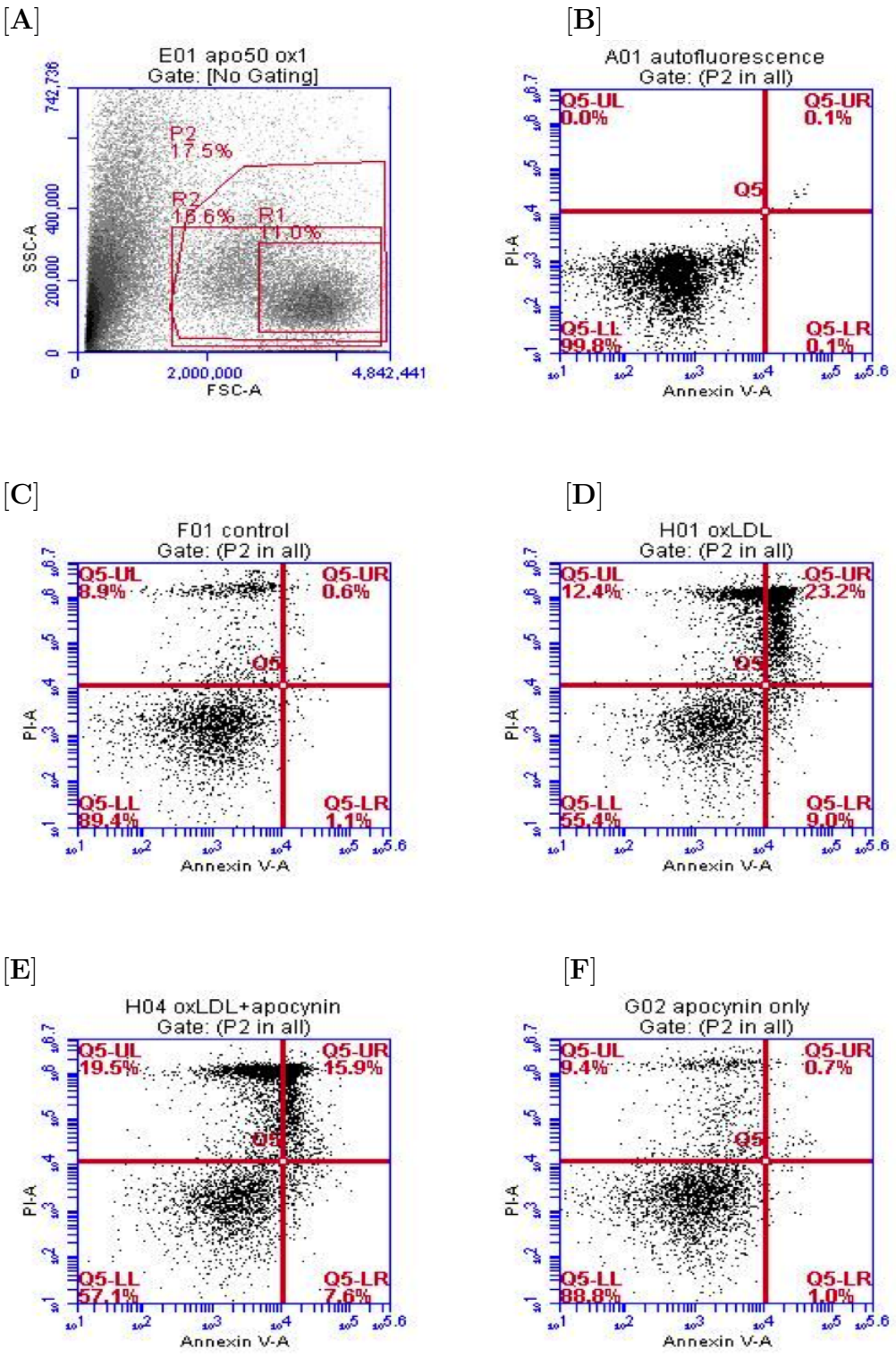

Figure 4.17: Annexin V and PI quadrant identification on flow cytometer output.

Break down of the flow cytometry output for Annexin V/PI HMDM cell staining is presented. **(A)** Gating for HMDM cells (P2 gate); **(B)** HMDM cells autofluorescence; **(C)** HMDM cells control; **(D)** oxLDL–treated HMDM cells; **(E)** oxLDL and apocynin–treated HMDM cells; **(F)** apocynin only control HMDM cells.

[A]

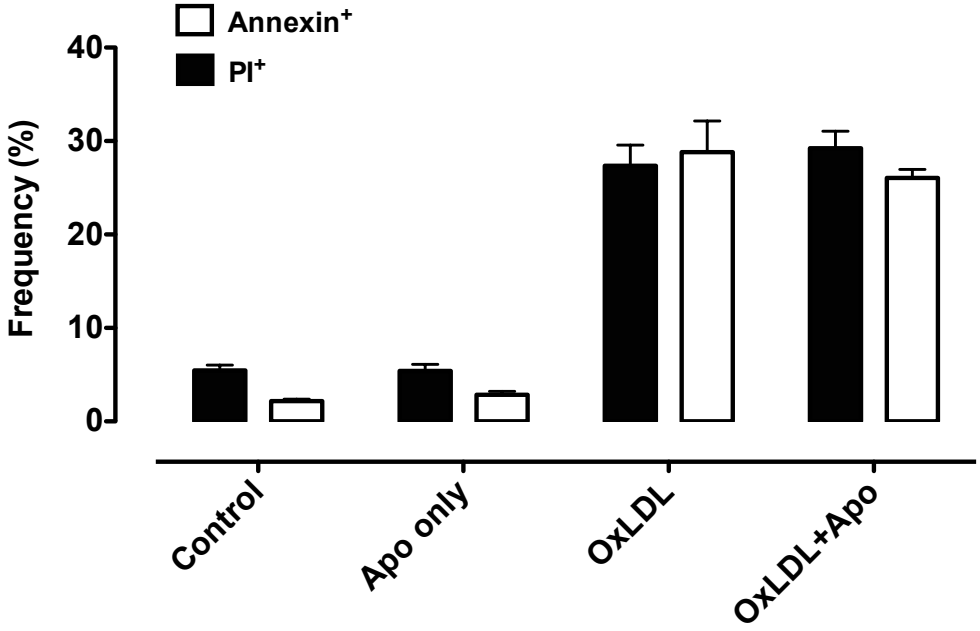

Figure 4.18: Apocynin does not protect HMDM cells against oxLDL at 200 μM (Annexin V and PI).

HMDM (1x10^5 cells mL^{-1}) pre-treated with 200 μM of apocynin (Apo) for 3 hours, were incubated with 2.5 mg/mL oxLDL in the presence of apocynin for a further 15 hours. The presence of apoptosis/necrosis was measured by flow cytometry after the cells were detached with Accutase™and stained for Annexin V and PI. Results are displayed as percentage of cells with the respective staining **(A)** or in the respective quadrant **(B: next page)**, displayed as mean ± SEM of triplicate measurements from a single experiment. No statistically significant difference was detected between ± Apo treatments (one-factor ANOVA with Bonferroni post test comparing ± Apo on oxLDL–treated HMDM cells).

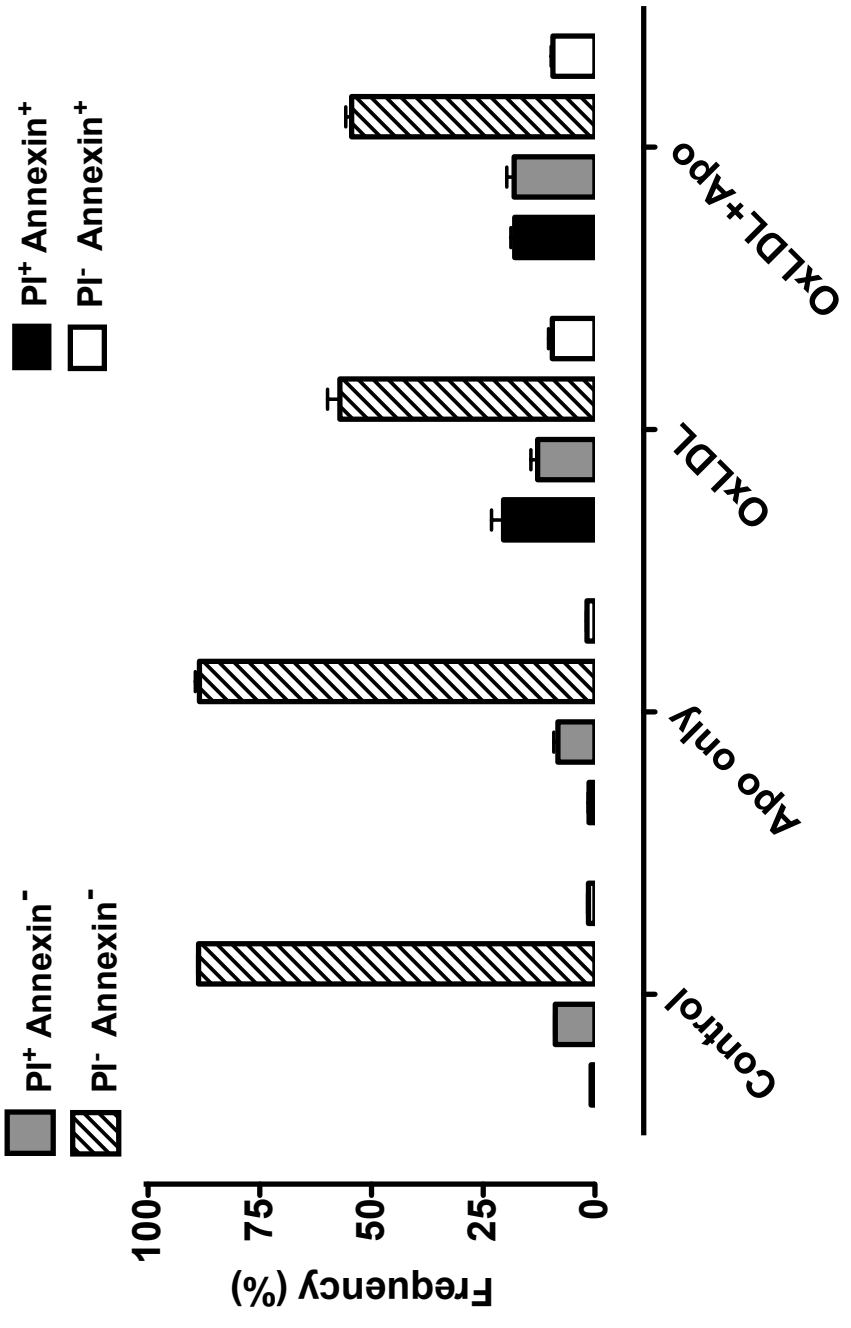

[B] Figure 4.18. Continued.

[A]

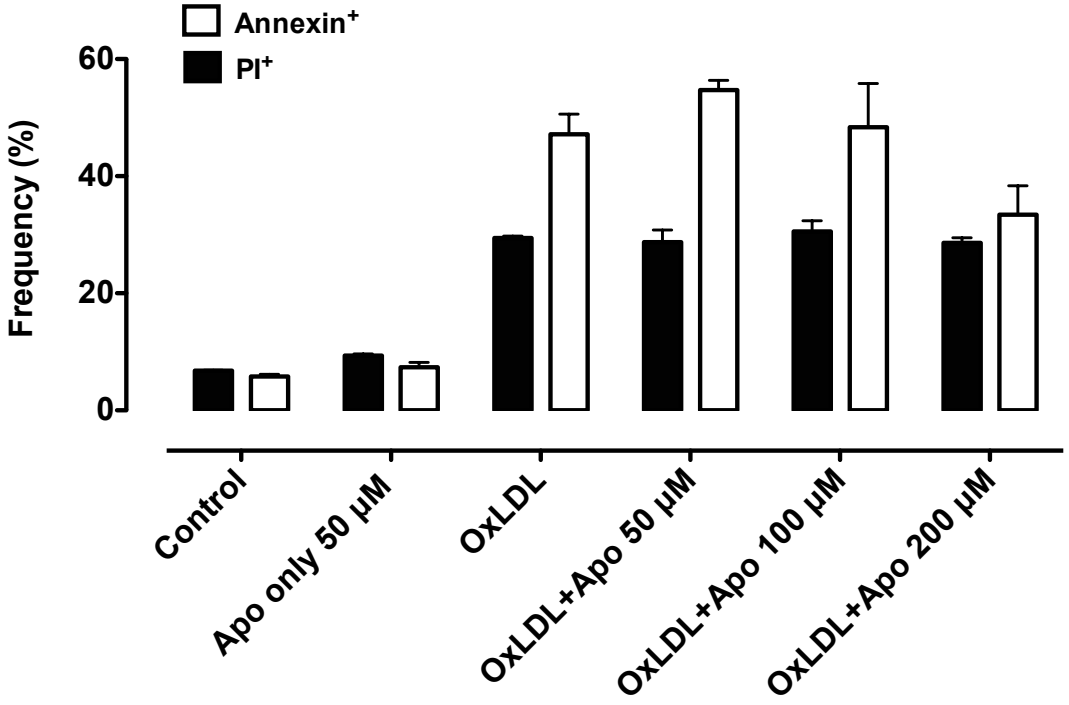

Figure 4.19: Apocynin at a range of concentrations does not protect HMDM cells against oxLDL (Annexin V and PI).
HMDM (1x10^5 cells mL^{-1}), pre-treated with the indicated concentrations of apocynin (Apo) for 3 hours, were incubated with 2.5 mg/mL oxLDL in the presence of apocynin for a further 15 hours. The presence of apoptosis/necrosis was measured by flow cytometry after the cells were detached with Accutase™and stained for Annexin V and PI. Results are displayed as percentage of cells with the respective staining **(A)** or in the respective quadrant **(B: next page)**, displayed as mean ± SEM of triplicate measurements from a single experiment. No statistically significant difference was detected between ± Apo treatments (one-factor ANOVA with Dunnett's post test comparing to oxLDL–treated HMDM cells).

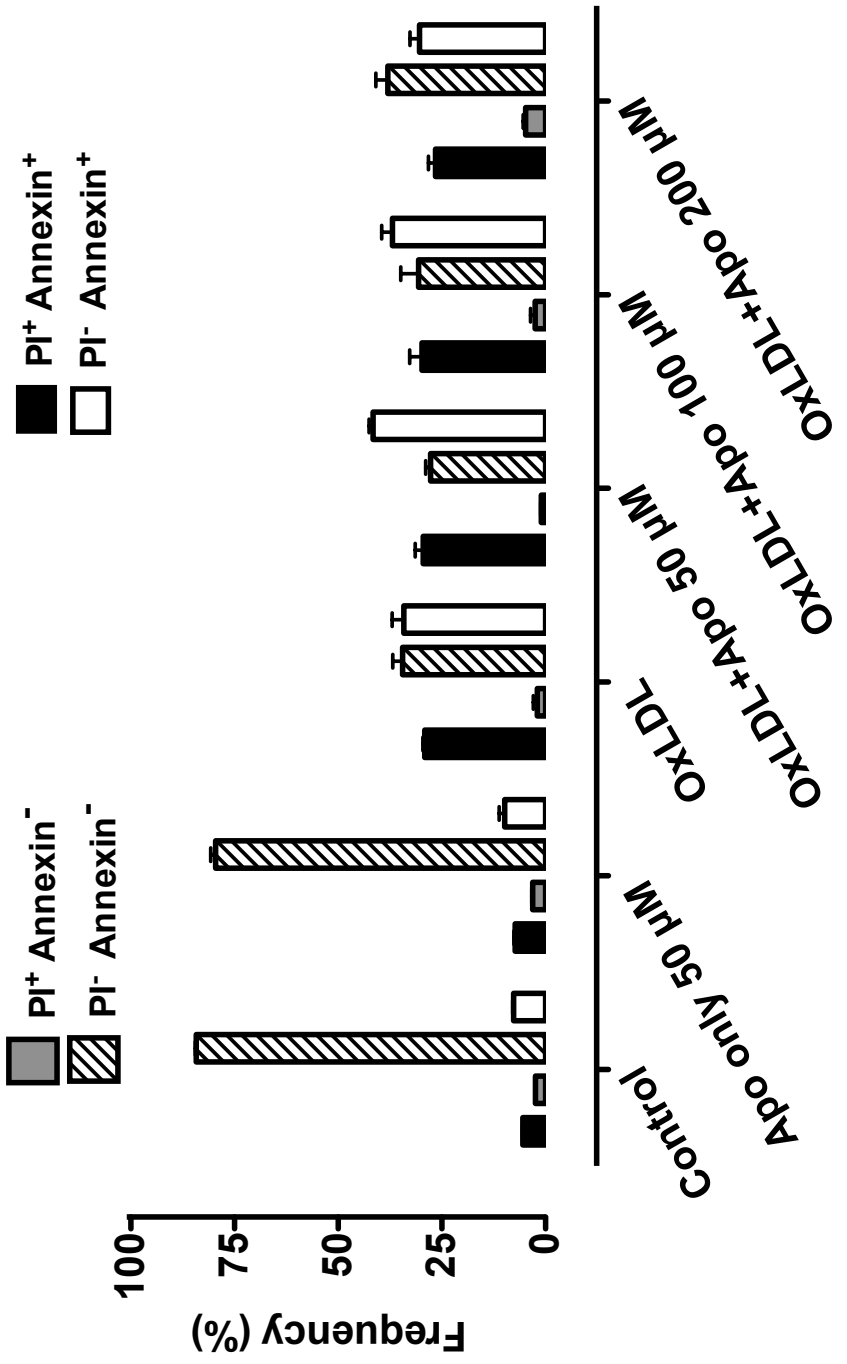

[B] Figure 4.19. Continued.

4.3 Discussion

4.3.1 7,8-NP–mediated protection of HMDM from oxLDL

Although 7,8-dihydroneopterin has been shown to protect HMDM cells from oxLDL–mediated death (Gieseg *et al.*, 2010a; Katouah, 2012), the result had to be confirmed in the current experimental setting to avoid any cell-specific artifacts. The present study successfully confirmed that exogenously applied 200 μM 7,8-NP protects HMDM cells from acute cellular death triggered by oxidatively modified lipoprotein (fig. 4.1). The study went on to show that 200 μM 7,8-NP effectively inhibited oxLDL–mediated HMDM cell viability loss at all time points over the course of 24 hours, providing, on average, a 30% protection at LC_{50} (fig. 4.2). The protective effect was almost absolute at 12 hours, but reduced in the second half of the incubation as indicated by a steeper slope (fig. 4.2b). A similar trend was observed previously with 7,8-NP–mediated protection against GSH loss, characterised by complete inhibition in the first 12 hours, followed by a gradual decrease over the 12–24 hours (Gieseg *et al.*, 2010a). Such kinetics could indicate either that the magnitude of 7,8-NP protection was a constant 30% of the remaining cell viability or that the effect of 7,8-NP–mediated protection diminished after the first 12 hours of acute toxic exposure to oxLDL. The latter could result from two mechanisms: the nature of the oxidative processes triggered in HMDM by oxLDL and/or a reduction of 7,8-NP uptake by the cells.

4.3.2 Antioxidant activity of 7,8-NP

7,8-NP reduces oxidative flux in HMDM cells

Our research group has previously proposed that antioxidant properties of 7,8-NP mediate cell protection against oxLDL damage (Baird *et al.*, 2005; Gieseg *et al.*, 2010a). This was based on the observations of 7,8-NP inhibiting GSH loss and protein hydroperoxide formation in THP-1 and monocyte cells treated with AAPH (Duggan *et al.*, 2002; Kappler *et al.*, 2007). The present work is the first to quantitatively assess the magnitude of 7,8-NP–mediated reduction of intracellular ROS as triggered by oxLDL. 7,8-NP was most effective at scavenging/inhibiting ROS during the time of severe oxidative flux (fig. 4.9). The highest rate of ROS production was observed during the first 6 hours and the highest mean intracellular ROS was detected at 12 hours after oxLDL addition (fig. 4.9). This corresponded to the time period when 7,8-NP was most effective at suppressing intracellular ROS at 3, 6 and, to a lesser

degree, 12 hours (fig. 4.9b). Higher 7,8-NP protection coincided with high oxidative flux suggesting that 7,8-NP might be protecting HMDM via scavenging of ROS.

The slope of the cell viability regression in the absence of 7,8-NP was steeper during the 0–12 hours than during 12–24 hours (fig. 4.2), indicating that toxic processes during the first stage had more impact on the loss of metabolic capacity than the processes in the second stage. The slope of viability loss by 7,8-NP-protected cells was less steep during the first stage than during the second stage, indicating higher protection. A hypothesis is proposed that antioxidant 7,8-NP is effective at protecting HMDM cells from the detrimental effects of early acute oxidative flux, but is less likely to confer protection over the second half of acute oxLDL exposure, perhaps, due to cellular processes of a different nature. The ability of 7,8-NP to suppress initial ROS produced by HMDM cells in response to acutely toxic oxLDL concentration may be highly beneficial in maintaining intracellular redox balance, as well as the reducing environment within a plaque, thus delaying plaque development. In support of this hypothesis, Gieseg *et al.* (2010a) reported that 7,8-NP completely protected intracellular GSH from oxLDL up to 12 hours. This protection decreased by approximately 18% over the following 12 hours of incubation . The rate of intracellular GSH loss was identical during 12–24 hours between 7,8-NP–treated and untreated HMDM cells, which also suggests that the processes during the second half of incubation may involve non-7,8-NP–amenable mechanisms. Taken together, the data suggest that the nature of oxLDL toxicity (manifested as ROS generation and oxidative stress) during the first 12 hours of incubation determined the effectiveness of 7,8-NP in protecting HMDM from oxLDL-mediated cell death during this time period.

7,8-NP's effect on viability and ROS decline may be due to its ability to scavenge peroxyl radical as shown by Duggan *et al.* (2001, 2002); Oettl *et al.* (1997). Trolox, also a peroxyl radical scavenger, was shown to restore mitochondrial polarisation and completely prevent human macrophage death from oxLDL–induced death (Asmis & Begley, 2003). Research from our laboratory demonstrated that 7,8-NP inhibited cellular damage to erythrocytes and the monocyte-like U937 cells from a range of oxidants such as hydrogen peroxide, hypochlorite, aqueous peroxyl and direct plasma membrane oxidation by ferrous ions (Duggan *et al.*, 2002; Gieseg *et al.*, 2001a,b). Thus, radical scavenging capacity of 7,8-NP may explain its effectiveness at the initial stages of ROS formation. Atherosclerotic plaques are often considered oxidative environments (Stocker & Keaney, 2004). Extracellular availability of 7,8-NP in such

environment would be advantageous at suppressing oxidative damage.

Inhibition of ROS formation by 7,8-NP was not investigated as part of this work due to difficulty in discerning inhibition vs. direct scavenging of oxidants when measuring oxidative flux. The inhibition of NOX assembly via $p47^{phox}$ phosphorylation in a U937 monocyte-like cell line was found to be unaffected by 7,8-NP (Chen, 2012). U937 cells are often used as a model for human macrophages due to the similarity in manifestation of oxLDL–mediated toxicity, such as absence of caspase activation, rapid oxidative stress and necrotic cell lysis as opposed to apoptotic cell shrinkage (Baird *et al.*, 2004; Katouah, 2012). This fact and the ability of 7,8-NP to protect both U937 and HMDM cells (Baird *et al.*, 2005; Gieseg *et al.*, 2010a) suggest that 7,8-NP may act similarly in both cell types and, therefore, not inhibit NOX assembly in HMDM cells. There is some evidence that neopterin, however, displays NOX inhibition. Kojima *et al.* (1992) reported weak scavenging activity of neopterin in the xanthine/xanthine oxidase system with 50% inhibitory concentration (IC_{50}) of 370 μM and a stronger inhibitory activity in splenic macrophage/PMA-reaction system with IC_{50} of 1.1 μM. On the basis of high vs. low IC_{50}, the authors suggested that neopterin acted as a scavenger in the former but inhibited the $O_2^{\bullet-}$ production in the latter system. The same group of authors also demonstrated that neopterin competitively inhibited the superoxide generation in the whole-cell macrophage/PMA reaction system; IC_{50} for neopterin was 1.39 μM and K_i was 6.5 μM (Kojima *et al.*, 1993). The authors did not propose a mechanism, but the structural similarity of neopterin/7,8-NP to flavin adenine dinucleotide (FAD), a NOX co-factor, could play a role. At present, it is difficult to evaluate whether neopterin-mediated inhibition of NOX took place in the HMDM cells exposed to oxLDL in this study. ROS and $O_2^{\bullet-}$ in particular, measured by DHE-product fluorescence decreased after the 12^{th} hour of incubation, when intracellular neopterin levels started to raise, indicating potential association. Yet, the concentration of extracellular neopterin after the 3^{rd} hour was close to or above 5 μM even in the control (no oxLDL) wells (fig. 4.3b), which exceeded the IC_{50} and approached K_i reported by Kojima *et al.* (1993) and Kojima *et al.* (1992). Thus, conclusive assessment of the NOX inhibitory action of neopterin generated through 7,8-NP oxidation in this study cannot be made and will require further investigation.

Neopterin formation from 7,8-NP in HMDM upon oxLDL exposure

If 7,8-NP were scavenging ROS generated by HMDM cells in response to oxLDL, it would be oxidised in the process (Gieseg *et al.*, 2001a). Indeed, an oxLDL–dependant elevation of intracellular neopterin was observed in 7,8-NP–treated HMDM cells in response to oxLDL (fig. 4.10). The rate of neopterin formation after the first 3 hours was relatively constant. It is likely that the neopterin measured at 3 hours, was taken up by the cells from the extracellular medium. The three hour sample was the first one collected after the addition of 7,8-NP. It showed a similar level of neopterin in treatment and control cells and followed similar kinetics to those observed in the cell-free RPMI-1640 (fig. 4.3b). The process of cell culture alone has been proposed to generate substantial oxidative stress (Halliwell, 2003), perhaps contributing to the baseline oxidation of 7,8-NP. Neopterin formation above control levels was evident as early as at 6 hours, coinciding with the timing of oxidative stress. Intracellular neopterin formed by the end of the 24 hour oxLDL incubation constituted 34 ± 11 % (SEM) of the total intracellular pterin in HMDM cells. Linearity of increase demonstrated a constant rate of neopterin formation, and, therefore, a constant rate of 7,8-NP oxidation over the course of the experiment. This implied a constant rate of oxidant generation, which was contrary to the oxidative stress measurement by DHE, as the rate of ethidium (E^+)/2-OH-HE formation showed a third order polynomial kinetics (Prism5). The DHE probe measured $O_2^{\bullet-}$ and, potentially, other oxidants like H_2O_2 in the presence of heme proteins (Fernandes *et al.*, 2006), whereas 7,8-NP oxidation to neopterin was the result of a reaction with HOCl (Widner *et al.*, 2000). The reaction of 7,8-NP with HOCl is the only known physiologically relevant mechanism that generates neopterin from 7,8-NP that has been experimentally demonstrated (Fuchs *et al.*, 2009; Widner *et al.*, 2000). Macrophages differentiated with GM-CSF contain MPO and produce HOCl (Sugiyama *et al.*, 2001), thus making this mechanism a likely route for 7,8-NP oxidation. This area deserves further investigation.

At this stage it is impossible to infer the relationship between $O_2^{\bullet-}$ and the formation of downstream ROS, such as peroxide and peroxyl radicals. The cumulative reaction of a suite of such species with DHE may show a variable rate of ROS formation as seen in fig. 4.9. Alternatively, non-linear rate of activation of ROS–producing enzymes may account for the increasing rate of ROS formation in the first 6 hours post oxLDL addition. 7,8-NP was shown to delay (by 3 hours) and suppress this chain of reactions (fig. 4.9). As opposed to superoxide measurement, neopterin formation is a secondary marker of oxidative stress, it is not the initial product of radical gener-

ation, and thus, could have different kinetics than the initial ROS release measured by DHE.

Other ROS involvement in 7,8-oxidation.

To gain further understanding of the kinetics of 7,8-NP oxidation in cells, the level of intracellular 7,8-NP during HMDM cell exposure to oxLDL was assessed. Due to the nature of the assay, 7,8-NP was calculated as the difference between total pterin and neopterin (figures 4.11 and 4.10). HMDM cells were found to maintain a relatively constant level of 7,8-NP between control and oxLDL–treated cells throughout incubation (fig. 4.12). Total pterin was slightly elevated in the oxLDL–treated cells, starting between 3 and 6 hours after initial exposure, which was due to neopterin increase in these cells (fig. 4.11). HMDM cells displayed a small difference between control and oxLDL–exposed cells 7,8-NP levels at around 9 and 12 hours, but the regression lines converged again at 24 hours (fig. 4.12). This difference was 17% at 12 hours as defined by the regression curves. One possible explanation for it could be that oxLDL up-regulated the transport of 7,8-NP into the HMDM cells through oxidative signaling, for example, IFN-γ which had been shown to rise after oxLDL treatment Huang *et al.* (1995) and this cytokine can regulate concentrative nucleoside transporter (CNT) (Soler *et al.*, 2001). CNT is partially responsible for trafficking of 7,8-NP into the cells (Tejraj Janmale, unpublished observations).

Extracellular total pterin showed a 10% difference (20 μM of initial 200 μM) between the oxLDL–treated and non-treated cells (fig. 4.13). Due to the magnitude of inter-experimental error, the result has to be interpreted with caution. Yet figure 4.13, perhaps, points towards a process, either intra- or extracellular, that guided a conversion of 7,8-NP to a non-neopterin product in oxLDL–treated cells. This was expected because the available literature proposes that a) oxygen–centered radicals, like $O_2^{\bullet-}$ and H_2O_2 and peroxyl radicals oxidise 7,8-NP into 7,8-DXP b) 7,8-NP had been shown to react with these radicals (Gieseg *et al.*, 2001a; Oettl *et al.*, 1997) and c) 7,8-NP had suppressed the intracellular $O_2^{\bullet-}$ flux in this study (fig. 4.9).

7,8-NP decreased the levels of DHE–reactive ROS, proposed to be primarily $O_2^{\bullet-}$ and H_2O_2-derivatives (Kobzik *et al.*, 1990; Rothe & Valet, 1990; Tarpey, 2004), suggesting that 7,8-NP could scavenge these oxidants. The rate constants for reactions of 7,8-NP with $O_2^{\bullet-}$ and peroxyl radical are $10^3 M^{-1}s$ and $10^7 M^{-1}s$, respectively (Oettl *et al.*, 1997), suggesting that 7,8-NP was likely scavenging peroxyl radicals rather

than $O_2^{\bullet-}$. 7,8-NP was also more likely to react with $ONOO^-$, a product of $O_2^{\bullet-}$ reaction with , rather than superoxide itself (Oettl *et al.*, 2004b), as $ONOO^-$ formation approaches the rate of diffusion (Beckman & Koppenol, 1996). Taken together, the data indicates that during oxLDL-mediated oxidative stress, 7,8-NP could also scavenge peroxyl radicals, not just HOCl, and the evidence for this is found in the extracellular medium. Unfortunately, due to the maintenance of constant 7,8-NP in the cell, the existence of these two processes could not be compared intracellularly. Thus, the results discussed so far have established that oxLDL triggered oxidative stress in HMDM cells that is partially suppressed by 7,8-NP. There is some debate, however, over the source of these oxidants.

NOX as a source of oxidants that yield neopterin

The literature on phagocytic NOX suggests that it plays a pivotal role in the generation of ROS, and that NOX inhibition and ROS reduction result in alleviated oxidative stress and cell survival (Aviram *et al.*, 1996; Bae *et al.*, 2009; Park *et al.*, 2009; Paterniti *et al.*, 2010; Sukhanov *et al.*, 2006). It was, therefore, hypothesised that inhibition of NOX in HMDM cells would decrease oxLDL–triggered oxidative processes and improve cell survival.

Although no specific inhibitors of NOX are known (Bedard & Krause, 2007), apocynin has been widely used for this purpose. Apocynin is a well known inhibitor of NOX (Bedard & Krause, 2007). Although recently a new class of NOX inhibitors with improved specificity has emerged (Wingler *et al.*, 2011), apocynin was used in this study due to its availability. Most of known limitations of apocynin did not present a problem for the present study. Firstly, apocynin is a pro-drug activated by cellular peroxidases, including MPO (Stolk *et al.*, 1994), which is present in the HMDM cells cultured with GM-CSF as was done in this study (Sugiyama *et al.*, 2001). Secondly, the cytosolic subunits, whose translocation to the plasma membrane is inhibited by apocynin are present in the phagocytic NOX2 homologue, classic of macrophages (Bedard & Krause, 2007; Stolk *et al.*, 1994). Thirdly, because this work focused on phagocytes, a recent report of apocynin's ROS scavenging activity in non-phagocytic cells did not present an obstacle (Heumüller *et al.*, 2008). Thus, it was chosen as a NOX inhibitor, while 7,8-NP oxidation to neopterin was used as an intracellular ROS probe.

Apocynin, incubated with 7,8-NP–containing HMDM cells for 12 hours in the presence of oxLDL, prevented the increase in intracellular 7,8-NP oxidation to neopterin by half (fig. 4.14), suggesting that NOX is one of the key sources of ROS that lead to 7,8-NP oxidation. Indeed, NOX has been responsible for oxLDL–mediated ROS release in a number of cells: mouse peritoneal macrophages and HMDM cells (Park *et al.*, 2009), SMCs (Sukhanov *et al.*, 2006) and J774 cells (Bae *et al.*, 2009). Based on this preliminary results, the following mechanism of ROS flux in oxLDL–mediated cells is proposed: generation of $O_2^{\bullet -}$ by activated NOX, which is then dismutated into H_2O_2 by SOD, which is then reacted with chloride ion (Cl^-) via myeloperoxidase (MPO) to produce HOCl that oxidises 7,8-NP to neopterin. Since NOX inhibition did not prevent oxidation completely, the remaining HOCl could have had a different source. For example, superoxide produced through the uncoupling of the mitochondrial electron transport chain. Recently, Chen (2012) demonstrated that mitochondrial superoxide was elevated upon oxLDL treatment of this monocyte-like cell line. By analogy, this may be a mechanism for HMDM cells. Sukhanov *et al.* (2006) also showed that apocynin and another NOX blocker only partially prevented GAPDH downregulation by oxLDL, while Park *et al.* (2009) demonstrated a 40% restoration by apocynin of macrophage migration inhibited by oxLDL. Since 7,8-NP was able to recover/react with ROS from multiple sources, it was considered a more effective intervention than NOX inhibitor apocynin, in terms of its oxidative-stress–mediating action. Alternatively, incomplete inhibition of 7,8-NP oxidation could have been due to the lack of specificity of apocynin, as NOX inhibitor. The use of recently developed inhibitors of VAS family is suggested for future investigation of the relative contribution of ROS sources during oxLDL–mediated oxidative flux (Altenhöfer *et al.*, 2012).

Significance of apocynin-mediated NOX inhibition for HMDM cell death

The developing hypothesis of this study alluded to ROS scavenging by 7,8-NP as a protective mechanism against oxLDL–mediated cellular death. NOX inhibition by apocynin reduced neopterin formation, suggesting reduced oxidative flux. Thence, the role of apocynin–inhibitable ROS in oxLDL–mediated toxicity to HMDM cells was also tested. Apocynin alone was not toxic to HMDM cells at the 50–200 μM range of concentrations but was slightly toxic at 300 μM (fig. 4.15). Contrary to the expectation, apocynin at the concentration that partially prevented neopterin oxidation did not protect HMDM cells from cellular death (see below). This was tested with both an MTT viability assay, which measures cellular metabolic activity,

and with the ApoAlert kit, which is able to distinguish apoptosis and necrosis. Both assays confirmed the absence of statistically significant protection (figures 4.16, 4.18, 4.19).

Apocynin concentrations of 50, 100 or 200 μM did not convey any protection against oxLDL toxicity when tested with the MTT assay at 24 hours (fig. 4.16). The mode of MTT cell viability assay is not completely understood but reports of both cytosolic and mitochondrial mechanisms of formazan reduction have been made (Bernas & Dobrucki, 2002). To exclude the possibility of an assay-specific result, conventional apoptosis–necrosis labelling was used for the subsequent cell viability experiments (ApoAlert kit, Clontech Laboratories, USA). To test the effect of the inhibitor during a shorter time-frame, lest the oxidative processes lost relevance towards the 24^{th} hour of incubation, apoptosis and necrosis were determined at 15 rather than 24 hours after the addition of oxLDL (figures 4.18, 4.19). Apocynin treatment did not influence the frequencies of total cells staining with annexin$^+$ and PI$^+$ (figures 4.18a, 4.19a) or distribution to Annexin V and PI staining quadrants (figures 4.17, 4.18b, 4.19b). In one instance, a small decrease of cell frequency in the annexin$^+$ corresponding to apoptosis or secondary necrosis quadrants of the flow cytometer output was observed at 200 μM (fig. 4.19b). The decrease in annexin$^+$ cells may indicate a reduction in apoptotic marker phosphatidyl serine exposure. Yet the overall frequencies of cellular death remained almost unchanged (fig. 4.19a). It is thus possible to conclude that despite the contribution that NOX-generated oxidative flux may have at the initial stages of oxLDL–mediated cell death, the effect of its inhibition by apocynin does not provide significant protection from cellular death at the end of the acute incubation period. The result was surprising given the abundance of literature that implicates NOX involvement in cellular death. Despite the wealth of publications on the ROS-generating effect of NOX in macrophages and other cells (Bedard & Krause, 2007; Brandes *et al.*, 2010; Dröge, 2001), the evidence to prove the direct effect of NOX on cell viability during oxLDL treatment in macrophages is lacking. This could be due to the specificity issues associated with the known NOX inhibitors like and apocynin (Altenhöfer *et al.*, 2012). A possibility of non-specific effects of apocynin also exists (personal communication with Dr. DeHaan, Baker IDI, Australia). Similarly, the results observed in this study could be confirmed with a more reliable NOX inhibitor (Wingler *et al.*, 2011).

Another interpretation of the results would be that either other non-NOX sources

of ROS were sufficient to illicit cellular damage that resulted in cell death or that cell death was not a consequence of oxidative processes at all. The latter is less likely since ROS scavenger 7,8-NP could prevent HMDM cell death from acute oxLDL toxicity. Furthermore, other antioxidants have been shown to inhibit cellular death and the associated perturbations of cellular redox balance in oxLDL–treated cells (Hardwick *et al.*, 1999; Hsieh *et al.*, 2001; Siow *et al.*, 1999, 1998). This, however, was not true of all antioxidant in all circumstances (Harris *et al.*, 2006; Hsieh *et al.*, 2001). In addition, only 50% of 7,8-NP oxidation to neopterin was prevented by apocynin, thus indicating that other source(s) of ROS contribute(s) to the oxidative flux and these ROS are also scavenged by 7,8-NP. For example, mitochondrial ROS generation could present a likely candidate for future investigation. Complex III was especially identified as a source of $O_2^{\bullet -}$ in compromised cells (Turrens, 2003). Asmis & Begley (2003) showed that oxLDL–mediated mitochondrial depolarisation and dysfunction contribute to macrophage cell death. It is also possible that oxidative processes, despite being the initial cellular response to oxLDL, are not the only contributor to cellular death, and in the absence of the first, non-oxidative processes such as lysosome destabilisation become more apparent and lead to the same net result of HMDM cell death (Yuan *et al.*, 1997; Zhang *et al.*, 2010). The higher protection mediated by 7,8-NP suggests that it has an effect on other cellular processes and/or their products and outcomes as well.

4.3.3 Intracellular levels of 7,8-NP

Intracellular 7,8-NP after exogenous addition

7,8-NP was rapidly internalised by HMDM cells, peaking at 12 hours and decreasing by 10-20% over the 12–24 hours of incubation (figures 4.4 and 4.12b). This decrease was unlikely to cause a loss of protection as the level of 7,8-NP at 24 hours was identical to that of 6 hours when the protection was full. HMDM cells seemed to maintain intracellular 7,8-NP levels even despite a drop in the extracellular 7,8-NP availability (fig. 4.3). It is conceivable that an increased rate of disappearance of extracellular 7,8-NP in the second half of the incubation contributed somewhat to the changed protection slope. In the future, this could be addressed by a two-step addition of freshly prepared 7,8-NP at 0 and 12^{th} hour of incubation. In comparison to the present study, Gieseg *et al.* (2010a) observed no decrease in intracellular 7,8-NP, but the reason for this disparity is unknown.

The effective intracellular concentration of 7,8-NP in HMDM cells was of interest since no data is available on the concentration of this compound in macrophages *in vivo*. The majority of published studies report plasma concentrations of neopterin and, occasionally, 7,8-NP (see section 1.7.2), but these are only remotely relevant to understanding the physiological role of these compounds in the inflammatory sites. The intracellular concentration of 7,8-NP within HMDM cells reached, on average, ∼1.3 nmol/mg protein or 180 pmol/well (fig. 4.5). To calculate the cellular 7,8-NP concentration, the following empirical exercise was performed. Considering the cell number to be 22,000 per well (appendix I), 7,8-NP amount could be calculated as 8.18 fmol/cell. In the absence of information on the exact distribution of HMDM cell volume, the radius of HMDM cell was assumed at 20 μm, the concentration of active 7,8-NP in the cell (assuming equal distribution inside a spherical cell) would be $33.49 \times 10^{-15} / 8.18 \times 10^{-15} = 0.24$ M (or 0.51 M assuming 15 μm HMDM radius). This figure is a rough estimate and there are factors it does not take into account, thus it will only be used as a guide. For comparison, intracellular GSH concentration is reported to range from 0.2 to 10 mM, much lower than the calculated 7,8-NP (Anderson, 1998). A more precise estimation of intracellular 7,8-NP on per cell basis could be carried out by measuring the distribution of cellular volume of HMDM cell population by flow cytometry in conjunction with pterin measurement by HPLC.

The protective 200 μM concentration of 7,8-NP in the experimental medium was higher than that in serum during immune activation, such as 68 nM neopterin detected in the plasma of coronary heart disease patients undergoing angioplasy (Genet, 2011). However, when activated monocytes, macrophages and T-lymphocytes accumulate at the inflammatory sites and release pteridines locally into a confined environment, the concentration of 7,8-NP in the proximity of those cells may be much higher than that in serum. At present, the levels of neopterin reported to be generated in cell culture are much lower than the levels required to account for the neopterin levels in the blood of CVD patients. This could be illustrated by a rough calculation. According to Weiss *et al.* (1999) polymorphonuclear blood monocytic cells (PBMC) cells produce 14.9 nmol/L neopterin per 10^6 cells per mL when activated with 250 U/mL IFN-γ over 48 hours. This is equivalent to 0.31 pmol/10^6cells/hour given that neopterin accumulation proceeded without any loss. Assuming an average person has 3 liters of plasma (5% of bodyweight) (Barrett *et al.*, 2010), the total amount of neopterin carried (during acute CVD event) is 68 nmol/L x 3 L = 204 nmol (Genet, 2011). The half life of neopterin in the body is estimated to be 90 minutes (Fuchs

et al., 1994). Therefore, to replenish 102 nmoles of neopterin within 90 minutes will require action of 102 x 10^{-9} mol / 0.31 x 10^{-12} mol per 10^6cells x 1 hr / 1.5 hr = 219.35 x 10^9 cells. Human blood contains, on average 540 monocytes per μL (Barrett *et al.*, 2010). It would require 219.35 x 10^9 / 540 = 406 L of blood to replenish excreted neopterin even if all blood monocytes were activated to the degree reported by Weiss *et al.* (1999). The same calculation can be performed for 12.11 nmol/L (instead of 68 nmol/L), reported as the predictive threshold for acute coronary complications by Ray *et al.* (2007), to yield 72 L, which is still very high. The magnitude of the outcome suggests that there are other sources of neopterin and 7,8-NP rather than cells in the circulation with a much higher production rate than is currently reported. Inflammatory sites were suggested as such a source (Firth *et al.*, 2008b; Gieseg *et al.*, 2008). Therefore, the comparison of plasma 7,8-NP and neopterin concentrations with effective concentration of these compounds in the inflammatory sites is unreasonable at this stage. It suggests that with the current knowledge of 7,8-NP production mechanisms it is impossible to draw conclusions on the presence of effective 7,8-NP concentrations used in this study in macrophages *in vivo*.

The intracellular 7,8-NP concentrations after exogenous addition varied between HMDM cell preparations from different donors (fig. 4.5). Two distinct groups of low and high uptake were identified. Correction for cellular protein did not eliminate this difference, suggesting that the number of cells per well was not the determining factor. The same HMDM preparations were assessed for baseline control levels of 7,8-NP in an attempt to explain the observed variation (fig. 4.6). Baseline total pterin levels, although varying between 12-well and 48-well seeded HMDM cells, were consistent within each group, indicating that the observed disparity in experimental concentration was not associated with the different starting values.

The difference in total 7,8-NP uptake between preparations and the kinetics of uptake over 24 hours may be associated with the variable levels of **e**quilibrative and **c**oncentrative **n**ucleoside **t**ransporters, ENT and CST respectively. These have been shown to orchestrate pterin internalisation (Ohashi *et al.*, 2011) but no details of 7,8-NP cellular uptake kinetics have been published. As the name suggests, ENTs facilitate pterin diffusion while CNTs couple nucleoside transport to the inwardly directed sodium gradient (Beal *et al.*, 2004; Gray *et al.*, 2004). Multiple studies detected large genetic and functional variation in human nucleoside transporters, highlighting that the cumulative effects of multiple nucleoside alleles in the population are very

complex (Leabman *et al.*, 2003; Li *et al.*, 2007; Owen *et al.*, 2005). In addition, some variants display substrate-specific defects in transport (Urban, 2005) and regulation in response to the extracellular stimuli. For example, the levels of ENT1 were reported to change during the course of differentiation from monocyte into macrophage (Soler *et al.*, 2001). Also, activation by IFN-γ inhibited this change but up-regulated the levels of CNT1 and CNT2 (Soler *et al.*, 2001). Thus, it is possible that the HMDM cell preparations from three donors on figure 4.5 possessed higher function of nucleoside transporters and were able to acquire and retain a higher level of 7,8-NP. The mechanisms for this cannot be established at present. The present sample size of five HMDM cell preparations is too small to draw comprehensive conclusions and lacks the depth of investigation into mechanisms. Yet this pilot study is suggested to be sufficient to highlight this area as one that warrants future investigation.

Intracellular 7,8-NP production

In vitro, only IFN-γ, TNF-α and bacterial LPS have been shown to enhance neopterin production (Henderson *et al.*, 1991; Weiss *et al.*, 1999), yet *in vivo* other stimuli have been suggested to drive neopterin elevation (Sghiri *et al.*, 2005). As serum neopterin was elevated in patients with CVD, it was not surprising to find that oxLDL slightly up-regulated intracellular 7,8-NP level in HMDM cells (fig. 4.7). This was an order of magnitude lower that the effective intracellular 7,8-NP detected in the HMDM cells supplemented exogenously, (95 pmol/mg protein vs 1.3 nmol/mg protein). Toxic levels of oxLDL induced a higher production of 7,8-NP than sub-toxic, producing 95.0 pmol/mg protein vs 5.5 pmol/mg protein (figures 4.7 and 4.8). Small neopterin elevation was also observed in the toxic samples, but was below the detection limit in the non-toxic samples. Published literature on the subject abounds with values for neopterin released into supernatant, but intracellular concentration of 7,8-NP is not available and even neopterin is scarce (Andert *et al.*, 1992; Franscini *et al.*, 2003; Huber *et al.*, 1984; Weiss *et al.*, 1999). Werner *et al.* (1989) reported an increase in intracellular HMDM neopterin from 1.95 $\pm$ 1.27 (SD) to 159.63 $\pm$ 51.22 (SD) pmol/mg protein over 48 hours in the presence of 250 U/mL IFN-γ. The increase from 6.4 to 20.0 pmol/mg protein observed in the present study was very low compared to that, but the incubation time was also shorter. The present result agreed well, however, with that of Werner-Felmayer *et al.* (1990), which reported an increase from "not determined" to 18 $\pm$ 2 pmol intracellular neopterin /mg protein in undifferentiated THP-1 cells incubated with 250 U/mL of IFN-γ for 24 hours. Another study determined that EC over 24 hour of stimulation produced from 1.0 $\pm$ 0.3 (SD) to 1.9 $\pm$ 1.1

(250 U/mL IFN-γ) or 2.8 $\pm$ 0.9 pmol/10^6 cells (Werner-Felmayer *et al.*, 1993), which was lower than the increase in the present study: from 1.23 $\pm$ 2.54 to 5 $\pm$ 3.5 (SD) pmol/10^6 cells. However the latter is not surprising as macrophages are known to produce higher amounts of neopterin. The results of the present work are comparable in magnitude of neopterin production to some published reports, therefore suggesting that oxLDL might be a physiologically-relevant stimulus for neopterin production in some circumstances.

The spread of data in the present study, however, suggests that oxLDL–induced pterin production is dependent on the individual HMDM cell preparations. Such inter-experimental variability is expected when dealing with donor-associated variability of primary cells and small concentrations, those approaching the limit of detection. To the best of the author's knowledge, this is the first attempt to investigate an effect of oxLDL as an agent stimulating 7,8-NP production by human monocyte–derived macrophages. The small increase may be attributable to oxLDL induction of inflammatory mediators such as TNF-α or IFN-γ, which, in turn, enhance 7,8-NP production. This is plausible in the view that toxic concentration of oxLDL, which elicited a higher inflammatory response in HMDM, caused a higher level of 7,8-NP production. These experiments also showed that the effective intracellular 7,8-NP concentration during experiments conducted in this study was primarily derived from the uptake of exogenous 7,8-NP.

4.4 Summary

The research presented in this chapter demonstrated that antioxidant capacity of 7,8-NP is a likely mechanism that protects HMDM cells from acute oxLDL toxicity. This work provides evidence that 7,8-NP scavengers ROS produced by HMDM cells in response to oxLDL and is oxidised to neopterin in the process. The scavenging of DHE-reactive ROS by 7,8-NP was an early event, while oxidation to neopterin proceeded at a constant rate during the 24 hour incubation. These results suggest that protection against oxidative damage through oxidant scavenging may be a physiological role of 7,8-NP in macrophages exposed to oxLDL within atherosclerotic plaques.

The present study identified NOX as a potential contributor to ROS formation during oxLDL–mediated stress in HMDM cells. Intracellular neopterin oxidation was inhibited by half in the presence of apocynin, a NOX enzyme assembly inhibitor. However,

contrary to the current view of cellular processes during oxLDL cytotoxicity and the original hypothesis, NOX inhibition by apocynin failed to prevent oxLDL–mediated HMDM cell death. In conjunction with incomplete inhibition of neopterin formation by apocynin, the result calls for a further investigation into the sources of ROS upon oxLDL exposure. This, however, should be confirmed with a more specific NOX inhibitor than apocynin. It is an important direction for future work, as relative contribution of ROS sources may inform pharmaceutical design for disease treatment. Mitochondrial and lysosomal destabilisation may provide initial targets.

Based on the results presented in this chapter, mechanistic pathway worthy of further investigation is proposed: NOX activation $\rightarrow O_2^{\bullet -} \rightarrow H_2O_2 \rightarrow$ HOCl (MPO–catalysed).

A retrospective pilot study detected inter-donor variation in macrophage 7,8-NP uptake, which could be addressed in a prospective and targeted investigation. Since 7,8-NP and neopterin are emerging as inflammatory markers of macrophage activation in disease, the knowledge of inter-individual variation in uptake and/or production of these compounds will be valuable in the clinical setting. The information about kinetics of 7,8-NP uptake by HMDM cells will be beneficial for any future cell culture based investigation that builds on the results of the present work.

5

Effect of 7,8-dihydroneopterin on oxLDL uptake by macrophages

5.1 Introduction

Foam cell formation and cell death underpin the development and progression of atherosclerotic plaques (Ball *et al.*, 1995; Naito *et al.*, 1997). Foam cells are characterised by the accumulation of cholesterol esters (CE) and oxidation products similar to those found in oxidatively modified lipoproteins (Jessup & Kritharides, 2000). *In vitro*, macrophages were found to accumulate CE and oxysterols when exposed to oxisided and aggregared LDL (Asmis & Jelk, 2000a; Bostrom, 2006; Brown *et al.*, 1996). Moreover, oxLDL was shown to contribute to macrophage death *in vitro* (Reid & Mitchinson, 1993) and was suggested to do so within an atherosclerotic plaque (Ball *et al.*, 1995; Li *et al.*, 1998). The exact mechanisms of these biological processes are disputed; however, binding, uptake and intracellular processing of oxLDL are important determinants of cell fate (Steinberg, 2009). Ultimately, the understanding of these processes will allow researchers to target "weak links" in the cellular design and, potentially, prevent, delay or alleviate atherosclerotic burden in the patient. This chapter is concerned with the second aspect of the 7,8-NP–mediated protection against oxLDL. It will examine the evidence for the effect of 7,8-NP on oxLDL internalisation and investigate the underlying mechanisms.

Scavenger receptors on the cell surface recognise oxidised epitopes on oxLDL (Boullier *et al.*, 2001). As discussed in the Introduction (section 1.4.1), CD36 and scavenger receptor A are considered to be the main mediators of oxLDL binding and uptake, however, other scavenger receptors are also capable of binding oxLDL (Horiuchi *et al.*,

2003). It is highly possible that CD36–facilitated uptake, processing, and accumulation of oxLDL are controlled by multiple cellular processes, because the results of CD36 binding or signalling inhibition studies vary significantly. These range from complete inhibition of uptake (Rahaman *et al.*, 2006) to no effect on uptake (Wintergerst *et al.*, 2000).

CD36 protein and mRNA levels are up-regulated by its ligands, such as oxLDL, in a number of cell types including macrophages (Han *et al.*, 1997; Munteanu *et al.*, 2006; Nakagawa *et al.*, 1998; Ricciarelli *et al.*, 2000). The regulatory mechanism includes nuclear hormone receptor PPAR-γ, which, once activated by a lipid-like ligand, drives transcriptional activation of CD36 expression (Munteanu *et al.*, 2006; Tontonoz *et al.*, 1998). PPAR-γ also plays a role in CD36 protein and mRNA down-regulation mediated by a number of agents including α-TocH and lovastatin (Pietsch *et al.*, 1996; Ricciarelli *et al.*, 2000).

When taken up by macrophage scavenger receptors (SRs), modified lipoproteins are delivered to endosomes and then lysosomes (Brown *et al.*, 2000; Maor & Aviram, 1994). There, their cholesterol ester (CE) content is hydrolysed into free cholesterol and fatty acids at acidic pH (Sekiya *et al.*, 2011). Since SRs are not regulated by intracellular cholesterol concentration, oxLDL uptake leads to accumulation of free cholesterol, which is then re-esterified by ACAT. This leads to accumulation of large pools of esterified cholesterol in the cytosol. Evidence suggests that esterification of toxic oxLDL components to their less toxic esters is a protective response (Monier *et al.*, 2003). Under normal conditions, excessive LDL cholesterol is effluxed out of the cells through a process called reverse cholesterol transport (RCT). RCT is characterised by CE hydrolysis, performed by a a family of enzymes with carboxyl ester hydrolase/esterase activity. Cholesterol and cholestrol products are then transported out of the cell onto HDL (Johnson *et al.*, 1991) via ATP–binding cassette transporters ABCA1 and ABCG1 (Yvan-Charvet *et al.*, 2010). However, LDL modification have been shown to reduce or inhibit the rate of its degradation and efflux from the macrophage (Hoff *et al.*, 1993; Jessup & Kritharides, 2000; Jessup *et al.*, 2002). Thus, not only oxLDL is internalised in higher amounts, but its efflux is reduced, facilitating the formation of foam cells.

The research in this chapter aims to confirm the 7,8-NP–mediated regulation of oxLDL uptake by HMDM cells with a different methodology to DiI (used in Gieseg

et al. (2010a)). OxLDL uptake by cells will be measured using 7-ketocholesterol (7KC), an inherent component of Cu-oxLDL. This marker will then be used to confirm the 7,8-NP–mediated inhibition of oxLDL uptake.

The mechanisms of oxLDL uptake regulation by 7,8-NP were unclear from the previous study (Amit, 2008). CD36 scavenger receptor down-regulation was proposed to play a role in the process but was not identified with certainty. Thus, this chapter will further explore the effect of 7,8-NP on CD36 receptor. It will also investigate the contribution of this process to 7,8-NP–mediated protection from oxLDL toxicity. The presence of CD36 and 7,8-NP in the plaque will be assessed. Finally, an alternative hypothesis of the mechanism of 7,8-NP–facilitated regulation of oxLDL in HMDM cells will be proposed and discussed.

5.2 Results

5.2.1 Measuring oxLDL uptake in macrophages with 7-ketocholesterol

7-Ketocholesterol (7KC) was used to measure the levels of intracellular oxLDL in HMDM cells. 7KC is an advanced product of cholesterol oxidation in Cu–oxidised LDL (Brown *et al.*, 1996), and is taken up by the cells within the oxLDL particle (Kritharides *et al.*, 1995; Rutherford & Gieseg, 2012). 7KC was a suitable marker of oxLDL uptake because oxLDL treated cells contained significantly higher levels of intracellular 7KC than the untreated control (fig. 5.1). 7KC was measured as both free and total (free+esterified) 7KC. The latter was expected to provide an overall measure of oxLDL internalised by the HMDM cells. Average total 7KC in oxLDL was 28.4 mol 7KC per mol of oxLDL and to 9.3 mol/mol of free 7KC. The ratio of total to free 7KC in oxLDL was 3.4 $\pm$ 0.5 (SD, n=8), which meant that 7KC esters comprised approximately 75% of the total 7KC in oxLDL.

HMDM cells in the whole medium (RPMI-1640 supplemented with 10% human serum and antibiotics) were treated with 1mg/mL oxLDL (a sub-toxic level). The intracellular concentration of total 7KC and, therefore, oxLDL, increased gradually over a 24 hour period (fig. 5.1). During the first 6 hours, this rise was due to the increase in free 7KC (4.5 nmol 7KC per mg cellular protein) (fig. 5.1). This indicated that cellular oxysterols derived from oxLDL particle were de-esterified at the initial stage of oxLDL

exposure. After the first 6 hours, however, the levels of free 7KC plateaued, while the levels of total 7KC continued to rise (fig. 5.1). This suggested that esterification of the internalised oxLDL oxysterol(s) (and other components) was taking place. The levels of total 7KC did not reach a maximum during the 24 hours of incubation indicating further uptake of oxLDL (the cells contained 12 and 22 nmol total 7KC per mg cell protein at 24 hours in two experiments, fig. 5.1). Total intracellular 7KC increased by about 50% from 6 to 24 hours, which was due to the increase in 7KC esters.

HMDM cells contained baseline levels of total 7KC. These were most likely derived from the serum supplemented medium in which the cells were cultured for 2 weeks prior to the experiment. The mean values of 7KC in the sera used in cell culture were 11.67 ± 5.36 (SD) μM of free 7KC and 65.44 ± 23.87 (SD) μM of total 7KC. This comprised less than 1.3% of the total reported serum cholesterol (Asmis & Jelk, 2000a). Two out of 8 batches of sera contained significantly lower levels of total 7KC (fig. 5.2). Serum lipoproteins were likely the source of 7KC in the medium, as medium supplemented with lipoprotein deficient serum (LPDS) contained less total 7KC than the medium supplemented with normal serum. Brown *et al.* (1996) also reported trace amounts of total 7KC in LDL.

[A]

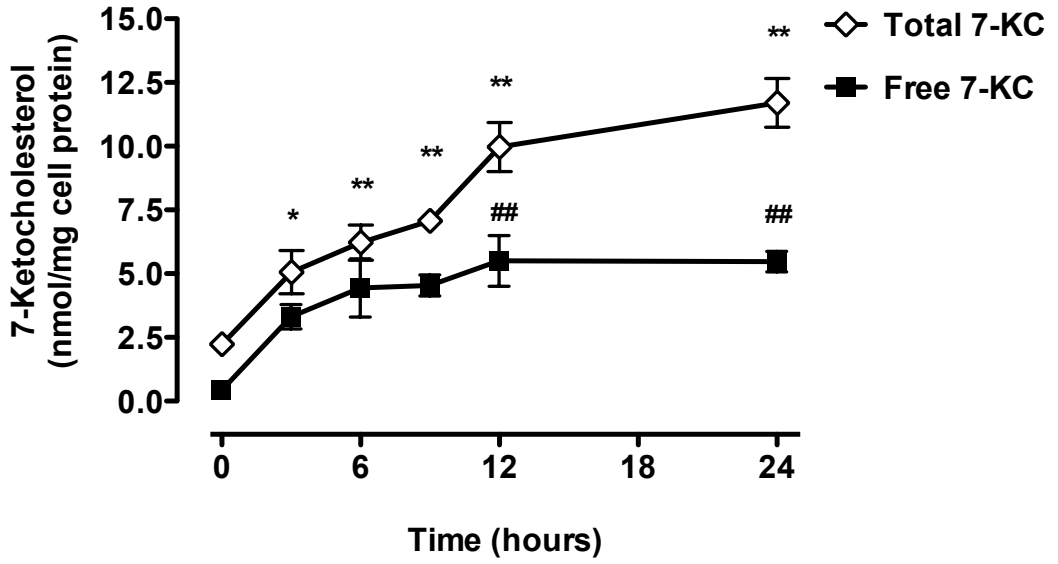

[B]

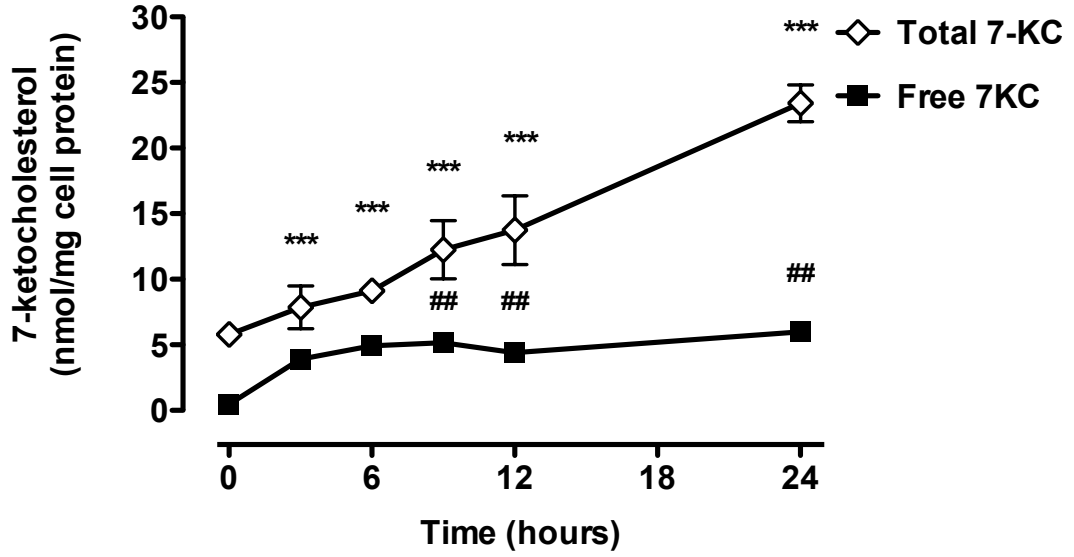

Figure 5.1: Intracellular 7-ketocholesterol (7KC) accumulation in HMDM cells exposed to oxLDL.

HMDM cells ($5x10^6$ cells/mL) were treated with 1 mg/mL oxLDL. Cell lysates were collected at the indicated time points and assessed for intracellular free (filled squares) and total (clear diamonds) 7KC via HPLC. Protein was determined by BCA assay and used to control for cellular content per well. Average protein concentrations in 0 hour control cells were 194 μg/well for A and 253 μg/well for B. Results are displayed as mean ± SEM of triplicates from two separate experiments (**A** and **B**). Statistical analysis: one-factor ANOVA with Dunnett's test to compare each type of 7KC at each time point to the 0h control (*) and Bonferroni test to compare types of 7KC at each time point (#), *, $p<0.05$, **,##, $p<0.01$, ***, $p<0.001$. For B, *** refers to free 7KC.

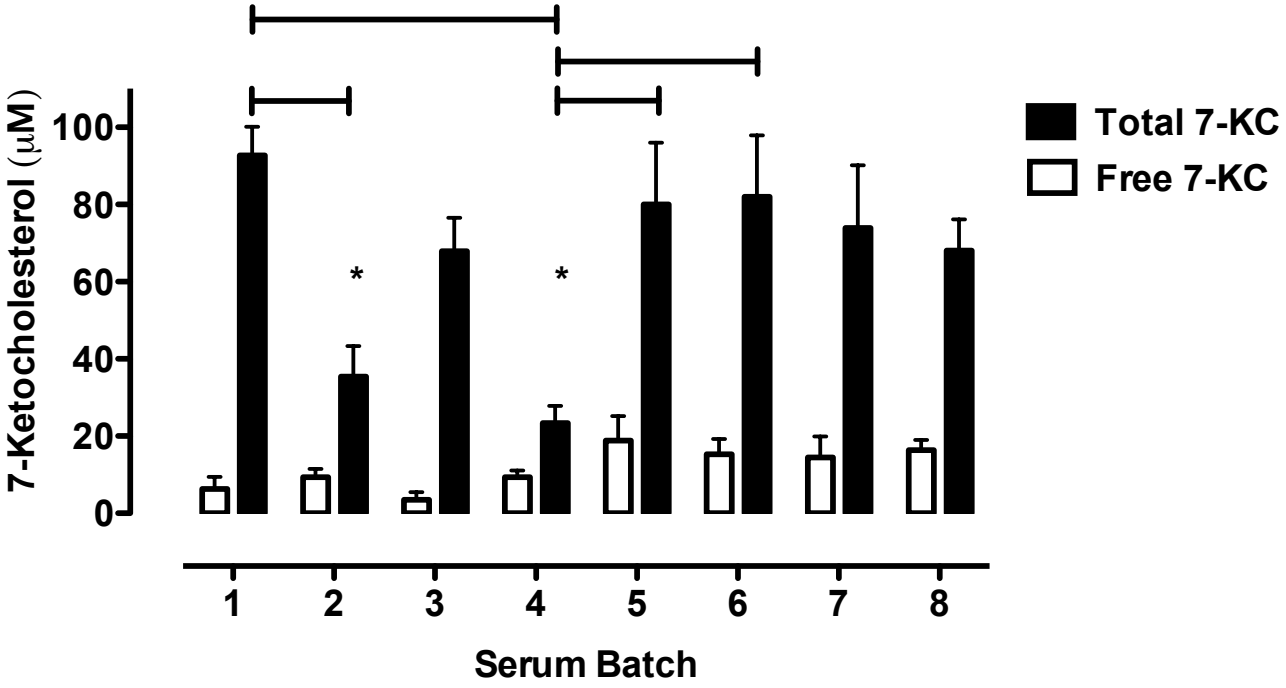

Figure 5.2: 7KC levels in human sera used in cell culture.
Human sera used in the culture of HMDM cells was analysed for total (black bars) and free (clear bars) 7KC levels by HPLC analysis. Results are presented as mean ± SEM of triplicate measurements. Significance (one-factor ANOVA with Turkey post test) is as indicated: *, $p<0.05$, horizontal lines outline the significant treatments.

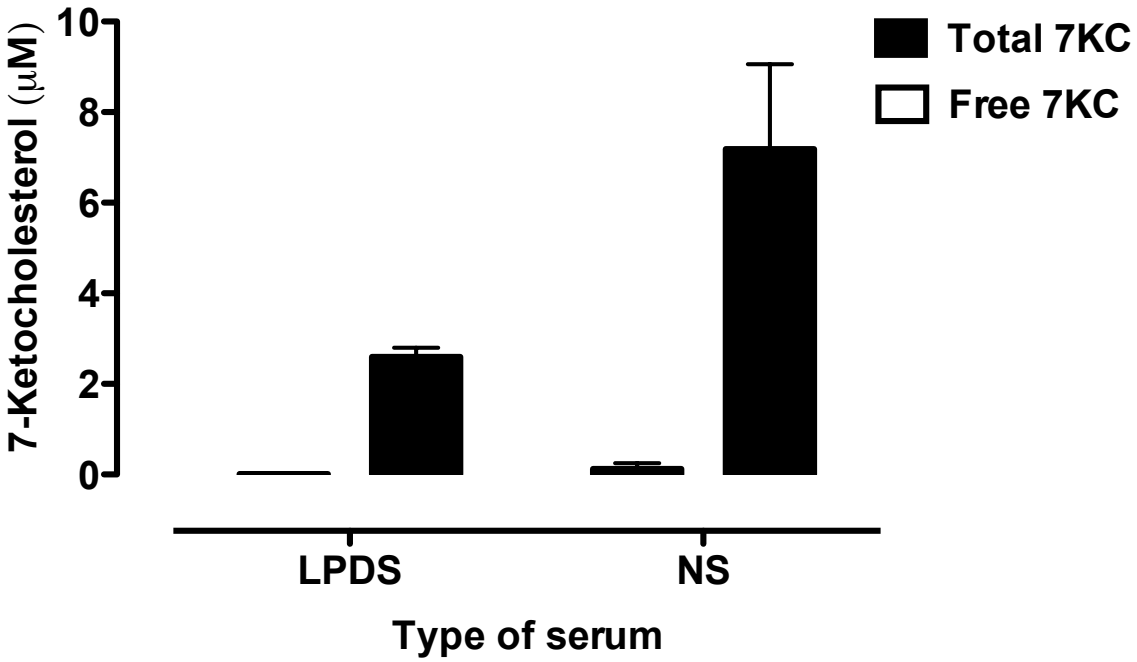

Figure 5.3: Serum lipoproteins are the primary source of 7KC in culture medium.

Total (black bars) and free (clear bars) 7KC concentration was measured in RPMI-1640 supplemented with 10% normal (NS) or lipoprotein deficient (LPDS) human serum after 24 hour incubation in the absence of cells. Results are presented as mean ± SEM of duplicate measurements from a single experiment. Statistical significance: t-test p=0.14.

5.2.2 7,8-NP reduces intracellular oxLDL uptake in HMDM cells

7,8-NP reduces intracellular 7KC accumulation in HMDM cells

Gieseg *et al.* (2010a) have shown that 7,8-NP affected the accumulation of DiI–labelled oxLDL by HMDM cells. Due to potential interference of DiI with cellular redox processes (see discussion), this study aimed to confirm oxLDL uptake down-regulation with a different intracellular marker of uptake, 7KC. The effect of 7,8-NP on the intracellular 7KC levels was observed during the 24 hour incubation with 1 mg/mL oxLDL (fig. 5.4). The presence of 7,8-NP had no effect on the total 7KC levels up to 9 hours, but caused a decrease in total 7KC levels at 12 hours and a statistically significant decrease at 24 hours (fig. 5.4a). Coincidentally, the free 7KC levels had plateaued by the time 7,8-NP started to have an effect. 7,8-NP had a significant effect on the levels of total 7KC but caused only a minor decrease (1 nmol/mg protein) in the free 7KC levels (fig. 5.4b). This suggested that 7,8-NP only affected the esterified 7KC. The magnitude of oxLDL uptake reduction by 7,8-NP was approximately 40%.

After establishing the time-frame of the 7,8-NP effect (24 hours) the experiment was replicated four more times (fig. 5.5)[1]. Total 7KC in HMDM cells was, as before, reduced in the presence of 7,8-NP (40 to 60%), while free 7KC was unaffected.

[1]The intracellular 7KC concentrations between the figures 5.4 and 5.5 are different due to change in plating density for repeated experiments.

[A]

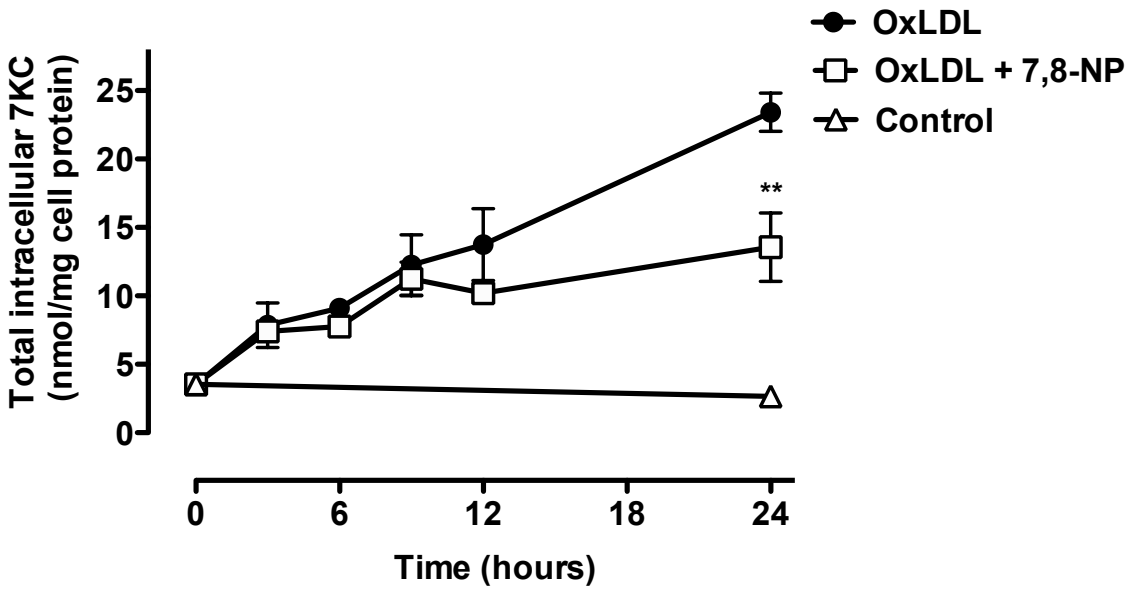

[B]

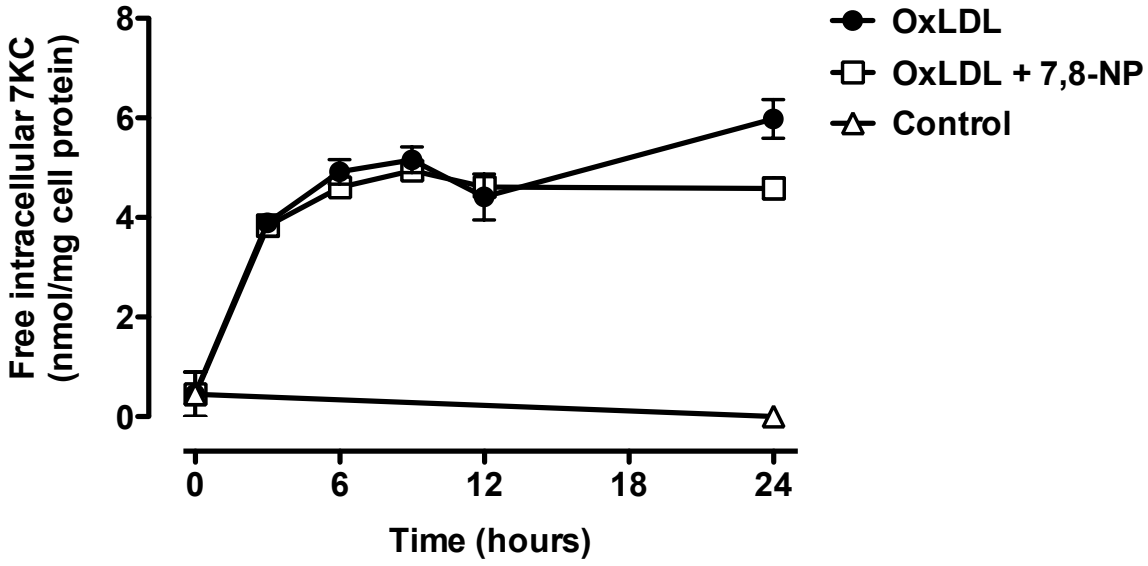

Figure 5.4: Time course of intracellular 7KC accumulation in HMDM cells exposed to oxLDL in the presence and absence of 7,8-NP.
HMDM cells ($5x10^6$ cells/mL) in whole medium were treated with 1 mg/mL oxLDL, with (empty squares) or without (filled circles) 200 μM 7,8-NP. Cell lysates were collected at the indicated time points and assessed for intracellular 7KC and protein. Results are displayed as mean ± SEM of triplicates from a single experiment: (**A**) total (free and esterified) intracellular 7KC, (**B**) free intracellular 7KC. Significance is indicated between the treatments (one-factor ANOVA with Bonferroni comparison between treatments at each time point), **, $p<0.01$.

[A]

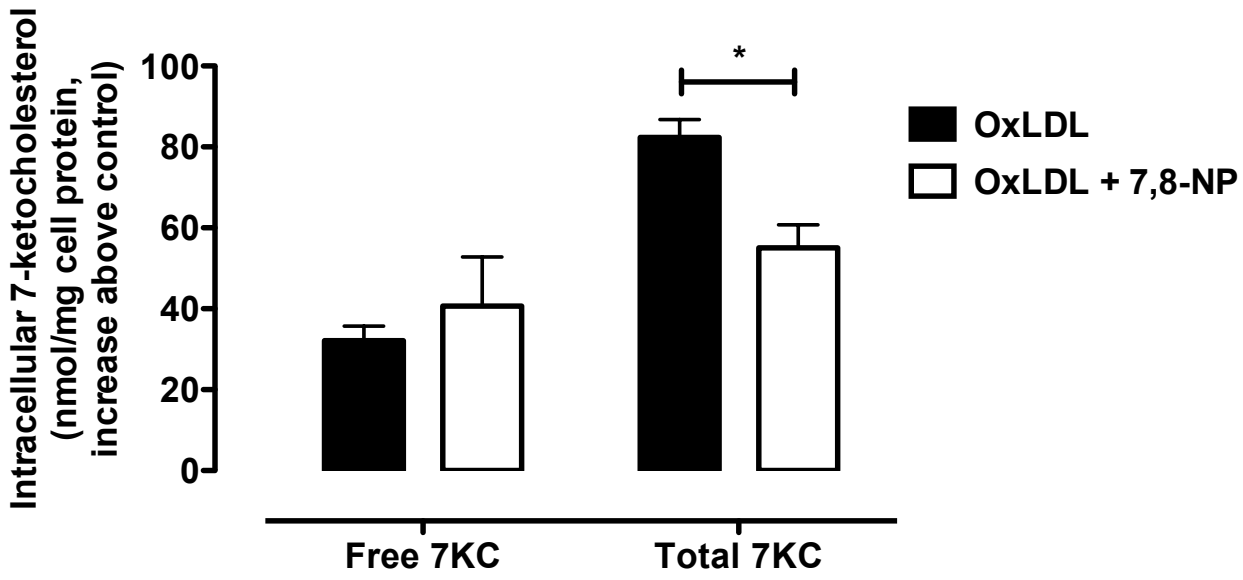

[B]

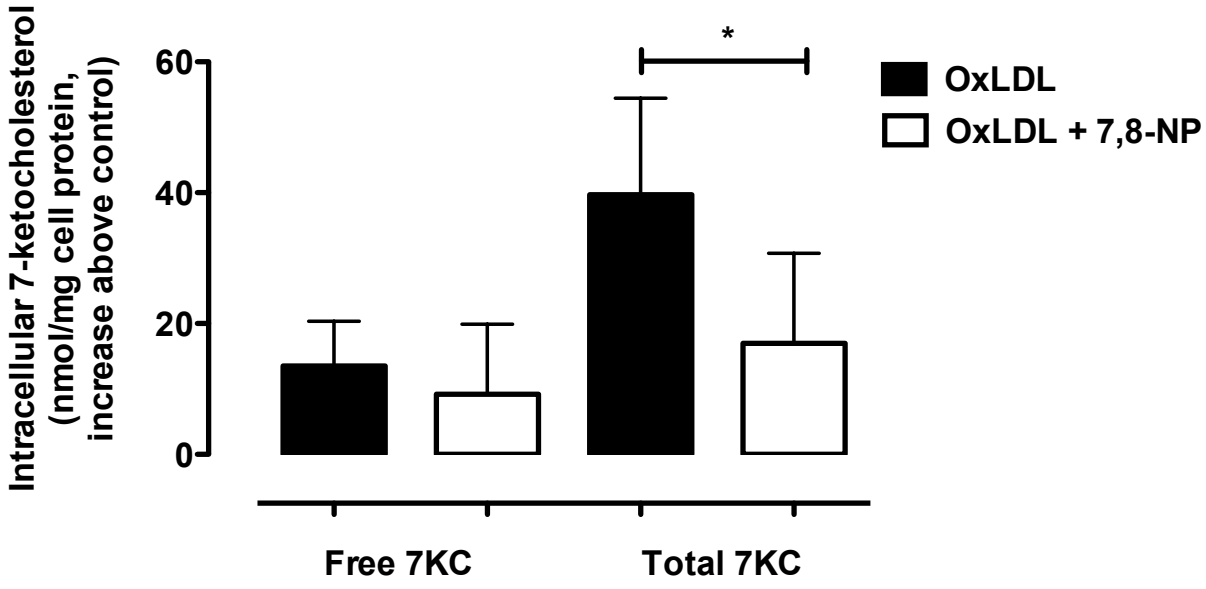

Figure 5.5: 7,8-NP mediates reduction of intracellular total 7KC in HMDM cells exposed to oxLDL.

HMDM cells (1x10^6 cells/mL) in the whole medium were treated with 1 mg/mL oxLDL in the presence (empty bars) or absence (filled bars) of 200 μM 7,8-NP for 24 hours. Cell lysates were assessed for intracellular free and total 7KC and protein and expressed as increase above respective no oxLDL control. (Average control values over four treatments: 13 and 23 nmol/mg protein for free and total 7KC, respectively). Results are displayed as mean ± SEM of triplicates from (**A**) single experiment, (**B**) four separate experiments combined. Paired t-test was performed on the data from 4 experiments, significance as indicated, *, $p<0.05$.

5.2.3 7,8-NP reduces the expression of CD36 scavenger receptor protein in HMDM

To establish the mechanism(s) of 7,8-NP mediated uptake reduction, the levels of scavenger receptor for oxLDL, CD36, were assessed via immunoblotting. HMDM cells were incubated in RPMI-1640 with 10% human serum containing increasing concentrations of 7,8-NP for 24 hours. Subsequently, the cells were washed and lysed in the presence of protease inhibitor. The lysates were immunoblotted for CD36 and β-actin was used as loading control. Both visual and numerical data are presented in figure 5.6. Densitometry analysis was done with GeneTool (SynGene) and ImageJ64 processing software and the CD36 intensity data were normalised by the respective β-actin band intensity. At 200 and 250 μM, 7,8-NP caused a 50 and 60% decrease in the CD36 100 kDa protein (fig. 5.6). The 83 kDa band was also decreased by 20% in the presence of 250 μM 7,8-NP. Different bands represent different glycosylation isoforms of CD36 protein. The 83 kDa band was reported to be the incompletely glycosylated protein located in the Golgi, while fully glycosylated band >100 kDa was shown to reside on plasma membrane (Alessio *et al.*, 1996).

The time–course of CD36 down-regulation was investigated in order to compare it to the time frame of uptake reduction (fig. 5.7). Two hundred μM 7,8-NP reduced the levels of 100 kDa CD36 protein by 20% after 12 hours and by 40% after 24 hours of incubation, compared to 0 hour control (fig. 5.7b). This conferred with the uptake data temporally. CD36 levels in control cells were unaffected over the course of the 24 hour incubation (fig. 5.7a). A quarter of HMDM cells preparations did not respond to 7,8-NP by down–regulating CD36 protein (data not shown). Lack of effect was also observed during the 7KC uptake experiments in a quarter of the experiments, suggesting a common cause.

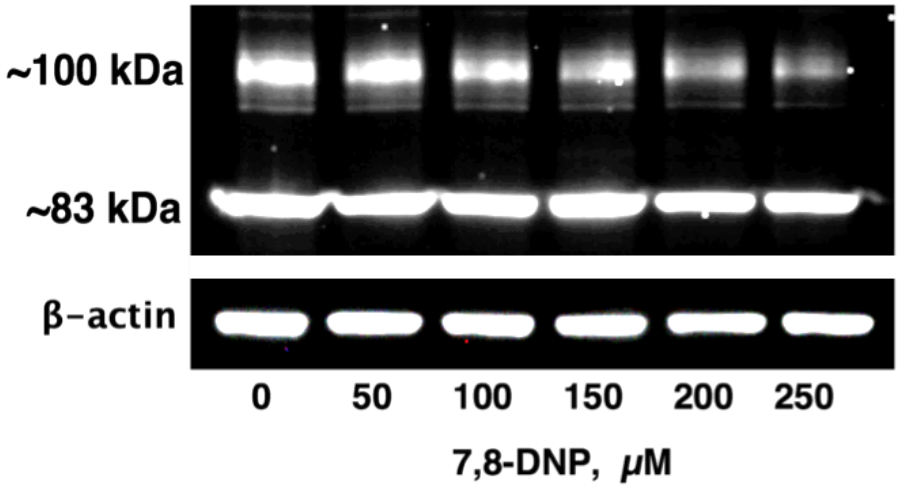

[B]

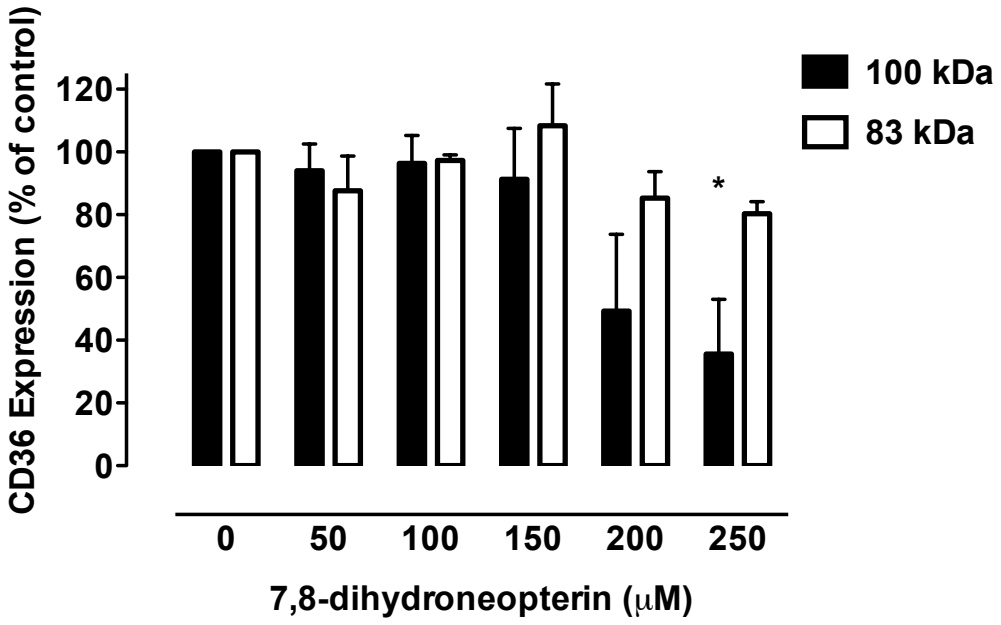

Figure 5.6: 7,8-NP reduces the expression of 100 kDa band of CD36 protein in HMDM in a concentration–dependent manner.
HMDM cells ($5x10^6$ cells/mL) were treated with increasing concentrations of 7,8-NP for 24 hours. Cell lysate was assessed for CD36 protein expression via Western blot (**A**). Quantitative densitometry of Western blots displays down-regulation of the CD36 protein (incompletely glycosylated) 83 and (fully glycosylated) 100 kDa bands, relative to the respective controls (**B**). Results were normalised by β-actin and displayed as mean ± SEM of triplicate experiments.
Figure published in Gieseg *et al.* (2010a).

[A]

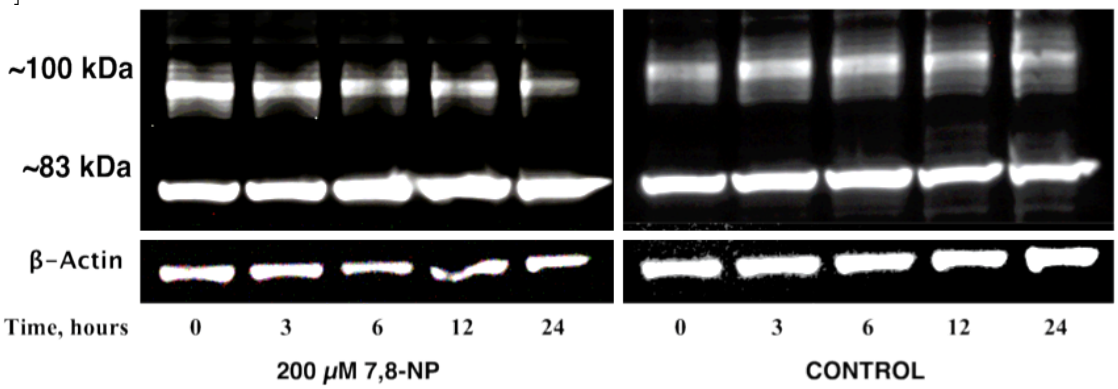

[B]

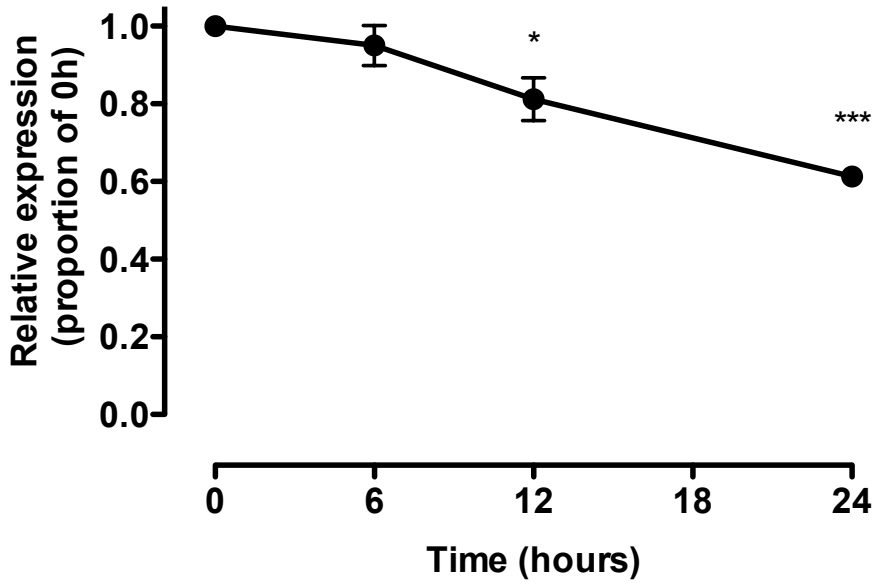

Figure 5.7: Time course of 7,8-NP–mediated down-regulation of CD36 protein.

HMDM cells (5x10^6 cells/mL) were treated with 200 μM of 7,8-NP in the whole medium for the indicated time. Cell lysate was assessed for CD36 protein expression via western blot **(A)**. **(B)** Quantitative densitometry of Western blots displaying time-dependent down-regulation of the fully glycosylated 100 kDa band relative to 0 hour control. Results were normalised by actin and displayed as mean ± SEM of triplicate experiments.

5. EFFECT OF 7,8-DIHYDRONEOPTERIN ON OXLDL UPTAKE BY MACROPHAGES

As seen previously (chapter 4), 7,8-NP could be oxidised to 7,8-dihydroxanthopterin (7,8-DXP) or neopterin. The effect of these oxidation products on CD36 was established to determine if 7,8-NP alone was responsible for the CD36 down-regulation (fig. 5.8). Neopterin slightly up-regulated the intensity of 100 kDa CD36 band, whereas 7,8-DXP slightly down-regulated it. Overall, neither 7,8-DXP nor neopterin oxidation products could be responsible for the 7,8-NP–mediated reduction in the CD36 levels.

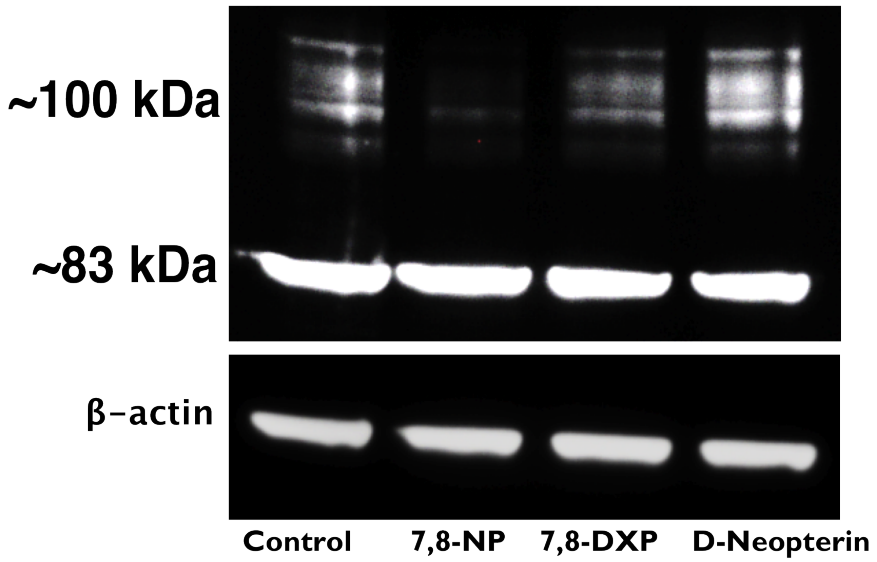

Figure 5.8: Effect of 7,8-NP degradation products, D-neopterin and 7,8-dihydroxanthopterin on the level of CD36.
HMDM cells ($5x10^6$ cells/mL) were treated with 250 μM solutions of 7,8-NP, D-neopterin and 7,8-dihydroxanthopterin (freshly dissolved in degassed RPMI-1640) for 24 hours. Cell lysates were assessed for CD36 protein expression via Western blot. Results are displayed as a representative Western blot (n=3).

5.2.4 7,8-NP reduces the mRNA expression of CD36 in HMDM cells

To test the mechanism of 7,8-NP–mediated down-regulation of the CD36 protein in HMDM cells, its effect on the CD36 mRNA was investigated. The RT-qPCR method development is outlined in Appendix I. The cells were treated with varying concentrations of 7,8-NP for 24 hours as for immunoblotting, but harvested into Trizol. mRNA was isolated from Trizol samples, converted into cDNA and the cDNA was tested on real time RT qPCR for a change of relative CD36 mRNA copy number. The target gene expression was normalised by the expression of reference genes β-actin and using REST2009 software (Pfaffl *et al.*, 2002). The data generated from three separate experiments were combined on one graph using Prism5 (fig. 5.9).

CD36 mRNA expression decreased by 30% in the presence of 100 μM 7,8-NP and by 40% in the presence of 200 μM 7,8-NP respectively (fig. 5.9). Three hundred μM of 7,8-NP did not down-regulate CD36 mRNA levels (fig. 5.9).

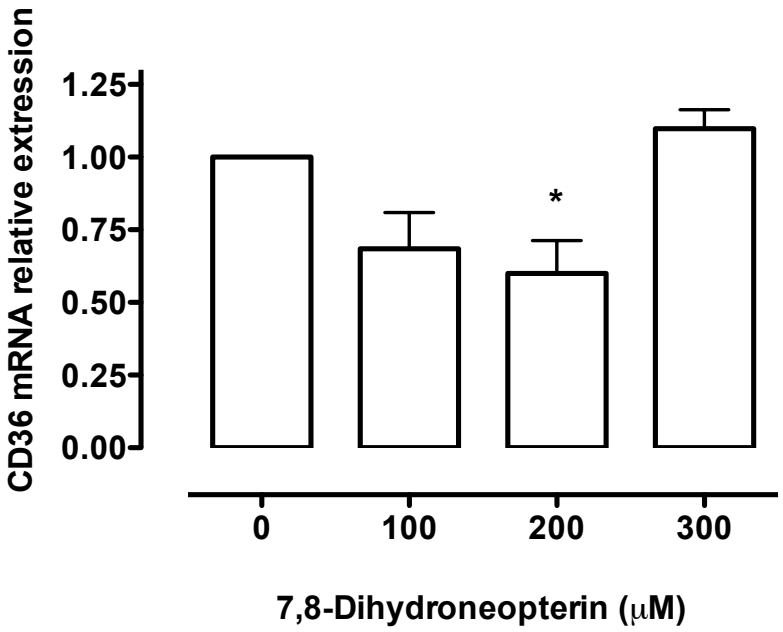

Figure 5.9: 7,8-NP reduces the CD36 mRNA expression in HMDM cells. HMDM cells (1x10^6 cells/mL) in RPMI-1640 supplemented with 10% human serum were treated with increasing concentrations of 7,8-NP for 24 hours. Two to three wells per treatment were collected into TRIzol and assessed for CD36 mRNA expression levels relevant to the untreated control. Reference genes were actin and HPRT and assessment was done using real time RT qPCR. The data was normalised to reference gene expression in REST2009 and plotted as a combined value from three separate experiments using Prism5. Results are displayed as mean ± SEM. Significant difference from 0 μM 7,8-NP using repeated measures one-way ANOVA with Dunnett's post test is indicated with *,$p<0.05$.

5.2.5 Significance of 7,8-NP–mediated CD36 down–regulation

Relative abundance of 7,8-NP and CD36 in the atherosclerotic plaque

One approach to evaluate the significance of 7,8-NP–modulation of CD36 levels was to assess the levels of both 7,8-NP and CD36 within atherosclerotic plaques. It was hypothesised that higher 7,8-NP levels would coincide with low CD36 levels. Atherosclerotic plaque material, sectioned longitudinally into 3 mm slices, was processed as described in Materials and Methods, section 2.5.3. 7,8-NP was measured via HPLC by T. Janmale and CD36 was assessed via Western blot. Two types of sample were prepared: the whole homogenate and the 'supernatant only' soluble fraction (homogenate centrifuged at 11,000 g for 10 minutes). Both sample types were tested for protein using BCA assay and loaded onto SDS-PAGE gel according to the protein content (50 μg of sample protein per well). Immunoblotting was performed as for the CD36 protein quantification in section 5.2.3.

The sample loading onto the wells, although standardised for the overall protein content, could not be standardised for the macrophage content. Immunoblotting for the macrophage marker CD68 was unsuccessful (data not shown). Thus, qualitative assessment of the data is presented. CD36 protein levels differed from section to section along the length of the plaque (figures 5.10a and 5.11a). Tissue-bound and soluble CD36 also showed different profiles along the plaque. In plaque A, soluble CD36 was present in sections 2, 3 and 6 (fig. 5.10a-top), but tissue-bound CD36 was absent from section 3 and present in sections 1, 2, 4 and 6 (fig. 5.10a-bottom), with sections 2, 4 and 6 containing both 80 and 100 kDa isoforms. Plaque B showed 100 kDa protein in the soluble fraction of sections 6–8, and 71 kDa in section 2 (fig. 5.11a-top); whereas the whole homogenate had high levels of both isoforms in section 8, 100 kDa in section 7 and 71 kDa in sections 2 and 3 (fig. 5.11a-bottom). Overall, plaque supernatant contained mostly the 100 kDa isoform, which supported the idea that 100 kDa is the surface protein that is shed into the extracellular space by the cells (Koonen *et al.*, 2011). Section 2 of plaque B was an exception. No pattern of CD36 presence in sections was evident with respect to plaque morphology.

7,8-NP detected in the plaque sections (figures 5.10b and 5.11b) did not associate (inversely, as per hypothesis) with the levels of CD36 protein along the plaque. Section 1 of plaque A contained the highest amount of 7,8-NP per g plaque protein (fig. 5.10b), and this section did not contain soluble CD36 (fig. 5.10a-top). Sections 4 and 5, however, which were low in 7,8-NP did not contain any soluble CD36 as well.

Similarly, an absence of any trend was observed in plaque B with section 3 being high in 7,8-NP and low in soluble CD36 (figures 5.11b and 5.11a-top, respectively). Yet, out of sections 3-6 with medium relative 7,8-NP levels (fig. 5.11b), sections 4 and 6 contained some soluble CD36 (fig. 5.11a-top). The difference between 7,8-NP levels in sections 1, 2, 7, 8 and 9 of plaque B was small (fig. 5.11b), but their profiles of CD36 in whole plaque homogenate and soluble fraction are large (fig. 5.11a). No association between low 7,8-NP levels and high CD36 levels was thus apparent in the two plaques used for the pilot study.

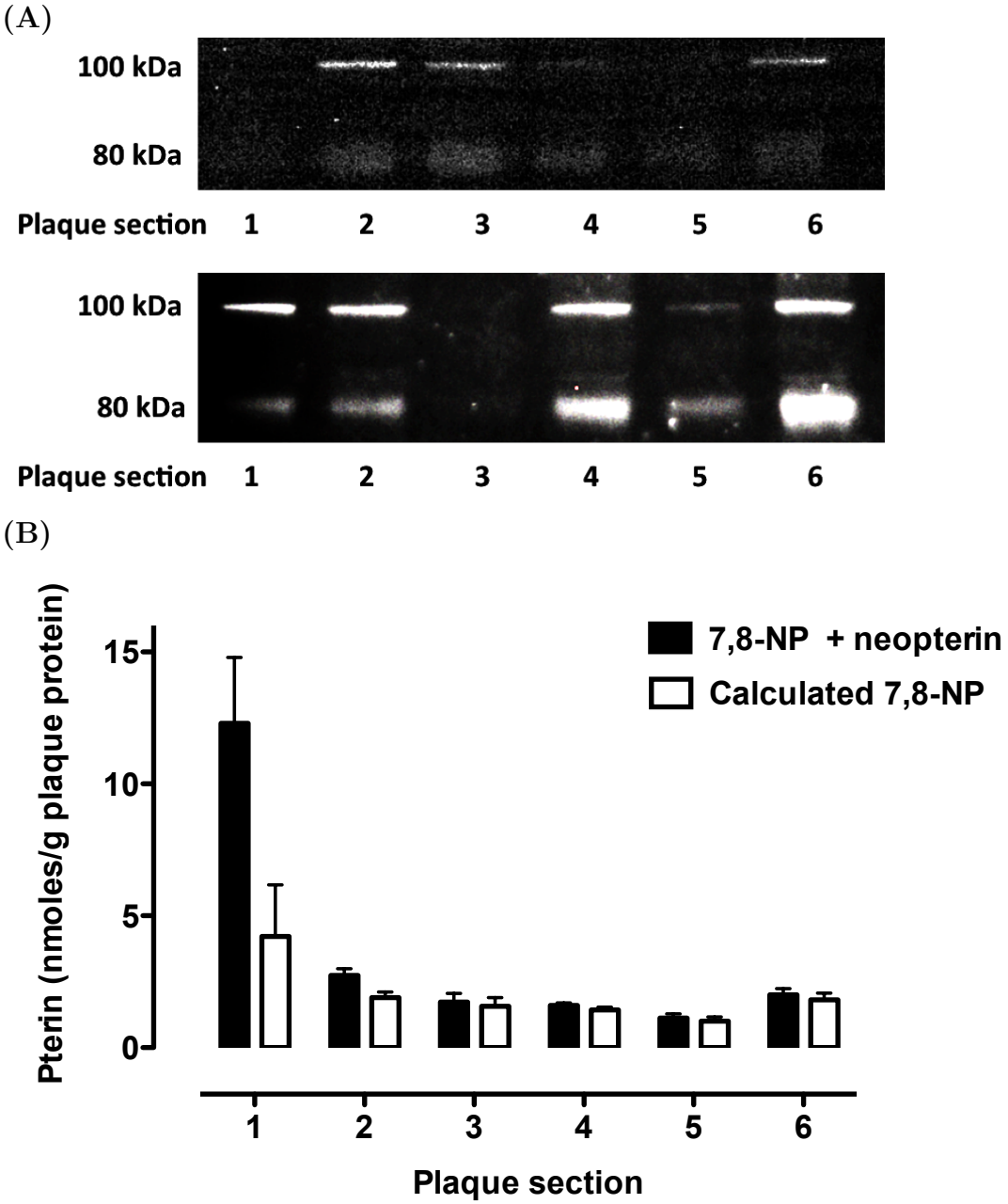

Figure 5.10: CD36 and 7,8-NP levels are differentially distributed across the length of atherosclerotic plaque A.

(A) Homogenized atherosclerotic plaque sections were assessed for soluble and tissue-bound CD36 by Western blot. The loading was normalised by the amount of protein per section and the transfer efficiency was assessed by Coomassie Blue. CD36 in soluble fraction (top) and whole homogenate (bottom) of atherosclerotic plaque.

(B) Neopterin and total pterin levels in homogenised atherosclerotic plaque sections were measured by T. Janmale via HPLC. 7,8-NP was calculated by subtracting neopterin values from total neopterin for the section. Results are displayed as mean ± SEM from triplicate measurements.

(A)

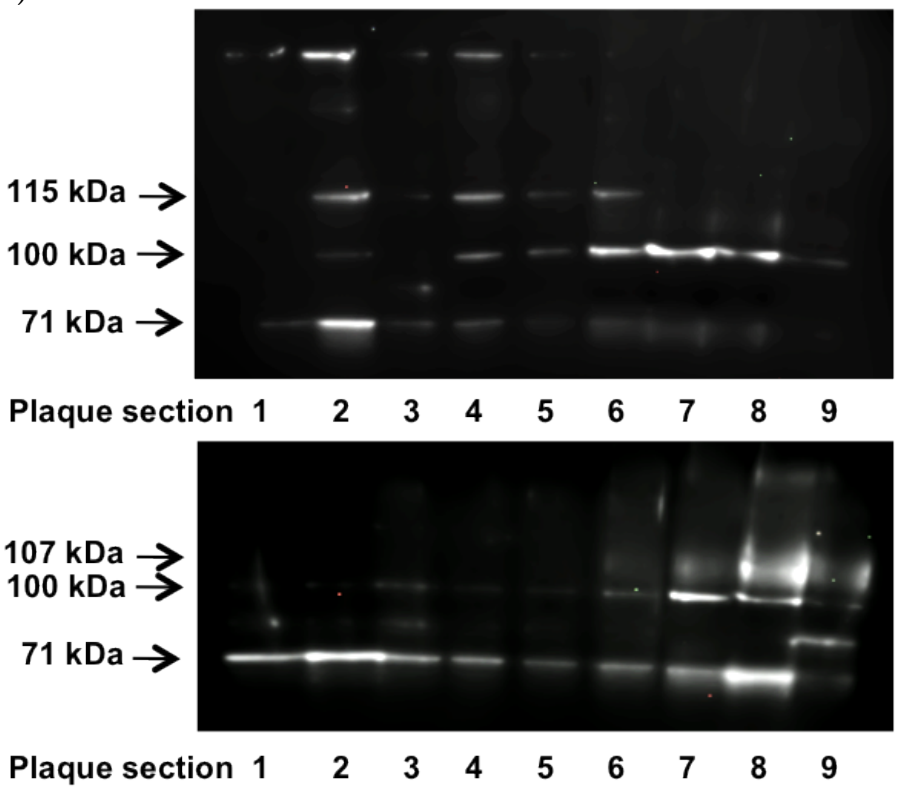

(B)

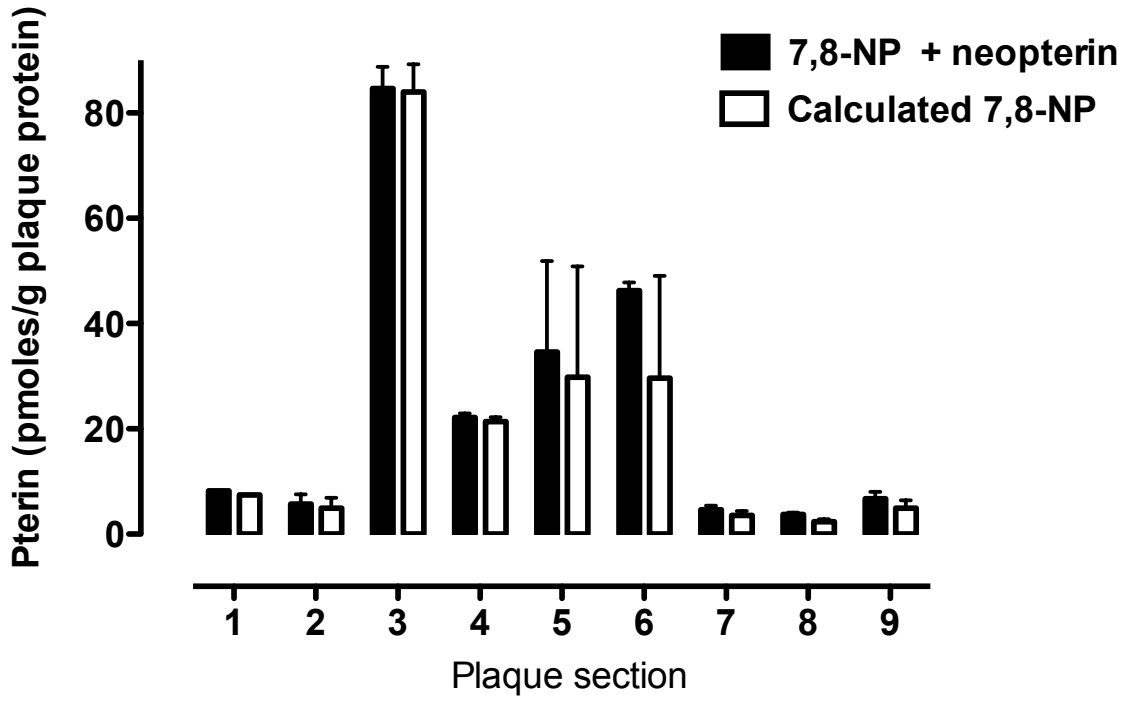

Figure 5.13: CD36 and 7,8-NP levels are differentially distributed across the length of atherosclerotic plaque B.

Figure 5.11: CD36 and 7,8-NP levels are differentially distributed across the length of atherosclerotic plaque B.
(A) Homogenized atherosclerotic plaque sections were assessed for soluble and tissue-bound CD36 by Western blot. The loading was normalised by the amount of protein per section and the transfer efficiency was assessed by Coomassie Blue. CD36 in soluble fraction (top) and whole homogenate (bottom) of atherosclerotic plaque.
(B) Neopterin and total pterin levels in homogenised atherosclerotic plaque sections were measured by T. Janmale via HPLC. 7,8-NP was calculated by subtracting neopterin values from total neopterin for the section. Results are displayed as mean ± SEM from triplicate measurements.

Effect of 7,8-NP–mediated down-regulation on cell survival

OxLDL toxicity has been the core theme of this project. Thus, the capacity for 7,8-NP–mediated CD36 down–regulation to prevent oxLDL toxicity to HMDM cells was investigated. As shown in chapter 3, a 6 hour exposure to oxLDL was sufficient to induce cellular death. Down-regulated CD36 protein did not recover until after 6 hours post–7,8-NP removal[1] (fig. 5.13). This fact was used to develop an experiment which tested the effect of 7,8-NP–mediated down-regulation alone (fig. 5.12). HMDM cells were pre-incubated with 200 μM of 7,8-NP for 24 hours to down-regulate CD36, after which 7,8-NP was removed from the extracellular medium. The cells were rinsed thoroughly and treated with increasing concentrations of oxLDL for 6 hours. As was shown in chapter 3, oxLDL treatment of HMDM cells for 6 hours resulted in an irreversible cell death. After 6 hours, the oxLDL–containing medium was replaced with fresh medium and the cells were incubated for another 18 hours. At the end of the second 24 hour period, cellular viability was measured via MTT reduction (fig. 5.14). 7,8-NP pre-treatment did not protect HMDM cells from oxLDL–induced cell death. At concentrations below LC_{50}, the metabolic capacity of the pre-treated cells was approximately 10% higher than that of non pre-treated cells, yet such an effect of 7,8-NP was also observed in the non-oxLDL–treated HMDM (fig. 5.14a). Combined data showed an even smaller protection of pre-treatment with 7,8-NP (fig. 5.14b). Thus, pre-incubation with 7,8-NP was not protective.

[1]The recovery of the down-regulated CD36 band was small in the 6 hours post incubation with 7,8-NP. The level of 100 kDa protein, corrected for loading changed from 0.5 to 0.68 in the 6 hours after the 7,8-NP removal. Western blot images were artificially enhanced for best appearance in print, therefore the relative visual intensity of the bands may appear different from the quantitative analysis, which was performed on the raw images.

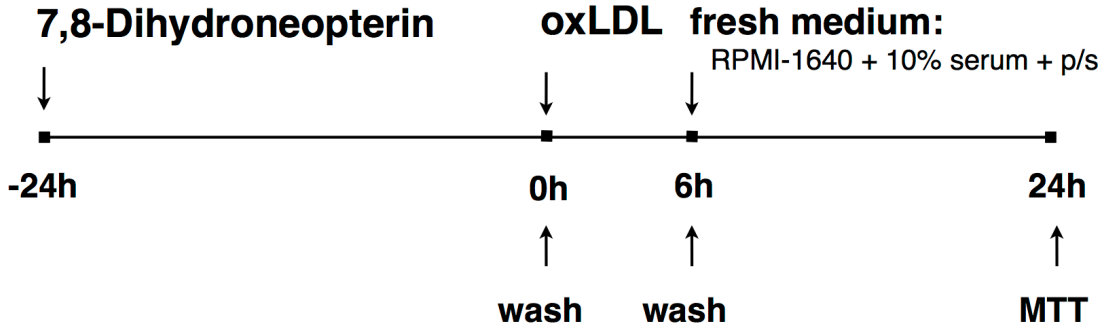

Figure 5.12: Experiment diagram.
Experiment designed to test the significance of 7,8-NP–mediated CD36 down-regulation in the context of oxLDL toxicity to HMDM cells. HMDM cells were pre-treated with 200 of μM 7,8-NP for 24 hours to down–regulate CD36. The cells were then washed thoroughly and incubated with oxLDL for 6 hours. After this oxLDL was aspirated, the cells were washed and re-supplemented with fresh whole medium for additional 18 hours. Cellular viability was measured via MTT assay at the end of a 24 hour period from the addition of oxLDL.

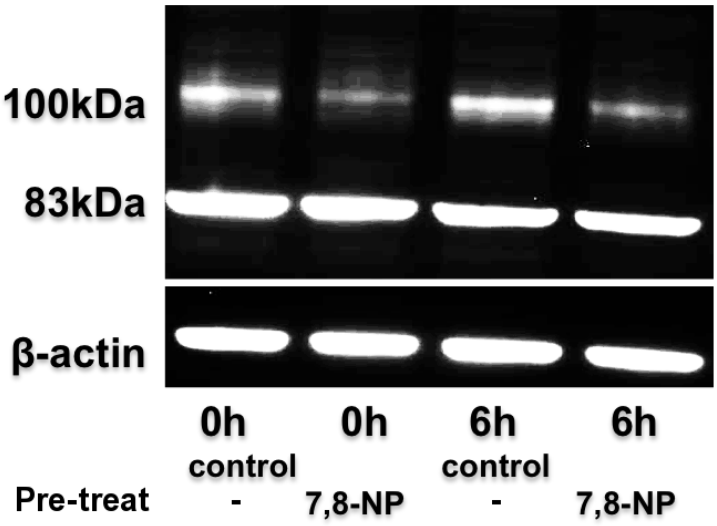

Figure 5.13: CD36 recovery after 7,8-NP pre-treatment does not occur until after 6 hours.

HMDM cells (5x10^6 cells/mL) were treated with (7,8-NP, 0h) or without (0h control) 200 μM of 7,8-NP for 24 hours, washed and collected 6 hours later. Cell lysate was assessed for CD36 protein expression via western blot. Quantitative densitometry of the fully glycosylated 100 kDa band, corrected for actin, was 0.5 at 0 hour relative to control at 0 hour and 0.68 at 6 hours post pre-treatment compared to 0.92 at 6 hours post–0 hour control.

[A]

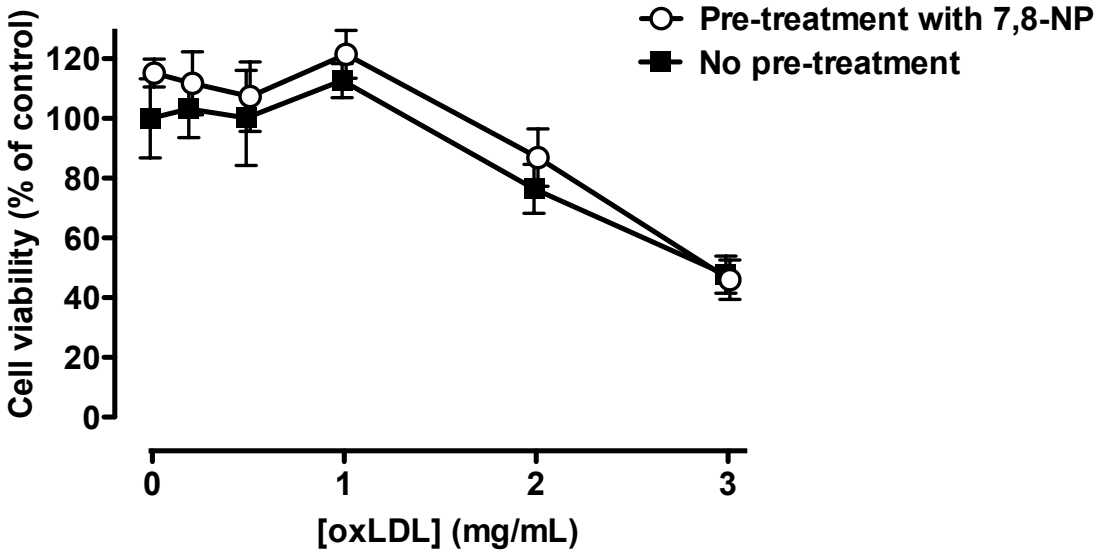

[B]

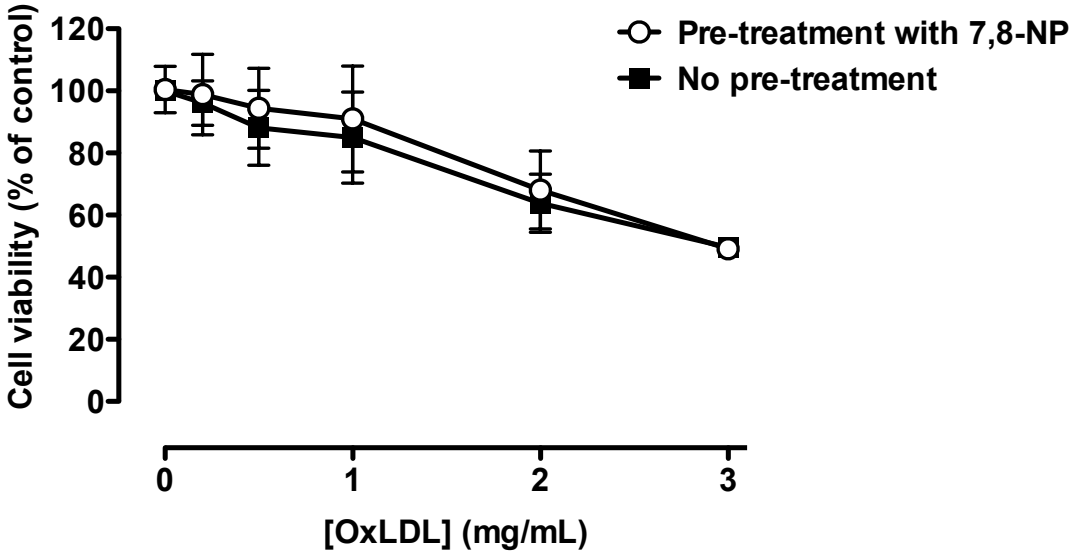

Figure 5.14: Pre-treatment with 7,8-NP to down-regulate CD36 does not protect HMDM cells from oxLDL–induced cell death.
HMDM cells ($5x10^6$ cells/mL) in the whole medium were pre-treated (empty circles) or not (filled squares) with 200 of μM 7,8-NP to down-regulate CD36 and thoroughly washed to remove residual 7,8-NP. The cells were then exposed to the increasing concentrations of oxLDL for 6 hours, washed and incubated in the fresh whole medium for 18 more hours. Cellular viability was assessed via MTT reduction at the end of the 24 hour period post-oxLDL addition and expressed as a percentage of the untreated control. Results are displayed as **(A)** mean ± SEM of triplicates from a single experiment, **(B)** mean ± SEM from three experiments combined. Difference between treatments was not significant (two-factor AVOVA).

5. EFFECT OF 7,8-DIHYDRONEOPTERIN ON OXLDL UPTAKE BY MACROPHAGES

Pre-incubation with 7,8-NP led to a slight increase of intracellular GSH level in HMDM cells exposed to oxLDL in comparison to non-pre–treated cells (fig. 5.15). HMDM cells were treated as described above (fig. 5.12) and analysed for intracellular GSH at the end of the second 24 hour period. At all oxLDL concentrations tested the pre-treated HMDM cells had a slightly increased level of GSH, Δ of 1 nmol/well at 0 mg/mL oxLDL, 3 nmol/well at 1 mg/mL and 2 nmol/well at 2 and 3 mg/mL oxLDL. This can be interpreted as a result of reduced oxidative flux. HMDM cells with down-regulated CD36 receptor showed lower oxidative damage, especially at the lower oxLDL exposure concentration (1 mg/mL).

Ultimately, the level of intracellular 7-ketocholesterol in the pre-treated cells was assessed to determine whether pre-treatment was successful at reducing the uptake of oxLDL (fig. 5.16). Contrary to the original hypothesis, the intracellular concentration of 7KC in the pre-treated cells was not different from the non-pre-treated cells (fig. 5.16). This indicated that down-regulation of CD36 did not result in reduced uptake of oxLDL over the first 6 hours of exposure. The hypothesis of CD36–driven oxLDL uptake down-regulation was, therefore, reconsidered.

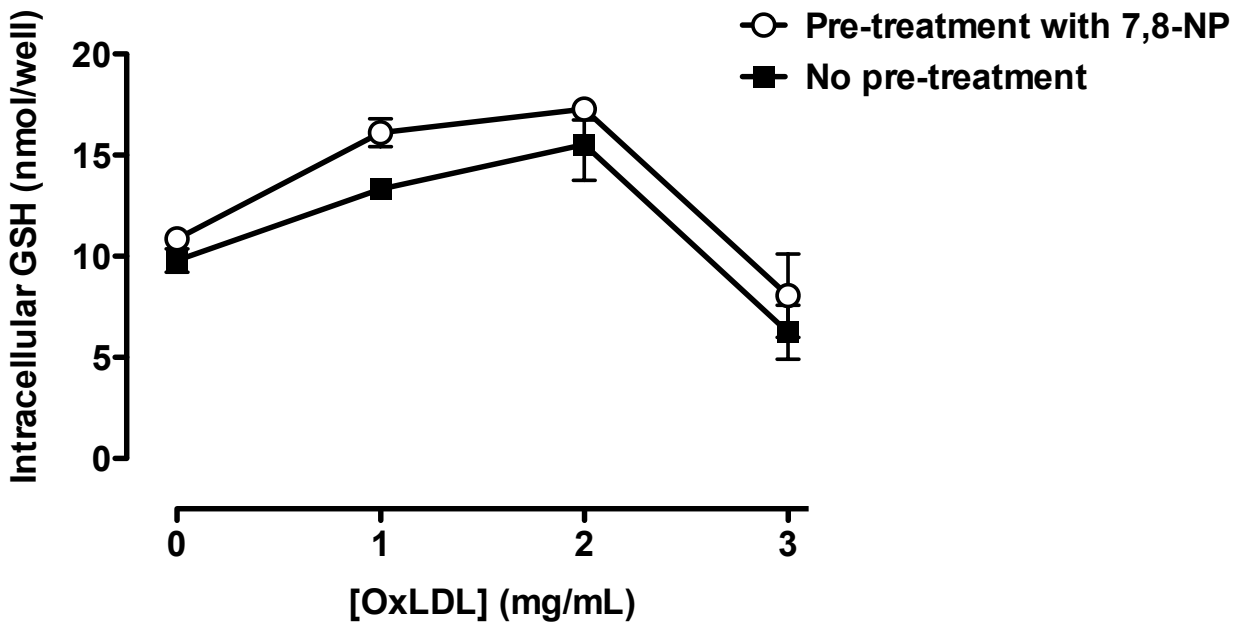

Figure 5.15: Pre-treatment with 7,8-NP leads to a small increase of intracellular GSH after subsequent exposure of HMDM to oxLDL.
HMDM cells (5x10^6 cells/mL) in the whole medium were pre-treated (empty circles) or not (filled squares) with 200 μM 7,8-NP and thoroughly washed to remove residual 7,8-NP. The cells were then treated with the increasing concentrations of oxLDL for 6 hours, washed and incubated in the whole medium for additional 18 hours. Cell lysates were analysed for GSH 24 hours after the addition of oxLDL. Results are displayed as mean ± SEM of triplicates from a single experiment. Statistical significance: two-factor ANOVA showed a significant difference between GSH levels in pre-treated and non-pre-treated cells, $p<0.05$. Interaction between oxLDL concentration and treatment was not significant.

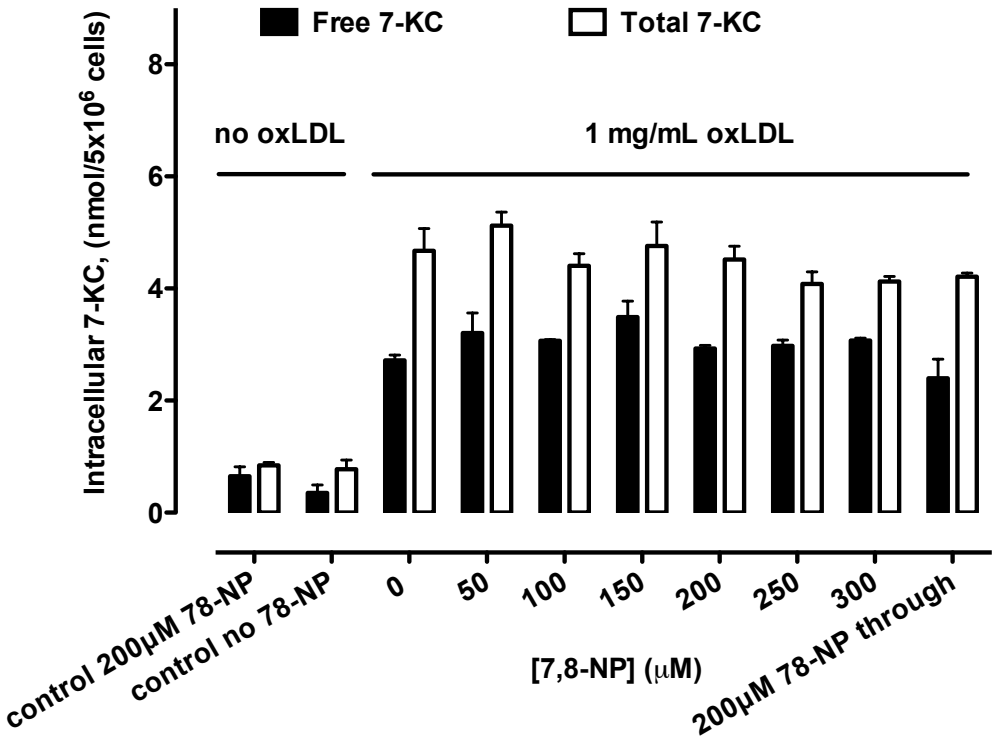

Figure 5.16: Pre-treatment with 7,8-NP does not affect free or total 7KC uptake in HMDM exposed to oxLDL for 6 hours.
HMDM cells (5x10^6 cells/mL) in the whole medium were pre-treated (except for the no 7,8-NP control) with the indicated concentrations of 7,8-NP for 24 hours, thoroughly washed to remove residual 7,8-NP, treated with 1 mg/mL oxLDL for 6 hours, collected and assessed for free and total 7-ketocholesterol on the HPLC. The last treatment on the left, "200 through" corresponds to the sample re-supplemented with 200 μM 7,8-NP for the duration of the 6 hour incubation with oxLDL. Results are displayed as mean $\pm$ SEM of triplicate measurements from a single experiment. Difference between 7,8-NP concentrations was not significant (one-factor ANOVA with Dunnett post test).

5.2.6 7,8-NP–mediated reduction of intracellular 7KC is serum dependant

The effect of 7,8-NP on total 7KC levels in HMDM cells was, therefore, tested in the absence of serum (fig. 5.17). Cholesterol efflux onto extracellular serum HDL is well documented and is the final stage of reverse cholesterol transport . The decrease in total 7KC was only observed in the presence but not the absence of extracellular human serum supplemented at 10%. The overall level of total 7KC in the absence of serum was lower than that in the serum–supplemented cells in one experiment and higher in other, thus the combined experimental data is presented (fig. 5.17b). The level of 7,8-NP–inhibited 7KC (serum present) was lower than that in cells incubated with 7,8-NP and oxLDL in the absence of serum. This result indicated a preliminary route that should be pursued through further experimentation.

[A]

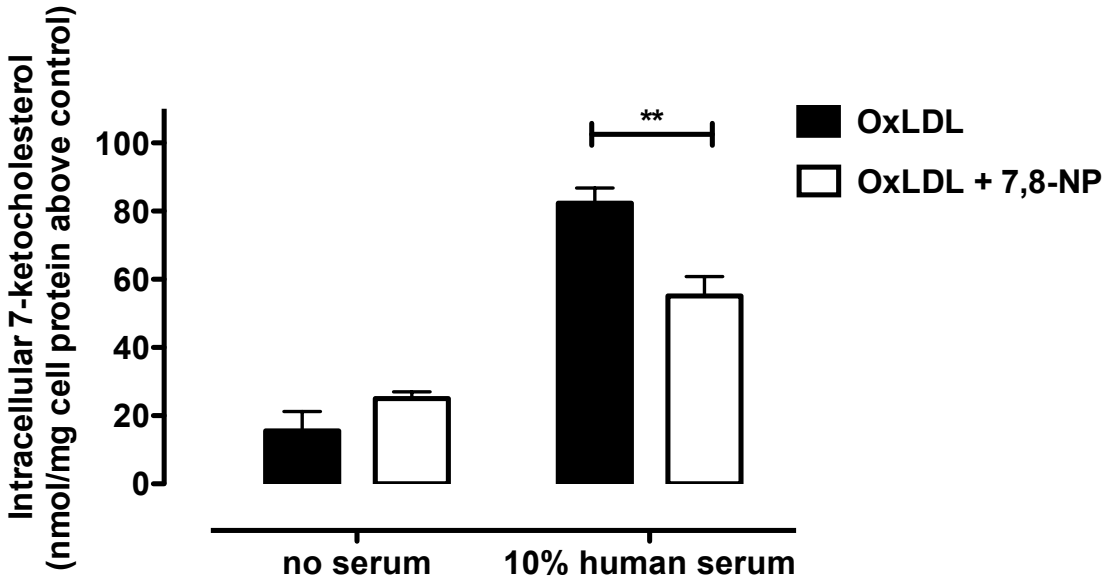

[B]

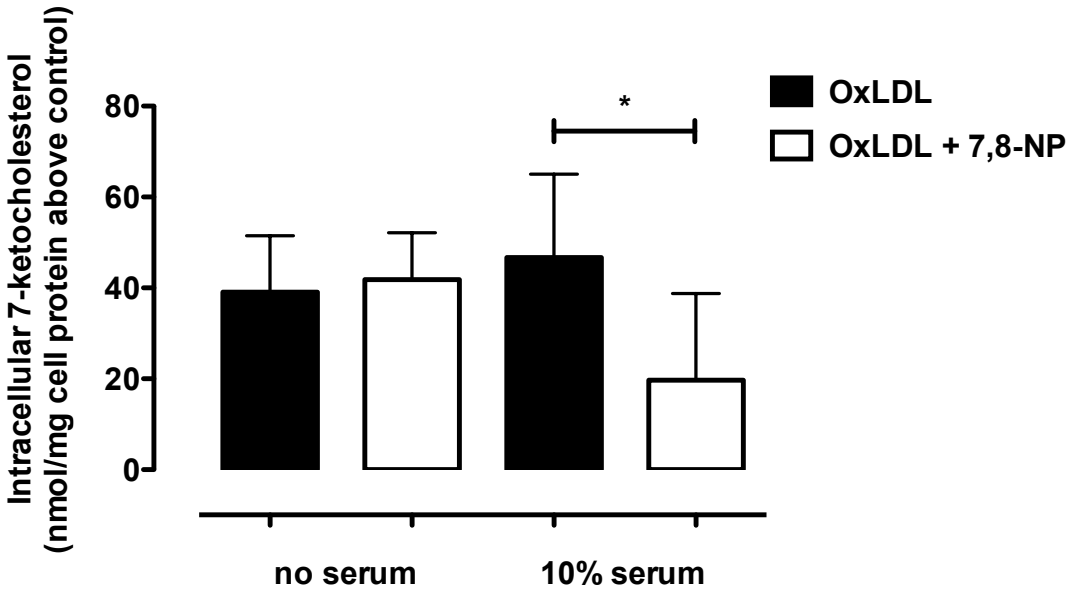

Figure 5.17: 7,8-NP mediates the reduction of intracellular total 7KC in HMDM cells exposed to oxLDL only in the presence of extracellular serum. HMDM cells ($1x10^6$ cells/mL) were treated with 1 mg/mL oxLDL in the presence or absence of serum and with (empty bars) or without (filled bars) 200 μM 7,8-NP for 24 hours. Cell lysates were assessed for intracellular total 7-ketocholesterol and protein and expressed as increase above respective no oxLDL control (average control values over three experiments: 19 and 29 nmol/mg protein for no serum and 10% serum respectively). Results are displayed as **(A)** mean ± SEM of triplicates from a single experiment; **(B)** average values ± SEM from three experiments combined. Paired t-test was done on the data from 3 experiments, significance (paired and unpaired t-test) as indicated, *, $p<0.05$, **, $p<0.01$.

5.3 Discussion

The research in this chapter attempted to confirm the down-regulation of macrophage oxLDL uptake by 7,8-NP and investigated the mechanisms and significance of this phenomenon. This chapter contributes to the overall aim of the thesis by characterising the effect of 7,8-NP on oxLDL internalisation during acute oxLDL–induced toxicity to HMDM cells.

5.3.1 7,8-NP down-regulates the levels of oxLDL in HMDM cells

7KC as a marker of oxLDL uptake

Previous research showed 7,8-NP–mediated reduction of DiI–labelled intracellular oxLDL (Gieseg *et al.*, 2010a). However, due to the limitations associated with DiI, the data had to be confirmed with a different oxLDL probe. DiI was thought to be unreliable as probe for a number of reasons. Fluorescent DiI was unstable and faded with time, suggesting it was being oxidised. Whether the oxidation proceeded via singlet oxygen or other ROS–mediated reaction was not clear, but both these processes decreased the reliability of the label. In addition, previous work in the laboratory indicated that DiI–labelled oxLDL lost some of its toxicity and this was inhibitory to the types of experiments that had to be performed with it. 7KC was preferred over a fluorescent lipid label like DiI, because this oxysterol occurs naturally within the oxLDL particle. It does not, therefore, unnaturally interfere with oxLDL clearance in the cell or with other cellular processes. 7KC was also superior because its measurement provided insight into oxLDL cholesterol metabolism in HMDM cells, as the assay measured the levels of free and esterified 7KC in each sample. Average total 7KC was 28.4 mol 7KC per mol of oxLDL compared to 9.3 mol/mol of free 7KC. Such results were comparable to the values of 143 $\pm$ 20 nmol/mg LDL protein (or 28.6 $\pm$ 4 mol 7KC per mol LDL) reported in Gerry *et al.* (2008). A proportion of baseline intracellular esterified 7KC levels was likely derived from the extracellular serum over the course of investigation. Sixty five μM levels of 7KC were detected in the human serum used for cell culture. On average, the content of total 7KC in the serum was less than 1.3% (fig. 5.2), as the concentration of total cholesterol in plasma of apparently healthy donors was determined to be 5.11 $\pm$ 1.01 mM (Asmis & Jelk, 2000a).

Kinetics of 7KC and oxLDL uptake and processing

OxLDL was consistently taken up by HMDM cells over the course of 24 hour incubation (fig. 5.1) as measured by 7KC accumulation. The ratio of total 7KC to free 7KC in cells differed from that in oxLDL (1:1 *de novo* uptake in cells vs. 3.37 in oxLDL), which implied that oxLDL contents such as 7KC were processed by the cell. Internalised oxLDL is initially compartmentalised in the endosomes/lysosomes (Brown *et al.*, 2000; Itabe *et al.*, 2000; Maor & Aviram, 1994; Wang *et al.*, 2005). During the first 6 hours of incubation, the HMDM cells in this study contained predominantly free 7KC, which suggested that oxLDL components were hydrolysed by the action of cellular esterases and lipases within those compartments (Brown *et al.*, 1979; Jerome & Yancey, 2003; Wang *et al.*, 2005). Modified LDL, however, and, especially, oxysterols, have been shown to reduce the rate and inhibit oxLDL degradation the efflux from the macrophage (Hoff *et al.*, 1993). 7KC has been shown to inhibit the action of cholesterol transporters (Jessup & Kritharides, 2000; Jessup *et al.*, 2002). OxLDL moieties were reported to raise lysosomal pH, inactivating lysosomal enzymes and thus inhibiting further oxLDL processing (Cox *et al.*, 2007). These changes of cellular homeostasis lead to excessive cholesterol accumulation in the form of re-esterified cholesterol and its products (Brown *et al.*, 1979). Evidence of this process was observed in the present study when, after 9-12 hours HMDM cells started accumulating 7KC esters (fig. 5.1). This was likely due to the action of acyl coenzymeA : cholesterol acyltransferase-1 (ACAT-1) (Rudel *et al.*, 2001).

A few studies have claimed that oxLDL incubation with macrophages had not led to CE accumulation in cells in the same way that aggregated oxLDL did (Asmis & Jelk, 2000a; Maor & Aviram, 1994). In this study, however, 7KC esters were evident in the oxLDL–treated cells. Either oxLDL in the present study underwent a slight aggregation sufficient to promote CE storage or the current HMDM experimental design differs from the ones described by Asmis & Jelk (2000a) and Maor & Aviram (1994).

Effect of 7,8-NP on oxLDL uptake

Two hundred μM of 7,8-NP reduced the levels of intracellular total 7KC and, therefore, oxLDL by 40–60% by the end of a 24 hour exposure (figures 5.4 and 5.5). This agreed with the magnitude of inhibition observed by Gieseg *et al.* (2010a). The effect was predominantly evident in total 7KC, suggesting that esterified rather than free component of intracellular 7KC was decreased in the presence of 7,8-NP. The

effect was evident as early as 12 hours after the initial exposure and was significant at 24 hours (5.4). Partial inhibition of total 7KC levels observed in this study was on a similar time-frame as the onset of esterification (the implications of which will be discussed below). Conversely, Gieseg *et al.* (2010a) observed a reduction in the DiI–associated oxLDL as early as 3 hours after the exposure. The difference in the time-frame could either signal the 7,8-NP–mediated interference of DiI probe with oxidative stress induced by oxLDL, or the processing of DiI–labelled oxLDL in a mode that degrades the DiI probe. The latter is possible as some of the data presented here suggest that 7,8-NP affects oxLDL processing by the cells.

A similar magnitude (40%) of oxLDL uptake inhibition was observed by (Nozaki *et al.*, 1995) in macrophages of CD36 scavenger receptor-deficient patients. In contrast, Wintergerst *et al.* (2000) reported only a small 20% inhibition of oxLDL uptake in the presence of CD36 ligands like thrombospondin and antibodies to to CD36, OKM-5 and SMO. CD36 scavenger receptor is prominent in atherosclerosis research (Collot-Teixeira *et al.*, 2007; Silverstein *et al.*, 2010). It has been associated with decreased uptake of modified lipoproteins and implicated in oxLDL toxicity (Higashi *et al.*, 2005; Nozaki *et al.*, 1995; Park *et al.*, 2009; Wintergerst *et al.*, 2000). Therefore, CD36 receptor down-regulation was examined as a potential mechanism of 7,8-NP mediated reduction in intracellular oxLDL.

5.3.2 CD36 down-regulation by 7,8-NP: levels and significance

Previous work by Amit (2008) determined that the levels of SR-A were not affected by 7,8-NP, but the levels of CD36 protein were down-regulated in 40% of the experiments. This effect on CD36 protein was confirmed by the present study (figures 5.6 and 5.7). However, the absence of down-regulation in a quarter of the experiments was also observed. This proportion was similar to that observed with the lack of 7,8-NP effect on uptake. These results suggest that there are likely to be as yet undetermined factors contributing to this process. Some of the discrepancy could, perhaps, be attributed to the heterogeneity of primary HMDM cell preparations both in cholesterol processing (Kruth, 2001) and CD36 level expression (Wintergerst *et al.*, 1998).

7,8-NP decreased the protein expression of both ∼100 and ∼80 kDa CD36 glycosylation products (fig. 5.6). Alessio *et al.* (1996) showed that the higher molecular

weight protein was a mature, plasma-membrane–expressed protein species while the lower MW product (74 kDa in the original publication) was the developing, not fully glycosylated receptor present in the Golgi. Hoosdally *et al.* (2009), however, demonstrated that some of the non-fully glycosylated CD36 protein isoforms were successfully expressed on the cellular membrane. There are 10 putative glycosylation sites on CD36. Not all of them are glycosylated to the same extent in different cell types. 53kDa is unglycosylated protein weight, while most studies report 71, 74, 84, 88, 95 kDa glycosylated CD36 protein. Overall, CD36 glycosylation is considered to be important for the trafficking of the protein to plasma membrane, rather than ligand binding (Hoosdally *et al.*, 2009). Significant down-regulation of 100 kDa protein by 50-60% was observed at 200 and 250 μM. This result, however, was variable in magnitude since the time-course data for 200 μM 7,8-NP showed a consistent 40% decrease of the 100 kDa band (fig. 5.4). The difference in absolute values could be associated with different expression level of CD36 in macrophage culture as Wintergerst *et al.* (1998) reported between 35 and 75% of CD36–positive cells per well on the 10^{th} day of HMDM cell culture.

The 100 kDa CD36 protein down-regulated by 20% after the first 12 hours of incubation and by 40% after 24 hours (fig. 5.7). This down-regulation was likely due to the decrease in mRNA copy number, as it was down by 40% by the end of 24 hours (fig. 5.7). This was different from the effect of ceramides reported by Luan & Griffiths (2006). Ceramide, a signalling molecule, was shown to reduce both CD36 expression and oxLDL uptake (Luan & Griffiths, 2006). The effect was not dependant on mRNA expression inhibition and was suggested to be caused by CD36 protein trafficking blockade (Luan & Griffiths, 2006). The down-regulation with 7,8-NP is also different from the inhibition of CD36 transcription induced by another antioxidant, α-TocH (Ricciarelli *et al.*, 2000). While in the present study a baseline down-regulation of 7,8-NP was observed, α-TocH had an antagonistic effect on oxLDL-induced up-regulated CD36. Ricciarelli *et al.* (2000) and Munteanu *et al.* (2006) reported that oxLDL induced CD36 expression via enhancing the presence of PPAR-γ regulatory element. Han *et al.* (1997) showed that incubation of macrophages with BSA and HDL caused a dose-dependent reduction in the expression of CD36 mRNA. This was independently confirmed by (Carvalho *et al.*, 2010) The authors suggested that alterations of cellular cholesterol levels due to efflux onto HDL and BSA were responsible for the observed effect. This was confirmed in the authors' subsequent publication

(Han *et al.*, 1999). Thus, cholesterol efflux is another mechanism that is able to regulate CD36.

Significance

OxLDL binding to CD36 has been suggested to mediate oxLDL uptake, activate the production and release of pro-inflammatory cytokines and ROS (Boyle, 2005; Moore, 2006; Park *et al.*, 2009; Silverstein *et al.*, 2010). The range of possible effects of the CD36 signalling includes cellular death, inflammatory gene expression, adhesion, and migration (Park *et al.*, 2009). Therefore, the significance of the observed CD36 down-regulation by 7,8-NP was investigated.

A pilot qualitative assessment of two atherosclerotic plaques was performed to determine whether there was an inverse correlation between 7,8-NP and CD36 levels along the longitudinal axis of a plaque (figures 5.10 and 5.11). CD36 has been detected in atherosclerotic plaques previously (Collot-Teixeira *et al.*, 2008; Nakata *et al.*, 1999), but never in relation to 7,8-NP. The analysis was carried out despite the obstacles with signal standardisation of CD36 (as alluded to in section 5.2.5). If this work continued, an alternative protocol of standardising or referencing the gel loading should be investigated. No association between the high 7,8-NP and CD36 levels was observed. The absence of correlation between 7,8-NP and CD36 levels was not surprising considering the a plaque is a milieu of material that had undergone extensive remodelling over the decades of development (Gieseg *et al.*, 2009). In addition, plaque sectioning and homogenisation of the 3 mm slices might lack the necessary precision needed to identify a subtle correlation between the markers. Other tests, for example, direct immunoblotting of plaque slices with macrophage, CD36 and 7,8-NP specific antibodies, might be more appropriate for this application. The difference in the total and soluble CD36 profiles for each section probably reflects the complexity of the interactions within the plaque. The variability between the plaque sections can reflect a number of factors, including cellular content of those sections, inflammatory status including the suite of cytokines/small signalling molecules present and plaque section history, past and present activity (Gieseg *et al.*, 2009; Shchepetkina, 2008).

The effect of CD36 down-regulation on HMDM cell death was also investigated. The CD36 level was down-regulated by 7,8-NP treatment, after which the pterin was

washed off and the cells were incubated with oxLDL for 6 hours (fig. 5.12). During this time, the 7,8-NP–mediated CD36 knock-down did not recover (fig. 5.13). No oxLDL–induced CD36 up-regulation was observed (data not shown) and the literature suggests that oxLDL–induced up-regulation takes place over a period of 24 hours (Munteanu *et al.*, 2006; Rios *et al.*, 2011). This experiment tested the effect of CD36 knock-down on oxLDL cell viability in the absence of added 7,8-NP that could scavenge oxidants. Cell viability was measured 18 hours after the removal of oxLDL, or 24 hours after initial addition of oxLDL. This experiment, therefore, repeated the conditions outlined in chapter 3. No significant protection was observed in the presence of 7,8-NP pre-treatment (fig. 5.14). It suggests that the down-regulation of CD36 did not play a significant role in 7,8-NP–mediated protection against oxLDL toxicity to the macrophage, which was contrary to the initial expectation.

Wintergerst *et al.* (2000) reported that binding of oxLDL to CD36 led to the rapid activation of caspase-3 and resulted in apoptosis of human macrophages. However, no caspase-3 activation was observed in the experimental design used in Gieseg *et al.* (2010a). Whether the latter also implied that CD36 is not involved in oxLDL–mediated toxicity remains to be seen. Such conclusion, however, would contradict the observations of Higashi *et al.* (2005) and Park *et al.* (2009) who also showed the importance of CD36 for oxLDL–mediated cell death. The down-regulation of CD36 receptor by 7,8-NP in the present study was not complete. At least 50% of CD36 was still available for oxLDL binding. Moreover, another scavenger receptor could have facilitated the uptake of oxLDL into the cells with down-regulated levels of CD36 (Horiuchi *et al.*, 2003). Nozaki *et al.* (1995) illustrated this by showing a 40% uptake reduction in CD36–negative macrophages. 7,8-NP pre-treatment and CD36 receptor reduction did not affect the uptake of 7KC and, therefore, oxLDL by the cells (fig. 5.16), suggesting that some of the aforementioned mechanisms took place.

Intracellular GSH levels were, however, slightly protected by the pre-treatment, especially at a sub-toxic oxLDL concentration. The higher GSH levels might indicate a reduced oxidative damage in the pre-treated cells. A possible mechanism was demonstrated by Park *et al.* (2009): CD36–mediated NADPH oxidase activation and subsequent ROS release. Nevertheless, this small increase of GSH levels did not lead to a significant gain in cell viability.

Alternative hypothesis

Assuming that total 7KC is the reflection of oxLDL internalised by the cell, the reduction of total 7KC in the presence of 7,8-NP could be interpreted as down-regulation of uptake, especially in combination with the down-regulation of CD36 scavenger. However, the down-regulation of the CD36 receptor by 7,8-NP (for 24 hours) did not reduce oxLDL uptake in the first 6 hours of subsequent exposure (fig. 5.16). Moreover, the 7,8-NP–mediated down-regulation of intracellular 7KC ester levels was only observed in the presence of extracellular human serum (fig. 5.17). (Complete absence of serum, although, might have an adverse effect on HMDM cells, which could not be ruled out). The combination of these results suggests that the effect of 7,8-NP might be associated with cholesterol reverse cholesterol trafficking and efflux rather than the uptake. Serum contains HDL apolipoprotein A1, which acts as an extracellular acceptor for cholesterol and oxysterols (Johnson *et al.*, 1991). 7KC esterification directly preceded the divergence of 7,8-NP and non-7,8-NP mediated rise in total 7KC (figures 5.1b and 5.4). Thus it can be speculated, that 7,8-NP may interfere with the esterification by ACAT-1 or ester hydrolysis by neutral ester hydrolase. Furthermore, it would explain the absence of 7,8-NP–mediated effect over the first 6 hours of exposure to oxLDL, as the esterification did not commence until after 6 hours.

CD36 protein and mRNA were also down-regulated by the presence of 7,8-NP. It is plausible that 7,8-NP down–regulation of CD36, while not being the cause of lower intracellular oxLDL, is associated with the oxLDL processing and efflux and is a consequence of that. CD36 expression in mouse macrophage-like J774 cells was shown to be down-regulated by cholesterol efflux which was induced by cyclodextrins (Han *et al.*, 1999). Therefore, if 7,8-NP enhances efflux, the latter may reduce CD36 protein and mRNA expression.

No added protection from cell viability loss was observed in the pre-treated cells with the lower CD36 receptor levels (fig. 5.14). However, these cells showed slightly elevated GSH levels, suggesting that some oxidative damage was alleviated. The size of the effect, however, suggested that this process may not be a major protection mechanism.

Cholesteryl ester accumulation is a characteristic feature of foam cells. AcLDL was shown to inhibit CE efflux from foam cells (Brown *et al.*, 1979), although not fully (Kritharides *et al.*, 1995), and so did oxLDL (Kritharides *et al.*, 1995). Kritharides

et al. (1995) and Gelissen *et al.* (1996) also reported that 7-KC inhibited the efflux of sterols from macrophages. The authors concluded that it was "possible that this impairment of efflux from oxLDL-loaded cells influences the generation and persistence of the foam cell phenotype in vivo" (Kritharides *et al.*, 1995). If 7,8-NP was promoting the hydrolysis of oxidised cholestryl esters and governing the efflux of oxLDL components from foam cell macrophages it could play a role in alleviating the atherosclerotic burden.

Future work is required to verify this hypothesis. ACAT-1 inhibition was shown to facilitate efflux and lead to the depletion of CE content (Liu *et al.*, 2003). The effect of 7,8-NP on ACAT-1 activity could be investigated. Brown *et al.* (1979) suggested that hydrolysis and removal of the esterified cholesterol in their study was performed by non-lysosomal esterases. The authors also observed that the activity of the enzyme that hydrolyses cytoplasmic cholesteryl ester was suppressed during the incubation with acLDL. The enzyme responsible for this process and its cellular activation could be the first target of a future investigation of the mechanism of 7,8-NP effect on the RCT during oxLDL exposure. Harrison *et al.* (1990) showed that cholestryl ester hydrolase was responsible for hydrolysis of CE associated with lipid droplets as opposed to lysosomes. In addition, the effect of 7,8-NP on cholesterol transporter ABCA1 and ABCG1 activity could also be investigated since they constitute the final stage of the RCT pathway (Yvan-Charvet *et al.*, 2010).

5.4 Summary

The research in this chapter has shown that 200 μM 7,8-NP decreased the levels of intracellular total 7-ketocholesterol by at least 40% in HMDM cells over 24 hours. This coincided with the 40% reduction in CD36 receptor (100 kDa) and mRNA levels. Both of these were late effects, taking place in the second half of the 24 hour incubation. Thus, 7,8-NP–mediated reduction in cellular oxLDL levels was a late effect in the oxLDL toxicity. Since the majority of the HMDM cellular death occurred in the first 12 hours of oxLDL treatment (chapter 3) and was heavily influenced by the first 6 hours of exposure, the aforementioned processes might play a secondary role in 7,8-NP–mediated protection of macrophages in the setting of acute oxLDL toxicity.

The effect of 7,8-NP on the levels 7KC esters coincided with the onset of esterification of oxLDL components, and was dependent on the presence of extracellular

serum. Based on this information, a new hypothesis of 7,8-NP role in oxLDL uptake is proposed. 7,8-NP could mediate oxLDL efflux by promoting cholesteryl ester hydrolysis. in particular reverse cholesterol transport. Future research is necessary to test this hypothesis. Cholestryl ester hydrolase(s) activity and other stages of reverse cholesterol transport such as on ACAT-1 and cholesterol transporters ABCA1 and ABCG1 are proposed as potential targets.

5. EFFECT OF 7,8-DIHYDRONEOPTERIN ON OXLDL UPTAKE BY MACROPHAGES

6

HMDM cell culture method development and troubleshooting

6.1 Introduction

Variability and resistance of HMDM cell response to oxLDL toxicity was a significant problem throughout the project. It manifested in LC_{50} being outside the experimental range of 2-3 mg/mL. This chapter describes the attempts to standardise cell culture methodology and investigate potential mechanisms that determine the variability of response and resistance to toxicity. This chapter also aimed to compare and contrast the available literature on the basis on current findings, since a range of oxLDL concentrations and experimental conditions has been used by different research groups.

Methodological improvements reported in the first part of this chapter constitute an extension of the previous work in the laboratory (Amit, 2008; Firth, 2006; Yang, 2009) and are included for the benefit of future researchers. The data on HMDM cell growth efficiency in the presence of GM-CSF is provided for benchmarking purposes. HMDM cell growth in 48 well plates was investigated to improve experimental capacity per HMDM cell preparation as 12 well plates were found to be limiting in number. The present study addresses serum supplementation in greater detail than the original reports from our laboratory (Amit, 2008; Firth, 2006; Yang, 2009). This was carried out in an attempt to resolve the issue of variable oxLDL toxicity to macrophages.

The second and third parts of this chapter explore the factors governing variability and resistance of HMDM cell response to oxLDL toxicity. In particular, the second part of this chapter explores the effects of serum and cell density on macrophage cell

death mediated by oxidised LDL. In the literature, varying concentrations of human and bovine serum have been used to supplement macrophages and macrophage-like cells during oxLDL treatment. For instance, Hardwick *et al.* (1999) and Gerry & Leake (2008) used serum-free media, Terasaka *et al.* (2007) used 5% lipoprotein–deficient serum, Harris *et al.* (2006) used 10% and Gieseg *et al.* (2010a) used 10% heat–inactivated human serum (HIHS). In our laboratory, 5% serum was found to prevent oxLDL toxicity to U937 cells, yet the HMDM cell experiments were performed in the presence of 10% human serum (Katouah, 2012). The original experiments by Henriksen *et al.* (1979) and Hessler *et al.* (1979) also showed that LDL toxicity to ECs and SMCs was inhibited by the presence of serum in the incubation medium. This was confirmed in HMDM cells as well (Asmis & Wintergerst, 1998; Wintergerst *et al.*, 2000). The present study aimes to establish the optimal serum conditions for studying cell death in our laboratory and identify whether some of the variation in published oxLDL toxicity levels could be attributed to the different conditions used by those researchers. Another aspect of cell culture that had been largely overlooked in the literature is cell density. A few early studies identified that oxLDL toxicity decreased with the increased cell density and proliferative activity of SMC and fibroblasts (Hessler *et al.*, 1983, 1979). Therefore, effect of cell density on oxLDL toxicity to HMDM and U937 cells is investigated.

The third and final part of this chapter addresses the phenomenon of HMDM resistance to oxLDL, which was occasionally observed in cultured cells in this study. The investigation was carried out at different serum concentrations as serum supplementation was found to be a significant extracellular factor in oxLDL toxicity. The oxidative nature of the underlying processes is explored by examining ROS production and oxidative damage in "resistant" vs. "susceptible" HMDM cells. Overall, this chapter explores the variation in cell culture technique and attempts to explain and standardise the underlying causes.

6.2 Culture of human monocyte–derived macrophages

6.2.1 Effect of GM-CSF and overall HMDM culture success

Monocytes' metabolic capability was greatly enhanced upon differentiation and development into macrophages. The effect of GM-CSF on the HMDM cell growth and development in the present study was assessed on seven HMDM cell preparations (batches) (fig. 6.1). Cellular metabolism per well (measured via MTT assay)

was proportional to the number of differentiated macrophages as monocytes showed minor MTT turnover (data not shown). The cell number output of non-GMCSF–treated cells was normalised to the number of matched GM-CSF–treated cells. Cells that were not supplemented with GM-CSF only developed to 44 ± 31% (SD) of the number of supplemented cells (fig. 6.1). Thus, monocytes seeded without GM-CSF showed some development into macrophages but the well coverage was lower than in the presence of the growth factor. One batch of HMDM cells out of seven was observed to have abnormally high differentiation in the absence of GM-CSF, highlighting the inter-donor variability (fig. 6.1). The term "differentiation" will be used here to denote monocyte development into macrophage as based on morphology and metabolic capacity.

The overall percentage of successful HMDM cell development (referred to as "differentiation" from monocyte into macrophage) from different donors was investigated to provide a reference for future work in this laboratory. Each batch was given a rating (differentiated, marginal, not differentiated) based on cell morphology and the data from 45 preparations was combined (fig. 6.2). Over the course of this research, the HMDM were cultured in both Nunc® (Nalge Nunc Int., Roskilde, Denmark) and Cellstar® (Greiner bio-one, Neuburg, Germany) plates at seeding densities of 1 and $5x10^6$ cells/well. The data were pooled for all preparations cultured in the presence of GM-CSF, because no difference in HMDM cell culture was observed between plates (as discussed below). Almost 70% of the HMDM preparations showed extensive morphological differentiation to be considered fit for experimentation (fig. 6.2). The cells produced a uniform lawn and displayed round "poached egg–like" morphology with 10-30% cells showing slightly elongated morphology. Approximately 15% of the HMDM preparations developed marginally, where either the morphology or the well coverage were not acceptable. The remaining preparations failed to differentiate properly even in the presence of GM-CSF.

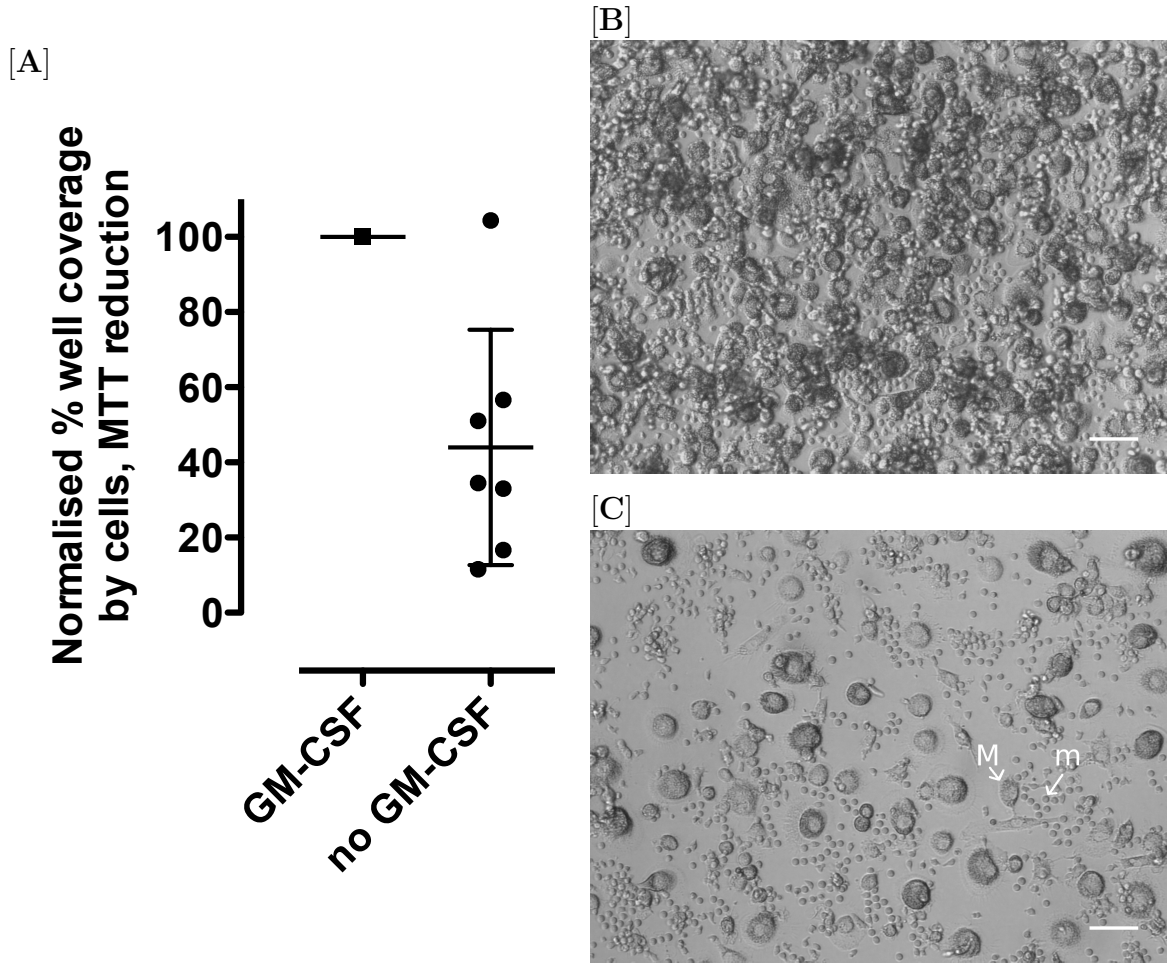

Figure 6.1: Effect of GM-CSF on HMDM cell differentiation.
HMDM (1x10^6 cells mL^{-1}) were cultured in the presence of 10% human serum with or without the initial 25 ng/mL GM-CSF. On days 11 to 14 of culture the HMDM cell number for both treatments was determined via MTT assay. The results for non-GM-CSF–treated HMDM were normalised to the cellular metabolism of matched GM-CSF–treated cells (n=7). The data is expressed as a scatter dot plot with mean ± SD. (**B**) and (**C**) represent HMDM cells cultured in the presence and absence of initial GM-CSF, respectively. Images are from a representative experiment. Arrows indicate macrophage (M)– and monocyte (m)–like morphology Scale bar = 50 μm.

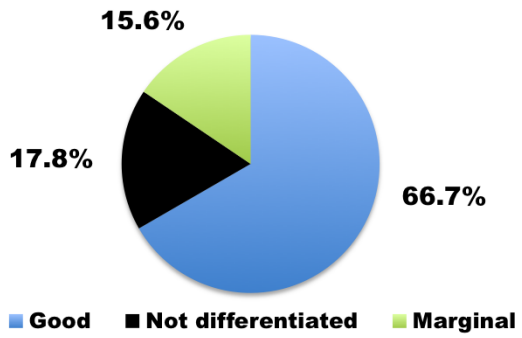

(a) % HMDM batches per category, n=45

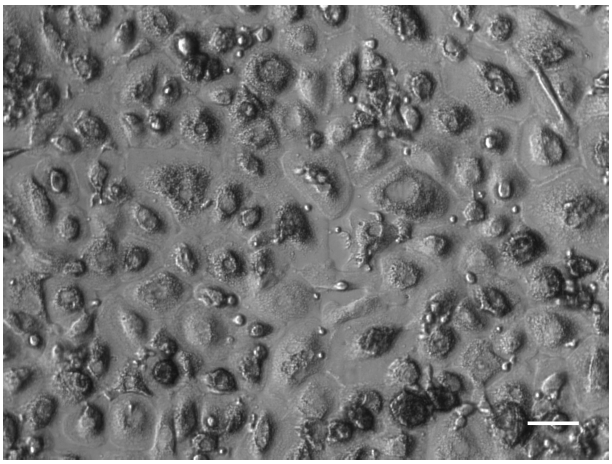

(b) good

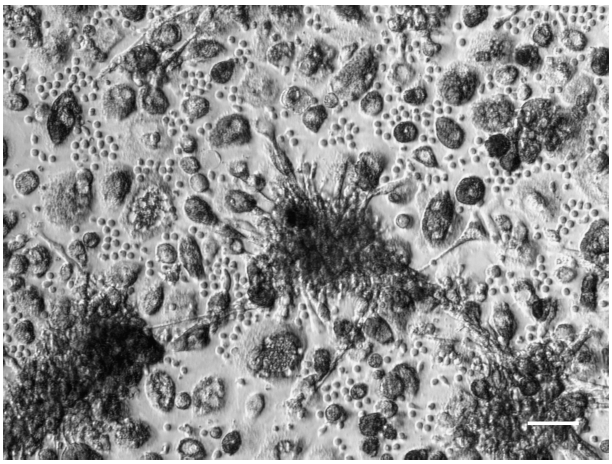

(c) marginal

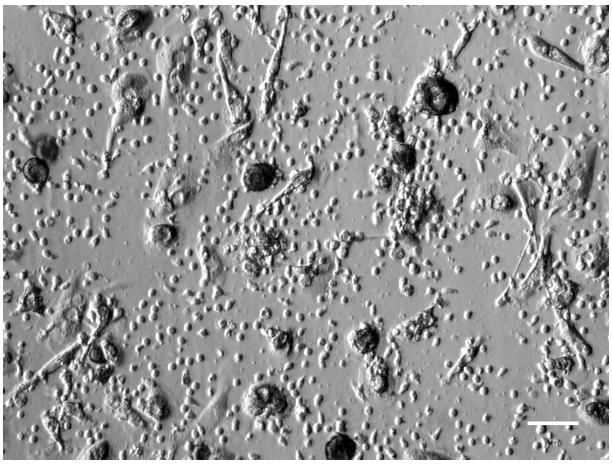

(d) not differentiated

Figure 6.2: Percentage of successful macrophage development in culture. HMDM differentiation and development into macrophage-like morphology was assessed over the course of the project. HMDM cells were cultured in either Nunc® or Cellstar®, 12 ($5x10^6$ cells mL^{-1}) or 48 well plates ($1x10^6$ cells mL^{-1}), in the presence of 10% human serum with an initial pulse of GM-CSF. The cells were given a rating of "good" (b), "marginal" (c) and "not differentiated" (d) according to the macrophage number and morphology approximately on day 12 after seeding (n=45). Scale bar=50μm.

6.2.2 Culture plate trial

Nunc vs. Cellstar plates for HMDM cell growth

Cellular adhesion and differentiation are processes that involve more than one mechanism. They are often cell type specific and, therefore, the selection of the growth surface for a particular cell line/type is based on the performance of the culture. Historically in this laboratory, the HMDM cells were cultured in 12 well Nunc adherent plates. Yet HMDM culture in Cellstar plates, if successful, could potentially reduce the cost of the operations. Thus, the two plate types were compared with respect to their ability to support HMDM cell growth (fig. 6.3). For one batch of HMDM (batch 2), Cellstar plate performed better than Nunc in sustaining cell differentiation and growth as indicated by the MTT reduction capacity of cells in that plate (fig. 6.3a). Since no negative growth data was observed and the morphology of HMDM cells grown in Cellstar and Nunc plates was identical, Cellstar plates were chosen for future experiments.

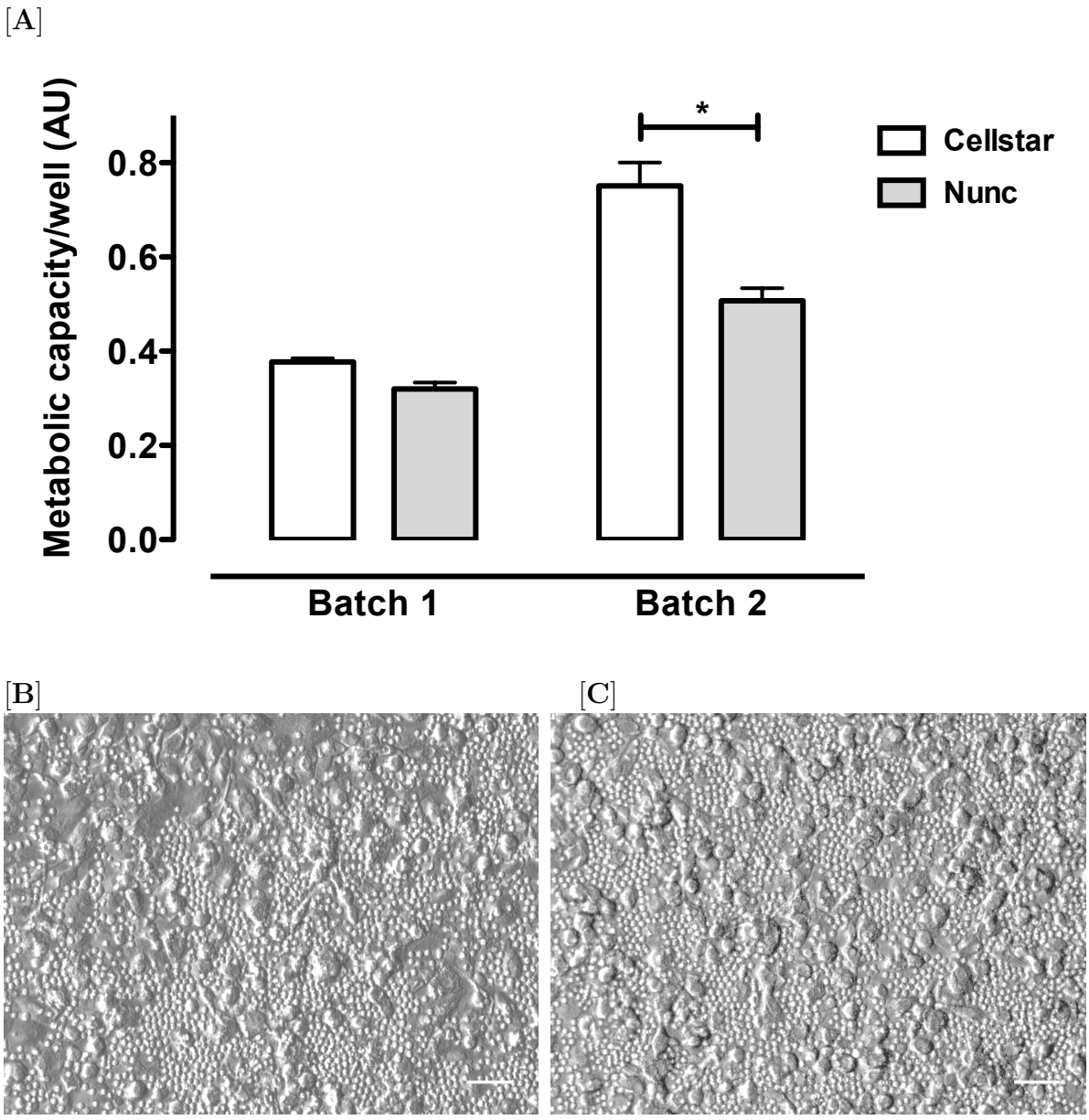

Figure 6.3: Effect of plate type on HMDM cell growth.
HMDM, seeded at 5x10^6 cells mL^{-1}, were cultured in 12 well plates (Cellstar **(B)** and Nunc **(C)**) in the presence of 10% human serum. Cell number/viability was assessed by MTT reduction on the 12th day of culture, images were taken on day 9. Results displayed as mean ± SEM of triplicate measurements from a single experiment **(A)**. HMDM batches 1 and 2 were from different donors. Significance (t-test) was as indicated, *, $p<0.05$. Scale bar = 50 μm.

Limitations of 12 well plates

Twelve well plates were initially used for HMDM growth. However, the low number of experimental units (i.e. wells) was an obstacle to experimental throughput. When seeded at $5x10^6$ per well, the largest HMDM preparation would reach approximately 120–140 wells, with an average of around 96 wells. This proved to be a very low number since every batch had to be tested for toxicity prior to any experiment. To overcome this problem, smaller wells were tested for HMDM growth. Two 48 well plates seeded at $1x10^6$ cells/well produced the same number of experimental units as the full batch previously, while constituting less than $1/3^{rd}$ of the cells isolated from an average donation. To determine the appropriate monocyte seeding density for a 48 well plate, the cells were seeded at 0.25 to $3x10^6$ cells/well (fig. 6.4). The number of viable cells per well was assessed via MTT assay 11 days after seeding. The differentiation success and capacity varied between the HMDM preparations, but $1x10^6$ resulted in the highest numbers of cells without causing over-crowding. It was, therefore, decided to seed $1x10^6$ monocytes per well.

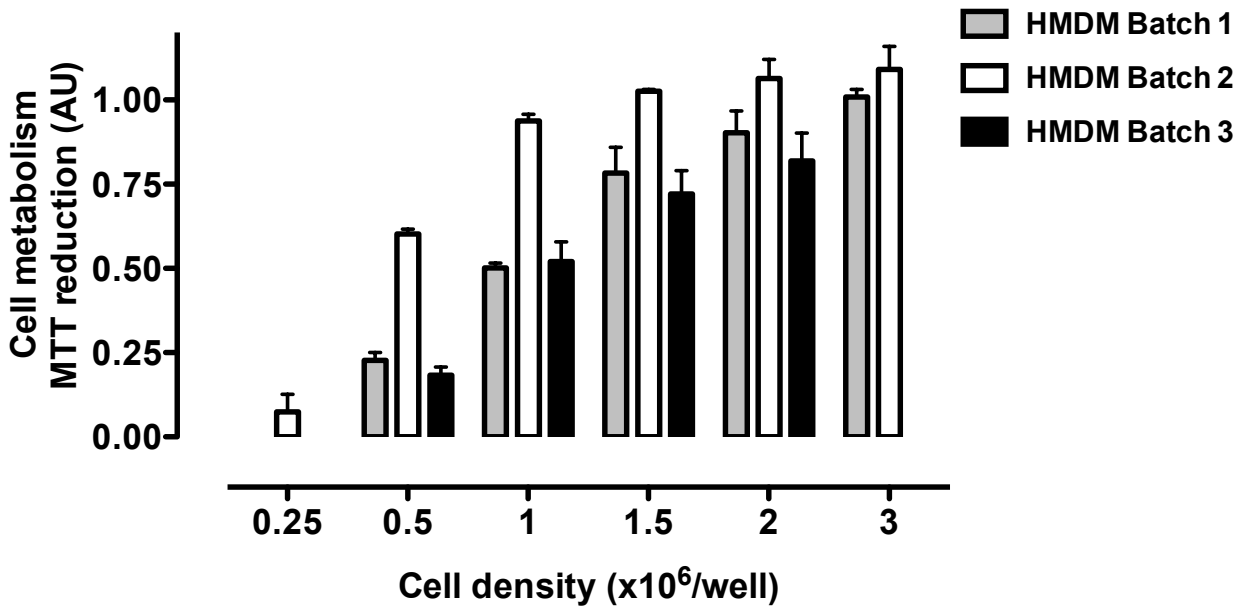

Figure 6.4: Determination of monocyte seeding density for HMDM cell growth in 48 well plate.

HMDM were seeded into 48 well plate at increasing cell densities. The cells were cultured in the presence of 10% human serum with an initial pulse of 25 ng/well GM-CSF. Cell viability was determined by MTT reduction 11 days after seeding (auto-zero on reagent only). Results are displayed as mean ± SEM of triplicate measurements from three batches of HMDM cells from different donors. Batches 1 and 3 lacked 0.25×10^6 and batch 3 lacked 3×10^6 measurements.

6.2.3 Effect of human serum on HMDM development and growth

Serum supplementation of monocyte/macrophage cultures is essential for successful cell growth. Batches of serum from different donors, however, varied in their capacity to promote macrophage differentiation (fig. 6.5). Monocytes were seeded in the presence of 10% serum in RPMI-1640 and the number of developed macrophages was assessed 12 days later by MTT assay. In order to achieve some replication, two HMDM batches from different donors were grown with each serum batch at the same time. Serum batches 2 and 7 in figure 6.5 a) and b), respectively, promoted higher HMDM differentiation than the rest of the sera in each test. The majority of the remaining sera (1,3 and 4,6) affected differentiation to a similar level (fig. 6.5b). An interaction between macrophage and serum batch was also observed as not all sera promoted differentiation in HMDM batches 1–4 equally (for example batches 6 and 7 in fig. 6.5b). Serum also played a role in HMDM growth after GM-CSF–facilitated differentiation (fig. 6.6). For GM-CSF–differentiated HMDM cells, batches 3, 6 and 7 yielded the highest macrophage growth and metabolism (fig. 6.6). All sera were non-autologous.

[A]

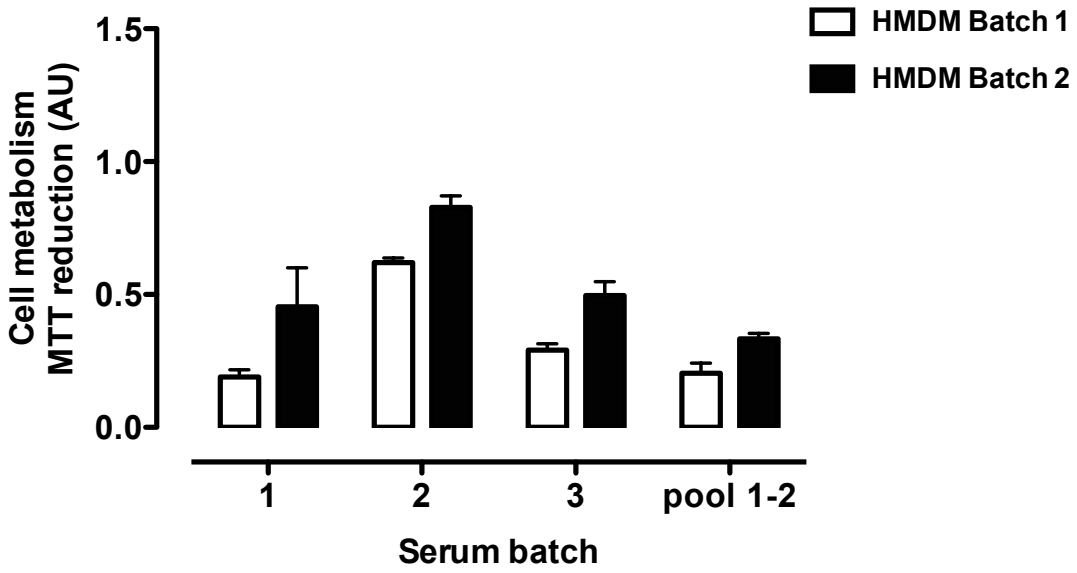

[B]

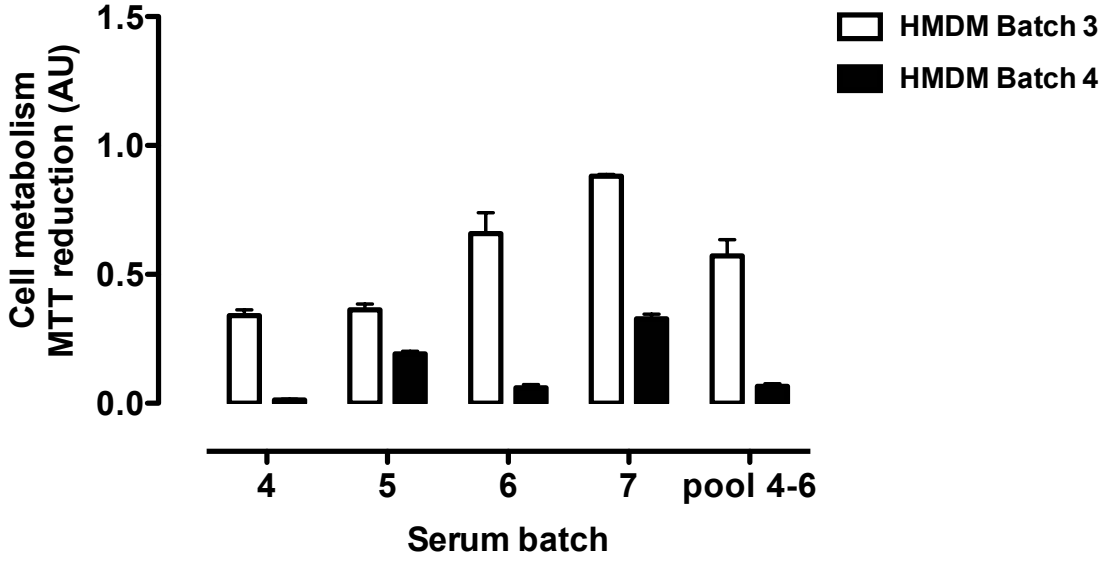

Figure 6.5: Effect of sera on HMDM cell development.
HMDM ($1x10^6$ cells mL^{-1}) seeded in the absence of GM-CSF were assessed for the cell number with MTT assay on the 12^{th} day of culture. Results are displayed as mean ± SEM of triplicate absorbance measurements. HMDM batches 1-4 and serum batches 1-7 were all from different donors. Pooled serum was made by combining the indicated batches of serum. "Cloudy" (lipid–rich) sera 3 and 7 were not pooled. Statistical significance (one-factor ANOVA with Turkey post test): **(A)**: serum 2 significantly different from sera 1 and pooled for both HMDM batch 1 and 2, $p<0.05$; **(B)** for HMDM batch 3: serum 7 significantly higher than all other sera, sera 4 and 5 significantly lower than sera 6 and 7 and pooled, $p<0.05$; for HMDM batch 4: sera 5 and 7 significantly higher than all other sera, $p<0.01$.

[A]

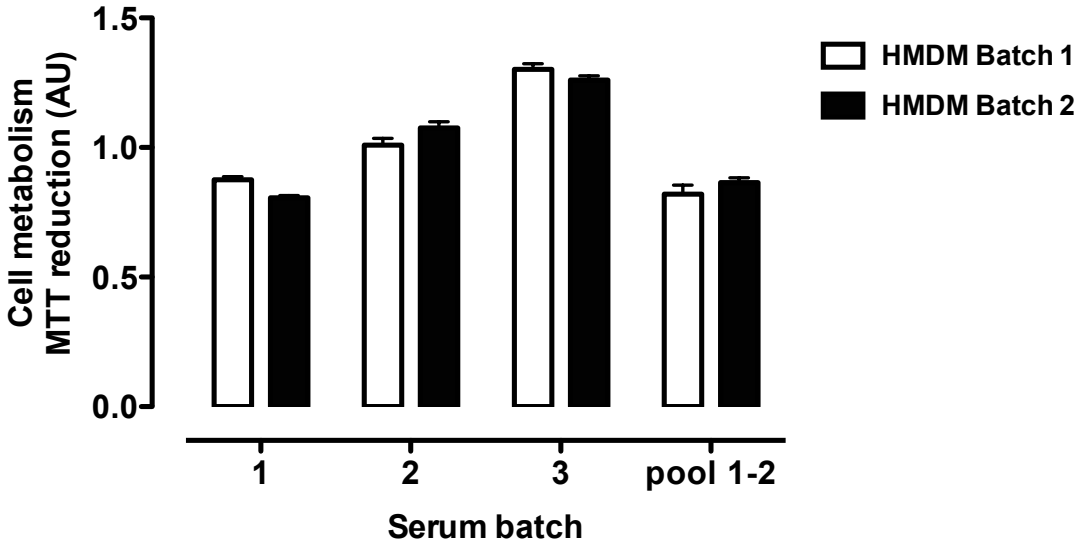

[B]

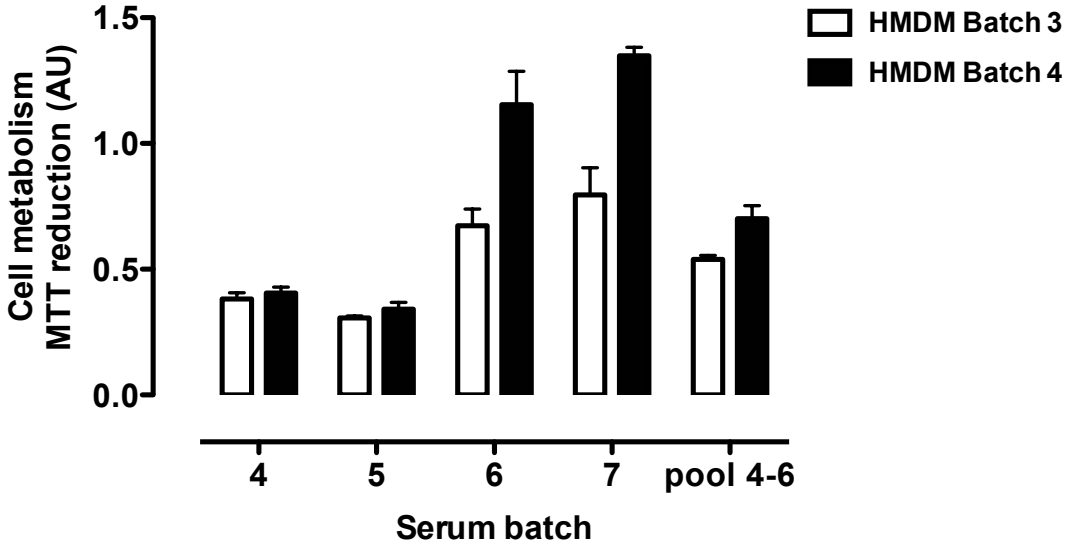

Figure 6.6: Effect of sera on GM-CSF–differentiated HMDM cell growth. HMDM ($1x10^6$ cells mL^{-1}) seeded in the presence of 25 ng/mg GM-CSF were assessed for the cell number with MTT assay on the 12^{th} day of culture. Results are displayed as mean ± SEM of triplicate absorbance measurements. HMDM batches 1-4 and serum batches 1-7 were from different donors. Pooled serum was made by combining the indicated batches of serum. "Cloudy" (lipid–rich) sera 3 and 7 were not pooled. Statistical significance (one-factor ANOVA with Turkey post test): **(A)**: sera 2 and 3 significantly different from sera 1 and pooled for both HMDM batch 1 and 2, sera 2 and 3 different from each other, $p<0.05$; **(B)** for HMDM batch 3: sera 4 and 5 significantly lower than sera 6 and 7, $p<0.05$; for HMDM batch 4: sera 4 and 5 significantly lower than sera 6 and 7, sera 6 and 7 significantly higher than pooled serum $p<0.05$.

Effect of heat–inactivation of human serum on HMDM cell growth

Human serum was heat–inactivated in the initial stages of the project, but this step was subsequently omitted (after the review of the literature (Biochrom AG, 2010; Hyclone®, 1996; Leshem *et al.*, 1999) and personal communication with Dr. S.P. Gieseg and Dr. B. Hock of Otago Medical School Christchurch, New Zealand). Heat–inactivation of serum had no effect on the cells' ability to reduce MTT to formazan after 24 hour incubation (fig. 6.6). This suggested that HMDM cell number and metabolic capacity was equal across the two serum treatments.

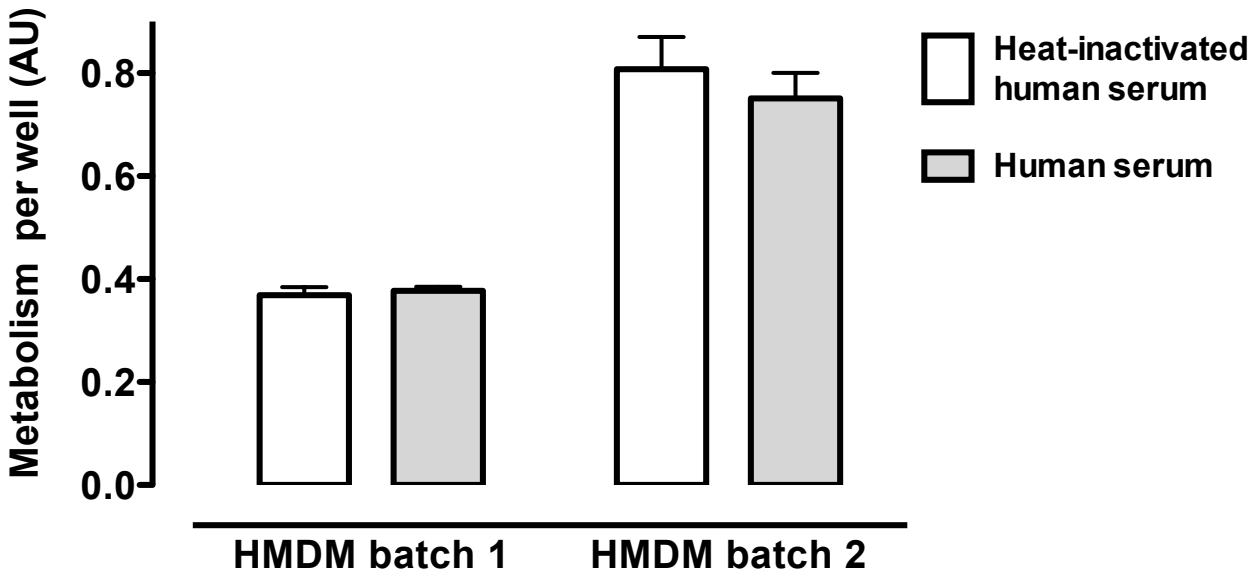

Figure 6.7: Heat–inactivation of human serum does not alter HMDM growth in culture.
HMDM ($1x10^6$ cells mL^{-1}) were cultured with 10% heat–inactivated (white bars) or non-heat–inactivated (grey bars) human serum. Cell metabolism was assessed by MTT reduction on the 12^{th} day of culture. Results displayed as mean ± SEM of triplicate measurements from two HMDM batches. The difference between heat–inactivated and non-heat–inactivated serum for each batch was not statistically significant (t-test).

6.3 Utility of U937 cells as a model of 7,8-NP–mediated oxLDL uptake regulation

The use of the U937 cell line for CD36 down-regulation experiments was assessed, since U937 cells comprised a more homogeneous system than primary HMDM cells. The effect of 7,8-NP on uptake and CD36 was tested in U937 cells. A range of 7,8-NP concentrations was tested on U937 cells incubated for 24 hours in the normal culture medium (RPMI-1640 supplemented with 5% FBS and antibiotics) (fig. 6.8). Monocyte-like U937 cells had a less prominent 100 kDa band than HMDM cells (fig. 6.8). 7,8-NP showed a concentration–dependant effect on the CD36 protein expression in U937 cells (fig. 6.8). The heavily glycosylated 100 kDa band was down–regulated , while the 80 kDa band was up-regulated with the increasing concentrations of 7,8-NP. At 250 μM, the 100 kDa band was 30% lower than control, while 80 kDa band was 45% higher than control.

OxLDL uptake in the presence of 7,8-NP in U937 cells was also measured (fig. 6.9). U937 cells (1x10^6 cells/mL) in RPMI-1640 (without FBS as per U937 protocol for oxLDL experiments in Katouah (2012)) were treated with 0.1 mg/mL oxLDL for 24 hours in the presence of increasing concentration of 7,8-NP. Sub-toxic level of oxLDL was used to ensure consistency with HMDM data. OxLDL caused a 40-50% rise in intracellular total 7KC levels compared to no oxLDL control (fig. 6.9). The presence of 7,8-NP did not alter intracellular 7KC levels significantly, suggesting the absence of effect on oxLDL uptake. Thus U937 cell were not used for the subsequent experiments.

[A]

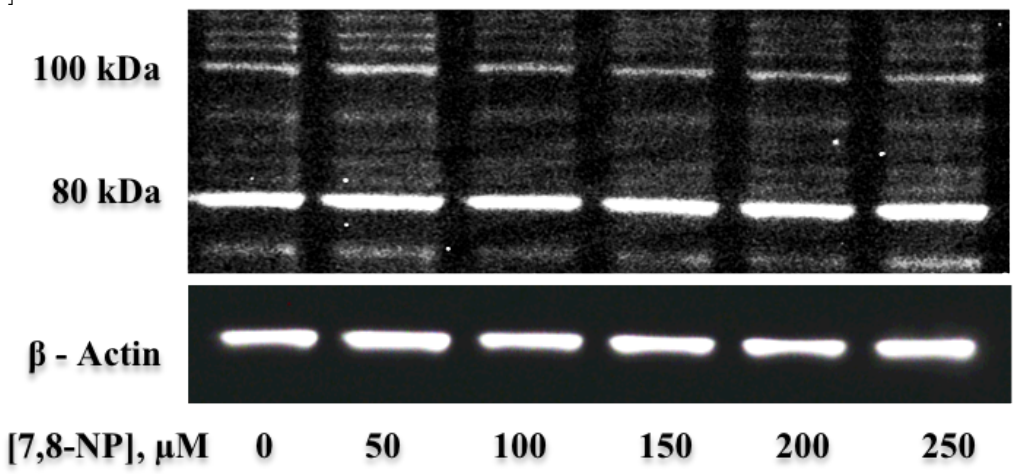

[(B)]

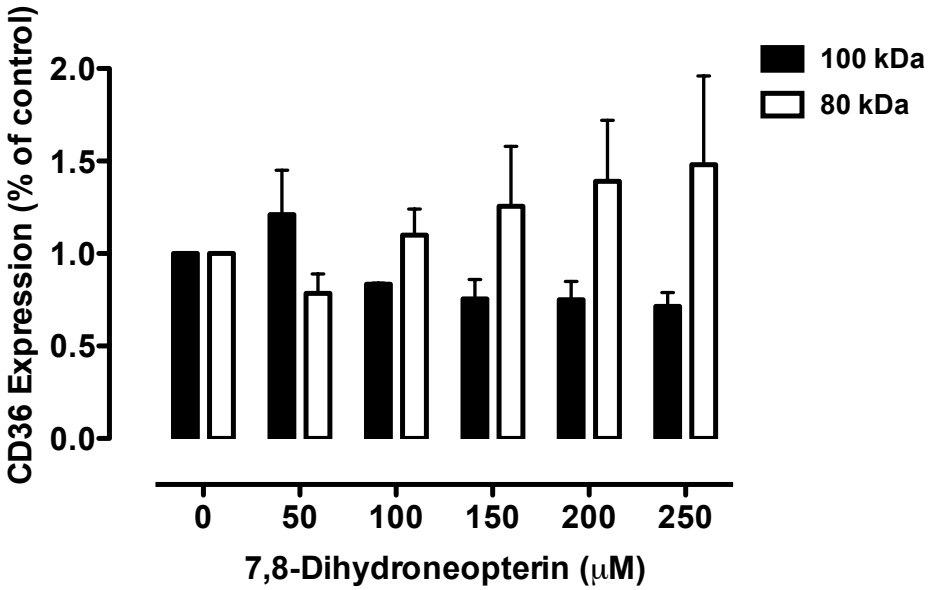

Figure 6.8: Effect of 7,8-NP on the CD36 protein expression in U937 cells. U937 cells were placed into BSA-coated wells at 10^6 cells/mL and incubated with increasing concentrations of 7,8-NP for 24 hours in RPMI containing 5% FBS. The presence of CD36 protein in cell lysates was assessed by immunoblotting. β-Actin was used as loading control. (**A**) A representative Western blot. (**B**) Quantitative densitometry of Western blots displaying concentration-dependent regulation of 80 and 100 kDa bands relative to 0 hour control. Results were normalised by actin and displayed as mean ± SEM of duplicate experiments. Neither decrease of fully glycosylated 100 kDa band nor increase of incompletely glycosylated 80 kDa band were statistically significant (one-factor ANOVA with Dunnett's post test).

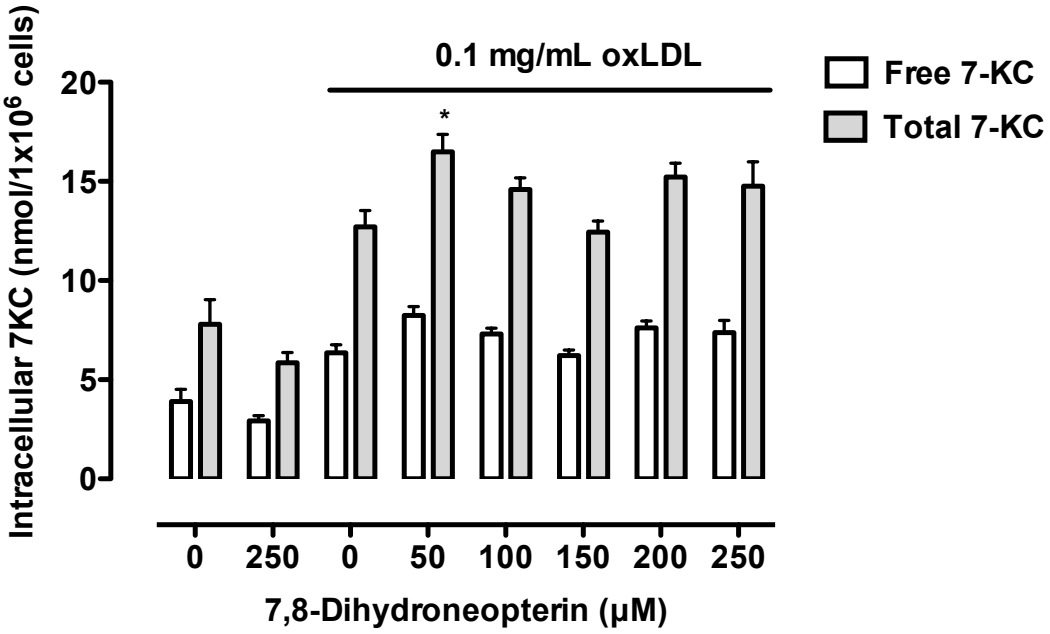

Figure 6.9: 7,8-NP has no effect on the intracellular 7KC uptake by the oxLDL–exposed U937 cells.

U937 cells ($1x10^6$ cells/mL) in RPMI-1640 were treated with 0.1 mg/mL oxLDL for 24 hours in the presence of increasing concentrations of 7,8-NP. The cells were collected and assessed for free (clear) and total (filled) 7KC via HPLC. Results are displayed as mean ± SEM of triplicates from a single experiment. Significant difference (one-factor ANOVA with Dunnett's post test) from 0 μM 7,8-NP exposed to oxLDL as indicated, *, $p<0.05$.

6.4 Extracellular experimental factors contributing to toxicity

6.4.1 Extracellular serum is a factor in oxLDL toxicity

OxLDL toxicity was established for each HMDM cell batch prior to conducting experiments. Two experimental protocols were used throughout the study. The original protocol involved treating cells (seeded at $5x10^6$ cells/well in 12 well plates) a decreasing human serum concentration with increasing oxLDL concentration as whole medium was pre-mixed to 10% serum before the addition of oxLDL. The results are presented in figure 6.10a. To analyse the effect of progressively decreasing serum concentration on oxLDL toxicity, a multiple regression analysis was performed on the toxicity data, taking into account individual serum concentrations for each data point. Linear mixed effects model analysis with [oxLDL] as a variate, [serum] as co-variate and experiment as factor, was performed in R (R Core Team, 2012). The effect of serum concentration was highly significant ($p<0.001$), as was the effect of oxLDL concentration and the interaction between the two variables ($p<0.05$).

For the subsequent experiments (performed on HMDM cells seeded at $1x10^6$ cells/well in 48 well plates), extracellular serum concentration was fixed at 10% (fig. 6.10b). In contrast to the original protocol, no cell viability loss was observed at 1 mg/mL oxLDL (fig. 6.10b). Direct comparison between figures 6.10a and 6.10b was not performed due to the different macrophage seeding density, but the effect of increasing serum concentration was pursued further.

[A]

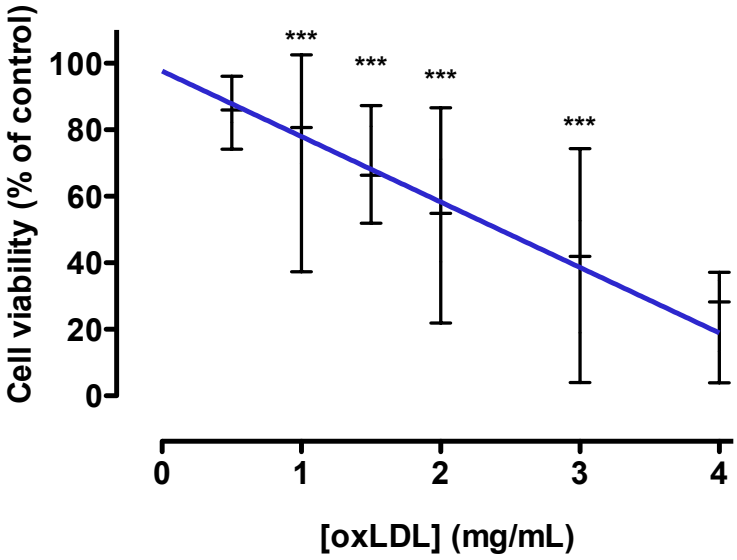

[B]

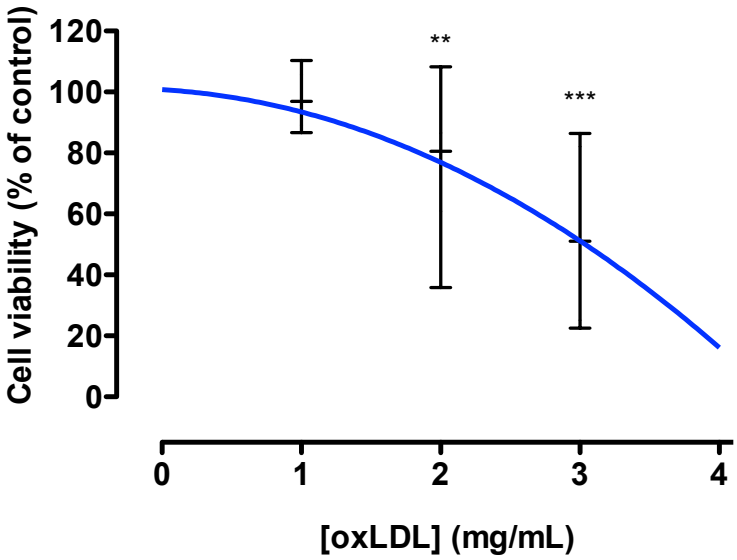

Figure 6.10: Effect of experimental protocol on oxLDL toxicity to HMDM. **(A)** HMDM cells ($5x10^6$ cells mL^{-1}) were incubated with increasing concentrations of oxLDL for 24 hours in the whole medium pre-mixed to 10% serum before the addition of oxLDL. Therefore, the amount of human serum decreased proportionally to the increase of oxLDL concentration. **(B)** HMDM cells ($1x10^6$ cells mL^{-1}) were incubated in the whole medium containing exactly 10% human serum. Cell viability was measured via MTT assay. The data are expressed as percentage of untreated control and the results are displayed as box-and-whiskers plots (mean ± range) of **(A)** n=14 experiments for [oxLDL] from 0 to 3 mg/mL and n=6 for [oxLDL]=4 mg/mL; **(B)** n=5 from 0 to 2 mg/mL, n=4 for 3 mg/mL, n=1 for 4 mg/mL. Significance (one-way ANOVA with Dunnetts post-test) is indicated from untreated control **, $p<0.01$, ***, $p<0.001$. Regression lines were fitted using Prism5.

A targeted experiment was performed to quantify the protective effect of human serum against oxLDL toxicity. The HMDM cells were incubated with 2 mg/mL oxLDL in the presence of increasing serum concentrations expressed as serum protein (fig. 6.11). Normal extracellular protein concentration of the whole medium at 10% human serum was ∼7 mg of protein per mL. (The average serum protein content was 70 ± 3 mg/mL (SD, n=12) which is in the published range (Barrett *et al.*, 2010) (p. 2)). Extracellular protein concentration above 2 mg/mL (2.86% serum, v/v) significantly prevented oxLDL–mediated HMDM cell viability loss when compared to oxLDL–treated HMDM in the absence of serum (fig. 6.11). The curve of extracellular serum effect plateaued after 3 mg of protein per mL (4.29% serum). In the current experimental design, the protection mediated by serum was almost complete (viability rise from 50 to 95%) (fig. 6.11b). The steep slope in the 0–2 mg/mL protein range indicated that incremental change in serum concentration within this range had a large effect on oxLDL–mediated toxicity. Large error bars at 0.75 and 1 mg/mL on the combined data (fig. 6.11b), but not on individual experimental data (fig. 6.11a) indicated the large variability between the experiments (indicative of variability in HMDM response between HMDM preparations) in this region of rapid change. It is worth noting that for all other points the SEM bars were a moderate ± 10% (fig. 6.11b), suggesting that experimental methodology was not the source of this large variation.

[A]

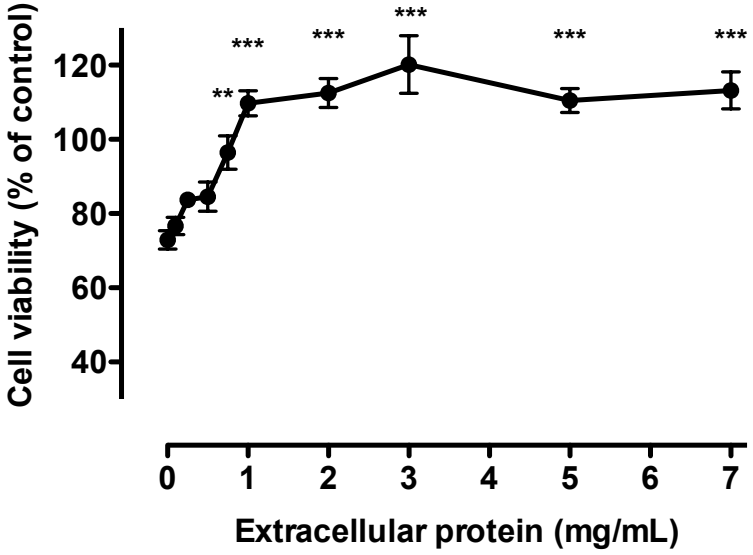

[B]

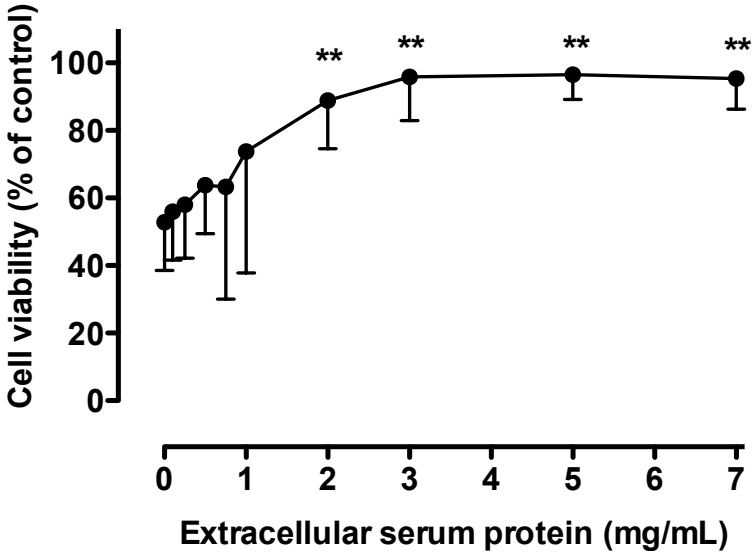

Figure 6.11: Extracellular serum inhibits oxLDL-mediated HMDM toxicity in a concentration–dependent manner.

HMDM cells ($1x10^6$ cells mL^{-1}) were treated with 2 mg/mL oxLDL for 24 hours in RPMI-1640 supplemented with increasing concentration of human serum (expressed as mg/mL serum protein). Cell viability was assessed via MTT reduction. Results are displayed as percentage of remaining cell viability relative to the respective control (no oxLDL, matched serum concentration), shown as mean ± SEM of **(A)** triplicate measurements from a single experiment, and **(B)** combined means from three separate experiments. Significance is indicated from control, **, $p<0.01$, ***, $p<0.001$ (one-way repeated measures ANOVA on A) single experiment B) combined data, Dunnetts post test).

Since albumin comprises the majority of serum protein and is the primary "sacrificial" antioxidant in serum, the ability of albumin to protect HMDM from oxLDL toxicity was investigated. A concentration of simple albumin solution (BSA dissolved in PBS) was matched to the concentration of serum protein and used to supplement oxLDL–treated HMDM cells. The effect of albumin in the extracellular medium almost exactly replicated the effect of serum (fig. 6.12), which suggested that the majority of the serum effect was attributable to serum albumin. However, at protein concentrations higher than 1 mg/mL a small but noticeable difference between the serum and BSA supplementation was observed (fig. 6.12). The difference was not statistically significant, but it was consistently replicated in the three experiments (fig. 6.12b), suggesting that the effect may have been real.

Asmis & Wintergerst (1998) showed that extracellular serum inhibited the uptake of Texas red–labelled oxLDL by HMDM cells. This experiment was repeated here, but amended to include extracellular protein. 7-Ketocholesterol (7KC), an advanced oxidation product of cholesterol in oxLDL, was used as a proxy of total intracellular oxLDL uptake. As discussed in chapter 5, 7KC is a good indicator of oxLDL uptake as it utilises an inherent component of oxLDL instead of being an exogenous compound like Texas red or DiI. Intracellular free and esterified 7KC was measured in HMDM cells exposed to a sub-toxic level of oxLDL for 24 hours (fig. 6.13). Extracellular serum and BSA inhibited 7KC and, therefore, oxLDL uptake, by 12 nmol/mg protein (or 25%) and by 18 nmol/mg protein (or 38%), respectively.

[A]

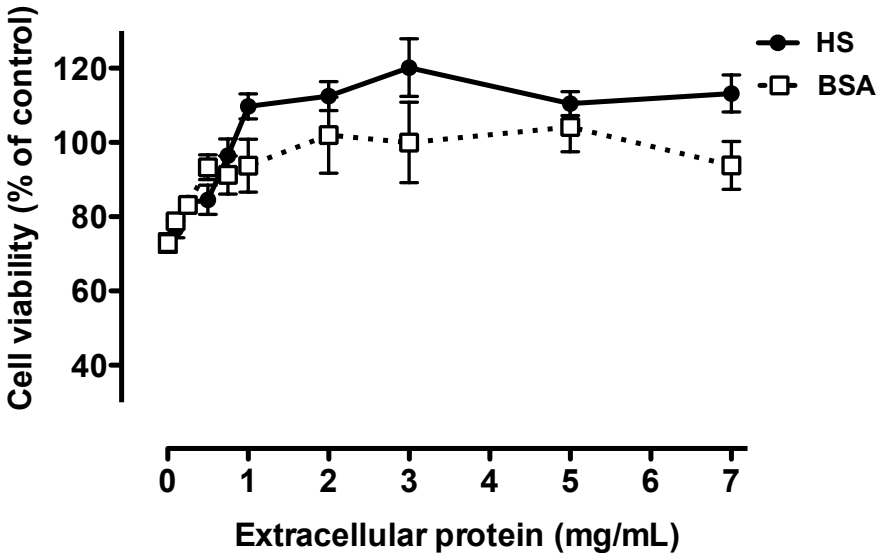

[B]

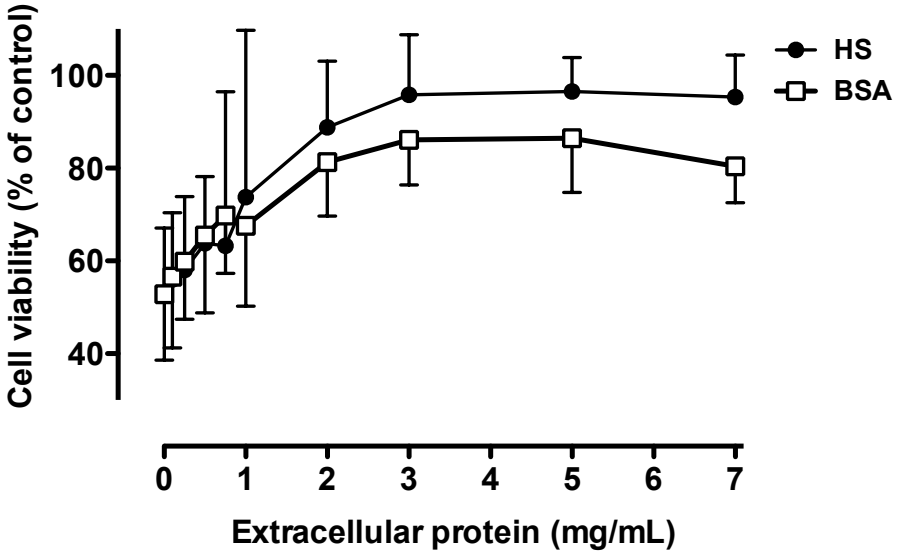

Figure 6.12: Extracellular protein inhibits oxLDL-mediated HMDM toxicity in a concentration–dependent manner.
HMDM cells ($1x10^6$ cells mL^{-1}) were treated with 2 mg/mL oxLDL for 24 hours in RPMI-1640 supplemented with the indicated concentration of protein added as native bovine serum albumin (BSA, squares) or human serum (human serum, HS, circles). Cell viability was assessed via MTT reduction. Results are displayed as percentage of remaining cell viability relative to the respective control (no oxLDL, matched serum concentration), shown as mean ± SEM of **(A)** triplicate measurements from a single experiment **(B)** combined means from three separate experiments. Treatments were not statistically different (one-way ANOVA, Bonferroni comparison of treatments at each concentration of (A) and (B)).

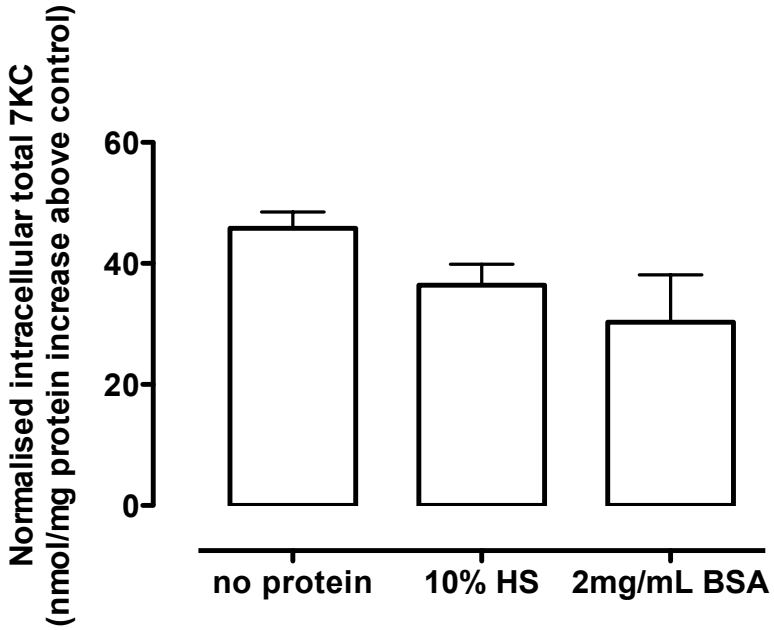

Figure 6.13: Effect of extracellular protein (added as BSA or as human serum) on oxLDL uptake by HMDM cells.
HMDM cells ($1x10^6$ cells mL^{-1}) were treated with 1 mg/mL oxLDL for 24 hours in RPMI-1640, RPMI-1640 supplemented with 10% human serum or 2mg/mL of native BSA. OxLDL uptake was assessed via total 7-ketocholesterol uptake. Results were normalised to the no oxLDL control and are displayed as mean ± SEM of triplicate measurements from a single experiment. No statistically significant difference was detected (one-way ANOVA with Dunnet's post test)

6.4.2 Cell density is a factor in oxLDL toxicity

Another variable of HMDM cell culture was the effective concentration of cells per well. Cellular density was suspected to influence the protection from oxLDL–mediated cell death when U937 cells failed to die in an experiment where cell number was tripled against the usual $5x10^5$ cells/mL. The effect of cell density on toxicity was identified as a potential source of variability between HMDM cell preparations, because the proportion of seeded monocytes which differentiated into HMDM cells was subject to inter-experimental variability.

U937 cells were used to test the effect of cell density on oxLDL–induced cell death, due to ease of controlling cell number compared to HMDM cells. Cell density was observed to have a large effect on oxLDL–induced cell toxicity in these cells. At the lowest density range ($0.1x\ 10^6$ cells mL^{-1}), virtually all cells were dead in the presence of 0.5 mg/mL oxLDL after 24 hours (examined through the microscope and via MTT assay) (fig. 6.14). Conversely, at the highest density range ($1.25–1.5\ x\ 10^6$ cells mL^{-1}), cellular viability remained above 60–80% at the end of 24 hour incubation. For U937 cell density above $0.5\ x\ 10^6$ cells/mL the decrease in oxLDL toxicity (increase in remaining cell viability) was 21% per $4x10^5$ cells (or 5.3% per $1x10^5$ cells). All tested cell densities fell within the linear detection range as indicated in figure 6.14a.

[A]

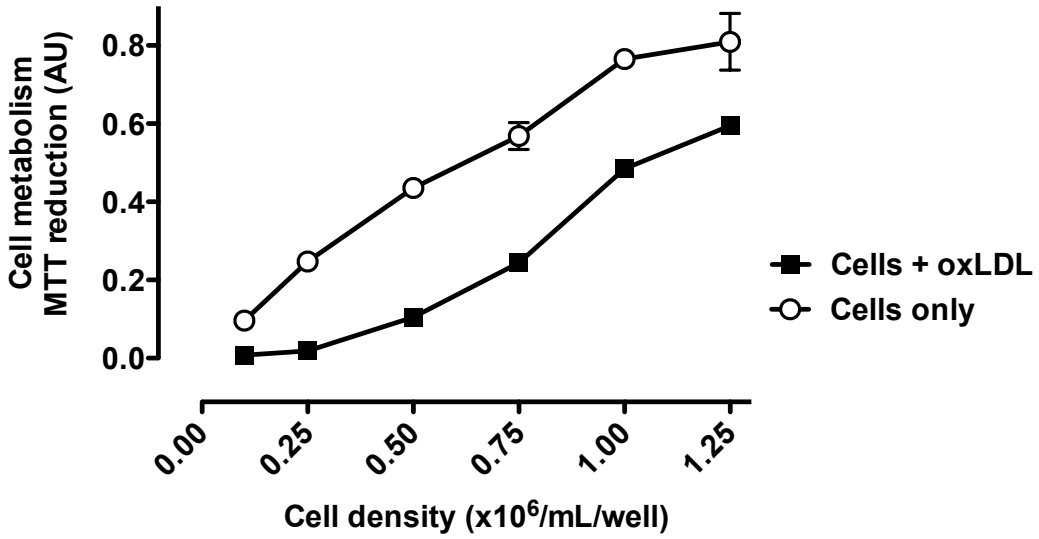

[B]

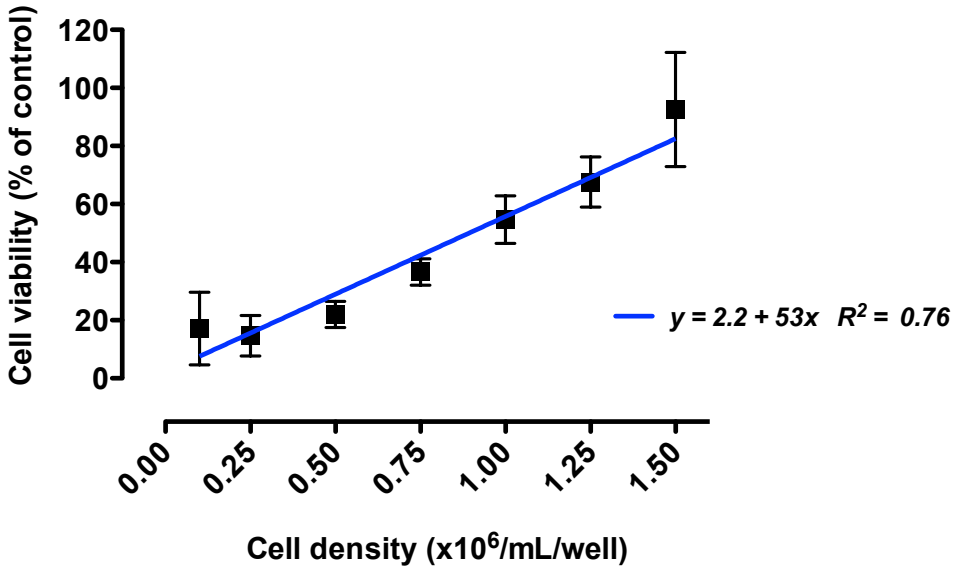

Figure 6.14: Effect of cell number on oxLDL–mediated U937 cell viability loss.

U937 cells incubated at increasing cell densities in 12 well plates were treated with (filled squares) or without (empty circles) 0.5 mg/mL of oxLDL in RPMI-1640 without phenol red for 24 hours. Cell viability was assessed by MTT reduction. Results are expressed as raw absorbance units displayed as mean ± SEM of **(A)** duplicate measurements from a single experiment, representative of three separate experiments and **(B)** as percentage remaining cell viability relative to the respective control, combined data from three experiments. OxLDL-mediated cell viability loss is influenced by cell density (two-factor ANOVA, interaction highly significant), ***, $p<0.001$.

6. HMDM CELL CULTURE METHOD DEVELOPMENT AND TROUBLESHOOTING

The experiment was repeated with HMDM cells. HMDM cells were cultured as usual, detached from the well with *Accutase*™, counted and re-plated at the indicated densities in the presence of 2% human serum (fig. 6.15). After a 20 hour adjustment period, the cells were incubated with 2.5 mg/mL oxLDL for 24 hours and assessed for cellular viability with *PrestoBlue*™. To yield linear response in the cell only control, the experimental design included a broad range of densities and oxLDL treatment was followed by 3 hour incubation with *PrestoBlue*™ (fig. 6.15). As with U937 cells, increasing cell density had a large protective effect against oxLDL toxicity (fig. 6.15). The result varied slightly with HMDM cell preparation, going from 10% to almost 90% cell viability gain in fig. 6.15b and from 35% to 75% in fig. 6.15d, or approximately 18 to 21% viability gain per $4x10^4$ cell density for both experiments (based on the regression slope).

[A]

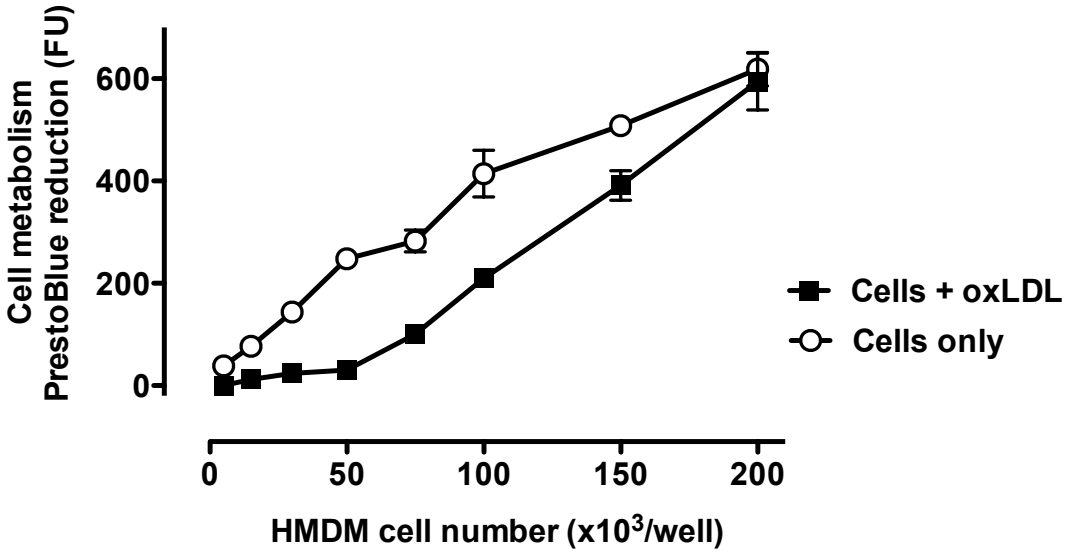

[B]

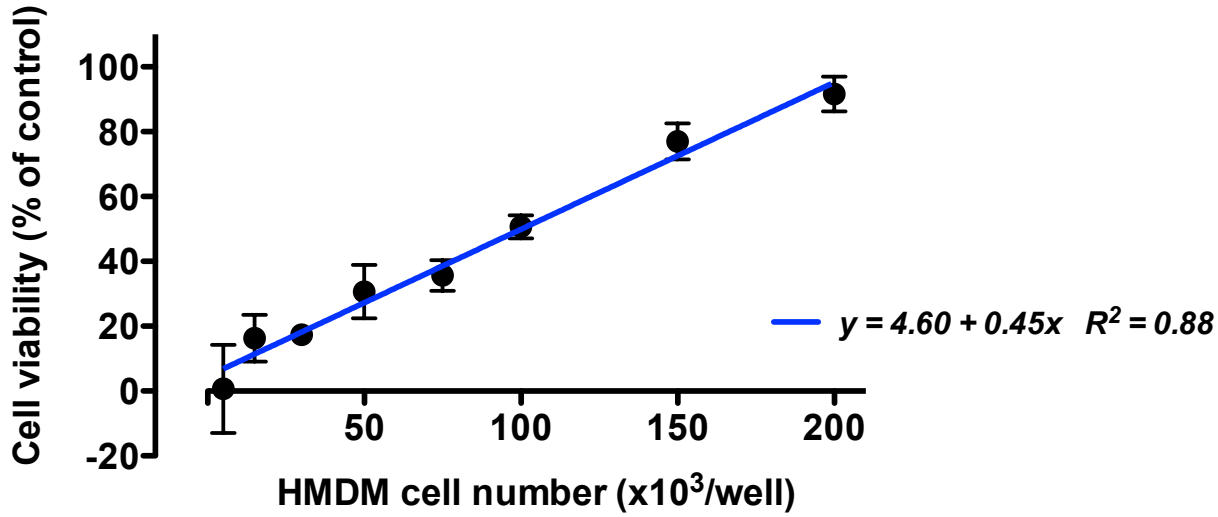

Figure 6.15: Effect of cell number on oxLDL–mediated HMDM cell viability loss, continued.

HMDM cells were lifted with *Accutase*™ treatment, counted and seeded at the indicated density into 48 well plates. After a 20 hour adjustment period, the cells were incubated with (filled squares) or without (empty circles) 2.5 mg/mL oxLDL for 24 hours in the presence of 2% human serum. Cell viability was assessed by *PrestoBlue*™ assay after 3 hour incubation. Results are mean ± SEM of triplicate measurements from two separate experiments (**A,B** and **C,D**); expressed as raw fluorescence values **(A,C)** and percentage of remaining cell viability relative to the respective no oxLDL control **(B,D)**. OxLDL–mediated cell viability loss was influenced by cell density (two-factor ANOVA, interaction highly significant, $p<0.001$) and the presence of oxLDL ($p<0.001$). Regression slopes were significantly non-zero, $p<0.001$.

[C]

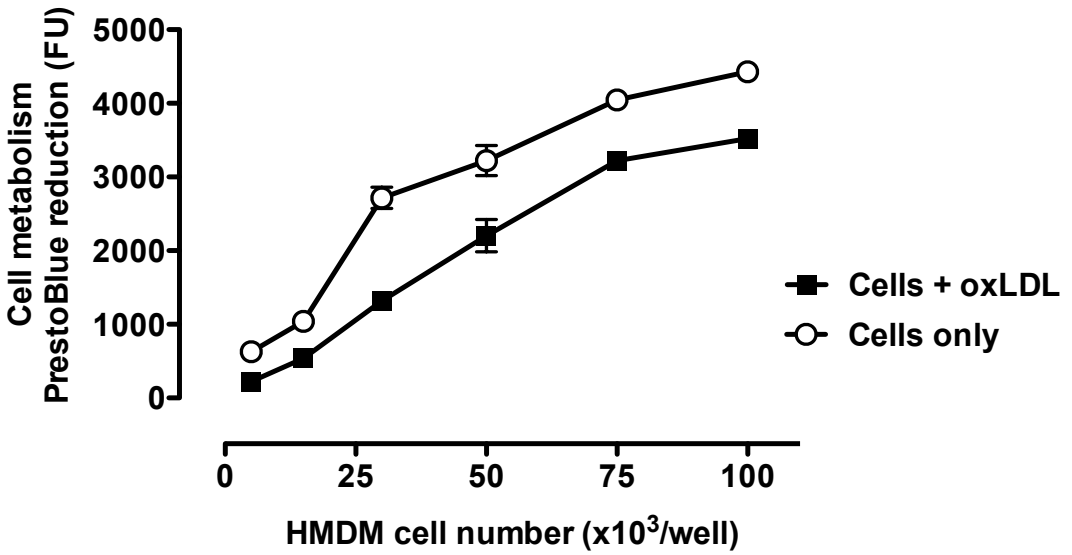
Cell metabolism
PrestoBlue reduction (FU)
5000
4000
3000
2000
1000
0
0
25
50
75
100
HMDM cell number (x10^3/well)
Cells + oxLDL
Cells only

[D]

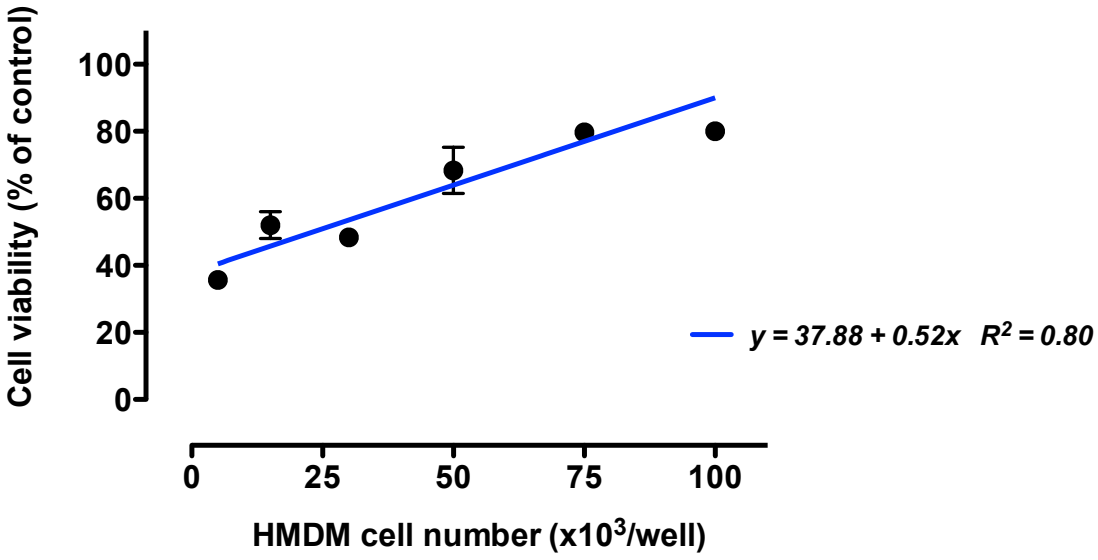
Cell viability (% of control)
100
80
60
40
20
0
0
25
50
75
100
HMDM cell number (x10^3/well)
y = 37.88 + 0.52x R^2 = 0.80

6.5 HMDM cell resistance to oxLDL toxicity

6.5.1 Defining HMDM cell resistance to oxLDL

The research presented in this section is a case study of HMDM cell resistance to oxLDL. It investigates the underlying mechanisms by characterising oxidative flux and damage in resistant cells. HMDM cells cultured in the presence of GM-CSF are robust to condition perturbations and toxic agents (personal communications with Dr. H. Kruth of National Heart Lund and Blood Institute, USA). As seen earlier, concentrations above 1–2 mg/mL oxLDL were required for any toxicity to occur. Among the overall robust culture, a proportion of HMDM preparations displayed little or no cell viability loss when exposed to otherwise toxic (2.5-3 mg/mL) concentrations of oxLDL (8 out of 20 since the start of observation). Although such cells were not used for the core experiments in this thesis, this persistent phenomenon was investigated further in an attempt to establish governing factors. This was necessary for the experiments that required toxicity. The "resistant" HMDM preparations were identified as showing no cell death when exposed to 2.5 mg/mL oxLDL for 24 hours in the culture medium supplemented with 0%, 2%, 5% or 10% human serum (fig. 6.16). A range of serum concentrations was tested because extracellular serum emerged as a protective factor against cellular death (fig. 6.4). More narrowly, the definition of resistant HMDM cells was chosen to be "HMDM cells that show less than 15% cell viability loss (when compared to cell only control, $p>0.05$) upon 24 hour incubation with 2.5 mg/mL oxLDL in the medium supplemented with 2% human serum" (as the complete absence of serum could be disputed as non-physiological). To unravel the mechanisms of this phenomenon, the investigation focused on two experimental components: oxLDL and HMDM cells.

[A]

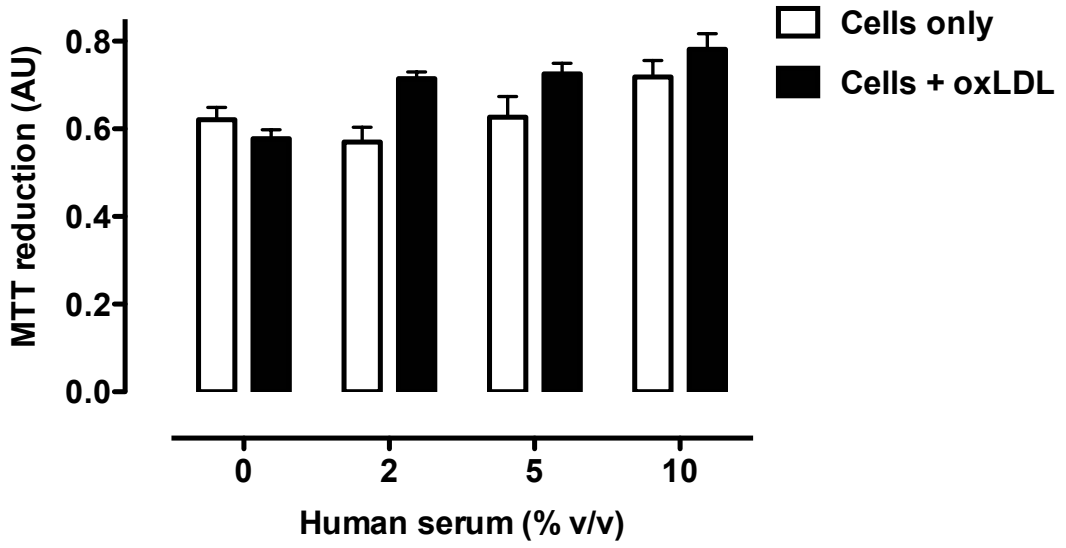

[B]

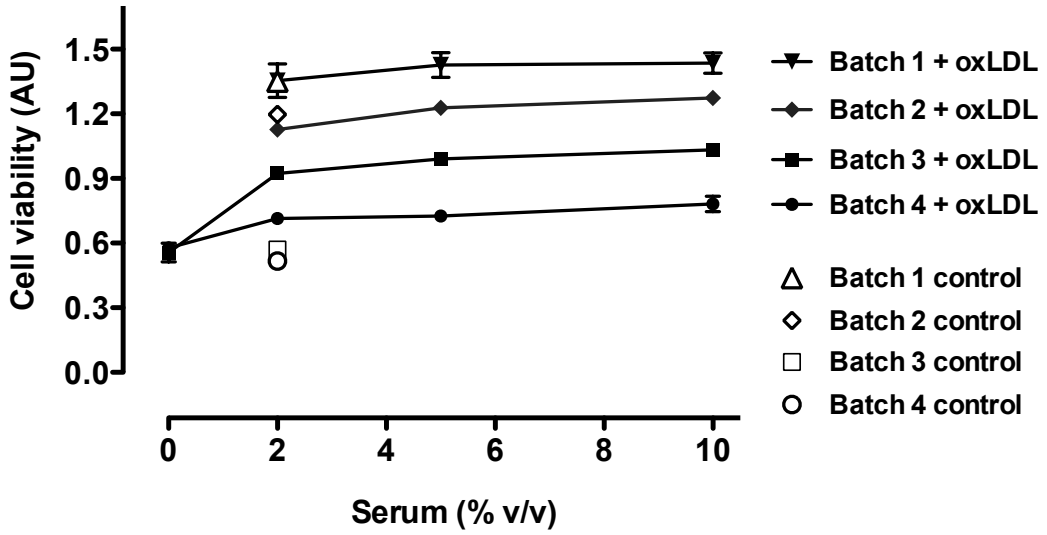

Figure 6.16: Resistance of HMDM to toxic concentration of oxLDL at a range of serum concentrations in the incubation medium.
HMDM cells ($1x10^6$ cells mL^{-1}) cultured in the whole medium, were treated with (filled signs and bars) or without (empty signs and bars) 2.5 mg/mL oxLDL for 24 hours in the medium containing the indicated concentration of serum. Cell viability was assessed by MTT reduction assay. Results are displayed as (**A**) mean ± SEM of triplicate measurements from a single experiment, (**B**) four separate experiments (only two of which had 0% serum measurement). None of the oxLDL treatments were statistically different from the respective no oxLDL control (one-factor ANOVA with Dunnett's post test).

6.5.2 LDL oxidation is not a factor in the HMDM cell resistance

The extent of LDL oxidation was measured to address the possibility that the oxLDL particle itself was the root of the resistance issue. LDL appeared to be fully oxidised after 24 hour oxidation with 500 μM Cu^{2+} ions at 37 °C. It lost its characteristic yellow colour and displayed increased relative electrophoretic mobility (REM) compared to native LDL on the native agarose gel (fig. 6.17). OxLDL in this study had a smaller REM of 3.65 compared to 4.20 ± 0.42 reported by Gerry *et al.* (2008). This REM was still high enough to indicate full oxidation. Amit (2008), who used a different methodology for Cu–mediated LDL oxidation, reported a REM of 2.67 and Katouah (2012), whose protocol was identical to the one used here, reported a REM of 3.33. Thus, the REM of oxLDL to which HMDM showed resistance was comparable to the published literature and the results obtained by the previous researchers in the same laboratory.

HMDM resistance was not due to a particular oxLDL preparation's inability to induce toxicity in cells. This was tested in U937 cells, a monocyte-like cell line shown to elicit similar response to HMDM cells when treated with oxLDL (U937 cellular death: Baird *et al.* (2004); HMDM cell death: Gieseg *et al.* (2010a), comparison: Katouah (2012)). OxLDL preparations that failed to kill HMDM cells were successful at killing U937 cells, thus eliminating oxLDL as the source of the problem. The remaining cell viability after 24 hour incubation of $5x10^5$ cells/mL with 0.5 mg/mL oxLDL was 44.7% ± 12.9 (SEM) (n=3). In view of these results, it was concluded that the source of HMDM resistance to oxLDL was not the properties of the oxLDL molecule, but the HMDM cells themselves and their response to oxLDL.

[A]

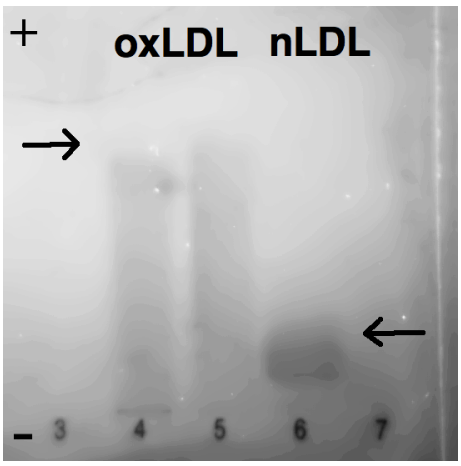

[B]

Oxidation method	REM
Published, Gerry et al. (2008)	4.20 ± 0.42
Present study	3.65

Figure 6.17: Lipoprotein gel electrophoresis.
Relative electrophoretic mobility (REM) of oxidised (lane 4, 5) and native (lane 6) LDL was established **(A)** and quantified **(B)** by native gel electrophoresis using Sebia© materials stained with sudan black. The arrows indicate the distance (mm) travelled by the lipoprotein, which was used to calculate the REM.

6.5.3 Delayed oxidative damage

Oxidative stress in oxLDL–resistant HMDM cells. A case study

To investigate the effect of oxLDL–mediated oxidative stress and damage, DHE fluorescence and GSH loss were assessed in "resistant" cell preparations. The following case study compares the development of oxidative flux over time in HMDM cell preparations that had varying susceptibility to oxLDL toxicity.

Two HMDM cell preparations cultured alongside each other were treated with 2.5 mg/mL oxLDL for 24 hours in the presence of varying concentrations of serum (fig. 6.18). The toxicity of oxLDL to batch A was only evident in the absence of serum. This batch was, therefore, called "resistant". OxLDL toxicity to batch B at 2% serum was statistically significant, and, thus, this batch was called "susceptible". Oxidative flux in "resistant" vs. "susceptible" HMDM cells was investigated, since oxidative stress had already been shown to be a prominent event in oxLDL toxicity to macrophages (fig. 3.3). Time-dependant intracellular ROS release was studied using a flow cytometry–based DHE fluorescence assay. After oxLDL treatment, the cells were detached with *Accutase*™, stained with DHE and analysed by flow cytometery. DHE product fluorescence was monitored in the FL3 channel and a shift to the right (higher fluorescence) was indicative of ROS increase. The gates were set as an overall FL3 gate, low fluorescence gate (determined based on control cell frequency distribution) and high fluorescence gate (high FL3 values) (fig. 6.19c-f). Control cells had minimal fluorescence in the right section of the FL3 flowgram. As the ROS flux increased, population frequency shifted to the right into the high fluorescence gate. The shift in median cellular fluorescence intensity (MFI) in the overall FL3 gate started at 24 hours and increased towards 48 hours in susceptible batch B (fig. 6.20). This shift was not apparent in control or cells from resistant batch A, which showed a significant shift only after 48 hours. Thus, overall oxidative burden was prominent at 24 hours in the susceptible batch, but was delayed in the resistant HMDM cells. At 48 hours, susceptible batch B cells reached 175,000 units, which was 25% higher than batch B increase at the same time (fig. 6.20).

The shift to higher DHE fluorescence was also evaluated as the proportion of total cells located in the high fluorescence region (fig. 6.21). The proportion of cells in this region at 24 hours was considerably lower for the resistant batch A, 25% vs. 50% for batch B. However, by the end of the 48^{th} hour, the proportion of cells staining highly for DHE in both batches converged and reached about 50%. This was also

reflected by the cellular viability (fig. 6.22). At 24 hours, the toxicity of resistant HMDM batch A was considerably lower than that of susceptible batch B, but this difference between batches was reduced by the 48^{th} hour (fig. 6.21). These results suggest that the oxidative stress manifesting as ROS release in the resistant HMDM cells was delayed (onset in the second rather than the first 24 hour period).

[A]

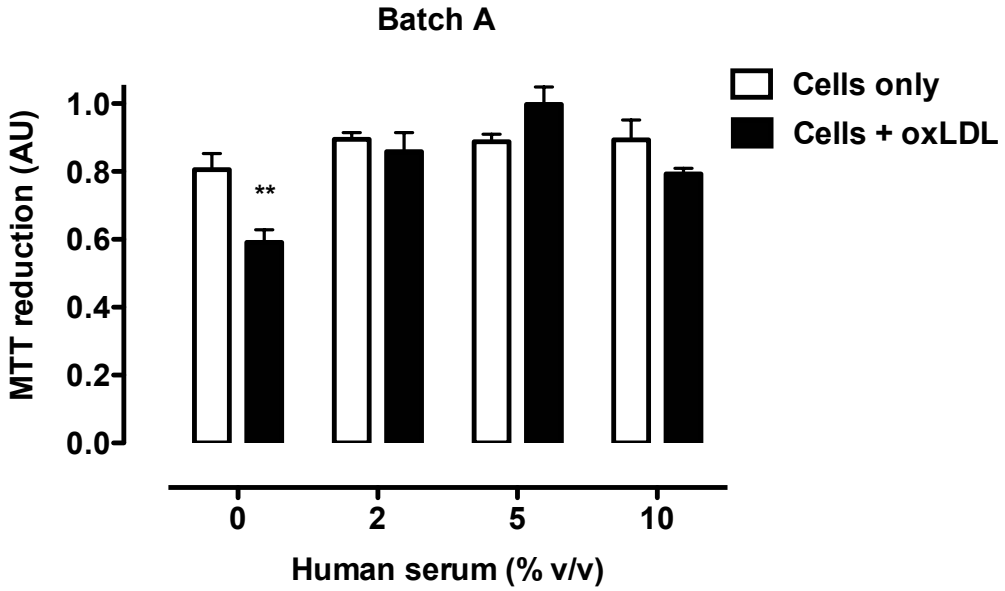

[B]

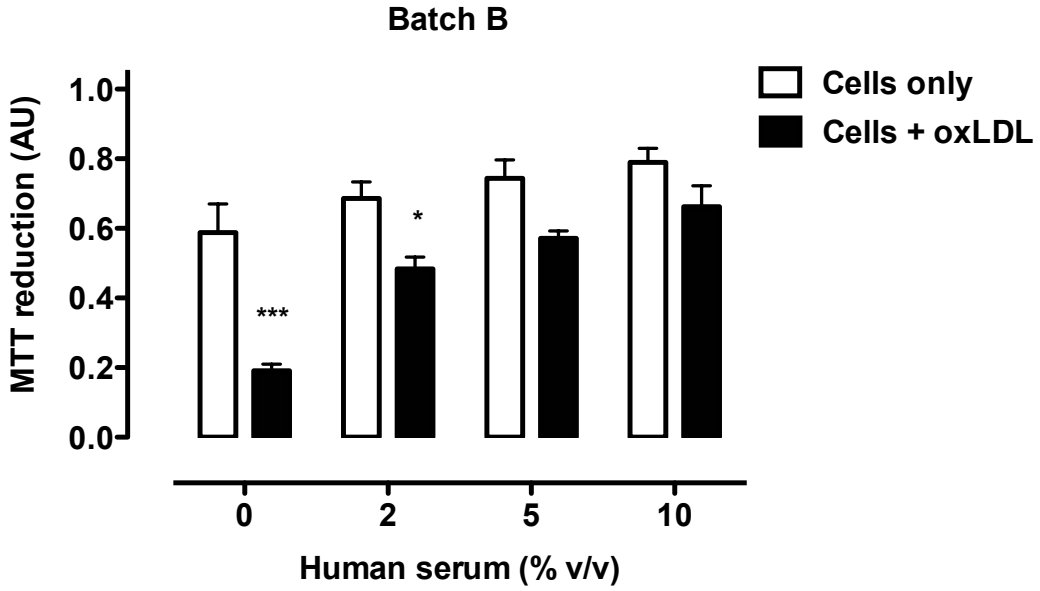

Figure 6.18: Differential oxLDL–mediated toxicity to HMDM preparations. HMDM cells ($1x10^6$ cells mL^{-1}), cultured in the whole medium, were treated with (filled bars) or without (empty bars) 2.5 mg/mL oxLDL for 24 hours in the medium containing the indicated concentration of serum. Cell viability was assessed by MTT reduction assay and displayed as mean ± SEM of triplicate measurements. (**A**) and (**B**) represent two HMDM cell batches grown alongside one another. Statistical significance as indicated (one-factor ANOVA with Bonferroni post test between the respective no oxLDL control and treatment): *, $p<0.05$, **, $p<0.01$, ***, $p<0.001$).

	Batch A, "resistant"	**Batch B, "susceptible"**
[0 hours]	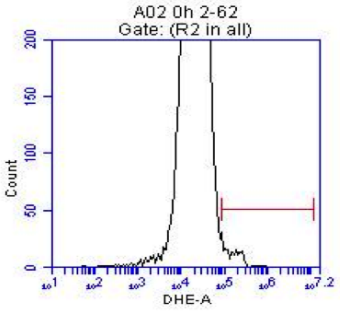	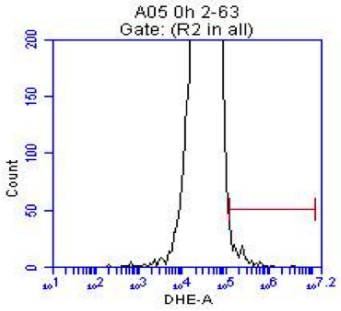
[6 hours]	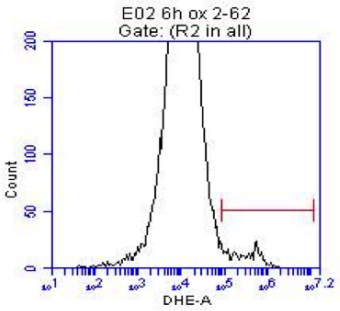	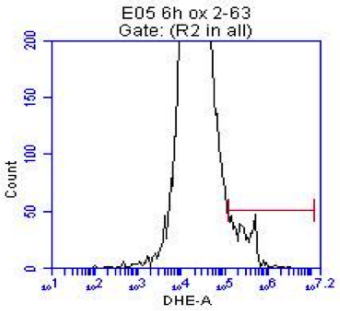
[12 hours]	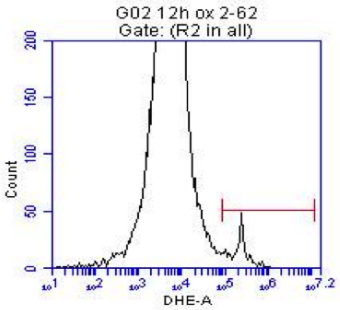	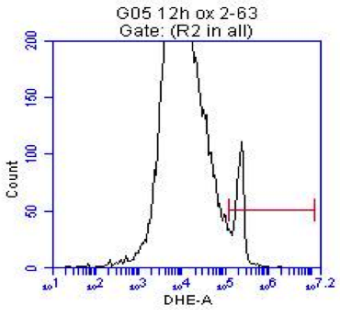
[24 hours]	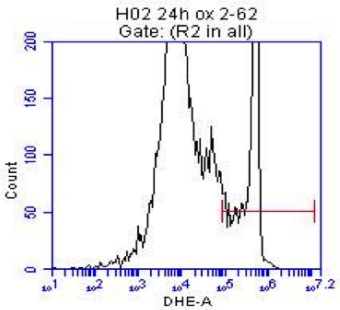	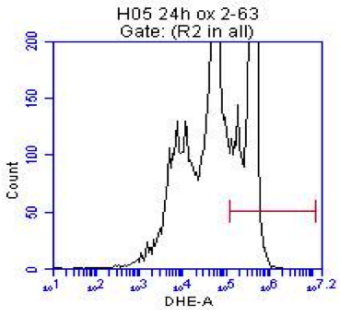
[48 hours]	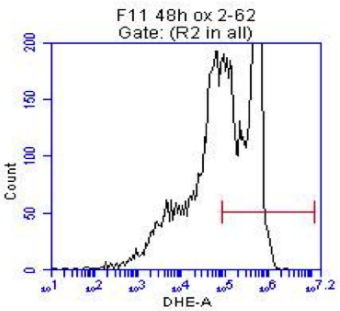	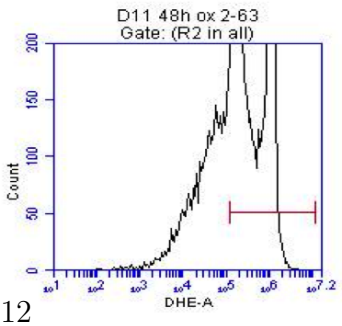

[Fig 1.17]

Figure 6.19: DHE measurement of resistant and susceptible oxLDL–treated HMDM cells.
HMDM (1x10^6 cells well^{-1}) were treated with 2.5 mg/mL oxLDL in the presence of 2% human serum for the indicated period of time. Cells were harvested into *Accutase*™ and assessed for ROS production using DHE probe. Presented are the histograms of cell count (out of 10,000 total events) in the FL3 channel. Shown is the "high DHE fluorescence" gate.

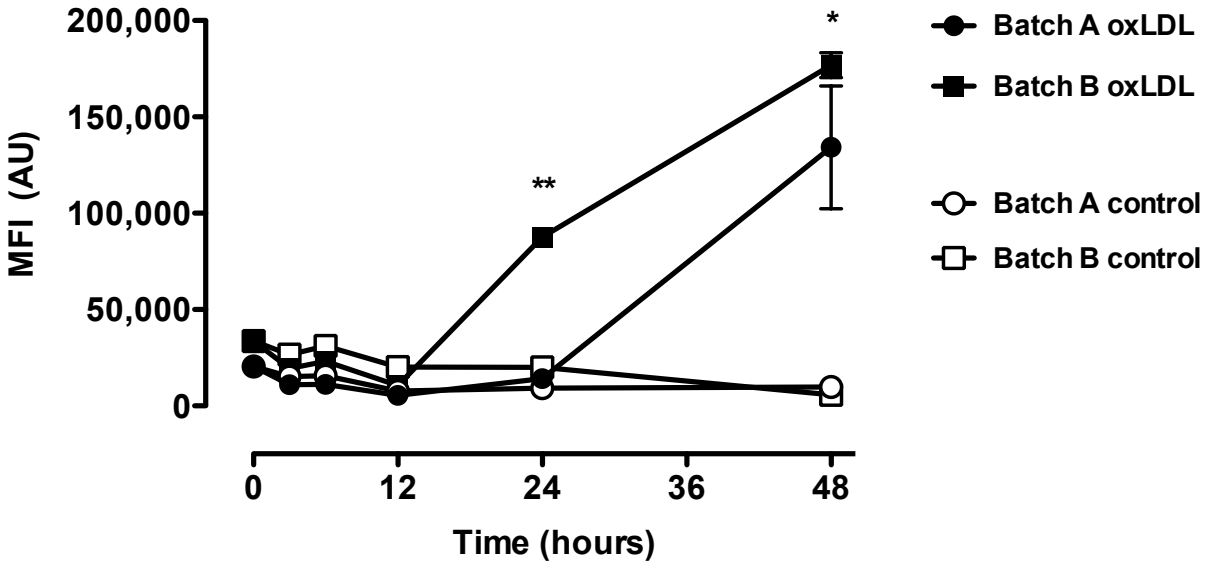

Figure 6.20: Differential oxLDL-mediated intracellular ROS flux in HMDM preparations.
HMDM cells (1x10^6 cells mL^{-1}) of batch A (circles) and batch B (squares), cultured in the whole medium, were treated with 2.5 mg/mL oxLDL for 24 hours in the medium containing 2% serum. Intracellular ROS was assessed by DHE flow cytometry-based assay. Results are displayed as mean ± SEM of fluorescence per "all-including" section based on 10,000 events. This experiment was performed once. Statistical significance is indicated between the batches at the respective time point (one-factor ANOVA with Bonferroni pairwise comparison, *, $p<0.05$, **, $p<0.01$.

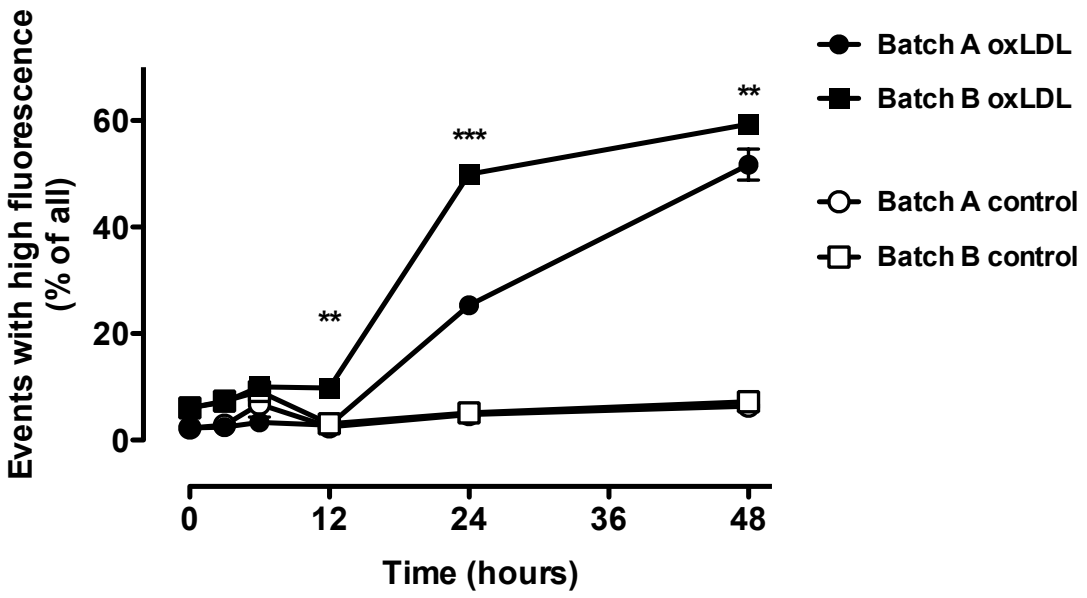

Figure 6.21: Differential oxLDL-mediated intracellular ROS flux in HMDM preparations, percentage shift into high DHE-fluorescence gate.
HMDM cells ($1x10^6$ cells mL^{-1}) of batch A (circles) and batch B (squares), cultured in the whole medium, were treated with 2.5 mg/mL oxLDL for 24 hours in the medium containing 2% serum. Intracellular ROS was assessed by DHE flow cytometry-based assay and expressed as percentage shift into "high DHE fluorescence" of total events in HMDM gate. Results are displayed as mean ± SEM of triplicate measurements from a single experiment. Statistical significance is indicated between the batches at the respective time point (one-factor ANOVA with Bonferroni pairwise comparison, **, $p<0.01$, ***, $p<0.001$.

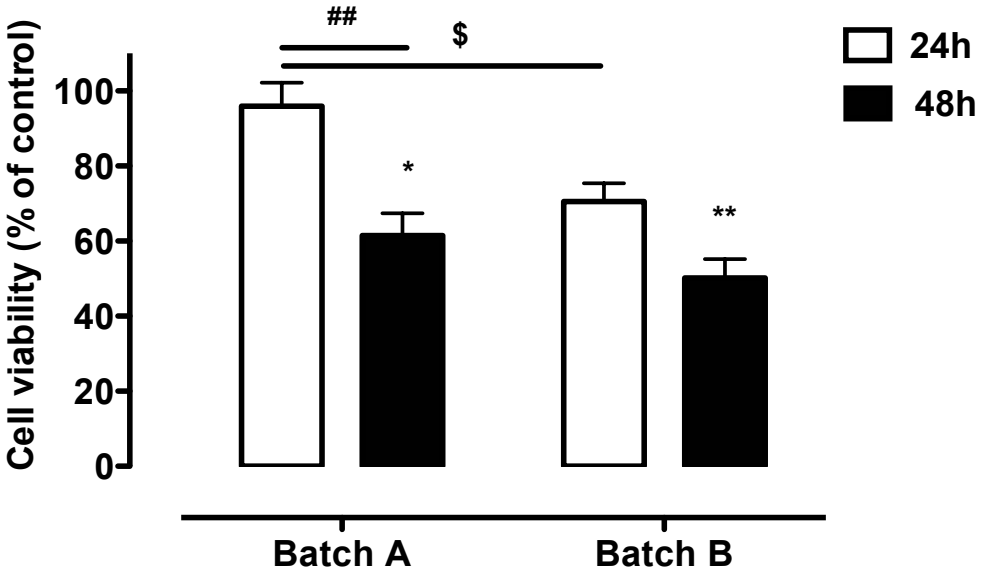

Figure 6.22: Cell viability after 24 vs. 48 hour incubation of HMDM cells with oxLDL.

HMDM cells ($1x10^6$ cells mL^{-1}) were incubated with 2.5 mg/mL oxLDL in the medium (2% serum) for 24 and 48 hours. Cell viability was assessed *via* MTT reduction assay. The data are expressed as a percentage of the untreated control. Results are displayed as mean ± SEM of triplicates from a single experiment. Statistical significance was determined by one-factor ANOVA with Bonferroni post test between the respective 0 hour control and treatment *, $p<0.05$, **, $p<0.01$; and between the 24–48 hour treatments ##, $p<0.01$, $, $p<0.05$.

GSH loss in "resistant" HMDM cells with oxLDL

Intracellular GSH loss was not observed in the "resistant" HMDM cells to the extent it was described in chapter 3. No GSH loss was observed over the course of incubation (fig. 6.23). A minor decrease at around 6 hours was observed, followed by a significant increase by the 24th hour. This result mirrored the one obtained by Cho *et al.* (1999) in kinetics, though not in magnitude.

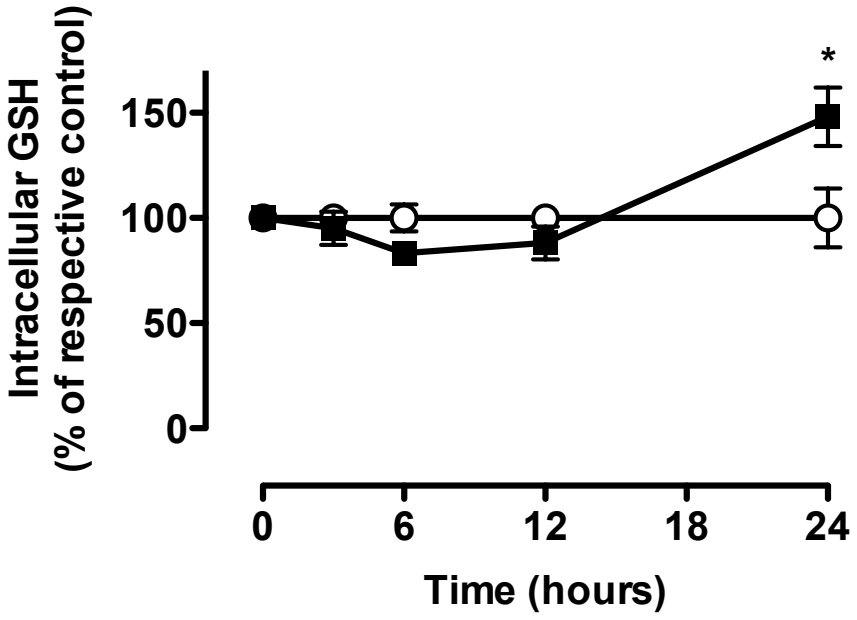

Figure 6.23: Time-course of intracellular GSH in "resistant" HMDM cells in response to oxLDL treatment.
HMDM cells (1x10^6 cells mL^{-1}) were incubated with (black squares) or without (white circles) 2.5 mg/mL oxLDL in RPMI-1640 supplemented with 5% human serum for the indicated period of time. Intracellular GSH was assessed via HPLC. The data are expressed as a percentage of the untreated control and displayed as mean ± SEM of triplicates from a single experiment. For reference, [GSH] in control cells was 5.2 nmol/well. Significance (t-test on raw data) is as indicated, *, $p<0.05$. [GSH] in control cells was 5.18 nmol/well.

The developing effect of oxLDL on GSH in a 24–48 hour time-frame was investigated further in two more HMDM preparations. Both experiments 1 and 2 showed no cell viability loss at 24 hours in the presence of 2.5 mg/mL oxLDL and 2% human serum and thus were considered "resistant" (figures 6.24a and 6.25a). In alignment with cell viability loss, both HMDM batches lost intracellular GSH in 0% serum within 24 hours (figures 6.24b and 6.25b). Also in agreement with the metabolic activity, GSH level in the rest of the treatments was did not change (figures 6.24b and 6.25b). At 48 hours (black bars), however, cell viability loss became evident in the 2% and 5% serum treatments (figures 6.24a and 6.25a). A similar pattern was observed for intracellular GSH confirming the colose association between oxidative damage and loss of cellular metabolism. Thence, oxidative damage in these "resistant" HMDM cells was delayed until after 24 hours. Metabolic activity loss followed the same trend.

[A]

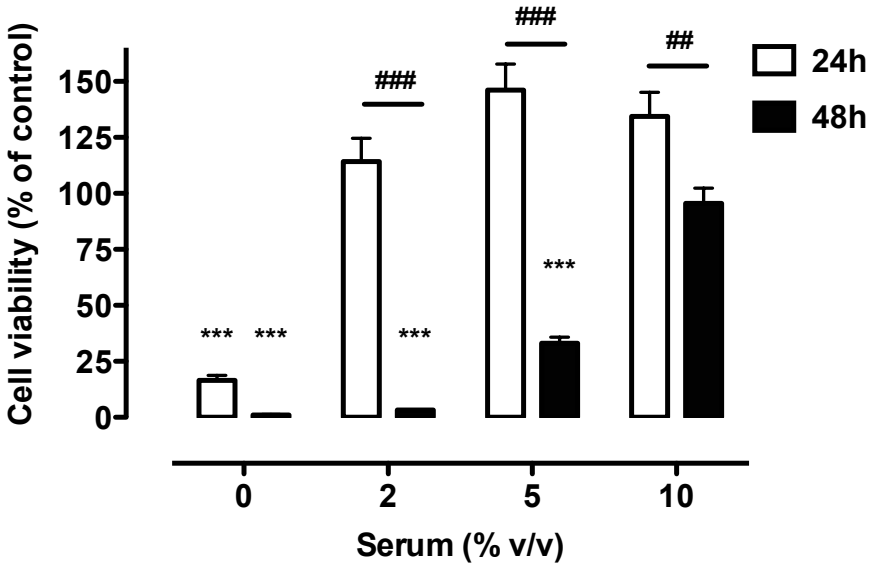

[B]

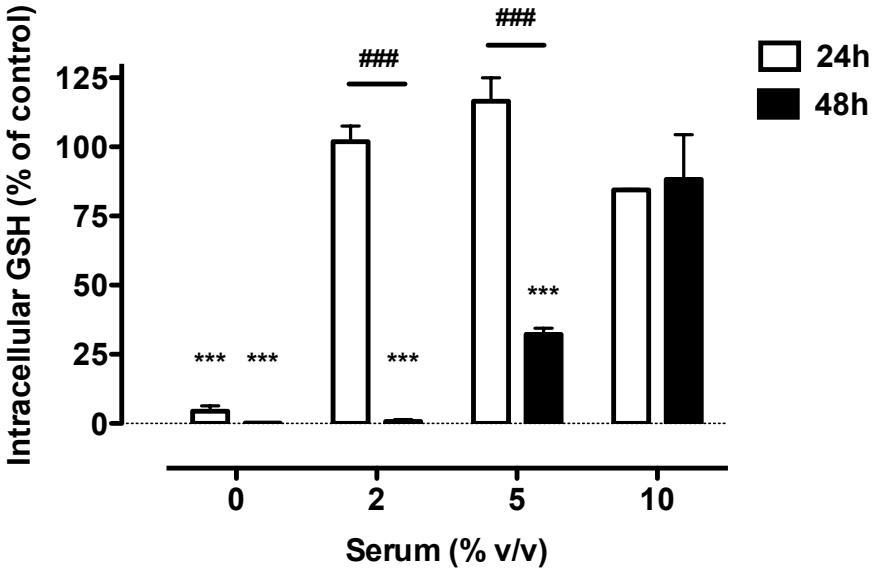

Figure 6.24: Viability and GSH loss in "resistant" HMDM cells at 24 and 48 hours after oxLDL treatment. Experiment 1.

HMDM cells ($1x10^6$ cells mL^{-1}) were incubated with 2.5 mg/mL oxLDL in RPMI-1640 supplemented with increasing concentrations of human serum for 24 (white bars) and 48 (black bars) hours. Cell viability and GSH were assessed via *PrestoBlue*™ reduction and MBB-HPLC assays, respectively. The data are expressed as a percentage of untreated control and displayed as mean ± SEM of triplicates from a single experiment. Statistical significance was determined by one-factor ANOVA with Bonferroni post test between the respective 0 hour control and treatment ***, $p<0.001$; and between the 24–48 hour treatments #, $p<0.01$, ###, $p<0.001$).

[A]

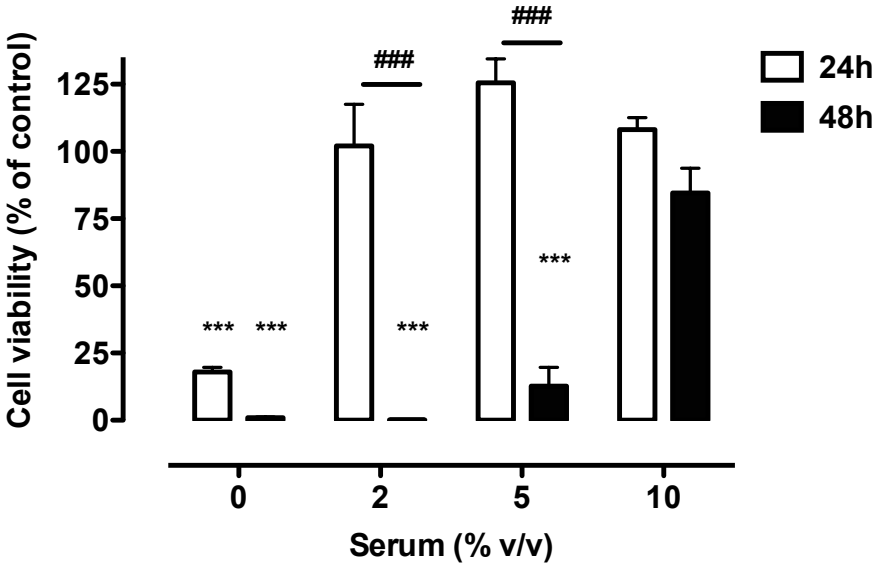

[B]

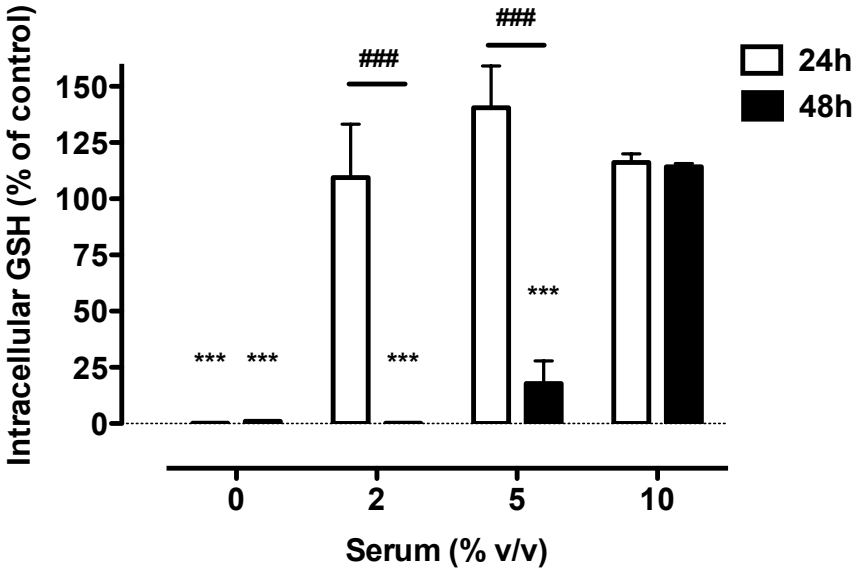

Figure 6.25: Viability and GSH loss in "resistant" HMDM cells at 24 and 48 hours after oxLDL treatment. Experiment 2.

HMDM cells ($1x10^6$ cells mL^{-1}) were incubated with 2.5 mg/mL oxLDL in RPMI-1640 supplemented with increasing concentrations of human serum for 24 (white bars) and 48 (black bars) hours. Cell viability and GSH were assessed via *PrestoBlue*™ reduction and MBB-HPLC assays, respectively. The data are expressed as a percentage of untreated control and displayed as mean ± SEM of triplicates from a single experiment. Statistical significance was determined by one-factor ANOVA with Bonferroni post test between the respective 0 hour control and treatment ***, $p<0.001$; and between the 24–48 hour treatments ###, $p<0.001$).

6.6 Discussion

6.6.1 HMDM cell culture

Reproducible culture and experimentation on primary cells is associated with challenges. This study attempted to standardise the methodology and explore the impact of the external experimental factors on oxLDL toxicity to cultured macrophages.

An overall success of HMDM cell culture in the presence of GM-CSF was quantified and is reported here for future reference, since no prior data on this subject is readily available. The growth and development of monocytes into macrophages was enhanced by 50% with the inclusion of the growth factor (fig. 6.1). Seventy percent of HMDM preparations grown with GM-CSF were of quality suitable for experiments (fig. 6.2). GM-CSF predominantly drives the differentiation of monocyte into the so called "M1" macrophage (Waldo *et al.*, 2008). This type was relevant to the present study, as IFN-γ, which is the *in vivo* stimulus for M1 macrophage differentiation, also enhances the production of 7,8-NP (Weiss *et al.*, 1999).

The effect of plate type and supplier on HMDM cell culture was tested with the goal of improving the uniformity of culture and increasing the experimental unit number. Cellstar were considered a superior plate type to Nunc based on the cost comparison, given a similar culture success rate (fig. 6.3). A move away from the 12 to 48 well plates was made after establishing the plating concentration of $1x10^6$ (fig. 6.4). This tripled the number of experimental units (i.e. wells) per batch of HMDM cells.

Serum supplementation was found to have a significant effect on HMDM cell differentiation and growth (figures 6.5 and 6.6). Three out of 7 serum batches tested conveyed a higher differentiation and growth–promoting capacity than the rest. At present, it is difficult to suggest a mechanism for the observed phenomenon. Cloudy or "lipid-rich" sera, which was most likely due to high triglyceride content, often resulted in higher macrophage differentiation and growth, although this trend was not restricted to cloudy serum. Due to time and funding restrictions, the underlying cause of serum–driven differentiation and growth disparity was not pursued further. The information gained through these experiments led to the combining (or "pooling") of multiple batches of sera in order to standardise the HMDM cell culture methodology. This allowed a reduction of some of the inter-donor variation and increased the volume of a "pooled" batch of serum. The latter enabled a higher number of experiments

to be performed in similar serum conditions. Serum pooling did not alter HMDM growth (figures 6.5 and 6.6). Heat–inactivation of human serum was discontinued after the review of the literature (Biochrom AG, 2010; Hyclone®, 1996; Leshem *et al.*, 1999). Heat–inactivation of serum neither induced nor inhibited HMDM cell growth (fig. 6.6).

6.6.2 Utility of U937 cells as a model of 7,8-NP–mediated oxLDL uptake regulation

The U937 cell line was tested as a potential replacement of the heterogeneous primary HMDM cell culture. As in HMDM cells, two protein products of molecular weights of 80 and 100 kDa were observed. Compared to HMDM cells, U937 monocytic cell line displayed an up-regulation of the lower molecular weight band (intracellular CD36, according to Alessio *et al.* (1996)) with increasing 7,8-NP concentrations (fig. 6.8). The higher molecular weight band (plasma membrane CD36) was down-regulated by 30% at 250 μM of 7,8-NP. This was almost 1.5–2 times lower compared to the HMDM cells' 50% down-regulation (fig. 6.8). This result suggested that despite having a less prominent 100 kDa protein product, U937 and HMDM cells share similar underlying processes in this area. Nakagawa *et al.* (1998) observed that CD36 levels increase with macrophage maturation. PMA–differentiation of U937 cells increased the amount of highly glycosylated CD36 (Alessio *et al.*, 1996). Thus PMA stimulus could be used to drive CD36 expression in U937 cells, if required for future study. However, the induction of protein kinase C and the activation of inflammatory status in such cells should be taken into account. Napolitano & Bravo (2003) reported that PMA–activated PKC pathways interfered with the optimal ligand-induced phosphorylation of the receptors, compromising the processes of degradation of modified LDL.

U937 cells showed no 7,8-NP–mediated decrease in oxLDL uptake (fig. 6.9). This might be due to the absence of serum in the experimental medium. The experimental conditions for U937 cells (RPMI-1640 in the absence of serum) could not be altered easily, as experiments with oxLDL toxicity to U937 cells were typically done in the absence of serum (Katouah, 2012). This made U937 cells an unsuitable substitute for HMDM cells for this work.

6.6.3 Extracellular factors

Serum supplementation is protective against oxLDL toxicity

The concentration–dependant oxLDL toxicity to HMDM cell varied substantially, as indicated by the mean ± range plots in figure 6.10. This presented a hindrance to the research because the cells for which LC_{50} was outside the common 2–3 mg/mL range were considered outliers and were not used for key experiments. Thus, conditions that favoured HMDM resistance to oxLDL toxicity were investigated.

The troubleshooting process started with investigating the effect of serum. As discussed above, different sera had different capacities to promote cellular differentiation and growth. However, minor difference in oxLDL toxicity was observed when the same batch of HMDM cells, that was cultured and incubated in sera from different donors, was treated with oxLDL (data not shown). Research indicates, however, that extracellular serum per se inhibits oxLDL toxicity to HMDM, ECs and SMC cells (Asmis & Wintergerst, 1998; Henriksen *et al.*, 1979; Hessler *et al.*, 1979; Wintergerst *et al.*, 2000). The effect of serum supplementation was, therefore, pursued as a potential factor of HMDM resistance.

The effect of serum supplementation was investigated further, revealing that it was highly protective against oxLDL–induced toxicity (fig. 6.11). Extracellular serum above ∼3% (v/v) almost completely protected against the toxicity of 2 mg/mL oxLDL. The curve of extracellular serum effect plateaued after 3 mg of protein per mL (or 4.86% serum), indicating a saturation effect. (Normal extracellular protein concentration of the whole medium at 10% human serum was a consistent ∼7 mg of protein per mL). The steep slope in the 0–2 mg/mL serum protein range indicated that incremental change in serum concentration within this range had a large effect on oxLDL–mediated toxicity. There was large variability between the experiments in this region of rapid change. This was not associated with experimental error, since a) higher concentration points showed lower variability and b) individual experimental replicates showed consistent variance at concentrations of 0.75 and 1 mg cell protein (fig. 6.12a). The sensitivity of this region of protein concentration could potentially be utilised in future experiments. If one was to pursue the inherent HMDM differences that cause differential response to toxicity, the experimental conditions within this region are more likely to yield a range of results.

Macrophage morphology during cell death was not affected by the reduction in serum

concentration, only the overall magnitude of toxicity. The presence of extracellular protein had no effect on apoptosis/necrosis ratio in U937 cells, only the timing of toxicity (data not shown). Thus, it appears that the cell death processes were delayed but not altered in the presence of serum. A similar theme emerged for the phenomenon of HMDM resistance, as will be discussed below.

Protein conveys the protective effect against oxLDL toxicity

Protection by serum factor(s) may occur either at the cellular level, rendering HMDM cells resistant to oxLDL, or at the level of oxLDL molecule, inactivating the cytotoxic moieties of oxLDL and hindering oxLDL binding sites (Asmis & Wintergerst, 1998). The majority of the protective effect was attributable to protein and not other components of serum (fig. 6.12). Simple protein solution and serum were equally protective against oxLDL up to a concentration of 0.75 mg protein/mL in the extracellular medium (fig. 6.12). From 1 mg/mL onwards, the protective effect of serum was, on average, 10% higher than that of BSA solution matched to serum by the concentration of protein (fig. 6.12). Thus, the majority of the serum protective effect was likely to be due to serum albumin.

The presence of serum and BSA reduced the levels of intracellular oxLDL by 25 and 40% as indicated by 7KC uptake (fig. 6.13). The flexibility of albumin tertiary structure enables it to bind a wide range of ligands, from metal ions to fatty acids (Roche *et al.*, 2008). Suginohara *et al.* (1996) also indicated that heparin-bound fraction of human lipoprotein–deficient serum inhibits endocytic uptake of oxLDL by macrophages. Thus, sequestration of oxLDL and its components by serum albumin was a possible protective mechanism. Also, some evidence exists that albumin acts as a cholesterol efflux acceptor, similar to HDL (Ha *et al.*, 2003; Han *et al.*, 1997). (The unphysiological state of HMDM cell culture in the absence of serum may have an unknown effect on the cells.)

Activated monocyte-macrophages are known to release extracellular ROS (Nakagawara *et al.*, 1981). Other cell types, like endothelial cells, also generated extracellular superoxide in response to oxLDL which was capable of promoting the induction of apoptosis (Harada-Shiba *et al.*, 1998). Albumin is a multifunctional protein that has been shown to act as an oxidant "sink" (Roche *et al.*, 2008). Albumin has been shown to effectively scavenge $O_2^{\bullet-}$, H_2O_2, HOCl reactive oxygen species in cell culture and in cell free conditions (Kouoh *et al.*, 1999; Roche *et al.*, 2008). Direct

antioxidant activity of albumin is associated with its abundance which enables it to act as a sacrificial target for ROS (Bourdon & Blache, 2001). A reduced cysteine residue, Cys34, and six methionine residues on human serum albumin are likely to be involved in ROS scavenging (Oettl & Stauber, 2007).

The remaining difference between serum and BSA–mediated protection (10%) could be attributed to the antioxidant effect of other components of human serum, although consensus on this topic is lacking. While some researchers observed a protective capacity of serum antioxidants such as ascorbate or dehydroascorbate against oxLDL (Asmis & Wintergerst, 1998; Siow *et al.*, 1998), others found no effect of ascorbate (Harris *et al.*, 2006) or α-TocH Asmis & Jelk (2000b). In a review, Bourdon & Blache (2001) also suggested that α-TocH or ascorbate provided a limited contribution to serum antioxidant activity. Lipid and lipoprotein deficient serum conveyed virtually the same protection as whole serum, indicating that lipid–associated antioxidants were not involved in protection (Asmis & Wintergerst, 1998; Hessler *et al.*, 1979). Extracellular GSH, on the other hand, has been unanimously protective (Baoutina & Dean, 2001; Hardwick *et al.*, 1999; Hultén *et al.*, 2005; Siow *et al.*, 1998; Wang *et al.*, 2006) and may have played a role in this study, as well. Another potential source of protection is cholesterol and oxidised cholestrol products' efflux onto HDL in serum (reviewed in Jessup *et al.* (2002) and Yvan-Charvet *et al.* (2010)).

Since protein emerged as the major protective component of serum, protein supplementation in cell culture could be used instead of serum supplementation. In experiments when serum components like lipoproteins, antioxidants and growth factors may interfere with the outcome being measured, serum could be substituted for BSA while retaining the beneficial effect on cells. Protein concentration in the sera batches used in this study was reasonably consistent (70 ± 3 mg/mL (SD)). This suggested that although serum protein may have been the source of HMDM resistance to toxicity it was unlikely to be the source of variation.

Increased cell density is protective against oxLDL cytotoxicity

Cell density also had a major effect on oxLDL toxicity to both U937 and HMDM cells. The magnitudes of the effects were approximately 20% protection per $4x10^5$ U937 and $4x10^4$ HMDM cells. To the author's knowledge this is the first attempt to quantitatively measure the effect of cell density on the oxLDL toxicity outcome.

Previously, Hessler *et al.* (1979) reported that for EC and SMC "cellular susceptibility to LDL toxicity appeared to be a function of culture density and possibly cell cycle phase". Doubling of the SMC culture density resulted in a 24% to 64% viability increase after 66 hour incubation with LDL (oxidised by cells) (Hessler *et al.*, 1979).

It is difficult to propose a mechanism of cell-density–mediated protection with any certainty. Potentially, spatial hindrance in high density cultures may lead to reduced binding and uptake of oxLDL as cell clumping leads to lower number of receptors available for oxLDL binding/uptake. This phenomenon has been described for LDL. Stein & Stein (1975) and Vlodavsky *et al.* (1977) (cited in Hessler *et al.* (1979)) have shown that SMC and EC cells internalise LDL depending on cell culture density (confluent vs. sub-confluent).

Another possible mechanism could be that cells release protective substances, such as growth factors, cytokines and thiol–containing proteins. Macrophages are known to release a suite of chemo– and cytokines in response to oxLDL (Hansson & Hermansson, 2011; McLaren *et al.*, 2011), some of which could be priming the neighbouring cells for resistance. In addition, HMDM cells have been shown to release extracellular thiols that could react with oxLDL components neutralising cholesteryl ester hydroperoxides in oxLDL, an antioxidant action that is proportional to cell number (Baoutina, 2000; Baoutina & Dean, 2001). HMDM cell density–associated thiol release had also been observed in this study (data not shown).

The implications of cell density–dependant toxicity for *in vitro* experiments are large. If oxLDL toxicity is dependant on density to the extent described here (20% per 40,000 fully grown HMDM cells), this would contribute to inter-batch variation between HMDM cells. As they differentiate from the seeded monocytes, the final number of cells per well would vary. Thus cell density is certainly a factor in the inter-batch variability between the HMDM cell cytotoxicity in response to oxLDL. Moreover, the effect of cell density would influence the magnitude of toxicity between the published studies that used different monocyte seeding densities. Indeed, cell density conditions varied between the laboratory groups presented in table 6.1. The Asmis group preferred seeding at 0.15 x 10^6 cells/well in 12 well plates or on 22 mm diameter Aclar film (Asmis & Begley, 2003; Asmis & Wintergerst, 1998; Asmis *et al.*, 2005; Wang *et al.*, 2006; Wintergerst *et al.*, 2000). Our group used 5 x 10^6 cells/well in 12 well plates (Gieseg *et al.*, 2009, 2010a), whereas Mitchinson's group favoured 3 x

10^3 cells/well in 24 well plates (Carpenter *et al.*, 2001; Hardwick *et al.*, 1996, 1999; Marchant *et al.*, 1995).

A collection of 15 studies featuring Cu-oxLDL toxicity to HMDM cells is presented in table 6.1. The following experimental parameters were included: time of exposure, concentration of oxLDL (in μg LDL protein/mL, which is 5 times smaller than the μg LDL cholesterol/mL used in this study), percentage cell death, either obtained from text or calculated from the figures of the manuscript, percentage cell death in the respective control (if applicable, depending on the assay), concentration of serum in the medium and cell seeding density. Since cellular death was measured by different means, the type of assay is also shown. For studies 2, 4, 6, 8, 12 and 15 more than one concentration of oxLDL or more than one time of exposure were included.

A number of observations could be made from the comparative analysis of the studies in the table 6.1. A third of the studies performed experiments in the absence of supplementary serum. Asmis & Wintergerst (1998) and Wintergerst *et al.* (2000) explicitly stated that the presence of serum inhibited oxLDL–mediated cell death at 100 mg/mL (equivalent to 0.5 mg/mL as used in the present study). Another third of the authors did not report serum concentration during experimental conditions (although most reported it during cell culture). Serum concentrations were a constant 10% in the remaining (but one) of the studies included in the table. Cell density also varied between the laboratory groups as outlined above.

Differences between the absolute oxLDL toxicity were also observed. The same oxLDL concentration often yielded a range of toxicity values. For the three studies that utilised 100 μg/mL oxLDL over 24 hours, the reported viability loss (using a variety of assays) ranged from 20% (Wintergerst *et al.*, 2000) to 50% (Asmis & Begley, 2003) to 27–65% (Hardwick *et al.*, 1996). Likewise, for the six studies that used 200 μg/mL oxLDL over 24 hours, the viability loss ranged from 0% (Gieseg *et al.*, 2009), to 40–50% (Carpenter *et al.*, 2001; Gieseg *et al.*, 2010a), to 75–86% (Hardwick *et al.*, 1996, 1999; Marchant *et al.*, 1995).

The hypothesis of the association between highest toxicity with lowest serum and lowest cell density values did not hold for this data set. Although some of the highest toxicity results coincided with serum-devoid experimental design (Hardwick *et al.*, 1999), others did not (Hardwick *et al.*, 1996; Marchant *et al.*, 1995). Similarly, the

studies with lowest HMDM seeding density (1-5, table 6.1) did not demonstrate the highest overall toxicity. Not all studies with at least one common author reported similar range of toxicity. For example, 50% in Asmis & Begley (2003) contrasts with 20% in Wintergerst *et al.* (2000); and 0% in Gieseg *et al.* (2009) contrasts with 50% in Gieseg *et al.* (2010a). Overall, these differences indicate that much more information is required to explain the inter-experimental variation within and between laboratories, than just level of serum and cell density. In the light of the current findings, the interpretation and comparison of relative oxLDL toxicity in the studies included in the table 6.1 should proceed with caution, as the interaction between the serum inclusion and cell seeding density could have unpredicted effect.

The extracellular composition within the atherosclerotic plaque is unknown. Plaques contain oxidised LDL constituents (Li *et al.*, 2006; Waddington *et al.*, 2003; Ylä-Herttuala *et al.*, 1989) in regions characterised by extensive cellular death (Hegyi *et al.*, 1996; Isner *et al.*, 1995; Kockx *et al.*, 1998; Martinet *et al.*, 2011). This suggests that LDL oxidation and cell death do take place. Since both of these are inhibited in the presence of serum (Henriksen *et al.*, 1979; Hessler *et al.*, 1979), the effective concentration of serum in plaque is probably low (unless its distribution is compartmentalised either spatially or temporally). If, indeed, a spectrum of serum conditions exists within the lesion (evidenced by the presence of serum-derived antioxidants (Carpenter *et al.*, 1995; Suarna *et al.*, 1995)), the *in vitro* experiments that model a range of serum conditions will all provide information on cellular behaviour in plaques.

Table 6.1: OxLDL toxicity to HMDM cells and experimental conditions in the published literature.

No	Study	Cell type	Time hr	Conc. μg/mL	Cell death %	Death in control %	Serum % v/v	Cell density x10^6 c/w
1	Asmis & Wintergerst (1998)	HMDM	15	100	15.1^{AV}, $22.2^{apo2.7}$, 11^{H}, $<1^{PI}$	$<2^{AV,\ apo2.7,\ PI}$, 12^{H}	–#	0.15
2	Asmis & Begley (2003)	HMDM	24	100	$\sim 50^{H}$	$<10^{H}$	NS	0.15
2	Asmis & Begley (2003)	HMDM	24	150	$\sim 90^{H}$	$<10^{H}$	NS	0.15
3	Asmis *et al.* (2005)	HMDM	48	100	100^{H}	6.4^{H}	NS	0.15
4	Wintergerst *et al.* (2000)	HMDM	24	100	$20^{apo2.7}$	$4^{apo2.7}$	–	0.15
4	Wintergerst *et al.* (2000)	HMDM	48	100	$37^{apo2.7}$	$20^{apo2.7}$	–	0.15
4	Wintergerst *et al.* (2000)	HMDM	48	100	$<2^{apo2.7}$	$<2^{apo2.7}$	5, HS	0.15
5	Wang *et al.* (2006)	HMDM	24	75	48^{H}	6^{H}	NS	0.15
6	Carpenter *et al.* (2001)	HMDM	24	200	38^{LDH}, $\sim 40^{H}$	15^{LDH}, $\sim 23^{H}$	–	likely 3^{x}
6	Carpenter *et al.* (2001)	HMDM	48	200	73^{LDH}, 55^{H}	15^{LDH}, 32^{H}	–	likely 3^{x}
7	Carpenter *et al.* (2003)	HMDM	48	200^{*}	67^{LDH}	47^{LDH}	–	likely 3^{y}
8	Hardwick *et al.* (1996)	HMDM	24	100	$\sim 40^{H}$, $\sim 27^{LDH}$, $\sim 65^{MTT}$	$<20^{H}$, $<15^{LDH}$, $<27^{MTT}$	10, LPD FCS	3-4
8	Hardwick *et al.* (1996)	HMDM	24	200	$\sim 80^{H}$, $\sim 37^{LDH}$, $\sim 75^{MTT}$	$<20^{H}$, $<15^{LDH}$, $<27^{MTT}$	10, LPD FCS	3-4
9	Hardwick *et al.* (1999)	HMDM	24	200	86^{H}	32^{H}	–	3
10	Isa *et al.* (2011)	HMDM	24	40	30^{MTS}	NA^{MTS}	NS	NS
11	Gerry & Leake (2008)	HMDM	48	200^{***}	$\sim 37^{AV}$	$\sim 5^{AV}$	20, FBS	1
12	Gieseg *et al.* (2009)	HMDM	24	600^{a}	$\sim 55^{MTT}$	NA^{MTT}	10, HIHS	5
12	Gieseg *et al.* (2009)	HMDM	24	200^{b}	$\sim 0^{MTT}$	NA^{MTT}	10, HIHS	5
13	Gieseg *et al.* (2010a)	HMDM	24	200^{b}	$\sim 50^{MTT}$	NA^{MTT}	10, HIHS	5
14	Marchant *et al.* (1995)	HMDM	24	200^{**}	$\sim 80^{H}$	23^{H}	10, LPD FBS	3
15	Muller *et al.* (2001)	HMDM	24	50^{**}	$\sim 5^{AV}$, $\sim 4.5^{AV+PI}$, $\sim 24^{LDH}$	$\sim 1^{AV}$, $\sim 2^{AV+PI}$, $\sim 24^{LDH}$	10, LPD FCS	0.1–2
15	Muller *et al.* (2001)	HMDM	48	50^{**}	$\sim 6^{AV}$, $\sim 11^{AV+PI}$, $\sim 36^{LDH}$	$\sim 1^{AV}$, $\sim 2^{AV+PI}$, $\sim 24^{LDH}$	10, LPD FCS	0.1–2

^{H}: H^3 radioactive adenine release, ^{LDH}: Lactate dehydrogenase release, ^{AV}: Annexin V, $^{apo2.7}$: apoptosis marker, ^{PI}: Propidium iodide, ^{MTT}: MTT assay, ^{MTS}: assay

NS: not stated, NA: not applicable; * moderately oxLDL; ** strongly oxLDL; *** oxysterol rich oxLDL

$^{\#}$ apoptosis was prevented in the presence of serum

^{a}: 3 mg/mL cholesterol; ^{b}: 1 mg/mL cholesterol; ^{x}: reference to Hardwick *et al.* (1996); ^{y}: reference toCarpenter *et al.* (2001)

6.6.4 HMDM cell *resilience* not resistance to oxLDL

At least 8 HMDM preparations were identified to be resistant to oxLDL during the last stage of the project. The phenomenon was defined as displaying no significant metabolic loss after 24 hours of oxLDL exposure in the presence of 2% serum (fig. 6.16). The presence of serum ensured that HMDM were not pro-apoptotic. Absence of cell death was not due to incomplete LDL oxidation, as colour, REM and cholesterol oxidation confirmed that LDL molecule was fully oxidised to the standard set by the literature (figures 6.17). In addition, such oxLDL caused U937 cells to loose viability, showing its potency (sec. 6.5.2).

Thus, the investigation focused on HMDM cell response to oxLDL. Oxidative stress and damage were assessed in two case studies. Firstly, oxidative stress detection with DHE revealed that the "resistant" cells had a delayed onset of ROS flux compared to more "susceptible" cells. By the 48^{th} hour of incubation with oxLDL, oxidative stress was prominent in both resistant and susceptible cells. Similarly, oxidative damage (as GSH loss) in resistant cells also developed between 24 and 48 hours of incubation. This tightly correlated with the loss of metabolic capacity (figures 6.23, 6.24, 6.25). These results suggested that oxLDL toxicity to the "resistant cells" was delayed rather than completely abolished. Those cells were, therefore, resilient rather than resistant to oxLDL toxicity.

A few authors had used 48 hour exposure time to observe oxLDL toxicity (Asmis *et al.*, 2005; Baird *et al.*, 2005; Carpenter *et al.*, 2001, 2003; Wintergerst *et al.*, 2000). The reason for using the 48 hour time-frame over any other was not specified. Yuan *et al.* (1997), Wintergerst *et al.* (2000), Carpenter *et al.* (2001), Harris *et al.* (2006) and Isa *et al.* (2011) observed an increase in cell death with prolonged exposure (24 vs. 48 hours). Similarly, in this study, the extended incubation time allowed moderately "susceptible" HMDM cells (made so in the presence of low serum concentration) to increase viability loss from 24 to 48 hours (figures 6.24 and 6.25).

Serum supplementation played an important role in HMDM resilience to oxLDL. The full application of this knowledge requires understanding of the serum protective mechanisms. As discussed earlier, (sec. 6.4) uptake prevention and antioxidant capacity of serum albumin may be involved in this phenomenon of cellular resilience. Cellular density could also be a factor (sec. 6.4), however, cell density was not measured routinely on the performed experiments so no data is available to test the

hypothesis. It is likely, however, that cell–specific mechanisms are also important. As shown in figure 6.18, the two HMDM preparations grown and treated in the presence of the same serum batch and the same serum concentration, responded to oxLDL differently. Intracellular GSH levels have been shown to influence HOCl–mediated macrophage loss, where higher starting GSH levels conveyed protection against the oxidant (Yang *et al.*, 2012). Due to the oxidative nature of oxLDL–inflicted damage, similar mechanism may be involved in the HMDM cell resilience to oxLDL. This could be pursued in further study, especially if the starting intracellular GSH levels are pre-determined by external stimuli or genetic background. Two enzymes in the GSH synthesis have been reported to influence the cellular GSH status. The first and rate limiting step in GSH synthesis is catalysed by γ-glutamate cysteine ligase (GCL) composed of catalytic (GCLC) and modifier (GCLM) subunits (Nichenametla *et al.*, 2008). There is known genetic variation in the promoter region of both GCLC and GCLM that appears to influence the inducibility of these genes and, hence, the expression of the encoded proteins (Nichenametla *et al.*, 2008). The variation in protein function may, in turn, determine the variability of GSH content between donors. The second step in GSH synthesis is catalysed by glutathione synthetase. A correlation between the glutathione synthetase activity and the level of glutathione in cultured fibroblasts was reported (Konrad *et al.* (1972) cited in Njälsson & Norgren (2005)).

Another source of resilience may be the antioxidant enzymes within macrophage cells. Manganese SOD (MnSOD), heme oxygenase-1 have been shown to respond to oxygen tension, and inflammatory cytokine regulation (Lakari *et al.*, 2001; Miao & Clair, 2009). Moreover, MnSOD genetic polymorphism have been shown to affect susceptibility to apoptosis and correlate with the occurrence of myocardial infarction (Fujimoto *et al.*, 2010). The presence of alanine instead of valine in the targeting peptide for human MnSOD cause an increase in enzyme activity due to more effective targeting of protein to mitochondria, which led to higher protection against oxLDL–induced apoptosis. The alanine allele was also found to reduce the risk of coronary artery disease and acute myocardial infarction (Fujimoto *et al.*, 2010). Moreover, macrophages within the plaques have been show to display differential MPO activity with both MPO-positive and MPO-negative macrophages being detected (Sugiyama *et al.*, 2001). Thus, a range of oxidant and antioxidant enzymatic expression could contribute to macrophage resilience to oxLDL. The understanding of these processes may provide prognostic value, if the mechanisms of HMDM resilience to oxLDL toxicity are, in part, genetic.

Another distinguishing factor may be macrophage cell heterogeneity. M2 macrophage subtypes show higher sensitivity to oxLDL *in vitro*, whereas M1 macrophages are more resistant (Isa *et al.*, 2011). M2 macrophage are thought to be responsible for anti-inflammatory and wound healing processes, while M1–polarised state predominantly displays pro-inflammatory characteristics. Thus if the cultures of HMDM cells were heterogeneous due to unknown serum components, some cells would have been more resilient than others. In the future, it would be beneficial to characterise cultured HMDM cell cultures with subtype-specific markers.

6.7 Summary

Experimental conditions have been found to heavily affect the overall level of oxLDL toxicity to HMDM cells. Extracellular serum inhibited oxLDL toxicity, conveying resilience to HMDM cells. This effect followed saturation kinetics and was largely dependant on the protein component of serum. Cell death was also inhibited by increased HMDM and U937 cell density, although the present study did not investigate the actual mechanism(s) of this phenomenon. It is likely that cell density was one of the factors behind the variability in oxLDL–driven HMDM cell death. The results obtained in this section provide insight into the mechanisms governing cellular interaction *in vitro*, but they could not be used to predict the relative toxicity between published studies. Nonetheless, these results indicate the direction in which cell culture conditions could be optimised in order to improve the consistency of oxLDL–mediated cell death response in HMDM culture.

HMDM cell resistance was a recurrent phenomenon. Such cells had a delayed onset of oxidative flux yet they too underwent oxidative damage and lost metabolic activity when exposed to oxLDL for a longer period of time. Hence, these HMDM cells were resilient rather than resistant to oxLDL. Inter-batch variation among the resilient/susceptible cells could not be explained by serum or cellular density alone. Thus, future work could focus on the intracellular mechanisms of protection, such as GSH, to provide an answer to the issue of variable cytotoxicity.

6. HMDM CELL CULTURE METHOD DEVELOPMENT AND TROUBLESHOOTING

7

General discussion, conclusions and future work

Primate macrophages produce 7,8-dihydroneopterin (7,8-NP) upon inflammatory stimulation. This thesis argues that in an atherosclerotic plaque, where macrophages are exposed to high levels of toxic oxidised lipoproteins, 7,8-NP could provide antioxidant protection against high intracellular oxidative stress associated with acute cell death. 7,8-NP could also modulate accumulation and processing of the modified lipids in lipid–loaded foam cells, thus potentially alleviating atherosclerotic burden.

7.1 Mechanisms of 7,8-NP–mediated protection: ROS scavenging vs. oxLDL processing

The research set out to investigate how 7,8-dihydroneopterin protects macrophage cells from acute oxLDL toxicity. We recently reported that 7,8-NP was able to protect HMDM cells from oxLDL toxicity and oxidative damage to glutathione (GSH). We demonstrated that 7,8-NP both inhibited the ROS generation and partially prevented DiI–labelled oxLDL uptake (Gieseg *et al.*, 2010a). However, the relative contribution of these processes was unclear. Therefore, two lines of evidence were pursued: the antioxidant capacity of intracellular 7,8-NP and its effect on oxLDL internalisation. The initial hypothesis stated that both mechanisms equally contributed to the 7,8-NP–mediated protection.

Acute oxLDL toxicity was defined as HMDM cell viability loss after 24 hour exposure to the LC_{50} levels of Cu-oxidised LDL. LC_{50} was established to be in the

range of 2–3 mg/mL oxLDL. Initially, the nature of the cellular response was investigated. As expected, oxLDL caused a concentration and time–dependant loss of cell viability in HMDM cells (figures 3.1 and 3.2). The majority of the damage took place during the first 12 hours of exposure (fig. 4.2). Furthermore, the exposure to toxic concentration of oxLDL for 6 hours with subsequent incubation in the absence of extracellular oxLDL was sufficient to irreversibly affect cellular metabolism (fig. 3.6). Neither concentrations nor time of exposure of macrophages to oxidised lipoproteins in atherosclerotic plaques are known. The evidence of cellular death in plaques favours the school of thought that the concentration of toxic agents is sufficient to cause cell death in such conditions (Ball *et al.*, 1995; Lusis, 2000; Moore & Tabas, 2011). The data presented here suggests that even a short-term exposure to the toxic concentration of oxLDL is sufficient to cause irreversible damage to cellular metabolism. Such quick inactivation of cell metabolism may explain the observed lack of mobility in macrophages that had been exposed to oxLDL. Previously oxLDL had been show to inhibit macrophage migration (Quinn *et al.*, 1987), induce actin depolymerisation and cell spreading (Park *et al.*, 2009) thus preventing the cells from exiting the atherosclerotic lesion. Rapid metabolic damage could also play a role in this process, perpetuating the disease, as monocytes/macrophages infiltrate the lesion attracted by cytokines and endothelial cell factors (Hansson & Hermansson, 2011; Ross, 1993).

The toxicity of oxLDL to HMDM cells was characterised by a rapid generation of ROS (as measured by DHE fluorescent probe) (fig. 3.3). Intracellular ROS levels were highly elevated at 3 hours, peaked at 12 hours and started declining in the next 12–24 hours. The rate of ROS production was highest in the first 6 hours. This coincided with the loss of intracellular GSH that occurred during the first 6 hours and reached maximum 9 hours after oxLDL exposure (fig. 3.5). The timing of events is significant as it permits the examination of the inter-relationship of the cellular processes that underpin pathology. ROS flux coincided with GSH loss indicating oxidative stress and damage within the first 6 hours of exposure and more generally in the first half of the 24 hour incubation. Meanwhile, 7,8-NP provided an almost complete protection during this time, which declined over the following 12 hours (fig. 4.2). The same trend was observed by Gieseg *et al.* (2010a) with 7,8-NP–mediated protection of intracellular GSH. This suggested that the protective mechanism of 7,8-NP was particularly suited to counter-balance the type of processes that caused early toxicity to HMDM cells.

The ability of 7,8-NP to prevent cell death and oxidation of cellular molecules has been documented (Duggan *et al.*, 2002; Gieseg *et al.*, 2001b). The authors reported a 10 to 20% protection against Fe^{++}, H_2O_2, HOCl and peroxyl radical–induced cell death in U937 cells, as well as inhibition of thiol loss and hydroperoxide, TBARS and dityrosine formation (Duggan *et al.*, 2002; Gieseg *et al.*, 2001b). Based on the chemistry, 7,8-NP was likely to react with cellular ROS, reducing the oxidative burden and its damaging effects. This hypothesis was supported by the data. 7,8–NP more than halved intracellular ROS produced by the HMDM cells in response to oxLDL (fig. 4.9). 7,8-NP was most effective at 3 and 6 hours of oxLDL exposure, which further supported the idea of an early oxidative stress. Moreover, 7,8-NP was oxidised into neopterin within HMDM cells treated with oxLDL (fig. 4.10) providing further evidence that it was reacting with intracellular oxidants. Indirect evidence suggested that 7,8-NP was also oxidised into 7,8-dihydroxanthopterin. The final levels of 7,8-NP in the media between control and oxLDL treatment for 24 hours showed a net loss of approximately 20 μM indicating potential oxidation into non-neopterin product (fig. 4.13). Thus, 7,8-NP was scavenging ROS generated by HMDM cells.

Other antioxidant compounds such as probucol, probucol analogs and vitamin E have also been shown to inhibit cellular death *in vitro* and inhibited the progression of atherosclerosis in the animal models, suggesting that ROS is important to the disease pathology (Steinberg, 2009). Interestingly, both vitamin E and probucol demonstrated additional effects: down-regulation of CD36 receptor (vitamin E: Ozer *et al.* (2006); Ricciarelli *et al.* (2000)) and acceleration of cholesterol efflux (probucol: (Zhong *et al.*, 2010)), which were also characteristic of 7,8-NP.

7,8-NP caused a 40% decrease in total 7-ketocholesterol accumulation, which was used as an oxLDL uptake marker (figures 5.4 and 5.5). This was primarily achieved through lowering the intracellular 7KC esters, which suggests a link to the foam cell formation (Brown *et al.*, 1979). In addition, 7,8-NP down-regulated CD36 scavenger receptor protein and mRNA levels by 40% (figures 5.6, 5.7 and 5.9). CD36 has been implicated in oxLDL signalling (Silverstein *et al.*, 2010), foam cell formation (Rahaman *et al.*, 2006) and cell death (Higashi *et al.*, 2005; Wintergerst *et al.*, 2000). In order to evaluate the role these processes play in 7,8-NP–mediated protection in the present study, their time-frame was considered. Contrary to the antioxidant activity of 7,8-NP, the down-regulation of oxLDL uptake, or what was later hypothesised as

effect on oxLDL processing, was a late effect. The onset of the regulation of total 7KC levels did not commence until the start of the esterification process which took place between 9 and 12 hours (figures 5.1 and 5.4). The down-regulation of CD36 protein also occurred no earlier than 12 hours into the incubation and was highly significant at 24 hours (fig. 5.7). mRNA down-regulation was measured at 24 hours (fig. 5.9). The timing of these processes suggested their importance in longer term foam cell formation and homoeostasis rather than acute cell death. Moreover, an experiment that investigated the effect of 7,8-NP pre-incubation on oxLDL toxicity during and after the 6 hour oxLDL exposure in the absence of 7,8-NP did not show any protection against cell death (fig. 5.14). Neither was oxLDL uptake inhibited by the lower CD36 availability due to pre-incubation (fig. 5.16). A minor protective effect of intracellular GSH levels was observed (fig. 5.15), suggesting oxidative flux was slightly reduced in the presence of down-regulated CD36, yet the effect did not transfer onto cell survival. Although the role of CD36 in oxLDL–mediated cell death is established (Higashi *et al.*, 2005; Rusiñol *et al.*, 2000; Wintergerst *et al.*, 2000), other SR receptors such as SR-A were also shown to facilitate cell death (DeVries-Seimon *et al.*, 2005). SR-A also mediated oxLDL uptake (Wintergerst *et al.*, 2000), which may explain the lack of effect in the presence of partially down-regulated CD36. Differences in cell type and methodology could limit the ability to make direct comparison between the studies.

Therefore, the main conclusion of this work is that 7,8-NP primarily acts as an antioxidant and ROS scavenger when protecting HMDM cells from acute oxLDL toxicity. Its effect on oxLDL processing may have a secondary effect in this cell death model. The latter process might be implicated in chronic cell death and foam cell formation (discussed below). Thus, in an atherosclerosis plaque, 7,8-NP might act as an indigenous antioxidant providing the initial protection against oxidative stress mounted by the cells in response to oxidised lipid. This action is dependant on sufficient intracellular 7,8-NP concentrations, which is still a matter of debate. However, an empirical calculation of provisional plasma 7,8-NP concentration in chapter 4 showed that our current knowledge of its production levels and mechanisms is unable to account for the elevated levels observed in disease pathology. Therefore, it may be possible that 7,8-NP concentrations in the vicinity of cells are sufficient to scavenge the generated oxidants.

7.2 Source and types of ROS during oxLDL toxicity to HMDM cells

While addressing the primary aim of the research project, the present study identified three areas that are highlighted for future investigation. These are the contribution of NADPH oxidase to oxLDL toxicity, the role of MPO–produced HOCl in oxLDL–mediated damage and the effect of 7,8-NP on the reverse cholesterol transport in macrophage foam cells.

NADPH oxidase as a source of ROS

NADPH oxidase was suspected to be the source of superoxide due to the exponential rise in DHE–reactive ROS in the first 6 hours of oxLDL treatment (fig. 3.3). NOX activation by oxLDL has been reported in Sukhanov *et al.* (2006) and Park *et al.* (2009). The NOX activity was investigated with the use of apocynin, a NOX inhibitor, and the chemical properties of 7,8-NP oxidation reaction. Approximately 50% of 7,8-NP oxidation to neopterin was blocked by the addition of apocynin (fig. 4.14), suggesting that a similar proportion of oxLDL–triggered ROS is produced by the cellular NOX. Despite this, cellular viability was not protected in the presence of apocynin (figures 4.16, 4.18 and 4.19). Lack of protection suggests potential involvement of other sources of ROS and oxidative damage upon oxLDL exposure, such as mitochondrial enzymes. This might have implications for pharmacological intervention (Paterniti *et al.*, 2010; Wingler *et al.*, 2011). If pro-atherogenic cellular ROS was targeted for therapy, a combined inhibition/scavenging of these ROS generating systems should be considered. The action of 7,8-NP was superior than that of apocynin at protecting cells, potentially due to its ability to scavenge oxidants from a variety of sources. This research proposed that NOX–mediated ROS production upon oxLDL treatment on the basis of apocynin inhibition studies. Reports have been made about the unspecific action of apocynin in NOX inhibition (Altenhöfer *et al.*, 2012; Wind *et al.*, 2010). Recently, a VAS family of more specific NOX inhibitors has emerged (Altenhöfer *et al.*, 2012). Therefore, it may be valuable to confirm the NOX involvement in ROS production and subsequent cellular death in oxLDL–exposed HMDM cells with these small molecule inhibitors.

HOCl as a mediator of oxidative damage

This study used chemical properties of 7,8-NP oxidation reaction to gain insight into the mechanisms of ROS production in cells exposed to oxLDL. HOCl is the only physiological oxidant known to produce neopterin from 7,8-NP as the primary reaction product (Widner *et al.*, 2000). Therefore, oxidation of 7,8-NP into neopterin in oxLDL–treated HMDM cells suggests an HOCl–mediated oxidative stress within these cells. HMDM cells cultured in the presence of GM-CSF are known to express active MPO which converts H_2O_2 and Cl^- into HOCl (Sugiyama *et al.*, 2001). A proposed route for ROS flux based on the use of neopterin as an ROS probe in this study is: NOX activation $\rightarrow O_2^{\bullet-} \rightarrow H_2O_2 \rightarrow$ HOCl (MPO–catalysed). This system could be explored further to obtain a direct evidence of HOCl, active MPO and quantify its activity in oxLDL–treated macrophages.

7.3 The effect of 7,8-NP on oxLDL processing: potential for cholesterol ester efflux regulation

As discussed above, 7,8-NP was found to have an effect on the accumulation of intracellular oxLDL as measured by total 7-ketocholesterol. Based on the data obtained through this study it was hypothesised that 7,8-NP may have affected the reverse cholesterol transport of oxLDL. This was based on three lines of evidence. Firstly, the down–regulation of total 7KC and, therefore, oxLDL in cells was found to coincide with the esterified portion of intracellular 7KC and commence after the esterification process started in control cells (figures 5.1 and 5.4). Cholesterol ester accumulation is a hallmark of foam cell formation and oxLDL is known to inhibit cholesterol efflux (Gelissen *et al.*, 1996; Jessup & Kritharides, 2000). Secondly, down-regulation of the CD36 receptor for 24 hours with subsequent oxLDL treatment for 6 hours did not lead to the reduction of intracellular 7KC and, thus, oxLDL uptake (figures 5.13 and 5.16). This could be explained by the observation that during the initial 6 hours of exposure, all incoming 7KC was hydrolysed and remained as free 7KC. Free cholesterol accumulation was the first part of oxLDL oxysterol trafficking (Brown *et al.*, 1979; Zanotti *et al.*, 2012) and was not affected by 7,8-NP. Thirdly, the down-regulation depended on the presence of extracellular serum, hinting at reverse cholesterol trafficking and efflux (fig. 5.17). A minor possibility of serum-less environment adversely affecting cellular processes is acknowledged. Ten percent serum supplemented medium contained HDL and ApoA-1 as well as serum albumin as cholesterol/7KC

acceptors (Amit, 2008; Han *et al.*, 1997; Johnson *et al.*, 1991). Further research is required to validate this hypothesis. Focusing on the enzymes and proteins that are involved in cholesterol esterification (ACAT) and hydrolysis (neutral hydrolase) and efflux (ABCA1 and ABCG1 transporters) (Zanotti *et al.*, 2012) is suggested. The research demonstrates that *in vivo* 7,8-NP may be involved in macrophage cholesterol ester homeostasis and foam cell development. Foam cell formation and death in the atherosclerotic plaque is associated with the development of plaque necrotic core (Hegyi *et al.*, 1996), and can promote its instability (Nishi *et al.*, 2002), which often leads to thromobosis (Rittersma, 2005). The relevance of 7,8-NP–mediated action on atherosclerotic plaque progression and morphology is unclear at present, as the concentration of 7,8-NP, time-frame and magnitude of the effect need to be considered. Since this contribution may be both positive and negative it is valuable to understand the underlying mechanisms.

7.4 Conclusion

This thesis set out to explore the mechanism of 7,8-dihydroneopterin–mediated protection of HMDM from acute oxLDL–mediated cell death. The results obtained suggest that antioxidant capacity of 7,8-NP in these cells is the most probable mechanism for the observed protection and may be so *in vivo*. Rapid rise of intracellular ROS levels, its effective scavenging by 7,8-NP and the resulting oxidation of 7,8-NP to neopterin all support this claim. This work showed that ROS production is the initial response of HMDM to toxic concentration of oxLDL and the majority of damage to cellular viability takes place during the first 6-12 hours of incubation.

7,8-NP was also found to decrease intracellular 7-ketocholesterol ester accumulation (as a proxy of oxLDL uptake) and down–regulate CD36 protein and mRNA expression in HMDM cells. These effects were delayed until after the 12^{th} hour of incubation, thus emerging as less probable protective mechanisms during acute oxLDL toxicity. However, 7,8-NP–mediated regulation of CD36 receptor and oxLDL uptake might be relevant during foam cell formation and chronic oxLDL–mediated cellular death. This work also opened up new exciting areas of 7,8-NP research, including its application in oxidative stress monitoring and effect on reverse cholesterol transport in foam cells.

Bibliography

Abumrad, N.N., Harmon, C.C. & Ibrahimi, A.A. (1998). Membrane transport of long-chain fatty acids: evidence for a facilitated process. *Journal of Lipid Research*, 39, 2309–2318.

Adachi, T., Naruko, T., Itoh, A., Komatsu, R., Abe, Y., Shirai, N., Yamashita, H., Ehara, S., Nakagawa, M., Kitabayashi, C., Ikura, Y., Ohsawa, M., Yoshiyama, M., Haze, K. & Ueda, M. (2007). Neopterin is associated with plaque inflammation and destabilisation in human coronary atherosclerotic lesions. *Heart (British Cardiac Society)*, 93, 1537–1541.

Aikawa, M., Sugiyama, S., Hill, C., Voglic, S.J., Rabkin, E., Fukumoto, Y., Schoen, F.J., Witztum, J.L. & Libby, P. (2002). Lipid lowering reduces oxidative stress and endothelial cell activation in rabbit atheroma. *Circulation*, 106, 1390–1396.

Al Gadban, M.M., Smith, K.J., Soodavar, F., Piansay, C., Chassereau, C., Twal, W.O., Klein, R.L., Virella, G., Lopes-Virella, M.F., Hammad, S.M. & Kanellopoulos, J. (2010). Differential trafficking of oxidized LDL and oxidized LDL immune complexes in macrophages: Impact on oxidative stress. *PLoS ONE*, 5, e12534.

Alessio, M., De Monte, L., Scirea, A., Gruarin, P., Tandon, N.N. & Sitia, R. (1996). Synthesis, processing, and intracellular transport of CD36 during monocytic differentiation. *The Journal of Biological Chemistry*, 271, 1770–1775.

Altenhöfer, S., Kleikers, P.W.M., Radermacher, K.A., Scheurer, P., Rob Hermans, J.J., Schiffers, P., Ho, H., Wingler, K. & Schmidt, H.H.H.W. (2012). The NOX toolbox: validating the role of NADPH oxidases in physiology and disease. *Cellular and Molecular Life Sciences*, 69, 2327–2343.

Amberger, A., Maczek, C., Jürgens, G., Michaelis, D., Schett, G., Trieb, K., Eberl, T., Jindal, S., Xu, Q. & Wick, G. (1997). Co-expression of ICAM-1, VCAM-1, ELAM-1 and Hsp60 in human arterial and venous endothelial cells in response to cytokines and oxidized low-density lipoproteins. *Cell Stress & Chaperones*, 2, 94–103.

Amit, Z. (2008). *A model of complex plaque formation: 7,8-Dihydroneopterin protects human monocyte-derived macrophages from oxidised low density lipoprotein-induced death*. Ph.D. thesis, University of Canterbury, Christchurch, New Zealand.

Andersen, C.L., Jensen, J.L. & Ørntoft, T.F. (2004). Normalization of real-time quantitative reverse transcription-PCR data: a model-based variance estimation approach to identify genes suited for normalization, applied to bladder and colon cancer data sets. *Cancer Research*, 64, 5245–5250.

Anderson, M.E. (1998). Glutathione: an overview of biosynthesis and modulation. *Chemo Biological Interactions*, 111-112, 1–14.

Andert, S.E., Griesmacher, A., Zuckermann, A. & Müller, M.M. (1992). Neopterin release from human endothelial cells is triggered by interferon-gamma. *Clinical and Experimental Immunology*, 88, 555–558.

Asch, A.S., Barnwell, J., Silverstein, R.L. & Nachman, R.L. (1987). Isolation of the thrombospondin membrane receptor. *The Journal of Clinical Investigation*, 79, 1054–1061.

Ashkenazi, A. & Dixit, V.M. (1998). Death receptors: signaling and modulation. *Science*, 281, 1305–1308.

Ashraf, M.Z. & Gupta, N. (2011). Scavenger receptors: Implications in atherothrombotic disorders. *The International Journal of Biochemistry & Cell Biology*, 43, 697–700.

Asmis, R. & Begley, J.G. (2003). Oxidized LDL promotes peroxide-mediated mitochondrial dysfunction and cell death in human macrophages: a caspase-3-independent pathway. *Circulation Research*, 92, 20–29.

Asmis, R. & Jelk, J. (2000a). Large variations in human foam cell formation in individuals: a fully autologous in vitro assay based on the quantitative analysis of cellular neutral lipids. *Atherosclerosis*, 148, 243–253.

Asmis, R. & Jelk, J. (2000b). Vitamin E supplementation of human macrophages prevents neither foam cell formation nor increased susceptibility of foam cells to lysis by oxidized LDL. *Arteriosclerosis Thrombosis and Vascular Biology*, 20, 2078–2086.

Asmis, R. & Wintergerst, E.S. (1998). Dehydroascorbic acid prevents apoptosis induced by oxidized low-density lipoprotein in human monocyte-derived macrophages. *The FEBS Journal*, 255, 147–155.

Asmis, R., Begley, J.G., Jelk, J. & Everson, W.V. (2005). Lipoprotein aggregation protects human monocyte-derived macrophages from OxLDL-induced cytotoxicity. *The Journal of Lipid Research*, 46, 1124–1132.

Assari, T. (2006). Chronic Granulomatous Disease; fundamental stages in our understanding of CGD. *Medical Immunology*, 5, 4.

Aviram, M., Rosenblat, M., Etzioni, A. & Levy, R. (1996). Activation of NADPH oxidase is required for macrophage-mediated oxidation of low-density lipoprotein. *Metabolism*, 45, 1069–1079.

Bae, Y.S., Lee, J.H., Choi, S.H., Kim, S., Almazan, F., Witztum, J.L. & Miller, Y.I. (2009). Macrophages generate reactive oxygen species in response to minimally oxidized low-density lipoprotein: toll-like receptor 4- and spleen tyrosine kinase-dependent activation of NADPH oxidase 2. *Circulation Research*, 104, 210–8, 21p following 218.

Baird, S.K., Hampton, M.B. & Gieseg, S.P. (2004). Oxidized LDL triggers phosphatidylserine exposure in human monocyte cell lines by both caspase-dependent and -independent mechanisms. *FEBS Letters*, 578, 169–174.

Baird, S.K., Reid, L., Hampton, M.B. & Gieseg, S.P. (2005). OxLDL induced cell death is inhibited by the macrophage synthesised pterin, 7,8-dihydroneopterin, in U937 cells but not THP-1 cells. *Biochimica et Biophysica Acta*, 1745, 361–369.

Ball, R.Y., Stowers, E.C., Burton, J.H., Cary, N.R., Skepper, J.N. & Mitchinson, M.J. (1995). Evidence that the death of macrophage foam cells contributes to the lipid core of atheroma. *Atherosclerosis*, 114, 45–54.

Baoutina, A. (2000). Macrophages can decrease the level of cholesteryl ester hydroperoxides in low density lipoprotein. *Journal of Biological Chemistry*, 275, 1635–1644.

Baoutina, A. & Dean, R. (2001). Antioxidant properties of macrophages toward low-density lipoprotein. *Trends in Cardiovascular Medicine*, 11.

BIBLIOGRAPHY

Barrett, K.E., Barman, S.M., Boitano, S. & Brooks, H. (2010). *Ganong's review of medical physiology*. McGraw-Hill Medical, 23rd edn.

Bea, F. (2003). Induction of glutathione synthesis in macrophages by oxidized low-density lipoproteins is mediated by consensus antioxidant response elements. *Circulation Research*, 92, 386–393.

Beal, P.R., Yao, S.Y.M., Baldwin, S.A., Young, J.D., King, A.E. & Cass, C.E. (2004). The equilibrative nucleoside transporter family, SLC29. *Pflugers Archiv European Journal of Physiology*, 447, 735–743.

Beckman, J. & Koppenol, W. (1996). Nitric oxide, superoxide, and peroxynitrite: the good, the bad, and ugly. *American Journal of Physiology*, 271, 1424–1437.

Bedard, K. & Krause, K.H. (2007). The NOX family of ROS-generating NADPH oxidases: physiology and pathophysiology. *Physiological Reviews*, 87, 245–313.

Bennett, S., Por, S.B., Stanley, E.R. & Breit, S.N. (1992). Monocyte proliferation in a cytokine-free, serum-free system. *Journal of Immunological Methods*, 153, 201–212.

Benov, L., Sztejnberg, L. & Fridovich, I. (1998). Critical evaluation of the use of hydroethidine as a measure of superoxide anion radical. *Free Radical Biology and Medicine*, 25, 826–831.

Berdowska, A. & Zwirska-Korczala, K. (2001). Neopterin measurement in clinical diagnosis. *Journal of Clinical Pharmacy and Therapeutics*, 26, 319–329.

Berliner, J.A. & Heinecke, J.W. (1996). The role of oxidized lipoproteins in atherogenesis. *Free Radical Biology and Medicine*, 20, 707–727.

Bernas, T. & Dobrucki, J. (2002). Mitochondrial and nonmitochondrial reduction of MTT: interaction of MTT with TMRE, JC-1, and NAO mitochondrial fluorescent probes. *Cytometry*, 47, 236–242.

Berridge, M., Tan, A., McCoy, K. & Wang, R. (1996). The biochemical and cellular basis of cell proliferation assays that use tetrazolium salts. *Biochemica*, 4, 15–20.

Bindokas, V.P., Jordán, J., Lee, C.C. & Miller, R.J. (1996). Superoxide production in rat hippocampal neurons: selective imaging with hydroethidine. *Journal of Neuroscience*, 16, 1324–1336.

Biochrom AG (2010). Latest findings on heat inactivation of sera.

Bird, D.A., Gillotte, K.L., Hörkkö, S., Friedman, P., Dennis, E.A., Witztum, J.L. & Steinberg, D. (1999). Receptors for oxidized low-density lipoprotein on elicited mouse peritoneal macrophages can recognize both the modified lipid moieties and the modified protein moieties: implications with respect to macrophage recognition of apoptotic cells. *Proceedings of the National Academy of Sciences of the United States of America*, 96, 6347–6352.

Bjorkerud, B. & Bjorkerud, S. (1996a). Contrary effects of lightly and strongly oxidized LDL with potent promotion of growth versus apoptosis on arterial smooth muscle cells, macrophages, and fibroblasts. *Arteriosclerosis Thrombosis and Vascular Biology*, 16, 416–424.

Bjorkerud, S. & Bjorkerud, B. (1996b). Apoptosis is abundant in human atherosclerotic lesions, especially in inflammatory cells (macrophages and T cells), and may contribute to the accumulation of gruel and plaque instability. *American Journal of Pathology*, 149, 367–380.

Bostrom, P. (2006). Hypoxia converts human macrophages into triglyceride-loaded foam cells. *Arteriosclerosis Thrombosis and Vascular Biology*, 26, 1871–1876.

Boullier, A., Bird, D.A., Chang, M.K., Dennis, E.A., Friedman, P., Gillotte-Taylor, K., Hörkkö, S., Palinski, W., Quehenberger, O., Shaw, P., Steinberg, D., Terpstra, V. & Witztum, J.L. (2001). Scavenger receptors, oxidized LDL, and atherosclerosis. *Annals of the New York Academy of Sciences*, 947, 214–223.

Bourdon, E. & Blache, D. (2001). The importance of proteins in defense against oxidation. *Antioxidants & Redox Signaling*, 3, 293–311.

Boyle, J.J. (2005). Macrophage activation in atherosclerosis: pathogenesis and pharmacology of plaque rupture. *Current Vascular Pharmacology*, 3, 63–68.

Brandes, R.P., Weissmann, N. & Schröder, K. (2010). NADPH oxidases in cardiovascular disease. *Free Radical Biology and Medicine*, 49, 687–706.

Bratslavska, O., Platace, D., Miklasevics, E., Fuchs, D. & Martinsons, A. (2007). Influence of neopterin and 7,8-dihydroneopterin on the replication of Coxsackie type B5 and influenza A viruses. *Medical Microbiology and Immunology*, 196, 23–29.

Brown, A.J., Leong, S.L., Dean, R.T. & Jessup, W. (1997). 7-Hydroperoxycholesterol and its products in oxidized low density lipoprotein and human atherosclerotic plaque. *Journal of Lipid Research*, 38, 1730–1745.

Brown, A.J., Mander, E.L., Gelissen, I.C., Kritharides, L., Dean, R.T. & Jessup, W. (2000). Cholesterol and oxysterol metabolism and subcellular distribution in macrophage foam cells: accumulation of oxidized esters in lysosomes. *The Journal of Lipid Research*, 41, 226–237.

Brown, A.J.A., Dean, R.T.R. & Jessup, W.W. (1996). Free and esterified oxysterol: formation during copper-oxidation of low density lipoprotein and uptake by macrophages. *Journal of Lipid Research*, 37, 320–335.

Brown, M.S., Goldstein, J.L., Krieger, M., Ho, Y.K. & Anderson, R.G. (1979). Reversible accumulation of cholesteryl esters in macrophages incubated with acetylated lipoproteins. *Journal of Cell Biology*, 82, 597–613.

Buettner, G.R.G. (1993). The pecking order of free radicals and antioxidants: lipid peroxidation, alpha-tocopherol, and ascorbate. *Archives of Biochemistry and Biophysics*, 300, 535–543.

Carmody, R.J. & Cotter, T.G. (2001). Signalling apoptosis: a radical approach. *Redox Report : Communications in Free Radical Research*, 6, 77–90.

Carpenter, K.L., Taylor, S.E., van der Veen, C., Williamson, B.K., Ballantine, J.A. & Mitchinson, M.J. (1995). Lipids and oxidised lipids in human atherosclerotic lesions at different stages of development. *Biochimica et Biophysica Acta*, 1256, 141–150.

Carpenter, K.L., Dennis, I., Challis, I., Osborn, D., Macphee, C., Leake, D.S., Arends, M. & Mitchinson, M.J. (2001). Inhibition of lipoprotein-associated phospholipase A2 diminishes the death-inducing effects of oxidised LDL on human monocyte-macrophages. *FEBS Letters*, 505, 357–363.

Carpenter, K.L.H., Challis, I.R. & Arends, M.J. (2003). Mildly oxidised LDL induces more macrophage death than moderately oxidised LDL: roles of peroxidation, lipoprotein-associated phospholipase A2 and PPAR. *FEBS Letters*, 553, 145–150.

BIBLIOGRAPHY

Carvalho, M.D.T., Vendrame, C.M.V., Ketelhuth, D.F.J., Yamashiro-Kanashiro, E.H., Goto, H. & Gidlund, M. (2010). High-density lipoprotein inhibits the uptake of modified low- density lipoprotein and the expression of CD36 and FcgammaRI. *Journal of Atherosclerosis and Thrombosis*, 17, 844–857.

Chen, A. (2012). *Role of intracellular oxidant release in oxidised low density lipoprotein-induced U937 cell death*. Master's thesis, University of Canterbury, Christchurch, New Zealand.

Cho, S., Hazama, M., Urata, Y., Goto, S., Horiuchi, S., Sumikawa, K. & Kondo, T. (1999). Protective role of glutathione synthesis in response to oxidized low density lipoprotein in human vascular endothelial cells. *Free Radical Biology and Medicine*, 26, 589–602.

Chroni, A., Nieland, T.J.F., Kypreos, K.E., Krieger, M. & Zannis, V.I. (2005). SR-BI mediates cholesterol efflux via its interactions with lipid-bound ApoE. Structural mutations in SR-BI diminish cholesterol efflux. *Biochemistry*, 44, 13132–13143.

Chung, B.H., Wilkinson, T., Geer, J.C. & Segrest, J.P. (1980). Preparative and quantitative isolation of plasma lipoproteins: rapid, single discontinuous density gradient ultracentrifugation in a vertical rotor. *The Journal of Lipid Research*, 21, 284–291.

Collins, R.F., Touret, N., Kuwata, H., Tandon, N.N., Grinstein, S. & Trimble, W.S. (2009). Uptake of oxidized low density lipoprotein by CD36 occurs by an actin-dependent pathway distinct from macropinocytosis. *The Journal of Biological Chemistry*, 284, 30288–30297.

Collot-Teixeira, S., Martin, J., McDermott-Roe, C., Poston, R. & McGregor, J.L. (2007). CD36 and macrophages in atherosclerosis. *Cardiovascular Research*, 75, 468–477.

Collot-Teixeira, S., Barbatis, C., Bultelle, F., Koutouzis, M., Pasterkamp, G., Fraser, P., Kyriakides, Z.S., Poston, R.N., Ristagno, A., Mcgregor, L., Boulanger, C.M., Leseche, G. & Mcgregor, J.L. (2008). CD36 is significantly correlated with adipophilin in human carotid lesions and inversely correlated with plasma ApoAI. *Journal of Biomedicine and Biotechnology*, 2008, 813236.

Cotgreave, I. & Moldeus, P. (1986). Methodologies for the application of monobromobimane to the simultaneous analysis of soluble and protein thiol components of biological systems. *Journal of Biochemical and Biophysical Methods*, 13, 231–249.

Cox, B.E., Griffin, E.E., Ullery, J.C. & Jerome, W.G. (2007). Effects of cellular cholesterol loading on macrophage foam cell lysosome acidification. *The Journal of Lipid Research*, 48, 1012–1021.

Dántola, M.L., Thomas, A.H., Braun, A.M., Oliveros, E. & Lorente, C. (2007). Singlet oxygen (O2(1Deltag)) quenching by dihydropterins. *The Journal of Physical Chemistry A*, 111, 4280–4288.

Dántola, M.L., Schuler, T.M., Denofrio, M.P., Vignoni, M., Capparelli, A.L., Lorente, C. & Thomas, A.H. (2008a). Reaction between 7,8-dihydropterins and hydrogen peroxide under physiological conditions. *Tetrahedron*, 64, 8692–8699.

Dántola, M.L., Vignoni, M., Capparelli, A.L., Lorente, C. & Thomas, A.H. (2008b). Stability of 7,8-dihydropterins in air-equilibrated aqueous solutions. *Helvetica Chimica Acta*, 91, 411–425.

de Lorenzo, F., Feher, M., Martin, J., Collot-Teixeira, S., Dotsenko, O. & McGregor, J.L. (2006). Statin therapy-evidence beyond lipid lowering contributing to plaque stability. *Current Medicinal Chemistry*, 13, 3385–3393.

De Meyer, G.R.Y. & Martinet, W. (2009). Autophagy in the cardiovascular system. *Biochimica et Biophysica Acta - Molecular Cell Research*, 1793, 1485–1495.

de Villiers, W.J. & Smart, E.J. (1999). Macrophage scavenger receptors and foam cell formation. *Journal of Leukocyte Biology*, 66, 740–746.

Deng, T., Xu, K., Zhang, L. & Zheng, X. (2008). Dynamic determination of Ox-LDL-induced oxidative/nitrosative stress in single macrophage by using fluorescent probes. *Cell Biology International*, 32, 8–8.

Denz, H., Fuchs, D., Hausen, A., Huber, H., Nachbaur, D., Reibnegger, G., Thaler, J., Werner, E.R. & Wachter, H. (1990). Value of urinary neopterin in the differential diagnosis of bacterial and viral infections. *Klinische Wochenschrift*, 68, 218–222.

DeVries-Seimon, T., Li, Y., Yao, P.M., Stone, E., Wang, Y., Davis, R.J., Flavell, R. & Tabas, I. (2005). Cholesterol-induced macrophage apoptosis requires ER stress pathways and engagement of the type A scavenger receptor. *The Journal of Cell Biology*, 171, 61–73.

Dornas, W.C., de TT Oliveira, T., Augusto, L.E.F. & Nagem, T.J. (2010). Experimental atherosclerosis in rabbits. *Arquivos Brasileiros de Cardiologia*, 95, 272–278.

Dröge, W. (2001). Free radicals in the physiological control of cell function. *Physiological Reviews*, 82, 47–95.

Duggan, S., Rait, C., Gebicki, J.M. & Gieseg, S.P. (2001). Inhibition of protein oxidation by the macrophage-synthesised antioxidant 7,8-dihydroneopterin. *Redox Report*, 6, 188–190.

Duggan, S., Rait, C., Platt, A. & Gieseg, S. (2002). Protein and thiol oxidation in cells exposed to peroxyl radicals is inhibited by the macrophage synthesised pterin 7,8-dihydroneopterin. *Biochimica et Biophysica Acta*, 1591, 139–145.

Edinger, A.L. & Thompson, C.B. (2004). Death by design: apoptosis, necrosis and autophagy. *Current Opinion in Cell Biology*, 16, 7–7.

Edwards, J.E. & Moore, R.A. (2003). Statins in hypercholesterolaemia: a dose-specific meta-analysis of lipid changes in randomised, double blind trials. *BMC Family Practice*, 4, 18–18.

Endemann, G., Stanton, L.W., Madden, K.S., Bryant, C.M., White, R.T. & Protter, A.A. (1993). CD36 is a receptor for oxidized low density lipoprotein. *Journal of Biological Chemistry*, 268, 11811–11816.

Enzinger, C., Wirleitner, B., Spöttl, N., Böck, G., Fuchs, D. & Baier-Bitterlich, G. (2002). Reduced pteridine derivatives induce apoptosis in PC12 cells. *Neurochemistry International*, 41, 71–78.

Ermak, N., Lacour, B., Goirand, F., Drüeke, T.B. & Vicca, S. (2010). Differential apoptotic pathways activated in response to Cu-induced or HOCl-induced LDL oxidation in U937 monocytic cell line. *Biochemical and Biophysical Research Communications*, 393, 783–787.

Esterbauer, H., Dieber-Rotheneder, M., Waeg, G., Striegl, G. & Jürgens, G. (1990). Biochemical, structural, and functional properties of oxidized low-density lipoprotein. *Chemical Research in Toxicology*, 3, 77–92.

Febbraio, M., Podrez, E.A., Smith, J.D., Hajjar, D.P., Hazen, S.L., Hoff, H.F., Sharma, K. & Silverstein, R.L. (2000). Targeted disruption of the class B scavenger receptor CD36 protects against atherosclerotic lesion development in mice. *The Journal of Clinical Investigation*, 105, 1049–1056.

BIBLIOGRAPHY

Febbraio, M., Hajjar, D.P. & Silverstein, R.L. (2001). CD36: a class B scavenger receptor involved in angiogenesis, atherosclerosis, inflammation, and lipid metabolism. *The Journal of Clinical Investigation*, 108, 785–791.

Fernandes, D.C., Wosniak, J., Pescatore, L.A., Bertoline, M.A., Liberman, M., Laurindo, F.R.M. & Santos, C.X.C. (2006). Analysis of DHE-derived oxidation products by HPLC in the assessment of superoxide production and NADPH oxidase activity in vascular systems. *American Journal of Physiology: Cell Physiology*, 292, C413–C422.

Fiers, W., Beyaert, R., Declercq, W. & Vandenabeele, P. (1999). More than one way to die: apoptosis, necrosis and reactive oxygen damage. *Oncogene*, 18, 7719–7730.

Firth, C., Crone, E., Flavall, E. & Roake, J. (2008a). Macrophage mediated protein hydroperoxide formation and lipid oxidation in low density lipoprotein are inhibited by the inflammation marker 7,8-dihydroneopterin. *Biochemica et Biophysica Acta*, 1783, 1095–1101.

Firth, C.A. (2006). *7,8-Dihydroneopterin-mediated protection of low density lipoprotein, but not human macrophages, from oxidative stress* . Ph.D. thesis, University of Canterbury, Christchurch, New Zealand.

Firth, C.A., Laing, A.D., Baird, S.K., Pearson, J. & Gieseg, S.P. (2008b). Inflammatory sites as a source of plasma neopterin: measurement of high levels of neopterin and markers of oxidative stress in pus drained from human abscesses. *Clinical Biochemistry*, 41, 1078–1083.

Flavall, E.A., Crone, E.M., Moore, G.A. & Gieseg, S.P. (2008). Dissociation of neopterin and 7,8-dihydroneopterin from plasma components before HPLC analysis. *Journal of Chromatography B: Biomedical Sciences and Applications*, 863, 167–171.

Fox, S. & Rossi, A. (2010). Macrophages. In C.N. Serhan, W.P. A & G.D. W, eds., *Fundamentals of Inflammation*, chap. 8, Cambridge University Press, 1st edn.

Franscini, N., Blau, N., Walter, R.B., Schaffner, A. & Schoedon, G. (2003). Critical role of interleukin-1beta for transcriptional regulation of endothelial 6-pyruvoyltetrahydropterin synthase. *Arteriosclerosis Thrombosis and Vascular Biology*, 23, e50–3.

Freshney, R.I. (2010). *Culture of animal cells*. A manual of basic technique and specialized applications, Wiley-Blackwell.

Fu, S., Davies, M., Stocker, R & Dean, R.T. (1998). Evidence for roles of radicals in protein oxidation in advanced human atherosclerotic plaque. *Biochemical Journal*, 333 (Pt 3), 519–525.

Fuchs, D., Milstien, S., Krämer, A., Reibnegger, G., Werner, E.R., Goedert, J.J., Kaufman, S. & Wachter, H. (1989). Urinary neopterin concentrations vs total neopterins for clinical utility. *Clinical Chemistry*, 35, 2305–2307.

Fuchs, D., Stahl-Hennig, C., Gruber, A., Murr, C., Hunsmann, G. & Wachter, H. (1994). Neopterin–its clinical use in urinalysis. *Kidney international Supplement*, 47, S8–11.

Fuchs, D., Avanzas, P., Arroyo-Espliguero, R., Jenny, M., Consuegra-Sanchez, L. & Kaski, J.C. (2009). The role of neopterin in atherogenesis and cardiovascular risk assessment. *Current Medicinal Chemistry*, 16, 4644–4653.

Fujimoto, H., Kobayashi, H., Ogasawara, K., Yamakado, M. & Ohno, M. (2010). Association of the manganese superoxide dismutase polymorphism with vasospastic angina pectoris. *Journal of Cardiology*, 55, 205 – 210.

Galle, J., Hansen-Hagge, T., Wanner, C. & Seibold, S. (2006). Impact of oxidized low density lipoprotein on vascular cells. *Atherosclerosis*, 185, 219–226.

Garcia-Cruset, S., Carpenter, K.L., Guardiola, F., Stein, B.K. & Mitchinson, M.J. (2001). Oxysterol profiles of normal human arteries, fatty streaks and advanced lesions. *Free Radical Research*, 35, 31–41.

Gelissen, I.C., Brown, A.J., Mander, E.L., Kritharides, L., Dean, R.T. & Jessup, W. (1996). Sterol efflux is impaired from macrophage foam cells selectively enriched with 7-ketocholesterol. *The Journal of Biological Chemistry*, 271, 17852–17860.

Genet, R.M. (2011). *A study of oxidation and inflammation using plaque and plasma of vascular disease patients*. Master's thesis, University of Canterbury, Christchurch, New Zealand.

Gerry, A.B. & Leake, D.S. (2008). A moderate reduction in extracellular pH protects macrophages against apoptosis induced by oxidized low density lipoprotein. *The Journal of Lipid Research*, 49, 782–789.

Gerry, A.B., Satchell, L. & Leake, D.S. (2008). A novel method for production of lipid hydroperoxide- or oxysterol-rich low-density lipoprotein. *Atherosclerosis*, 197, 579–587.

Gieseg, S.P. & Esterbauer, H. (1994). Low density lipoprotein is saturable by pro-oxidant copper. *FEBS Letters*, 343, 188–194.

Gieseg, S.P., Reibnegger, G., Wachter, H. & Esterbauer, H. (1995). 7,8-Dihydroneopterin inhibits low density lipoprotein oxidation in vitro. Evidence that this macrophage secreted pteridine is an anti-oxidant. *Free Radical Research*, 23, 123–136.

Gieseg, S.P., Maghzal, G. & Glubb, D. (2001a). Protection of erythrocytes by the macrophage synthesized antioxidant 7,8-dihydroneopterin. *Free Radical Research*, 34, 123–136.

Gieseg, S.P., Whybrow, J., Glubb, D. & Rait, C. (2001b). Protection of U937 cells from free radical damage by the macrophage synthesized antioxidant 7,8-dihydroneopterin. *Free Radical Research*, 35, 311–318.

Gieseg, S.P., Crone, E.M., Flavall, E.A. & Amit, Z. (2008). Potential to inhibit growth of atherosclerotic plaque development through modulation of macrophage neopterin/7,8-dihydroneopterin synthesis. *British Journal of Pharmacology*, 153, 627–635.

Gieseg, S.P., Leake, D.S., Flavall, E.M., Amit, Z., Reid, L. & Yang, Y.T. (2009). Macrophage antioxidant protection within atherosclerotic plaques. *Frontiers in bioscience : a journal and virtual library*, 14, 1230–1246.

Gieseg, S.P., Amit, Z., Yang, Y.T., Shchepetkina, A.A., & Katouah, H. (2010a). Oxidant production, oxLDL uptake, and CD36 levels in human monocyte-derived macrophages are downregulated by the macrophage-generated antioxidant 7,8-dihydroneopterin. *Antioxidants & Redox Signaling*, 13, 1525–1534.

Gieseg, S.P., Crone, E. & Amit, Z. (2010b). Oxidised low density lipoprotein cytotoxicity and vascular disease. In P.J. O'Brien & R.W. Bruce, eds., *Endogenous toxins*, 620–645, Wiley-VCH Verlag Gmbh & Co., Weinheim, Germany.

Glass, C.K. & Witztum, J.L. (2001). Atherosclerosis. the road ahead. *Cell*, 104, 503–516.

Gmünder, H., Eck, H.P., Benninghoff, B., Roth, S. & Dröge, W. (1990). Macrophages regulate intracellular glutathione levels of lymphocytes. Evidence for an immunoregulatory role of cysteine. *Cellular Immunology*, 129, 32–46.

Gordon, D., Reidy, E., Benditt, E. & Schwartz, S. (1990). Cell proliferation in human coronary arteries. *Proceedings of the National Academy of Sciences of the United States of America*, 87, 4600–4604.

Gotoh, N., Graham, A., Niki, E. & Darley-Usmar, V. (1993). Inhibition of glutathione synthesis increases the toxicity of oxidized low-density lipoprotein to human monocytes and macrophages. *The Biochemical Journal*, 296, 151–154.

Gough, P.J., Greaves, D.R., Suzuki, H., Hakkinen, T., Hiltunen, M.O., Turunen, M., Herttuala, S.Y., Kodama, T. & Gordon, S. (1999). Analysis of macrophage scavenger receptor (SR-A) expression in human aortic atherosclerotic lesions. *Arteriosclerosis Thrombosis and Vascular Biology*, 19, 461–471.

Gown, A.M., Tsukada, T. & Ross, R. (1986). Human atherosclerosis. II. Immunocytochemical analysis of the cellular composition of human atherosclerotic lesions. *American Journal of Pathology*, 125, 191–207.

Graham, A., Hassall, D., Rafique, S. & Owen, J. (1997). Evidence for a paraoxonase-independent inhibition of low-density lipoprotein oxidation by high-density lipoprotein. *Atherosclerosis*, 135, 193–204.

Gray, J.H., Owen, R.P. & Giacomini, K.M. (2004). The concentrative nucleoside transporter family, SLC28. *Pflugers Archiv European Journal of Physiology*, 447, 728–734.

Greilberger, J., Oettl, K., Cvirn, G., Reibnegger, G. & Jürgens, G. (2004). Modulation of LDL oxidation by 7,8-dihydroneopterin. *Free Radical Research*, 38, 9–17.

Groemping, Y. & Rittinger, K. (2005). Activation and assembly of the NADPH oxidase: a structural perspective. *The Biochemical Journal*, 386, 401–416.

Gu, L., Okada, Y., Clinton, S.K., Gerard, C., Sukhova, G.K., Libby, P. & Rollins, B.J. (1998). Absence of monocyte chemoattractant protein-1 reduces atherosclerosis in low density lipoprotein receptor-deficient mice. *Molecular Cell*, 2, 275–281.

Ha, J.S., Ha, C.E., Chao, J.T., Petersen, C.E., Theriault, A. & Bhagavan, N.V. (2003). Human serum albumin and its structural variants mediate cholesterol efflux from cultured endothelial cells. *Biochimica et Biophysica Acta - Molecular Cell Research*, 1640, 119–128.

Hägg, D., Englund, M.C.O., Jernås, M., Schmidt, C., Wiklund, O., Hultén, L.M., Ohlsson, B.G., Carlsson, L.M.S., Carlsson, B. & Svensson, P.A. (2006). Oxidized LDL induces a coordinated up-regulation of the glutathione and thioredoxin systems in human macrophages. *Atherosclerosis*, 185, 282–289.

Haider, L., Fischer, M.T., Frischer, J.M., Bauer, J., Höftberger, R., Botond, G., Esterbauer, H., Binder, C.J., Witztum, J.L. & Lassmann, H. (2011). Oxidative damage in multiple sclerosis lesions. *Brain*, 1–11.

Halliwell, B. (2003). Oxidative stress in cell culture: an underappreciated problem? *FEBS Letters*, 540, 3–6.

Halliwell, B. & Whiteman, M. (2004). Measuring reactive species and oxidative damage in vivoand in cell culture: how should you do it and what do the results mean? *British Journal of Pharmacology*, 142, 231–255.

Han, J., Hajjar, D.P., Febbraio, M. & Nicholson, A.C. (1997). Native and modified low density lipoproteins increase the functional expression of the macrophage class B scavenger receptor, CD36. *The Journal of Biological Chemistry*, 272, 21654–21659.

Han, J., Hajjar, D.P., Tauras, J.M. & Nicholson, A.C. (1999). Cellular cholesterol regulates expression of the macrophage type B scavenger receptor, CD36. *The Journal of Lipid Research*, 40, 830–838.

Han, J., Zhong, C.Q. & Zhang, D.W. (2011). Programmed necrosis: backup to and competitor with apoptosis in the immune system. *Nature Immunology*, 12, 1143–1149.

Handberg, A., Levin, K., Højlund, K. & Beck-Nielsen, H. (2006). Identification of the oxidized low-density lipoprotein scavenger receptor CD36 in plasma: a novel marker of insulin resistance. *Circulation*, 114, 1169–1176.

Hansson, G.K. & Hermansson, A. (2011). The immune system in atherosclerosis. *Nature Immunology*, 12, 204–212.

Harada-Shiba, M., Kinoshita, M., Kamido, H. & Shimokado, K. (1998). Oxidized low density lipoprotein induces apoptosis in cultured human umbilical vein endothelial cells by common and unique mechanisms. *The Journal of Biological Chemistry*, 273, 9681–9687.

Hardwick, S., Hegyi, L., Clare, K., Law, N., Carpenter, K.L., Mitchinson, M.J. & Skepper, J.N. (1996). Apoptosis in human monocyte-macrophages exposed to oxidized low density lipoprotein. *The Journal of Pathology*, 179, 294–302.

Hardwick, S., Carpenter, K.L., Allen, E.A. & Mitchinson, M.J. (1999). Glutathione (GSH) and the toxicity of oxidised low-density lipoprotein to human monocyte-macrophages. *Free Radical Research*, 30, 11–19.

Harris, L.K., Mann, G.E., Ruiz, E., Mushtaq, S. & Leake, D.S. (2006). Ascorbate does not protect macrophages against apoptosis induced by oxidised low density lipoprotein. *Archives of Biochemistry and Biophysics*, 455, 68–76.

Harris, P. & Ralph, P. (1985). Human leukemic models of myelomonocytic development: a review of the HL-60 and U937 cell lines. *Journal of Leukocyte Biology*, 37, 407–422.

Harrison, E.H., Bernard, D.W., Scholm, P., Quinn, D.M., Rothblat, G. & Glick, J.M. (1990). Inhibitors of neutral cholesteryl ester hydrolase. *Journal of Lipid Research*, 31, 2187–2193.

Hegyi, L., Skepper, J.N., Cary, N.R. & Mitchinson, M.J. (1996). Foam cell apoptosis and the development of the lipid core of human atherosclerosis. *The Journal of Pathology*, 180, 423–429.

Heinecke, J.W., Kawamura, M., Suzuki, L. & Chait, A. (1993). Oxidation of low density lipoprotein by thiols: superoxide-dependent and -independent mechanisms. *Journal of Lipid Research*, 34, 2051–2061.

Henderson, D.C., Sheldon, J., Riches, P. & Hobbs, J.R. (1991). Cytokine induction of neopterin production. *Clinical and Experimental Immunology*, 83, 479–482.

Henriksen, T., Evensen, S.A. & Carlander, B. (1979). Injury to human endothelial cells in culture induced by low density lipoproteins. *Scandinavian Journal of Clinical Laboratory Investigation*, 39, 361–368.

Henriksen, T., Mahoney, E.M. & Steinberg, D. (1983). Enhanced macrophage degradation of biologically modified low density lipoprotein. *Atherosclerosis*, 3, 149–159.

Hessler, J.R., Morel, D.W., Lewis, L.J. & Chisolm, G.M. (1983). Lipoprotein oxidation and lipoprotein-induced cytotoxicity. *Arteriosclerosis*, 3, 215–222.

Hessler, J.R.J., Robertson, A.L.A. & Chisolm, G.M.G. (1979). LDL-induced cytotoxicity and its inhibition by HDL in human vascular smooth muscle and endothelial cells in culture. *Atherosclerosis*, 32, 213–229.

BIBLIOGRAPHY

Heumüller, S., Wind, S., Barbosa-Sicard, E., Schmidt, H.H.H.W., Busse, R., Schröder, K. & Brandes, R.P. (2008). Apocynin is not an inhibitor of vascular NADPH oxidases but an antioxidant. *Hypertension*, 51, 211–217.

Higashi, Y., Peng, T., Du, J., Sukhanov, S., Li, Y., Itabe, H., Parthasarathy, S. & Delafontaine, P. (2005). A redox-sensitive pathway mediates oxidized LDL-induced downregulation of insulin-like growth factor-1 receptor. *Journal of Lipid Research*, 46, 1266–1277.

Ho, Y.K., Brown, S., Bilheimer, D. & Goldstein, J.L. (1976). Regulation of low density lipoprotein receptor activity in freshly isolated human lymphocytes. *The Journal of Clinical Investigation*, 58, 1465–1474.

Hodis, H.N., Kramsch, D.M., Avogaro, P., Bittolo-Bon, G., Cazzolato, G., Hwang, J., Peterson, H. & Sevanian, A. (1994). Biochemical and cytotoxic characteristics of an in vivo circulating oxidized low density lipoprotein (LDL-). *Journal of Lipid Research*, 35, 669–677.

Hoff, H.F. & O'Neil, J. (1988). Extracts of human atherosclerotic lesions can modify low density lipoproteins leading to enhanced uptake by macrophages. *Atherosclerosis*, 70, 29–41.

Hoff, H.F., Zyromski, N., Armstrong, D. & O'Neil, J. (1993). Aggregation as well as chemical modification of LDL during oxidation is responsible for poor processing in macrophages. *Journal of Lipid Research*, 34, 1919–1929.

Hoffmann, G. & Schobersberger, W. (2004). Neopterin: a Mediator of the Cellular Immune System. *Pteridines*, 15, 107–112.

Hoffmann, G., Schobersberger, W., Frede, S., Pelzer, L., Fandrey, J., Wachter, H., Fuchs, D. & Grote, J. (1996). Neopterin activates transcription factor nuclear factor-kappa B in vascular smooth muscle cells. *FEBS Letters*, 391, 181–184.

Hoffmann, G., Frede, S., Kenn, S., Smolny, M., Wachter, H., Fuchs, D., Grote, J., Rieder, J. & Schobersberger, W. (1998). Neopterin-induced tumor necrosis factor-alpha synthesis in vascular smooth muscle cells in vitro. *International Archives of Allergy and Immunology*, 116, 240–245.

Hoffmann, G., Wirleitner, B. & Fuchs, D. (2003). Potential role of immune system activation-associated production of neopterin derivatives in humans. *Inflammation Research*, 52, 313–321.

Holland, J.A., Meyer, J.W., Schmitt, M.E., Sauro, M.D., Johnson, D.K., Abdul-Karim, R.W., Patel, V., Ziegler, L.M., Schillinger, K.J., Small, R.F. & Lemanski, L.F. (1997). Low-density lipoprotein stimulated peroxide production and endocytosis in cultured human endothelial cells: mechanisms of action. *Endothelium*, 5, 191–207.

Hönlinger, M., Fuchs, D., Hausen, A., Reibnegger, G., Schonitzer, D., Werner, E.R., Reissigl, H., Dierich, M.P. & Wachter, H. (2008). Serum-Neopterinbestimmung zur zusätzlichen Sicherung der Bluttransfusion: Erfahrungen an 76 587 Blutspendern. *Deutsche medizinische Wochenschrift (1946)*, 114, 172–176.

Hoosdally, S.J., Andress, E.J., Wooding, C., Martin, C.A. & Linton, K.J. (2009). The Human Scavenger Receptor CD36: glycosylation status and its role in trafficking and function. *The Journal of Biological Chemistry*, 284, 16277–16288.

Horiuchi, S., Sakamoto, Y. & Sakai, M. (2003). Scavenger receptors for oxidized and glycated proteins. *Amino Acids*, 25, 283–292.

Hsieh, C.C., Yen, M.H., Yen, C.H. & Lau, Y.T. (2001). Oxidized low density lipoprotein induces apoptosis via generation of reactive oxygen species in vascular smooth muscle cells. *Cardiovascular Research*, 49, 135–145.

Huang, Y.H., Rönnelid, J. & Frostegard, J. (1995). Oxidized LDL induces enhanced antibody formation and MHC class II-dependent IFN-gamma production in lymphocytes from healthy individuals. *Arteriosclerosis Thrombosis and Vascular Biology*, 15, 1577–1583.

Huber, C., Batchelor, J., Fuchs, D., Hausen, A., Lang, A., Niederwieser, D., Reibnegger, G., Swetly, P., Troppmair, J. & Wachter, H. (1984). Immune response-associated production of neopterin. Release from macrophages primarily under control of interferon-gamma. *The Journal of Experimental Medicine*, 160, 310–316.

Hultén, L.M., Ullström, C., Krettek, A., Van Reyk, D., Marklund, S.L., Dahlgren, C. & Wiklund, O. (2005). Human macrophages limit oxidation products in low density lipoprotein. *Lipids in Health and Disease*, 4, 6.

Hyclone® (1996). Heat Inactivation— Are You Wasting Your Time? *Art to Science*, 15.

Ignarro, L.J. (2009). *Nitric oxide*. Biology and Pathobiology, Academic Press.

Isa, S.A., Ruffino, J.S., Ahluwalia, M., Thomas, A.W., Morris, K. & Webb, R. (2011). M2 macrophages exhibit higher sensitivity to oxLDL-induced lipotoxicity than other monocyte/macrophage subtypes. *Lipids in Health and Disease*, 10, 229.

Isner, J.M., Kearney, M., Bortman, S. & Passeri, J. (1995). Apoptosis in human atherosclerosis and restenosis. *Circulation*, 91, 2703–2711.

Itabe, H.H., Suzuki, K.K., Tsukamoto, Y.Y., Komatsu, R.R., Ueda, M.M., Mori, M.M., Higashi, Y.Y. & Takano, T.T. (2000). Lysosomal accumulation of oxidized phosphatidylcholine-apolipoprotein B complex in macrophages: intracellular fate of oxidized low density lipoprotein. *Biochimica et Biophysica Acta*, 1487, 233–245.

Jawień, J., Nastałek, P. & Korbut, R. (2004). Mouse models of experimental atherosclerosis. *Journal of Physiology and Pharmacology*, 55, 503–517.

Jedidi, I., Couturier, M., Thérond, P., Gardès-Albert, M., Legrand, A., Barouki, R., Bonnefont-Rousselot, D. & Aggerbeck, M. (2006). Cholesteryl ester hydroperoxides increase macrophage CD36 gene expression via PPARalpha. *Biochemical and Biophysical Research Communications*, 351, 733–738.

Jerome, W.G. & Yancey, P.G. (2003). The role of microscopy in understanding atherosclerotic lysosomal lipid metabolism. *Microscopy and Microanalysis*, 9, 54–67.

Jessup, W. & Kritharides, L. (2000). Metabolism of oxidized LDL by macrophages. *Current Opinion in Lipidology*, 11, 473–481.

Jessup, W., Wilson, P., Gaus, K. & Kritharides, L. (2002). Oxidized lipoproteins and macrophages. *Vascular Pharmacology*, 38, 239–248.

Johnson, W.J.W., Mahlberg, F.H.F., Rothblat, G.H.G. & Phillips, M.C.M. (1991). Cholesterol transport between cells and high-density lipoproteins. *Biochimica et Biophysica Acta - Bioenergetics*, 1085, 273–298.

Jürgens, G., Hoff, H.F., Chisolm III, G.M. & Esterbauer, H. (1987). Modification of human serum low density lipoprotein by oxidation — Characterization and pathophysiological implications. *Chemistry and Physics of Lipids*, 45, 315–336.

Kalyanaraman, B.B. (2011). Oxidative chemistry of fluorescent dyes: implications in the detection of reactive oxygen and nitrogen species. *Biochemical Society Transactions*, 39, 1221–1225.

Kanegae, M.P.P., da Fonseca, L.M., Brunetti, I.L., de Oliveira Silva, S. & Ximenes, V.F. (2007). The reactivity of ortho-methoxy-substituted catechol radicals with sulfhydryl groups: Contribution for the comprehension of the mechanism of inhibition of NADPH oxidase by apocynin. *Biochemical Pharmacology*, 74, 457–464.

Kappler, M., Gerry, A.B., Brown, E., Reid, L., Leake, D.S. & Gieseg, S.P. (2007). Aqueous peroxyl radical exposure to THP-1 cells causes glutathione loss followed by protein oxidation and cell death without increased caspase-3 activity. *Biochimica et Biophysica Acta*, 1773, 945–953.

Kaski, J.C., Consuegra-Sanchez, L., Fernandez-Berges, D.J., Cruz-Fernandez, J.M., Garcia-Moll, X., Marrugat, J., Mostaza, J., Toro-Cebada, R., González-Juanatey, J.R. & Guzmán-Martínez, G. (2008). Elevated serum neopterin levels and adverse cardiac events at 6 months follow-up in Mediterranean patients with non-ST-segment elevation acute coronary syndrome. *Atherosclerosis*, 201, 176–183.

Katouah, H. (2012). *Inhibition of macrophage metabolism by oxLDL*. Ph.D. thesis, University of Canterbury, Christchurch, New Zealand.

Katsuda, S., Boyd, H.C., Fligner, C., Ross, R. & Gown, A.M. (1992). Human atherosclerosis. III. Immunocytochemical analysis of the cell composition of lesions of young adults. *American Journal of Pathology*, 140, 907–914.

Kehrer, J.P. (2000). The Haber-Weiss reaction and mechanisms of toxicity. *Toxicology*, 149, 43–50.

Keyel, P.A., Tkacheva, O.A., Larregina, A.T. & Salter, R.D. (2012). Coordinate stimulation of macrophages by microparticles and TLR ligands induces foam cell formation. *Journal of Immunology*, 189, 4621–9.

Khan, O.F. & Sefton, M.V. (2010). Endothelial cell behaviour within a microfluidic mimic of the flow channels of a modular tissue engineered construct. *Biomedical Microdevices*, 13, 69–87.

Kielar, D., Dietmaier, W., Langmann, T., Aslanidis, C., Probst, M., Naruszewicz, M. & Schmitz, G. (2001). Rapid quantification of human ABCA1 mRNA in various cell types and tissues by real-time reverse transcription-PCR. *Clinical Chemistry*, 47, 2089–2097.

Kinscherf, R., Claus, R., Wagner, M., Gehrke, C., Kamencic, H., Hou, D., Nauen, O., Schmiedt, W., Kovacs, G., Pill, J., Metz, J. & Deigner, H.P. (1998). Apoptosis caused by oxidized LDL is manganese superoxide dismutase and p53 dependent. *The FASEB Journal*, 12, 461–467.

Klebanoff, S. (2005). Myeloperoxidase: friend and foe. *Journal of Leukocyte Biology*, 77, 598–625.

Kobzik, L.L., Godleski, J.J.J. & Brain, J.D.J. (1990). Oxidative metabolism in the alveolar macrophage: analysis by flow cytometry. *Journal of Leukocyte Biology*, 47, 295–303.

Kockx, M.M., De Meyer, G., Muhring, J., Jacob, W., Bult, H. & Herman, A. (1998). Apoptosis and related proteins in different stages of human atherosclerotic plaques. *Circulation*, 97, 2307–2315.

Kodama, T., Reddy, P., Kishimoto, C. & Krieger, M. (1988). Purification and characterization of a bovine acetyl low density lipoprotein receptor. *Proceedings of the National Academy of Sciences of the United States of America*, 85, 9238–9242.

Kojima, S., Icho, T., Kajiwara, Y. & Kubota, K. (1992). Neopterin as an endogenous antioxidant. *FEBS Letters*, 304, 163–166.

Kojima, S., Nomura, T., Icho, T., Kajiwara, Y., Kitabatake, K. & Kubota, K. (1993). Inhibitory effect of neopterin on NADPH-dependent superoxide-generating oxidase of rat peritoneal macrophages. *FEBS Letters*, 329, 125–128.

Konrad, P.N., Richards, F., Valentine, W.N. & Paglia, D.E. (1972). Gamma-Glutamyl-cysteine synthetase deficiency. A cause of hereditary hemolytic anemia. *New England Journal of Medicine*, 286, 557–561.

Koonen, D.P.Y., Jensen, M.K. & Handberg, A. (2011). Soluble CD36- a marker of the (pathophysiological) role of CD36 in the metabolic syndrome? *Archives of Physiology and Biochemistry*, 117, 57–63.

Kouoh, F., Gressier, B., Luyckx, M., Brunet, C., Dine, T., Cazin, M. & Cazin, J.C. (1999). Antioxidant properties of albumin: effect on oxidative metabolism of human neutrophil granulocytes. *Il Farmaco*, 54, 695–699.

Kritharides, L., Jessup, W., Gifford, J. & Dean, R.T. (1993). A method for defining the stages of low-density lipoprotein oxidation by the separation of cholesterol and cholesterol ester-oxidation products using HPLC. *Analytical Biochemistry*, 213, 79–89.

Kritharides, L., Jessup, W., Mander, E.L. & Dean, R.T. (1995). Apolipoprotein A-I-mediated efflux of sterols from oxidized LDL-loaded macrophages. *Arteriosclerosis Thrombosis and Vascular Biology*, 15, 276–289.

Kruth, H.S. (2001). Macrophage foam cells and atherosclerosis. *Frontiers in Bioscience*, 6, D429–D455.

Krysko, D.V., Berghe, T.T.V., D'Herde, K. & Vandenabeele, P. (2008). Apoptosis and necrosis: Detection, discrimination and phagocytosis. *Methods*, 44, 17–17.

Kuchibhotla, S., Vanegas, D., Kennedy, D.J., Guy, E., Nimako, G., Morton, R.E. & Febbraio, M. (2008). Absence of CD36 protects against atherosclerosis in ApoE knock-out mice with no additional protection provided by absence of scavenger receptor A I/II. *Cardiovascular Research*, 78, 185–196.

Kunjathoor, V.V., Febbraio, M., Podrez, E.A., Moore, K.J., Andersson, L., Koehn, S., Rhee, J.S., Silverstein, R., Hoff, H.F. & Freeman, M.W. (2002). Scavenger receptors class A-I/II and CD36 are the principal receptors responsible for the uptake of modified low density lipoprotein leading to lipid loading in macrophages. *The Journal of Biological Chemistry*, 277, 49982–49988.

Lai, J.P., Yang, J., Douglas, S., Wang, X., Riedel, E. & Ho, W.Z. (2003). Quantification of CCR5 mRNA in Human Lymphocytes and Macrophages by Real-Time Reverse Transcriptase PCR Assay. *Clinical and Vaccine Immunology*, 10, 1123–1128.

Laich, A.A., Neurauter, G.G., Wirleitner, B.B. & Fuchs, D.D. (2002). Degradation of serum neopterin during daylight exposure. *Clinica Chimica Acta; International Journal of Clinical Chemistry*, 322, 175–178.

Lakari, E.,]s, P.P., Pietarinen-Runtti, P.,][auml]kk[ouml], P.P., Soini, Y. & Kinnula, V.L. (2001). Expression and regulation of hemeoxygenase 1 in healthy human lung and interstitial lung disorders. *Human Pathology*, 32, 1257 – 1263.

Larsson, D.A., Baird, S., Nyhalah, J.D., Yuan, X.M. & Li, W. (2006). Oxysterol mixtures, in atheroma-relevant proportions, display synergistic and proapoptotic effects. *Free Radical Biology and Medicine*, 41, 9–9.

BIBLIOGRAPHY

Leabman, M.K., Huang, C.C., DeYoung, J., Carlson, E.J., Taylor, T.R., de la Cruz, M., Johns, S.J., Stryke, D., Kawamoto, M., Urban, T.J., Kroetz, D.L., Ferrin, T.E., Clark, A.G., Risch, N.N., Herskowitz, I.I. & Giacomini, K.M. (2003). Natural variation in human membrane transporter genes reveals evolutionary and functional constraints. *Proceedings of the National Academy of Sciences of the United States of America*, 100, 5896–5901.

Lee, C.F., Qiao, M., Schröder, K., Zhao, Q. & Asmis, R. (2010). Nox4 is a Novel Inducible Source of Reactive Oxygen Species in Monocytes and Macrophages and Mediates Oxidized Low Density Lipoprotein-Induced Macrophage Death. *Circulation Research*, 106, 1489–1497.

Leitner, K.L., Meyer, M., Leimbacher, W., Peterbauer, A., Hofer, S., Heufler, C., Müller, A., Heller, R., Werner, E.R.E., Thöny, B.B. & Werner-Felmayer, G.G. (2003). Low tetrahydrobiopterin biosynthetic capacity of human monocytes is caused by exon skipping in 6-pyruvoyl tetrahydropterin synthase. *Biochemical Journal*, 373, 681–688.

Leshem, B., Yogev, D. & Fiorentini, D. (1999). Heat inactivation of fetal calf serum is not required for in vitro measurement of lymphocyte functions. *Journal of Immunological Methods*, 223, 249–254.

Levitan, I., Volkov, S. & Subbaiah, P.V. (2010). Oxidized LDL: diversity, patterns of recognition, and pathophysiology. *Antioxidants & Redox Signaling*, 13, 39–75.

Li, L., Tan, C.M.F., Koo, S.H., Chong, K.T. & Lee, E.J.D. (2007). Identification and functional analysis of variants in the human concentrative nucleoside transporter 2, hCNT2 (SLC28A2) in Chinese, Malays and Indians. *Pharmacogenetics and Genomics*, 17, 783–786.

Li, W., Yuan, X.M. & Brunk, U.T. (1998). OxLDL-induced macrophage cytotoxicity is mediated by lysosomal rupture and modified by intralysosomal redox-active iron. *Free Radical Research*, 29, 389–398.

Li, W., Ostblom, M., Xu, L.H., Hellsten, A., Leanderson, P., Liedberg, B., Brunk, U.T., Eaton, J.W. & Yuan, X.M. (2006). Cytocidal effects of atheromatous plaque components: the death zone revisited. *The FASEB Journal*, 20, 2281–2290.

Libby, P. (2002). Inflammation in atherosclerosis. *Nature*, 420, 868–874.

Liu, S.M., Cogny, A., Kockx, M., Dean, R.T., Gaus, K., Jessup, W. & Kritharides, L. (2003). Cyclodextrins differentially mobilize free and esterified cholesterol from primary human foam cell macrophages. *Journal of Lipid Research*, 44, 1156–1166.

Luan, Y. & Griffiths, H.R. (2006). Ceramides reduce CD36 cell surface expression and oxidised LDL uptake by monocytes and macrophages. *Archives of Biochemistry and Biophysics*, 450, 89–99.

Lusis, A.J. (2000). Atherosclerosis. *Nature*, 407, 233–241.

Madamanchi, N.R. & Runge, M.S. (2007). Mitochondrial dysfunction in atherosclerosis. *Circulation Research*, 100, 460–473.

Malek, A.M., Alper, S.L. & Izumo, S. (1999). Hemodynamic shear stress and its role in atherosclerosis. *Journal of the American Medical Association*, 282, 2035–2042.

Manning-Tobin, J., Moore, K.J., Seimon, T.A., Bell, S.A., Sharuk, M., Alvarez-Leite, J.I., de Winther, M.P.J., Tabas, I. & Freeman, M.W. (2008). Loss of SR-A and CD36 activity reduces atherosclerotic Lesion complexity without abrogating foam cell formation in hyperlipidemic mice. *Arteriosclerosis Thrombosis and Vascular Biology*, 29, 19–26.

Maor, I. & Aviram, M. (1994). Oxidized low density lipoprotein leads to macrophage accumulation of unesterified cholesterol as a result of lysosomal trapping of the lipoprotein hydrolyzed cholesteryl ester. *The Journal of Lipid Research*, 35, 803–819.

Marchant, C., Law, N., van der Veen, C., Hardwick, S., Carpenter, K.L. & Mitchinson, M.J. (1995). Oxidized low-density lipoprotein is cytotoxic to human monocyte-macrophages: protection with lipophilic antioxidants. *FEBS Letters*, 358, 175–178.

Martinet, W., Schrijvers, D.M. & De Meyer, G.R.Y. (2011). Necrotic cell death in atherosclerosis. *Basic Research in Cardiology*, 106, 749–760.

Matés, J.M., Pérez-Gómez, C. & Núñez de Castro, I. (1999). Antioxidant enzymes and human diseases. *Clinical Biochemistry*, 32, 595–603.

McLaren, J.E., Michael, D.R., Ashlin, T.G. & Ramji, D.P. (2011). Cytokines, macrophage lipid metabolism and foam cells: Implications for cardiovascular disease therapy. *Progress in Lipid Research*.

Miao, L. & Clair, D.K.S. (2009). Regulation of superoxide dismutase genes: Implications in disease. *Free Radical Biology and Medicine*, 47, 344 – 356.

Mihalache, C.C. & Simon, H.U. (2012). Autophagy regulation in macrophages and neutrophils. *Experimental Cell Research*, 318, 1187–1192.

Miller, Y.I., Choi, S.H., Fang, L. & Harkewicz, R. (2009). Toll-like receptor-4 and lipoprotein accumulation in macrophages. *Trends in Cardiovascular Medicine*, 19, 227–232.

Monier, S., Samadi, M., Prunet, C., Denance, M., Laubriet, A., Athias, A., Berthier, A., Steinmetz, E., Jürgens, G.G., Negre-Salvayre, A.A., Bessède, G.G., Lemaire-Ewing, S.S., Néel, D.D., Gambert, P.P. & Lizard, G.G. (2003). Impairment of the cytotoxic and oxidative activities of 7 beta-hydroxycholesterol and 7-ketocholesterol by esterification with oleate. *Biochemical and Biophysical Research Communications*, 303, 814–824.

Moore, K.J. (2006). Scavenger receptors in atherosclerosis: beyond lipid uptake. *Arteriosclerosis Thrombosis and Vascular Biology*, 26, 1702–1711.

Moore, K.J. & Tabas, I. (2011). Macrophages in the pathogenesis of atherosclerosis. *Cell*, 145, 341–355.

Morel, Y. & Barouki, R. (1999). Repression of gene expression by oxidative stress. *The Biochemical Journal*, 342 (Pt 3), 481–496.

Mosmann, T. (1983). Rapid colorimetric assay for cellular growth and survival: Application to proliferation and cytotoxicity assays. *Journal Immunological Methods*, 65, 55–63.

Motulsky, H. (2007). Statistics Guide. GraphPad Software Inc.

Muijsers, R.B., van Den Worm, E., Folkerts, G., Beukelman, C.J., Koster, A.S., Postma, D.S. & Nijkamp, F.P. (2000). Apocynin inhibits peroxynitrite formation by murine macrophages. *British Journal of Pharmacology*, 130, 932–936.

Muller, C., Salvayre, R., gre Salvayre, A.N.e. & Vindis, C. (2010). HDLs inhibit endoplasmic reticulum stress and autophagic response induced by oxidized LDLs. *Cell Death and Differentiation*, 18, 817–828.

Muller, K., Dulku, S., Hardwick, S., Skepper, J.N. & Mitchinson, M.J. (2001). Changes in vimentin in human macrophages during apoptosis induced by oxidised low density lipoprotein. *Atherosclerosis*, 156, 133–144.

Munteanu, A., Taddei, M., Tamburini, I., Bergamini, E., Azzi, A. & Zingg, J.M. (2006). Antagonistic effects of oxidized low density lipoprotein and alpha-tocopherol on CD36 scavenger receptor expression in monocytes: involvement of protein kinase B and peroxisome proliferator-activated receptor-gamma. *The Journal of Biological Chemistry*, 281, 6489–6497.

Murr, C., Fuchs, D., Gössler, W., Hausen, A., Reibnegger, G., Werner, E.R., Werner-Felmayer, G., Esterbauer, H. & Wachter, H. (1994). Enhancement of hydrogen peroxide-induced luminol-dependent chemiluminescence by neopterin depends on the presence of iron chelator complexes. *FEBS Letters*, 338, 223–226.

Murr, C., Schroecksnadel, K., Schönitzer, D., Fuchs, D. & Schennach, H. (2005). Neopterin concentrations in blood donors differ between AB0 blood group phenotypes. *Clinical Biochemistry*, 38, 916–919.

Naghavi, M., Libby, P., Falk, E., Casscells, S.W., Litovsky, S., Rumberger, J., Badimon, J.J., Stefanadis, C., Moreno, P., Pasterkamp, G., Fayad, Z., Stone, P.H., Waxman, S., Raggi, P., Madjid, M., Zarrabi, A., Burke, A., Yuan, C., Fitzgerald, P.J., Siscovick, D.S., de Korte, C.L., Aikawa, M., Airaksinen, K.E.J., Assmann, G., Becker, C.R., Chesebro, J.H., Farb, A., Galis, Z.S., Jackson, C., Jang, I.K., Koenig, W., Lodder, R.A., March, K., Demirovic, J., Navab, M., Priori, S.G., Rekhter, M.D., Bahr, R., Grundy, S.M., Mehran, R., Colombo, A., Boerwinkle, E., Ballantyne, C., Insull, W., Schwartz, R.S., Vogel, R., Serruys, P.W., Hansson, G.K., Faxon, D.P., Kaul, S., Drexler, H., Greenland, P., Muller, J.E., Virmani, R., Ridker, P.M., Zipes, D.P., Shah, P.K. & Willerson, J.T. (2003). From vulnerable plaque to vulnerable patient: a call for new definitions and risk assessment strategies: Part I. *Circulation*, 108, 1664–1672.

Naito, M., Nomura, H., Esaki, T. & Iguchi, A. (1997). Characteristics of macrophage-derived foam cells isolated from atherosclerotic lesions of rabbits. *Atherosclerosis*, 135, 241–247.

Nakagawa, T., Nozaki, S., Nishida, M., Yakub, J.M., Tomiyama, Y., Nakata, A., Matsumoto, K., Funahashi, T., Kameda-Takemura, K., Kurata, Y., Yamashita, S. & Matsuzawa, Y. (1998). Oxidized LDL increases and interferon-gamma decreases expression of CD36 in human monocyte-derived macrophages. *Arteriosclerosis Thrombosis and Vascular Biology*, 18, 1350–1357.

Nakagawara, A., Nathan, C.F. & Cohn, Z.A. (1981). Hydrogen peroxide metabolism in human monocytes during differentiation in vitro. *The Journal of Clinical Investigation*, 68, 1243–1252.

Nakashima, Y., Plump, A.S., Raines, E.W., Breslow, J. & Ross, R. (1994). ApoE-deficient mice develop lesions of all phases of atherosclerosis throughout the arterial tree. *Arteriosclerosis Thrombosis and Vascular Biology*, 14, 133–140.

Nakashima, Y., Wight, T.N. & Sueishi, K. (2008). Early atherosclerosis in humans: role of diffuse intimal thickening and extracellular matrix proteoglycans. *Cardiovascular Research*, 79, 14–23.

Nakata, A., Nakagawa, Y., Nishida, M., Nozaki, S., Miyagawa, J., Nakagawa, T., Tamura, R., Matsumoto, K., Kameda-Takemura, K., Yamashita, S. & Matsuzawa, Y. (1999). CD36, a novel receptor for oxidized low-density lipoproteins, is highly expressed on lipid-laden macrophages in human atherosclerotic aorta. *Arteriosclerosis Thrombosis and Vascular Biology*, 19, 1333–1339.

Napolitano, M. & Bravo, E. (2003). Activation of protein kinase C by phorbol esters in human macrophages reduces the metabolism of modified LDL by down-regulation of scavenger receptor activity. *The International Journal of Biochemistry & Cell Biology*, 35, 1127–1143.

Nathan, C. (2008). Epidemic inflammation: pondering obesity. *Molecular Medicine*, 14, 485–492.

Nathan, C.F. (1986). Peroxide and pteridine: a hypothesis on the regulation of macrophage antimicrobial activity by interferon gamma. *Interferon*, 7, 125–143.

National Cholesterol Education Program NCEP Expert Panel on Detection, E. & of High Blood Cholesterol in Adults Adult Treatment Panel III, T. (2002). Third report of the National Cholesterol Education Program (NCEP) expert panel on detection, evaluation, and treatment of high blood cholesterol in adults (Adult Treatment Panel III) final report. The Program.

Nichenametla, S.N., Ellison, I., Calcagnotto, A., Lazarus, P., Muscat, J.E. & Richie, J.P., Jr. (2008). Functional significance of the GAG trinucleotide-repeat polymorphism in the gene for the catalytic subunit of gamma-glutamylcysteine ligase. *Free Radical Biology and Medicine*, 45, 645–650.

Nishi, K., Itabe, H., Uno, M., Kitazato, K.T., Horiguchi, H., Shinno, K. & Nagahiro, S. (2002). Oxidized LDL in carotid plaques and plasma associates with plaque instability. *Arteriosclerosis Thrombosis and Vascular Biology*, 22, 1649–1654.

Njålsson, R. & Norgren, S. (2005). Physiological and pathological aspects of GSH metabolism. *Acta Paediatrica*, 94, 132–137.

Nockengost, S. (2009). T042-NanoDrop-Spectrophotometers-Nucleic-Acid-Purity-Ratios.pub. Tech. Rep. T042, Thermo Scientific.

Nozaki, S., Kashiwagi, H., Yamashita, S., Nakagawa, T., Kostner, B., Tomiyama, Y., Nakata, A., Ishigami, M., Miyagawa, J. & Kameda-Takemura, K. (1995). Reduced uptake of oxidized low density lipoproteins in monocyte-derived macrophages from CD36-deficient subjects. *The Journal of Clinical Investigation*, 96, 1859–1865.

Oettl, K. & Stauber, R.E. (2007). Physiological and pathological changes in the redox state of human serum albumin critically influence its binding properties. *British Journal of Pharmacology*, 151, 580–590.

Oettl, K., Dikalov, S., Freisleben, H.J., Mlekusch, W. & Reibnegger, G. (1997). Spin trapping study of antioxidant properties of neopterin and 7,8-dihydroneopterin. *Biochemical and Biophysical Research Communications*, 234, 774–778.

Oettl, K., Greilberger, J., Dikalov, S. & Reibnegger, G. (2004a). Interference of 7,8-dihydroneopterin with peroxynitrite-mediated reactions. *Biochemical and Biophysical Research Communications*, 321, 379–385.

Oettl, K., Greilberger, J., Dikalov, S. & Reibnegger, G. (2004b). Interference of 7,8-dihydroneopterin with peroxynitrite-mediated reactions. *Biochemical and Biophysical Research Communications*, 321, 379–385.

Ohashi, A., Sugawara, Y., Mamada, K., Harada, Y., Sumi, T., Anzai, N., Aizawa, S. & Hasegawa, H. (2011). Membrane transport of sepiapterin and dihydrobiopterin by equilibrative nucleoside transporters: a plausible gateway for the salvage pathway of tetrahydrobiopterin biosynthesis. *Molecular Genetics and Metabolism*, 102, 18–28.

Ouimet, M., Franklin, V., Mak, E., Liao, X., Tabas, I. & Marcel, Y.L. (2011). Autophagy regulates cholesterol efflux from macrophage foam cells via lysosomal acid lipase. *Cell Metabolism*, 13, 655–667.

Owen, R.P., Gray, J.H., Taylor, T.R., Carlson, E.J., Huang, C.C., Kawamoto, M., Johns, S.J., Stryke, D., Ferrin, T.E. & Giacomini, K.M. (2005). Genetic analysis and functional characterization of polymorphisms in the human concentrative nucleoside transporter, CNT2. *Pharmacogenetics and Genomics*, 15, 83–90.

BIBLIOGRAPHY

Ozer, N.K., Negis, Y., Aytan, N., Villacorta, L., Ricciarelli, R., Zingg, J.M. & Azzi, A. (2006). Vitamin E inhibits CD36 scavenger receptor expression in hypercholesterolemic rabbits. *Atherosclerosis*, 184, 15–20.

Packard, R.R.S. & Libby, P. (2008). Inflammation in atherosclerosis: from vascular biology to biomarker discovery and risk prediction. *Clinical Chemistry*, 54, 24–38.

Park, Y.M., Febbraio, M. & Silverstein, R.L. (2009). CD36 modulates migration of mouse and human macrophages in response to oxidized LDL and may contribute to macrophage trapping in the arterial intima. *The Journal of Clinical Investigation*, 119, 136–145.

Patel, H.H. & Insel, P.A. (2009). Lipid rafts and caveolae and their role in compartmentation of redox signaling. *Antioxidants & Redox Signaling*, 11, 1357–1372.

Paterniti, I., Galuppo, M., Mazzon, E., Impellizzeri, D., Esposito, E., Bramanti, P. & Cuzzocrea, S. (2010). Protective effects of apocynin, an inhibitor of NADPH oxidase activity, in splanchnic artery occlusion and reperfusion. *Journal of Leukocyte Biology*, 88, 993–1003.

Pearson, T.A., Mensah, G.A., Alexander, R.W., Anderson, J.L., Cannon, R.O., Criqui, M., Fadl, Y.Y., Fortmann, S.P., Hong, Y., Myers, G.L., Rifai, N., Smith, S.C., Taubert, K., Tracy, R.P., Vinicor, F., Centers for Disease Control and Prevention & Association, A.H. (2003). Markers of inflammation and cardiovascular disease: application to clinical and public health practice: A statement for healthcare professionals from the Centers for Disease Control and Prevention and the American Heart Association.

Petukh, M.G., Semenkova, G.N., Fuchs, D. & Cherenkevich, S.N. (2009). [Pteridine-dependent oxygen activation in neutrophils]. *Tsitologiia*, 51, 824–829.

Pfaffl, M.W., Horgan, G.W. & Dempfle, L. (2002). Relative expression software tool (REST) for group-wise comparison and statistical analysis of relative expression results in real-time PCR. *Nucleic Acids Research*, 30, e36–e36.

Pietarinen-Runtti, P., Lakari, E., Raivio, K.O. & Kinnula, V.L. (2000). Expression of antioxidant enzymes in human inflammatory cells. *American Journal of Physiology, Cell physiology*, 278, C118–25.

Pietsch, A., Erl, W. & Lorenz, R.L. (1996). Lovastatin reduces expression of the combined adhesion and scavenger receptor CD36 in human monocytic cells. *Biochemical Pharmacology*, 52, 433–439.

Podrez, E.A., Abu-Soud, H.M. & Hazen, S.L. (2000). Myeloperoxidase-generated oxidants and atherosclerosis. *Free Radical Biology and Medicine*, 28, 1717–1725.

Potteaux, S., Gautier, E.L., Hutchison, S.B., van Rooijen, N., Rader, D.J., Thomas, M.J., Sorci-Thomas, M.G. & Randolph, G.J. (2011). Suppressed monocyte recruitment drives macrophage removal from atherosclerotic plaques of Apoe-/- mice during disease regression. *The Journal of Clinical Investigation*, 121, 2025–2036.

Quinn, M.T., Parthasarathy, S., Fong, L.G. & Steinberg, D. (1987). Oxidatively modified low density lipoproteins: a potential role in recruitment and retention of monocyte/macrophages during atherogenesis. In *Proceedings of the National Academy of Sciences of the United States of America*, 2995–2998.

R Core Team (2012). R: A Language and Environment for Statistical Computing.

Rahaman, S.O., Lennon, D.J., Febbraio, M., Podrez, E.A., Hazen, S.L. & Silverstein, R.L. (2006). A CD36-dependent signaling cascade is necessary for macrophage foam cell formation. *Cell Metabolism*, 4, 211–221.

Ramprasad, M.P., Terpstra, V., Kondratenko, N., Quehenberger, O. & Steinberg, D. (1996). Cell surface expression of mouse macrosialin and human CD68 and their role as macrophage receptors for oxidized low density lipoprotein. *Proceedings of the National Academy of Sciences of the United States of America*, 93, 14833–14838.

Ray, K.K., Morrow, D.A., Sabatine, M.S., Shui, A., Rifai, N., Cannon, C.P. & Braunwald, E. (2007). Long-term prognostic value of neopterin: a novel marker of monocyte activation in patients with acute coronary syndrome. *Circulation*, 115, 3071–3078.

Razumovitch, J.A., Semenkova, G.N., Fuchs, D. & Cherenkevich, S.N. (2003). Influence of neopterin on the generation of reactive oxygen species in human neutrophils. *FEBS Letters*, 549, 83–86.

Razumovitch, J.A., Fuchs, D., Semenkova, G.N. & Cherenkevich, S.N. (2004). Influence of neopterin on generation of reactive species by myeloperoxidase in human neutrophils. *Biochimica et Biophysica Acta*, 1672, 46–50.

Reibnegger, G., Fuchs, D., Fuith, L.C., Hausen, A., Werner, E.R., Werner-Felmayer, G. & Wachter, H. (1991). Neopterin as a marker for activated cell-mediated immunity: application in malignant disease. *Cancer Detection and Prevention*, 15, 483–490.

Reid, V. & Mitchinson, M.J. (1993). Toxicity of oxidised low density lipoprotein towards mouse peritoneal macrophages in vitro. *Atherosclerosis*, 98, 17–24.

Ren, Y., Silverstein, R.L., Allen, J. & Savill, J. (1995). CD36 gene transfer confers capacity for phagocytosis of cells undergoing apoptosis. *The Journal of Experimental Medicine*, 181, 1857–1862.

Rezk, B.M., Haenen, G.R.M., van der Vijgh, W.J.F. & Bast, A. (2003). Tetrahydrofolate and 5-methyltetrahydrofolate are folates with high antioxidant activity. Identification of the antioxidant pharmacophore. *FEBS Letters*, 555, 601–605.

Ricciarelli, R., Zingg, J.M. & Azzi, A. (2000). Vitamin E reduces the uptake of oxidized LDL by inhibiting CD36 scavenger receptor expression in cultured aortic smooth muscle cells. *Circulation*, 102, 82–87.

Rigotti, A., Acton, S.L. & Krieger, M. (1995). The class B scavenger receptors SR-BI and CD36 are receptors for anionic phospholipids. *Journal of Biological Chemistry*, 270, 16221–16224.

Rios, F.J.O., Gidlund, M. & Jancar, S. (2011). Pivotal role for platelet-activating factor receptor in CD36 expression and oxLDL uptake by human monocytes/macrophages. *Cellular Physiology and Biochemistry*, 27, 363–372.

Rittersma, S.Z.H. (2005). Plaque instability frequently occurs days or weeks before occlusive coronary thrombosis: a pathological thrombectomy study in primary percutaneous coronary intervention. *Circulation*, 111, 1160–1165.

Robinson, J.M. (2008). Reactive oxygen species in phagocytic leukocytes. *Histochemistry and Cell Biology*, 130, 281–297.

Roche, M., Rondeau, P., Singh, N.R., Tarnus, E. & Bourdon, E. (2008). The antioxidant properties of serum albumin. *FEBS Letters*, 582, 5–5.

BIBLIOGRAPHY

Roger, V.L., Go, A.S., Lloyd-Jones, D.M., Adams, R.J., Berry, J.D., Brown, T.M., Carnethon, M.R., Dai, S., De Simone, G., Ford, E.S., Fox, C.S., Fullerton, H.J., Gillespie, C., Greenlund, K.J., Hailpern, S.M., Heit, J.A., Ho, P.M., Howard, V.J., Kissela, B.M., Kittner, S.J., Lackland, D.T., Lichtman, J.H., Lisabeth, L.D., Makuc, D.M., Marcus, G.M., Marelli, A., Matchar, D.B., McDermott, M.M., Meigs, J.B., Moy, C.S., Mozaffarian, D., Mussolino, M.E., Nichol, G., Paynter, N.P., Rosamond, W.D., Sorlie, P.D., Stafford, R.S., Turan, T.N., Turner, M.B., Wong, N.D., Wylie-Rosett, J., Committee, A.H.A.S. & Subcommittee, S.S. (2011). Heart disease and stroke statistics–2011 update: a report from the American Heart Association. *Circulation*, 123, e18–e209.

Ross, R. (1986). The pathogenesis of atherosclerosis–an update. *New England Journal of Medicine*, 314, 488–500.

Ross, R. (1995). Cell biology of atherosclerosis. *Annual Review of Physiology*, 57, 791–804.

Ross, R. (1999). Atherosclerosis – an inflammatory disease. *New England Journal of Medicine*, 340, 115–126.

Ross, R.R. (1993). The pathogenesis of atherosclerosis: a perspective for the 1990s. *Nature*, 362, 801–809.

Rothe, G. & Valet, G. (1990). Flow cytometric analysis of respiratory burst activity in phagocytes with hydroethidine and 2',7'-dichlorofluorescin. *Journal of Leukocyte Biology*, 47, 440–448.

Rudel, L., Lee, R.G. & Cockman, T.L. (2001). Acyl coenzyme A: cholesterol acyltransferase types 1 and 2: structure and function in atherosclerosis. *Current Opinion in Lipidology*, 12, 121–127.

Rusiñol, A.E., Yang, L., Thewke, D., Panini, S.R., Kramer, M.F. & Sinensky, M.S. (2000). Isolation of a somatic cell mutant resistant to the induction of apoptosis by oxidized low density lipoprotein. *The Journal of Biological Chemistry*, 275, 7296–7303.

Rutherford, L.D. & Gieseg, S.P. (2012). 7-ketocholesterol is not cytotoxic to U937 cells when incorporated into acetylated low density lipoprotein. *Lipids*, 47, 239–247.

Ryan, L., O'Callaghan, Y.C. & O'Brien, N.M. (2003). Generation of an oxidative stress precedes caspase activation during 7 beta-hydroxycholesterol-induced apoptosis in U937 cells. *Journal of Biochemical and Molecular Toxicology*, 18, 50–59.

Sagara, Y., Dargusch, R., Chambers, D., Davis, J., Schubert, D. & Maher, P. (1998). Cellular mechanisms of resistance to chronic oxidative stress. *Free Radical Biology and Medicine*, 24, 1375–1389.

Salvayre, R., Auge, N., Benoist, H. & Nègre-Salvayre, A. (2002). Oxidized low-density lipoprotein-induced apoptosis. *Biochimica et Biophysica Acta*, 1585, 213–221.

Sando, G.N. & Rosenbaum, L.M. (1985). Human lysosomal acid lipase/cholesteryl ester hydrolase. Purification and properties of the form secreted by fibroblasts in microcarrier culture. *Journal of Biological Chemistry*, 260, 15186–15193.

Schobersberger, W., Hoffmann, G., Hobisch-Hagen, P., Bock, G., Volkl, H., Baier-Bitterlich, G., Wirleitner, B., Wachter, H. & Fuchs, D. (1996). Neopterin and 7,8-dihydroneopterin induce apoptosis in the rat alveolar epithelial cell line L2. *FEBS Letters*, 397, 263–268.

Schoedon, G., Troppmair, J., ADOLF, G., Huber, C. & Niederwieser, A. (1986). Interferon-gamma enhances biosynthesis of pterins in peripheral blood mononuclear cells by induction of GTP-cyclohydrolase I activity. *Journal of Interferon Research*, 6, 697–703.

Schroecksnadel, S., Jenny, M., Kurz, K., Klein, A., Ledochowski, M., Uberall, F. & Fuchs, D. (2010). LPS-induced NF-kappaB expression in THP-1Blue cells correlates with neopterin production and activity of indoleamine 2,3-dioxygenase. *Biochemical and Biophysical Research Communications*, 399, 642–646.

Seimon, T. & Tabas, I. (2009). Mechanisms and consequences of macrophage apoptosis in atherosclerosis. *Journal of Lipid Research*, 50, S382–7.

Sekiya, M., Osuga, J.I., Igarashi, M., Okazaki, H. & Ishibashi, S. (2011). The role of neutral cholesterol ester hydrolysis in macrophage foam cells. *Journal of Atherosclerosis and Thrombosis*, 18, 359–364.

Sghiri, R., Feinberg, J., Thabet, F., Dellagi, K., Boukadida, J., Ben Abdelaziz, A., Casanova, J.L. & Barbouche, M.R. (2005). Gamma interferon is dispensable for neopterin production in vivo. *Clinical and Diagnostic Laboratory Immunology*, 12, 1437–1441.

Shaikh, S., Brittenden, J., Lahiri, R., Brown, P., Thies, F. & Wilson, H.M. (2012). Macrophage subtypes in symptomatic carotid artery and femoral artery plaques. *European Journal of Vascular and Endovascular Surgery*, 44, 491–497.

Shapiro, H.M. (2003). *Practical flow cytometry*. Wiley-Liss, 4th edn.

Shchepetkina, A.A. (2008). Variation in antioxidant, oxidative and inflammatory biomarkers in atherosclerotic plaque, unpublished honour's thesis, University of Canterbury, Christchurch, New Zealand.

Sheehan, A.L., Carrell, S., Johnson, B., Stanic, B., Banfi, B. & Miller, F.J. (2011). Role for Nox1 NADPH oxidase in atherosclerosis. *Atherosclerosis*.

Shen, L. & Sevanian, A. (2001). OxLDL induces macrophage gamma-GCS-HS protein expression: a role for oxLDL-associated lipid hydroperoxide in GSH synthesis. *Journal of Lipid Research*, 42, 813–823.

Silverstein, R.L., Li, W., Park, Y.M. & Rahaman, S.O. (2010). Mechanisms of cell signaling by the scavenger receptor CD36: implications in atherosclerosis and thrombosis. *Transactions of the American Clinical and Climatological Association*, 121, 206–220.

Simard, S., Maurais, É., Gilbert, C. & Tremblay, M.J. (2008). LPS reduces HIV-1 replication in primary human macrophages partly through an endogenous production of type I interferons. *Clinical Immunology*, 127, 198–205.

Singh, U. & Jialal, I. (2006). Oxidative stress and atherosclerosis. *Pathophysiology*, 13, 129–142.

Siow, R.C., Richards, J., Pedley, K., Leake, D.S. & Mann, G. (1999). Vitamin C protects human vascular smooth muscle cells against apoptosis induced by moderately oxidized LDL containing high levels of lipid hydroperoxides. *Arteriosclerosis Thrombosis and Vascular Biology*, 19, 2387–2394.

Siow, R.C.M., Sato, H., Leake, D.S., Pearson, J.D., Bannai, S. & Mann, G. (1998). Vitamin C protects human arterial smooth muscle cells against atherogenic lipoproteins : effects of antioxidant vitamins C and E on oxidized LDL induced adaptive increases in cystine transport and glutathione. *Arteriosclerosis Thrombosis and Vascular Biology*, 18, 1662–1670.

Skulachev, V.P. (2006). Bioenergetic aspects of apoptosis, necrosis and mitoptosis. *Apoptosis*, 11, 473–485.

BIBLIOGRAPHY

Smith, C., Mitchinson, M.J., Aruoma, O. & Halliwell, B. (1992). Stimulation of lipid peroxidation and hydroxyl-radical generation by the contents of human atherosclerotic lesions. *Biochemical Journal*, 286, 901.

Smith, J.D., Trogan, E., Ginsberg, M., Grigaux, C., Tian, J. & Miyata, M. (1995). Decreased atherosclerosis in mice deficient in both macrophage colony-stimulating factor (op) and apolipoprotein E. *Proceedings of the National Academy of Sciences of the United States of America*, 92, 8264–8268.

Soler, C., García-Manteiga, J., Valdés, R., Xaus, J., Comalada, M., Casado, F.J., Pastor-Anglada, M., Celada, A. & Felipe, A.A. (2001). Macrophages require different nucleoside transport systems for proliferation and activation. *FASEB Journal*, 15, 1979–1988.

Speth, C., Stöckl, G., Fuchs, D., Wirleitner, B., Widner, B., Würzner, R., Mohsenipour, I., Lass-Flörl, C. & Dierich, M.P. (2000). Inflammation marker 7,8-dihydroneopterin induces apoptosis of neurons and glial cells: a potential contribution to neurodegenerative processes. *Immunobiology*, 202, 460–476.

Stary, H.C., Blankenhorn, D.H., Chandler, A.B., Glagov, S., Insull, W., Richardson, M., Rosenfeld, M.E., Schaffer, S.A., Schwartz, C.J. & Wagner, W.D. (1992). A definition of the intima of human arteries and of its atherosclerosis-prone regions. A report from the Committee on Vascular Lesions of the Council on Arteriosclerosis, American Heart Association. *Arteriosclerosis and Thrombosis*, 12, 120–134.

Stary, H.C., Chandler, A.B., Dinsmore, R.E., Fuster, V., Glagov, S., Insull, W., Rosenfeld, M.E., Schwartz, C.J., Wagner, W.D. & Wissler, R.W. (1995). A definition of advanced types of atherosclerotic lesions and a histological classification of atherosclerosis. *Circulation*, 92, 1355–1374.

Stefanska, J. & Pawliczak, R. (2008). Apocynin: molecular aptitudes. *Mediators of Inflammation*, 2008, 1–10.

Stein, O. & Stein, Y. (1975). Surface binding and interiorization of homologous and heterologous serum lipoproteins by rat aortic smooth muscle cells in culture. *Biochimica et Biophysica Acta*, 398, 377–384.

Steinberg, D. (2009). The LDL modification hypothesis of atherogenesis: an update. *Journal of Lipid Research*, 50, S376–81.

Steinberg, D. & Witztum, J.L. (2010). Oxidized low-density lipoprotein and atherosclerosis. *Arteriosclerosis Thrombosis and Vascular Biology*, 30, 2311–2316.

Steinberg, D., Parthasarathy, S., Carew, T.E., Khoo, J.C. & Witztum, J.L. (1989). Beyond cholesterol. Modifications of low-density lipoprotein that increase its atherogenicity. *The New England Journal of Medicine*, 320, 915–924.

Steinbrecher, U.P. (1999). Receptors for oxidized low density lipoprotein. *Biochimica et Biophysica Acta*, 1436, 279–298.

Stocker, R. & Keaney, J.F. (2004). Role of oxidative modifications in atherosclerosis. *Physiological Reviews*, 84, 1381–1478.

Stolk, J., Hiltermann, T.J., Dijkman, J.H. & Verhoeven, A.J. (1994). Characteristics of the inhibition of NADPH oxidase activation in neutrophils by apocynin, a methoxy-substituted catechol. *American Journal of Respiratory Cell and Molecular Biology*, 11, 95–102.

Suarna, C., Dean, R.T., May, J. & Stocker, R. (1995). Human atherosclerotic plaque contains both oxidized lipids and relatively large amounts of alpha-tocopherol and ascorbate. *Arteriosclerosis Thrombosis and Vascular Biology*, 15, 1616–1624.

Sucher, R., Schroecksnadel, K., Weiss, G., Margreiter, R., Fuchs, D. & Brandacher, G. (2010). Neopterin, a prognostic marker in human malignancies. *Cancer Letters*, 287, 13–22.

Suginohara, Y., Miyazaki, A., Hakamata, H., Sakamoto, Y., Ohta, T., Matsuda, I. & Horiuchi, S. (1996). The heparin-bound fraction of human lipoprotein-deficient serum inhibits endocytic uptake of oxidized low density lipoprotein by macrophages. *Atherosclerosis*, 120, 167–179.

Sugioka, K., Naruko, T., Matsumura, Y., Shirai, N., Hozumi, T., Yoshiyama, M. & Ueda, M. (2010). Neopterin and atherosclerotic plaque instability in coronary and carotid arteries. *Journal of Atherosclerosis and Thrombosis*, 17, 1115–1121.

Sugiyama, S., Okada, Y., Sukhova, G.K., Virmani, R., Heinecke, J.W. & Libby, P. (2001). Macrophage myeloperoxidase regulation by granulocyte macrophage colony-stimulating factor in human atherosclerosis and implications in acute coronary syndromes. *American Journal of Pathology*, 158, 879–891.

Sukhanov, S., Higashi, Y., Shai, S.Y., Itabe, H., Ono, K., Parthasarathy, S. & Delafontaine, P. (2006). Novel effect of oxidized low-density lipoprotein: cellular ATP depletion via downregulation of glyceraldehyde-3-phosphate dehydrogenase. *Circulation Research*, 99, 191–200.

Sundstrom, C. & Nilsson, K. (1976). Establishment and characterization of a human histiocytic lymphoma cell line (U-937). *International Journal of Cancer*, 17, 565–577.

Suzuki, H., Kurihara, Y., Takeya, M., Kamada, N., Kataoka, M., Jishage, K., Ueda, O., Sakaguchi, H., Higashi, T., Suzuki, T., Takashima, Y., Kawabe, Y., Cynshi, O., Wada, Y., Honda, M., Kurihara, H., Aburatani, H., Doi, T., Matsumoto, A., Azuma, S., Noda, T., Toyoda, Y., Itakura, H., Yazaki, Y. & Kodama, T. (1997). A role for macrophage scavenger receptors in atherosclerosis and susceptibility to infection. *Nature*, 386, 292–296.

Tarpey, M. (2004). Methods for detection of reactive metabolites of oxygen and nitrogen: in vitro and in vivo considerations. *American Journal of Physiology: Regulatory, Integrative and Comparative Physiology*, 286, 431R–444.

Taylor, F., Ward, K., Moore, T.H., Burke, M., Davey Smith, G., Casas, J.P. & Ebrahim, S. (2011). Statins for the primary prevention of cardiovascular disease. *Cochrane Database of Systematic Reviews (Online)*, CD004816.

Terasaka, N., Wang, N., Yvan-Charvet, L. & Tall, A.R. (2007). High-density lipoprotein protects macrophages from oxidized low-density lipoprotein-induced apoptosis by promoting efflux of 7-ketocholesterol via ABCG1. *Proceedings of the National Academy of Sciences of the United States of America*, 104, 15093–15098.

Terpstra, V., Kondratenko, N. & Steinberg, D. (1997). Macrophages lacking scavenger receptor A show a decrease in binding and uptake of acetylated low-density lipoprotein and of apoptotic thymocytes, but not of oxidatively damaged red blood cells. *Proceedings of the National Academy of Sciences of the United States of America*, 94, 8127–8131.

Tontonoz, P., Nagy, L., Alvarez, J.G., Thomazy, V.A. & Evans, R.M. (1998). PPARgamma promotes monocyte/macrophage differentiation and uptake of oxidized LDL. *Cell*, 93, 241–252.

Troyano, A., Sancho, P., Fernandez, C., De Blas, E., Bernardi, P. & Aller, P. (2003). The selection between apoptosis and necrosis is differentially regulated in hydrogen peroxide-treated and glutathione-depleted human promonocytic cells. *Cell Death and Differentiation*, 10, 889–898.

Turrens, J. (2003). Mitochondrial formation of reactive oxygen species. *The Journal of Physiology*, 552, 335–344.

Urban, T.J. (2005). Functional genomics of membrane transporters in human populations. *Genome Research*, 16, 223–230.

Valko, M., Leibfritz, D., Moncol, J., Cronin, M.T.D., Mazur, M. & Telser, J. (2007). Free radicals and antioxidants in normal physiological functions and human disease. *The International Journal of Biochemistry & Cell Biology*, 39, 44–84.

Vásquez-Vivar, J. (2009). Tetrahydrobiopterin, superoxide, and vascular dysfunction. *Free Radical Biology and Medicine*, 47, 1108–1119.

Vejux, A. & Lizard, G. (2009). Cytotoxic effects of oxysterols associated with human diseases: Induction of cell death (apoptosis and/or oncosis), oxidative and inflammatory activities, and phospholipidosis. *Molecular Aspects of Medicine*, 30, 153–170.

Verheye, S., Martinet, W., Kockx, M.M., Knaapen, M.W.M., Salu, K., Timmermans, J.P., Ellis, J.T., Kilpatrick, D.L. & De Meyer, G.R.Y. (2007). Selective clearance of macrophages in atherosclerotic plaques by autophagy. *Journal of the American College of Cardiology*, 49, 706–715.

Vlodavsky, I., Fielding, P., Fielding, C. & Gospodarowicz, D. (1977). Role of contact inhibition in the regulation of receptor-mediated uptake of low density lipoprotein in cultured vascular endothelial cells. *Proceedings of the National Academy of Sciences of the United States of America*, 75, 356–360.

Wachter, H., Fuchs, D., Hausen, A., Reibnegger, G. & Werner, E.R. (1989). Neopterin as marker for activation of cellular immunity: immunologic basis and clinical application. *Advances in Clinical Chemistry*, 27, 81–141.

Waddington, E.I., Croft, K.D., Sienuarine, K., Latham, B. & Puddey, I.B. (2003). Fatty acid oxidation products in human atherosclerotic plaque: an analysis of clinical and histopathological correlates. *Atherosclerosis*, 167, 111–120.

Waldo, S.W., Li, Y., Buono, C., Zhao, B., Billings, E.M., Chang, J. & Kruth, H.S. (2008). Heterogeneity of human macrophages in culture and in atherosclerotic plaques. *The American Journal of Pathology*, 172, 1112–1126.

Walter, R., Schaffner, A. & Schoedon, G. (2001). Tetrahydrobiopterin in the vascular system. *Pteridines*, 12, 93–120.

Wang, Y., Castoreno, A.B., Stockinger, W. & Nohturfft, A. (2005). Modulation of endosomal cholesteryl ester metabolism by membrane cholesterol. *Journal of Biological Chemistry*, 280, 11876–11886.

Wang, Y., Qiao, M., Mieyal, J.J., Asmis, L.M. & Asmis, R. (2006). Molecular mechanism of glutathione-mediated protection from oxidized low-density lipoprotein-induced cell injury in human macrophages: role of glutathione reductase and glutaredoxin. *Free Radical Biology and Medicine*, 41, 775–785.

Weisberg, S.P. (2003). Obesity is associated with macrophage accumulation in adipose tissue. *The Journal of Clinical Investigation*, 112, 1796–1808.

Weiss, G., Glaser, K., Kronberger, P., Ambach, E., Fuchs, D., Bodner, E. & Wachter, H. (1992). Distinct distributions of D-erythro-neopterin in arteries and veins and its recovery by an enterohepatic circulation. *Biological Chemistry Hoppe-Seyler*, 373, 289–294.

Weiss, G., Fuchs, D., Hausen, A., Reibnegger, G., Werner, E.R., Werner-Felmayer, G., Semenitz, E., Dierich, M.P. & Wachter, H. (1993). Neopterin modulates toxicity mediated by reactive oxygen and chloride species. *FEBS Letters*, 321, 89–92.

Weiss, G., Willeit, J., Kiechl, S., Fuchs, D., Jarosch, E., Oberhollenzer, F., Reibnegger, G., Tilz, G.P., Gerstenbrand, F. & Wachter, H. (1994). Increased concentrations of neopterin in carotid atherosclerosis. *Atherosclerosis*, 106, 263–271.

Weiss, G., Murr, C., Zoller, H., Haun, M., Widner, B., Ludescher, C. & Fuchs, D. (1999). Modulation of neopterin formation and tryptophan degradation by Th1- and Th2-derived cytokines in human monocytic cells. *Clinical and Experimental Immunology*, 116, 435–440.

Werner, E.R., Werner-Felmayer, G., Fuchs, D., Hausen, A., Reibnegger, G. & Wachter, H. (1989). Parallel induction of tetrahydrobiopterin biosynthesis and indoleamine 2,3-dioxygenase activity in human cells and cell lines by interferon-gamma. *The Biochemical Journal*, 262, 861–866.

Werner, E.R., Werner-Felmayer, G., Fuchs, D., Hausen, A., Reibnegger, R., Yim, J.J. & Wachter, H. (1991). Biochemistry and function of pteridine synthesis in human and murine macrophages. *Pathobiology*, 59, 276–279.

Werner-Felmayer, G., Werner, E.R., Fuchs, D., Hausen, A., Reibnegger, G. & Wachter, H. (1990). Neopterin formation and tryptophan degradation by a human myelomonocytic cell line (THP-1) upon cytokine treatment. *Cancer Research*, 50, 2863–2867.

Werner-Felmayer, G., Werner, E.R., Fuchs, D., Hausen, A., Reibnegger, G., Schmidt, K., Weiss, G. & Wachter, H. (1993). Pteridine biosynthesis in human endothelial cells. Impact on nitric oxide-mediated formation of cyclic GMP. *The Journal of Biological Chemistry*, 268, 1842–1846.

Werner-Felmayer, G., Baier-Bitterlich, G., Fuchs, D., Hausen, A., Murr, C., Reibnegger, G., Werner, E.R. & Wachter, H. (1995). Detection of bacterial pyrogens on the basis of their effects on gamma interferon-mediated formation of neopterin or nitrite in cultured monocyte cell lines. *Clinical and Diagnostic Laboratory Immunology*, 2, 307–313.

Wick, G., Knoflach, M. & Xu, Q. (2004). Autoimmune and inflammatory mechanisms in atherosclerosis. *Annual Review of Immunology*, 22, 361–403.

Widner, B., Mayr, C., Wirleitner, B. & Fuchs, D. (2000). Oxidation of 7,8-dihydroneopterin by hypochlorous acid yields neopterin. *Biochemical and Biophysical Research Communications*, 275, 307–311.

Williams, K.J. & Tabas, I. (1998). The response-to-retention hypothesis of atherogenesis reinforced. *Current Opinion in Lipidology*, 9, 471–474.

Wind, S., Beuerlein, K., Eucker, T., Müller, H., Scheurer, P., Armitage, M.E., Ho, H., Schmidt, H. & Wingler, K. (2010). Comparative pharmacology of chemically distinct NADPH oxidase inhibitors. *British Journal of Pharmacology*, 161, 885–898.

Wingler, K., Hermans, J., Schiffers, P., Moens, A.L., Paul, M. & Schmidt, H. (2011). NOX1, 2, 4, 5: counting out oxidative stress. *British Journal of Pharmacology*, 164, 866–883.

Wintergerst, E.S., Jelk, J. & Asmis, R. (1998). Differential expression of CD14, CD36 and the LDL receptor on human monocyte-derived macrophages. A novel cell culture system to study macrophage differentiation and heterogeneity. *Histochemistry and Cell Biology*, 110, 231–241.

Wintergerst, E.S., Jelk, J., Rahner, C. & Asmis, R. (2000). Apoptosis induced by oxidized low density lipoprotein in human monocyte-derived macrophages involves CD36 and activation of caspase-3. *European Journal of Biochemistry / FEBS*, 267, 6050–6059.

BIBLIOGRAPHY

Wirleitner, B., Baier-Bitterlich, G., Böck, G., Widner, B. & Fuchs, D. (1998). 7,8-Dihydroneopterin-induced apoptosis in Jurkat T lymphocytes: a comparison with anti-Fas- and hydrogen peroxide-mediated cell death. *Biochemical Pharmacology*, 56, 1181–1187.

Wirleitner, B., Czaputa, R., Oettl, K., Bock, G., Widner, B., Reibnegger, G., Baier, G., Fuchs, D. & Baier-Bitterlich, G. (2001). Induction of apoptosis by 7,8-dihydroneopterin: involvement of radical formation. *Immunobiology*, 203, 629–641.

Wirleitner, B., Reider, D., Ebner, S., Böck, G., Widner, B., Jaeger, M., Schennach, H., Romani, N. & Fuchs, D. (2002). Monocyte-derived dendritic cells release neopterin. *Journal of Leukocyte Biology*, 72, 1148–1153.

Wong, B.X.W., Kyle, R.A., Croft, K.D., Quinn, C.M., Jessup, W. & Yeap, B.B. (2011). Modulation of macrophage fatty acid content and composition by exposure to dyslipidemic serum in vitro. *Lipids*, 46, 371–380.

Wosniak, J., Santos, C.X.C., Kowaltowski, A.J. & Laurindo, F.R.M. (2009). Cross-talk between mitochondria and NADPH oxidase: effects of mild mitochondrial dysfunction on angiotensin II-mediated increase in Nox isoform expression and activity in vascular smooth muscle cells. *Antioxidants & Redox Signaling*, 11, 1265–1278.

Yang, Y.T. (2009). *Mechanism and inhibition of hypochlorous acid-mediated cell death in human monocyte-derived macrophages*. Ph.D. thesis, University of Canterbury, Christchurch, New Zealand.

Yang, Y.t.T., Whiteman, M. & Gieseg, S.P. (2012). Intracellular glutathione protects human monocyte-derived macrophages from hypochlorite damage. *Life Sciences*, 90, 682–688.

Ylä-Herttuala, S., Palinski, W., Rosenfeld, M.E., Parthasarathy, S., Carew, T.E., Butler, S., Witztum, J.L. & Steinberg, D. (1989). Evidence for the presence of oxidatively modified low density lipoprotein in atherosclerotic lesions of rabbit and man. *The Journal of Clinical Investigation*, 84, 1086–1095.

Yoshida, H., Kondratenko, N., Green, S., Steinberg, D. & Quehenberger, O. (1998). Identification of the lectin-like receptor for oxidized low-density lipoprotein in human macrophages and its potential role as a scavenger receptor. *Biochemical Journal*, 334 (Pt 1), 9–13.

Yuan, X.M., Li, W., Olsson, A.G. & Brunk, U.T. (1997). The toxicity to macrophages of oxidized low-density lipoprotein is mediated through lysosomal damage. *Atherosclerosis*, 133, 153–161.

Yvan-Charvet, L., Wang, N. & Tall, A.R. (2010). Role of HDL, ABCA1, and ABCG1 transporters in cholesterol efflux and immune responses. *Arteriosclerosis Thrombosis and Vascular Biology*, 30, 139–143.

Zanotti, I., Favari, E. & Bernini, F. (2012). Cellular cholesterol efflux pathways: impact on intracellular lipid trafficking and methodological considerations. *Current Pharmaceutical Biotechnology*, 13, 292–302.

Zeibig, S., Li, Z., Wagner, S., Holthoff, H.P., Ungerer, M., Bültmann, A., Uhland, K., Vogelmann, J., Simmet, T., Gawaz, M. & Münch, G. (2011). Effect of the oxLDL binding protein Fc-CD68 on plaque extension and vulnerability in atherosclerosis. *Circulation Research*, 108, 695–703.

Zhang, M., Aguilera, D., Das, C., Vasquez, H., Zage, P., Gopalakrishnan, V. & Wolff, J. (2006). Measuring cytotoxicity: a new perspective on LC50. *Anticancer Research*, 27, 35–38.

Zhang, Y.l., Cao, Y.j., Zhang, X., Liu, H.h., Tong, T., Xiao, G.d., Yang, Y.p. & Liu, C.f. (2010). The autophagy-lysosome pathway: A novel mechanism involved in the processing of oxidized LDL in human vascular endothelial cells. *Biochemical and Biophysical Research Communications*, 394, 6–6.

Zhao, H., Joseph, J., Fales, H.M., Sokoloski, E.A., Levine, R.L., Vásquez-Vivar, J. & Kalyanaraman, B. (2005). Detection and characterization of the product of hydroethidine and intracellular superoxide by HPLC and limitations of fluorescence. *Proceedings of the National Academy of Sciences of the United States of America*, 102, 5727–5732.

Zhong, J.K., Guo, Z.G., Li, C., Wang, Z.K., Lai, W.Y. & Tu, Y. (2010). Probucol alleviates atherosclerosis and improves high density lipoprotein function. *Lipids in Health and Disease*, 10, 210–210.

Zmijewski, J.W., Moellering, D.R., Le Goffe, C., Landar, A., Ramachandran, A. & Darley-Usmar, V.M. (2005). Oxidized LDL induces mitochondrially associated reactive oxygen/nitrogen species formation in endothelial cells. *American Journal of Physiology Heart and Circulatory Physiology*, 289, H852–61.

Appendix A

Method development and validation

Experimental techniques that were new to this laboratory were developed and validated during the course of this research project. These included: *PrestoBlue*™ cell viability test, *Accutase*™–facilitated detachment for flow cytometry and RT-qPCR protocol.

Cell viability assay comparison

Cell metabolism and viability were routinely measured via MTT assay, which utilises the reducing power of cellular metabolic products like NADH and NADPH (Mosmann, 1983; Shen & Sevanian, 2001). The reduced formazan product is quantified spectrophotometrically and provides a reliable measure of both the number of cells and their metabolic activity. Terminal nature of the measurement (both formazan crystal toxicity to cells and the requirement to solubilise them with a detergent) is a disadvantage of the MTT assay. *PrestoBlue*™ (Invitrogen) also measures the reducing power of cells per well based on their ability to reduce resazurin. It has the advantage of being non-toxic and can be measured without cell lysis. *PrestoBlue*™ was compared to MTT to establish the level of similarity between the two assays. MTT and *PrestoBlue*™ produced identical results of HMDM cell density measurement (fig. A.1). The measurement of cell viability upon exposure to toxic oxLDL treatment (2 mg/mL at different concentrations of extracellular serum) was also very similar for both assays (fig. A.2). These results indicated that the two assays could be interchanged without the need for correction.

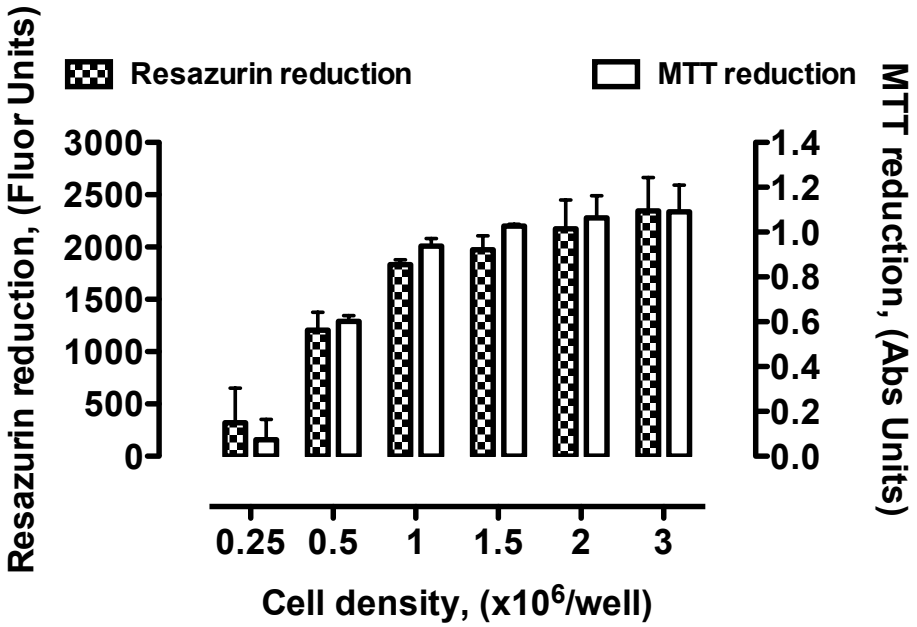

Figure A.1: Comparison of MTT and resazurin (*PrestoBlue*™) reduction assays in determining HMDM cell density.

HMDM cells were seeded at various cell densities in 48 well plates (with an initial pulse of 25 ng/well GM-CSF) and assayed for cell number/viability by MTT (clear bars) and resazurin (checked bars) reduction 11 days after seeding. Results are displayed as mean ± SEM of triplicate measurements from a single experiment. The results of the two assays were not significantly different (one-factor ANOVA with Bonferroni pairwise comparison).

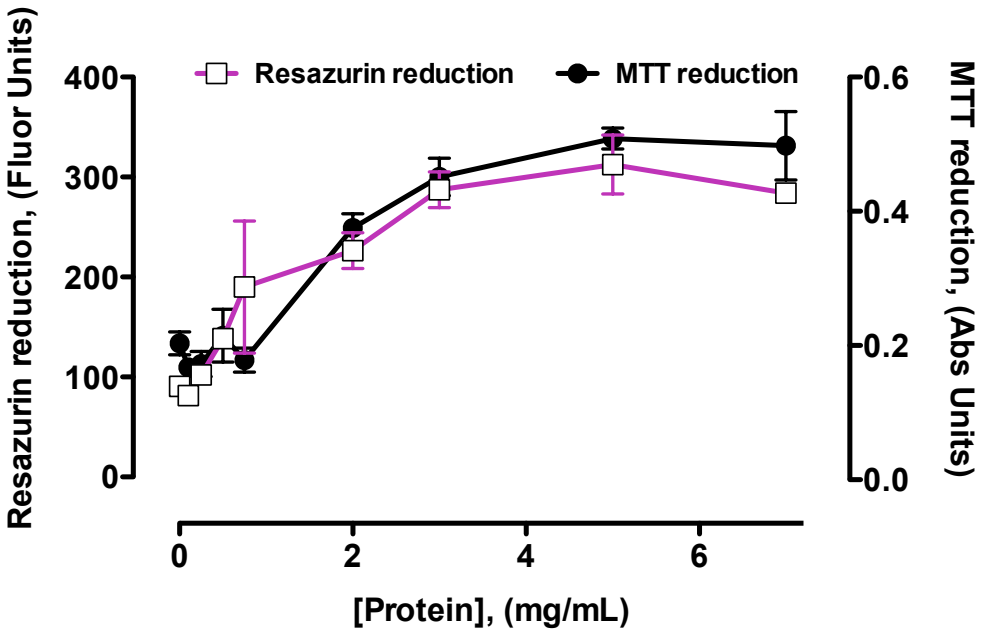

Figure A.2: Comparison of MTT and resazurin (*PrestoBlue*™) reduction assays in determining HMDM cell viability after oxLDL treatment.
HMDM (1x10^6 cells/well) treated with 2 mg/mL oxLDL in the presence of different concentrations of serum. MTT (filled circles) and resazurin (empty squares) reduction was performed concurrently on identical samples. Results are displayed as mean ± SEM of triplicate measurements from a single experiment. The results of the two assays were not significantly different (one-factor ANOVA with Bonferroni pairwise comparison)

Accutase™–facilitated harvesting of HMDM cells

Several analyses in this project required HMDM cell detachment from the plate. These included flow cytometry and experiments with specific HMDM cell density. A method for HMDM detachment with *Accutase*™ was, therefore, adopted from the one kindly suggested by Dr. H. Medbury (Sydney Medical School, Australia). Briefly, the adherent HMDM cells were rinsed with PBS and incubated with *Accutase*™ (130μL per well for 48 well plate) for 20 min at 37 °C. The cells were observed through the inverted microscope before and after being pipetted to dislodge the adherent cells (7-10 times with a 1mL pipette). HMDM cell detachment was facilitated by *Accutase*™ as seen from the figures A.3, A.4 and A.5. After incubation with *Accutase*™ the cells appeared more round and less spread (fig. A.3b). Pipetting, accompanied by light scraping of the well, was effective at dislodging the majority of cells (figures A.3c and A.4b). *Accutase*™ treatment was significantly more effective than control PBS at dislodging HMDM cells (fig. A.5). Moreover, *Accutase*™ was not toxic to HMDM cells up to 2h 50 minutes of treatment (fig. A.6). HMDM cells re-attached effectively when seeded into new plates after being dislodged with *Accutase*™ (fig. A.7)

[**A**] [**B**]

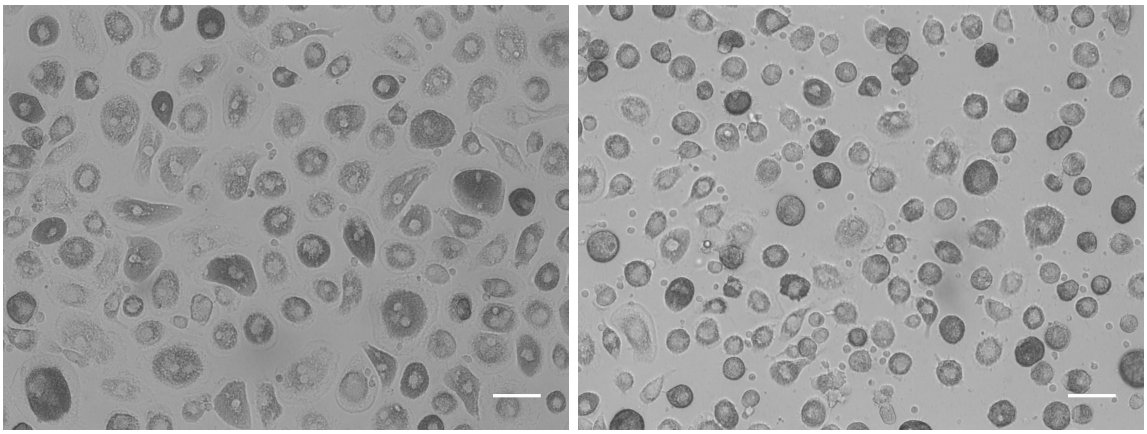

[**C**]

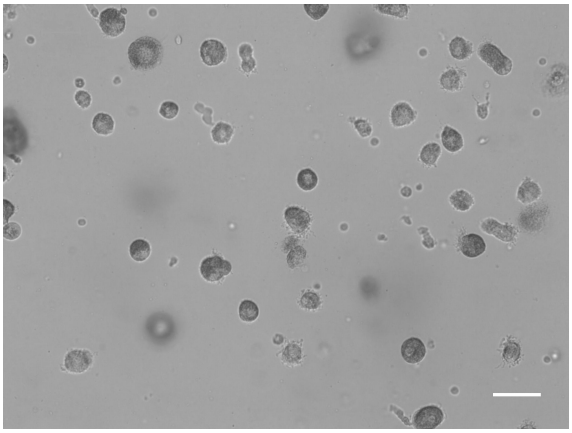

Figure A.3: HMDM cell morphology before and after *Accutase*™ treatment. HMDM were rinsed with warm PBS and treated with *Accutase*™ for 20 min, after which the cells were pipetted x10 to dislodge the adherent macrophages and aliquoted for further processing. **A**: before *Accutase*™ **B**: after incubation with *Accutase*™ **C**: after pipetting. Scale bar = 50 μm.

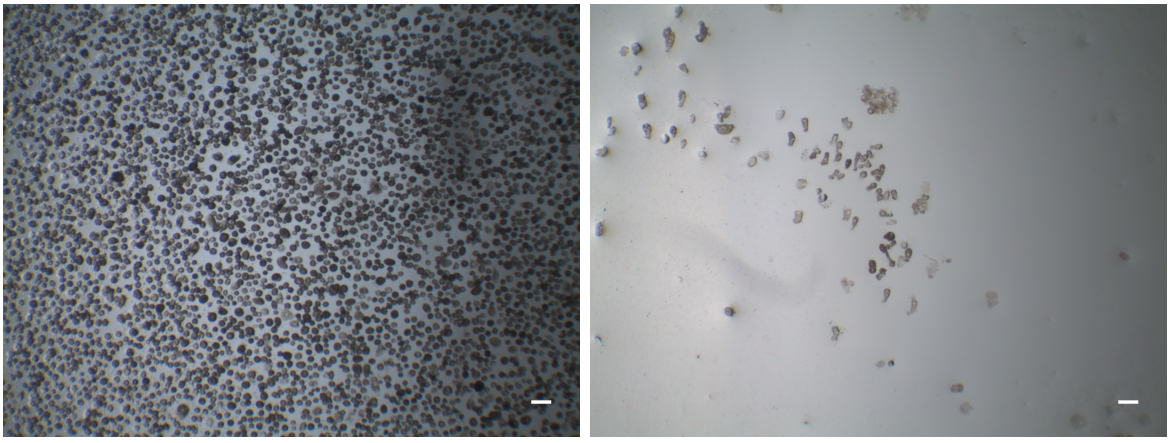

(a) before **(b)** after

Figure A.4: *Accutase*™ treatment of HMDM removes the majority of cells. HMDM were treated with *Accutase*™ (a) and removed by vigorous pipetting (b). Scale bar = 100 μm.

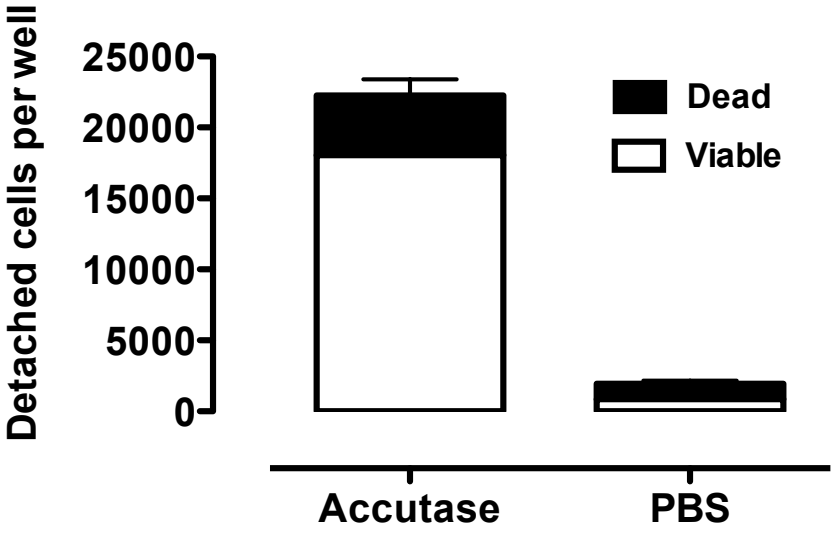

Figure A.5: Efficiency of *Accutase*™–facilitated detachment of HMDM cells. HMDM, cultured in 48 well plate in the whole medium were rinsed with PBS and incubated with either *Accutase*™ or PBS for 20 minutes. Cell number was counted with trypan blue assay after gentle re-pipetting of the cell suspension.

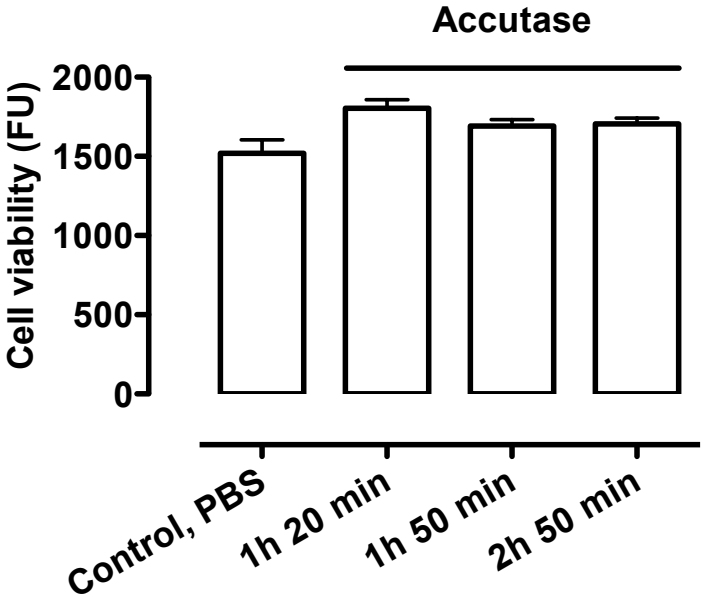

Figure A.6: *Accutase*™ **is not toxic to HMDM cells up to 3 hours after treatment.**
HMDM, cultured in 48 well plate (Cellstar®) in the whole medium were rinsed with PBS and incubated with either *Accutase*™ or whole medium followed by PBS for the indicated time. Cellular viability was assessed with *PrestoBlue*™ reagent added directly to the wells. No significant difference between the treatments was detected.

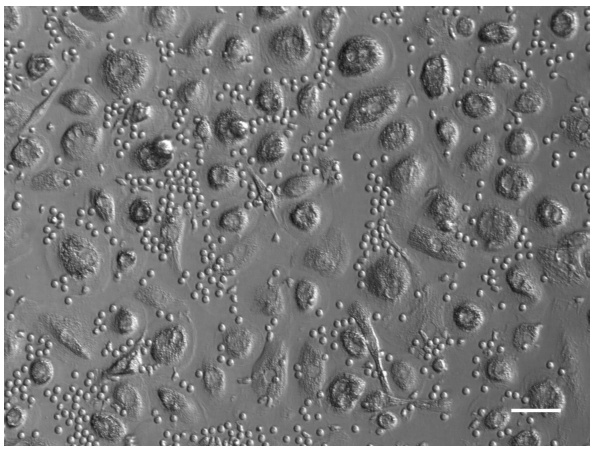

Figure A.7: HMDM cells re-attach effectively after *Accutase*™–facilitated removal.
HMDM were lifted up with *Accutase*™, re-plated at 2 x 10^5 cells/well (48 well), allowed to adhere and adjust for 19 hours and photographed. Scale bar = 50 μm.

PCR method development

Primer validation

Primer pairs for CD36 and a range of potential housekeeping genes were obtained from the published literature. CD36 and β-actin primer sequences were kindly provided by Wong *et al.* (2011); HPRT and RPL13A were from Jedidi *et al.* (2006); β-microglobulin and GAPDH were from Kielar *et al.* (2001) and e-GAPDH primers were from Lai *et al.* (2003). All primer pair sequences and expected amplicon sizes are presented in table A.1, together with actual amplicon sizes and melting temperatures, which were determined experimentally.

All primer pairs were checked for amplification success and amplicon specificity.

Table A.1: List of PCR primers tested.

Gene	Abbr.	Expected size, bp	Amplified size, bp	Melting temp., °C	Forward primer, Reverse primer
CD36 receptor	CD36	190	200	82	CTGGGGCTGTCATTGGTG TGTGGATTTTGCACATCA
β-Microglobulin	B2M	236	140	82.7	CTCGCGCTACTCTCTCTTTCT TGTCGGATTGATGAAACCCAG
Glyceraldehyde-3-phosphate dehydrogenase	GAPDH	270	270	90.1	TTGGTATCGTGGAAGGACTCA TGTCATCATATTTGGCAGGTTT
Ribosomal protein L13A	RPL13A	126	125	82	CCTGGAGGAGAAGAGGAAAGAGA TTGAGGACCTCTGTGTATTTGTCAA
Hypoxanthine phosphoribosyl transferase 1	HPRT	94	95	82	TGACACTGGCAAAACAATGCA GGTCCTTTTCACCAGCAAGCT
Glyceraldehyde-3-phosphate dehydrogenase	GAPDH-e	127	120	88	GGTGGTCTCCTCTGACTTCAACA GTTGCTGTAGCCAAATTCGTTGT
β-Actin	actin	352	330	90.5	CTGGCACCACACCTTCTA GGTGGTGAAGCTGTAGCC

Undiluted cDNA from untreated HMDM cells was amplified in the presence of CD36 and potential reference gene primers to verify the amplification of the desired product. The PCR products were electrophoresed on an agarose gel and visualised under the UV illumination. Figure A.8 presents the gel, and the calculated amplification product sizes are incorporated into table A.1. All primer pairs specifically amplified the desired products (see expected vs. amplified in the table). Amplicon melting temperatures were also determined, as these were used to confirm product identity post-RT qPCR (table A.1).

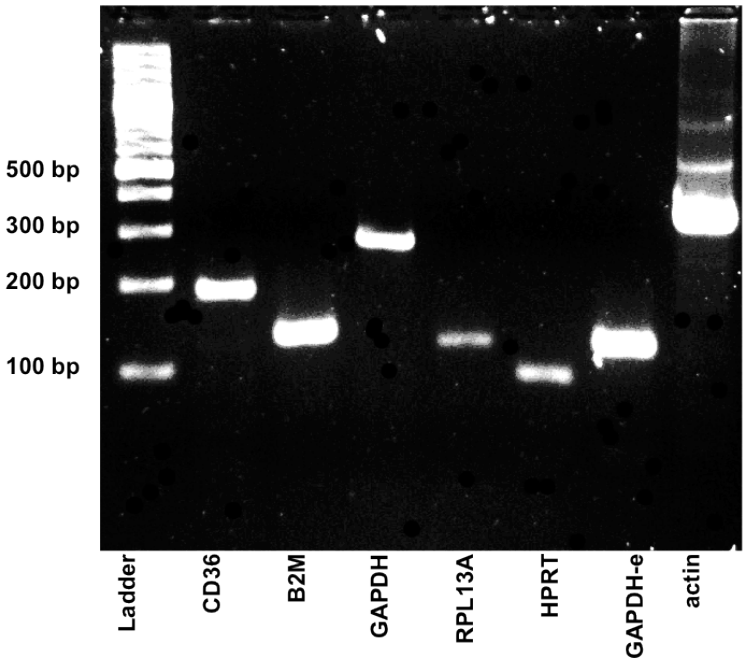

Figure A.8: Primer product size verification.
cDNA of untreated HMDM cells was amplified in the presence of the CD36 primers and potential reference gene primers to verify the amplification of the desired product(s). The PCR products were run on an agarose gel and visualised under the UV illumination.

"Housekeeping" gene selection

Since all of the chosen reference gene primers amplified products, reference genes for CD36 RT-qPCR assay were chosen on the basis of a combination of Normafinder™ output (Andersen *et al.*, 2004) and personal judgement. GAPDH was ruled out because its C_q values varied between the control and the highest treatment concentration (300 μM 7,8-NP). β-Actin was chosen due to its ubiquity and because it was also used as a reference gene in CD36 Western blots. HPRT and RPL13A had a similar likelihood of being suitable (Normfinder, Andersen *et al.* (2004)) and HPRT was chosen arbitrarily. The trio: CD36, β-actin and HPRT was then assessed for suitability using a PCR standard curve (fig. A.9). A standard curve of five cDNA dilutions was run on the qPCR machine to establish amplification efficiency and compare the slopes between gene of interest (CD36) and reference genes (HPRT and β-actin). Amplification efficiency was 100 $\pm$ 4% and the slopes were identical (fig. A.9). Together these results indicated that the combination primers for the gene of interest and reference genes was suitable for the assay. A typical RT-qPCR output of CD36, HPRT, and β-actin is presented in figure A.10.

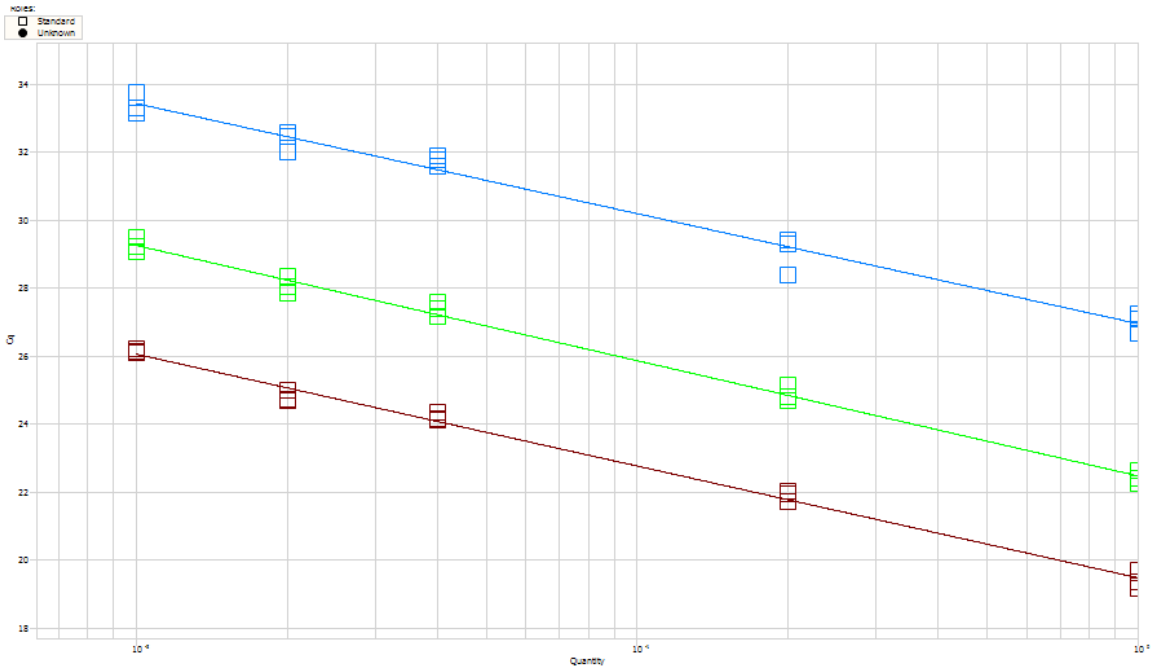

Figure A.9: RT-qPCR standard curve of CD36, HPRT and β-actin primer amplification.

A standard curve of five cDNA dilutions was run on the qPCR machine to establish amplification efficiency and compare the slopes between gene of interest (CD36, green) and reference genes (HPRT, blue, and β-actin, brown). Amplification efficiency was $100 \pm 4\%$ and the slopes were identical.

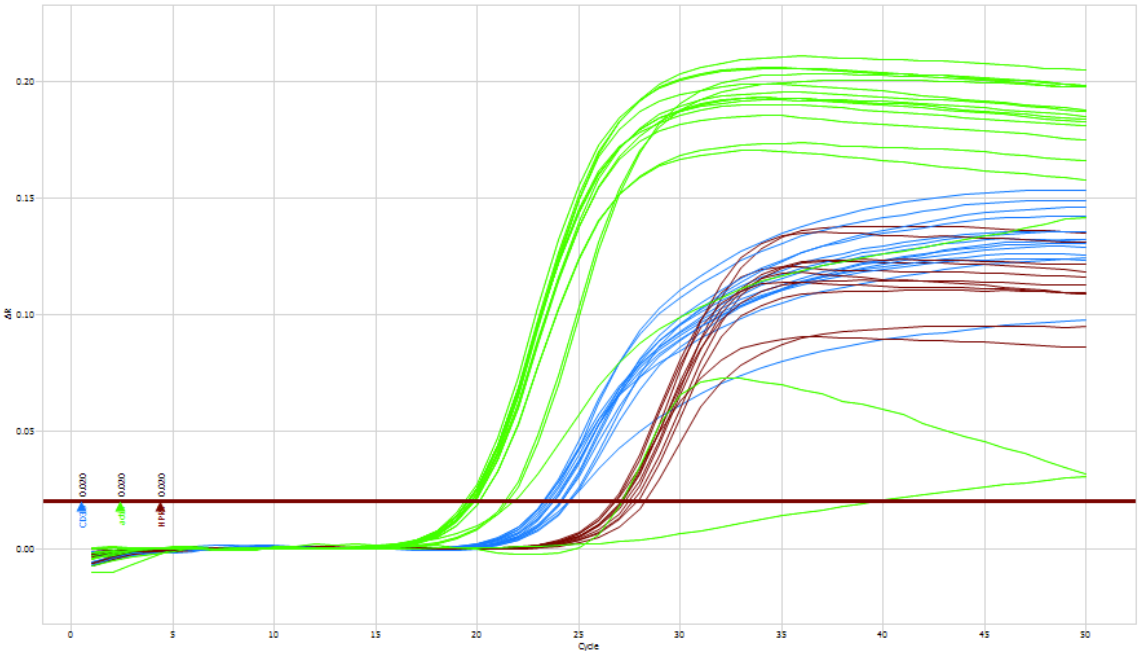

Figure A.10: Typical RT-qPCR amplification curve of CD36, HPRT and β-actin primers.

A typical RT-qPCR output of CD36 (blue) and two reference gene primers: HPRT (brown) and β-actin (green) is presented. Briefly, 7,8-NP–treated HMDM cells were collected into TRIzol. Sample RNA was isolated and converted to cDNA with subsequent amplification on a RT-qPCR.

Appendix B

Publication

The following paper, "Oxidant production, oxLDL uptake, and CD36 levels in human monocyte-derived macrophages are downregulated by the macrophage–generated antioxidant 7,8-dihydroneopterin", includes one figure (fig. 7b,c) that was generated during this PhD thesis.

ANTIOXIDANTS & REDOX SIGNALING
Volume 13, Number 10, 2010

DOI: 10.1089/ars.2009.3065

FORUM ORIGINAL RESEARCH COMMUNICATION

Oxidant Production, oxLDL Uptake, and CD36 Levels in Human Monocyte–Derived Macrophages Are Downregulated by the Macrophage-Generated Antioxidant 7,8-Dihydroneopterin

Steven P. Gieseg, Zunika Amit, Ya-Ting Yang, Anastasia Shchepetkina, and Hanadi Katouah

Abstract

The severity of atheroma burden in patients strongly correlates to increasing levels of plasma neopterin, the oxidation product of 7,8-dihydroneopterin. Interferon-γ stimulation of macrophages causes the synthesis of 7,8-dihydroneopterin, a potent antioxidant that inhibits oxidative damage to cells, and the cytotoxicity of oxidized low-density lipoprotein (oxLDL) to monocyte-like U937 cells but not THP-1 cells. With human monocyte–derived macrophages (HMDMs), oxLDL triggered a large oxidative stress, causing the rapid loss of cellular glutathione, glyceradehyde-3-phosphate dehydrogenase (GAPDH) inhibition, and eventual loss of viability without caspase-3 activation. Inhibition of oxLDL cytotoxicity to HMDMs occurred at 7,8-dihydroneopterin concentrations $>100\,\mu M$. The oxLDL-mediated glutathione loss and GAPDH inactivation was inhibited by 7,8-dihydroneopterin. 7,8-Dihydroneopterin rapidly entered the HMDMs, suggesting that much of the protective effect was scavenging of intracellular oxidants generated in response to oxLDL. OxLDL uptake by HMDMs was reduced by 30% by 7,8-dihydroneopterin. Immunoblot analysis suggests that this decrease in oxLDL uptake was due to a significant downregulation in the levels of CD36. These results imply that 7,8-dihydroneopterin protects human macrophages both by scavenging oxidants generated in response to oxLDL and by decreasing CD36-mediated uptake of oxLDL. *Antioxid. Redox Signal*. 13, 1525–1534.

Introduction

Increased clinical use of plasma neopterin is seen as a marker of a patient's level of inflammation in conditions as diverse as cancer and tuberculosis infection. Neopterin is the oxidation product of 7,8-dihydroneopterin, a pterin synthesized by macrophages when stimulated by γ-interferon released by Th-1 cells (17, 52). The increase of plasma neopterin levels has been strongly correlated with increased atherosclerotic burden (1, 43, 47). Significant amounts of neopterin and 7,8-dihydroneopterin have been reported in the interior of an atherosclerotic plaque (13, 17), which represents localized sites of chronic inflammation (36). Although neopterin is a sensitive marker of inflammation, it is becoming increasingly apparent that 7,8-dihydroneopterin and neopterin have distinct biologic properties. They may have significant influence on the inflammatory process, especially in chronic inflammation, such as atherosclerosis.

In vitro studies have shown that 7,8-dihydroneopterin is a potent antioxidant that can protect a range of biomolecules and cells from various oxidants, including hydroxyl and peroxyl radicals (21, 24, 25, 31). Oxidized low-density lipoprotein (OxLDL) formation with copper, peroxyl, or cellular oxidants is effectively inhibited by scavenging of the chain carrying lipid-peroxyl radical within the LDL particle by 7,8-dihydroneopterin (13, 15, 23, 24). 7,8-Dihydroneopterin accelerates copper-mediated oxidation if added after the lag phase because of increased metal reduction (26).

7,8-Dihydroneopterin is effective in protecting the monocyte-like U937 cells from the cytotoxic effects of oxidized low-density lipoprotein (oxLDL) (5). Cell death due to oxLDL cytotoxicity is considered to be a major factor in the development of a necrotic core in advanced atherosclerotic plaques (28, 30). Our previous studies have shown 7,8-dihydroneopterin protects U937 cells from oxLDL by preventing the loss of intracellular glutathione and the initiation of necrosis (5).

Free Radical Biochemistry Laboratory, School of Biological Sciences, University of Canterbury, Christchurch, New Zealand.

Although oxLDL itself is not capable of directly generating oxidants, exposure to U937 cells causes a large intracellular oxidant flux, which can be scavenged or inhibited by 7,8-dihydroneopterin.

Surprisingly, 7,8-dihydroneopterin cannot protect the related monocyte-like THP-1 cells from oxLDL-induced cytotoxicity (5). In THP-1 cells, oxLDL triggers caspase activation and apoptosis without the loss of glutathione (4). This non-oxidative stress mechanism in THP-1 cells does not appear to be inhibited by 7,8-dihydroneopterin. OxLDL-induced cell death occurs through a number of mechanisms, depending on the type of cell under study and the level to which the LDL has oxidized (22). The proposed mechanisms include calpain activation through oxysterol-induced alterations in lipid rafts–associated calcium channels (6), dephosphorylation and inhibition of protein kinase B, leading to mitochondrial dysfunction through Bcl-2 and MAPK (9, 45), lysozyme destabilization (7, 34), and CD36-linked NADPH oxidase activation (33, 37).

Human macrophages derived from peripheral blood monocytes, usually described as human monocyte–derived macrophages (HMDMs) have been described undergoing both caspase and caspase-independent cell death (3, 22, 53). We have observed oxLDL causing HMDMs to undergo a caspase-independent cell death characterized by a rapid loss of glutathione, caspase inactivation, and the appearance of necrotic cell morphology (22). In this study, we examined whether 7,8-dihydroneopterin can inhibit oxLDL-induced death in HMDMs and whether the mechanism involves the reduction of intracellular oxidative stress, as observed with U937 cells.

Materials and Methods

All reagents and chemicals were AR grade or better and obtained from either the Sigma Chemical Company (St. Louis, MO) or BDH Chemicals New Zealand Limited. Solutions were prepared by using high-purity water generated from an NANOpure ultrapure water system from Barnstead/Thermolyne (Dubuque, IA). Cells were grown in Nunc plates supplied by In Vitro New Zealand Ltd., and the remaining plastic ware was supplied by Greiner Bio-one through Raylab New Zealand Ltd. Neopterin and 7,8-dihydroneopterin were obtained from Schirck's Laboratories, Jona, Switzerland. Phosphate-buffered saline (PBS) solution consisted of 150 m*M* sodium chloride and 10 m*M* sodium phosphate, pH 7.4.

LDL was purified by buoyant density-gradient ultracentrifugation by using a Beckman SW41 rotor from EDTA-treated plasma collected by venipuncture from healthy male and female donors after an overnight fast, as previously described (5, 10, 23). LDL concentration (total mass) was determined by enzymatic cholesterol assay with the Chol MPR 2 kit supplied by Roche Chemicals (Bern, Switzerland) (20). Heavily oxidized oxLDL with the properties previously described (5) was prepared by incubating LDL at a concentration of 3 mg/ml (600 μg/ml protein) with 400 μM $CuCl_2$ solution for 24 h at 37°C before stirring with chelex-100 resin for 2 h to remove copper ions. The oxLDL was concentrated by using a Vivapore membrane concentrator (Millipore, Billerica, MA) before filter sterilization through a 0.22-μm membrane filter and then stored at 4°C.

Human monocyte–derived macrophages (HMDMs) were prepared from whole blood donated by clinically healthy hemochromatosis patients at the NZ Blood Services (Christchurch) under ethics approval CTY/98/07/069 granted by the New Zealand Upper South B Ethics Committee. The monocytes were purified by centrifugation over Lymphoprep and differentiated into adherent macrophages in adherent 12-well plates (14). The cells were maintained in RPMI 1640 supplemented with 10% heat-inactivated human serum plus 100 U/ml penicillin and 100 μg/ml streptomycin. Cell viability was determined by MTT reduction (38). Cell protein concentration was determined by using the BCA Protein Determination kit supplied by Pierce, (Rockford, IL) with bovine serum albumin as the standard.

Cellular glutathione levels were measured by derivation with monobromobimane and reverse-phase C_{18} high-performance liquid chromatography (HPLC) analysis of the fluorescent derivative by using monobromobimane-derivatized GSH as a standard (11). Neopterin and 7,8-dihydroneopterin were measured with reverse-phase HPLC analysis of cell lysates after removal of proteins by precipitation with trichloroacetic acid (13, 21). GAPDH activity was measured in cell lysates by monitoring the rate of conversion of $NADP^+$ to NADPH in the presence of glyceraldehyde-3-phosphate over a 4-min period (49). OxLDL uptake by HMDMs was measured by using DiI-labelled oxLDL (12, 50). The DiI uptake was measured by lysing cells into isopropanol and measuring the native DiI fluorescence intensity. The cellular protein concentration was determined by analysis of cell pellets collected after centrifugation of the isopropanol. Intracellular superoxide release was detected with dihydroethidium (DHE) staining (8) of cells grown on sterile glass coverslips. The cells were incubated for 20 min with DHE before examination with fluorescence microscopy.

Caspase-3, CD36, and scavenger receptor-A (SCR-A) were detected by immunoblotting after SDS-PAGE electrophoresis cells were harvested by scraping in lysis buffer (40 m*M* HEPES, 50 m*M* NaCl, 1 m*M* EDTA, and 1 m*M* EGTA, plus one tablet of Roche Complete mini protease inhibitor per 10 ml). Immunoblots were probed with either anti-CD36 rabbit polyclonal (NB400-145, Novus Biologicals, Cambridge, UK), diluted 1:1,000, followed by peroxidase-conjugated goat polyclonal anti-rabbit IgG (NB730-H, Novus Biologicals) at 1:2,000 dilution; or anti-caspase-3 (E-8) (SC-7272, Santa Cruz Biotechnology, Santa Cruz, CA) followed by conjugated goat anti-mouse IgG (F_c) (31434; Pierce Biotechnology); or anti-SR-A (I-20) (SC-20441, Santa Cruz Biotechnology) followed by peroxidase-conjugated donkey anti-goat IgG (SC-2020, Santa Cruz Biotechnology). Lane loading was accessed by reblotting with anti-β-actin (A5316, Sigma-Aldrich Chemical, St. Louis, MO) followed by peroxidase-conjugated sheep anti-mouse IgG (RPN4401, Amersham Biosciences, Amersham, England). Immunoblots were visualised by using Supersignal West Dura chemiluminescence from Pierce. The image was recorded on a Syngene Chemigenius-2 bioimaging system by using Genesnap software (Global, Aotearoa, NZ).

Phosphatidylserine (PS) translocation to the cell surface as a marker of apoptosis was measured by staining cells grown on coverslips with annexin-V-FITC by using the Annexin V Apoptosis Kit form Santa Cruz Biotechnology and viewing by fluorescence microscope by using Zeiss AxioImager.M1 epi-fluorescent microscope.

The data were analyzed by using the Prism software package supplied by Graphpad Software Inc. (San Diego,

CA). Comparisons among treatments were performed by using one-way analysis of variance (ANOVA). All results are expressed as the mean ± SD of triplicate treatments. Results shown are from single experiments, representative of a minimum of three. Where appropriate, significance is indicated as (***)$p \leq 0.001$; (**)$p \leq 0.01$, or (*)$p \leq 0.05$.

Results

OxLDL induced cell death in the HMDMs only after 12 h of incubation (Fig. 1A). Up to the 12-h time point, the cell morphology appeared normal, but after this, increasing numbers of lysed cells were observed. The appearance of lysed cells corresponded with the loss of cell viability, as measured by the ability to reduce MTT to the purple formazan product. The oxLDL-induced loss of viability was significantly inhibited by 50 μM 7,8-dihydroneopterin added 10 min before the oxLDL treatment (Fig. 1B). One hundred micromolar 7,8-dihydroneopterin reduced the loss of viability to a mean value of 20%, with the majority of the cells displaying normal morphology.

To understand the nature of the 7,8-dihydroneopterin protection, the mechanism of the oxLDL-induced death in the HMDMs was further examined, as conflicting reports in the literature exist on the oxLDL-induced death mechanism (22). Western blot analysis constantly failed to show any sign of proteolytic activation of caspase-3 in the oxLDL-treated HMDMs. The 32-kDa band of procaspase-3 was clearly seen (Fig. 2A), but no active 17- or 20-kDa band was evident. This confirms our earlier investigations, in which no caspase enzyme activity was observed with oxLDL exposure (22). Phosphatidylserine externalization in the plasma membrane appeared to increase, as indicated by staining with annexin-V after 3 and 6 h after the treatment with oxLDL (Fig. 2B–E). This process was significantly slowed and reduced in the presence of 7,8-dihydroneopterin (Fig. 2F–H). Although the effector caspase-3 appears not to be activated by oxLDL exposure, phosphatidylserine translocation, another classic marker of apoptosis, occurs.

We previously observed the loss of caspase activity during oxLDL-induced death of U937 cells (4). This was also accompanied by a large loss of glutathione, suggesting inhibition of caspase-3 activity through oxidative loss of key thiols within the enzyme. With the HMDMs, we observed a similar and very rapid loss of glutathione (Fig. 3A). Within 6 h of adding the oxLDL, nearly 50% of the glutathione was lost, with the level dropping to 36% of the control by 24 h. Generally, no significant loss was observed in the absence of oxLDL, although a small loss was observed at 24 h in this experiment. As with previous studies using 7,8-dihydroneopterin on macrophage-like cells (5, 25), addition of 7,8-dihydroneopterin alone had no significant effect on the levels of glutathione, but in the presence of oxLDL, a dose-dependent protection of the glutathione levels was noted at the end of a 24-h incubation (Fig. 3B). The 200 μM 7,8-dihydroneopterin maintained the glutathione level at 68% of the control value.

Based on studies with monocyte-like U937 cells (4, 29) and endothelial cells (51), we suspect that oxLDL induced the HMDM cells to generate reactive oxidants that depleted the intracellular glutathione levels. Treatment of cells with the fluorescent dye DHE confirmed that oxLDL was inducing an oxidative stress over the first 6 h (Fig. 4A–C), which was reduced by the addition of 7,8-dihydroneopterin (Fig. 4D and E). This suggested that the 7,8-dihydroneopterin was either inhibiting the oxidant production or scavenging the oxidant directly.

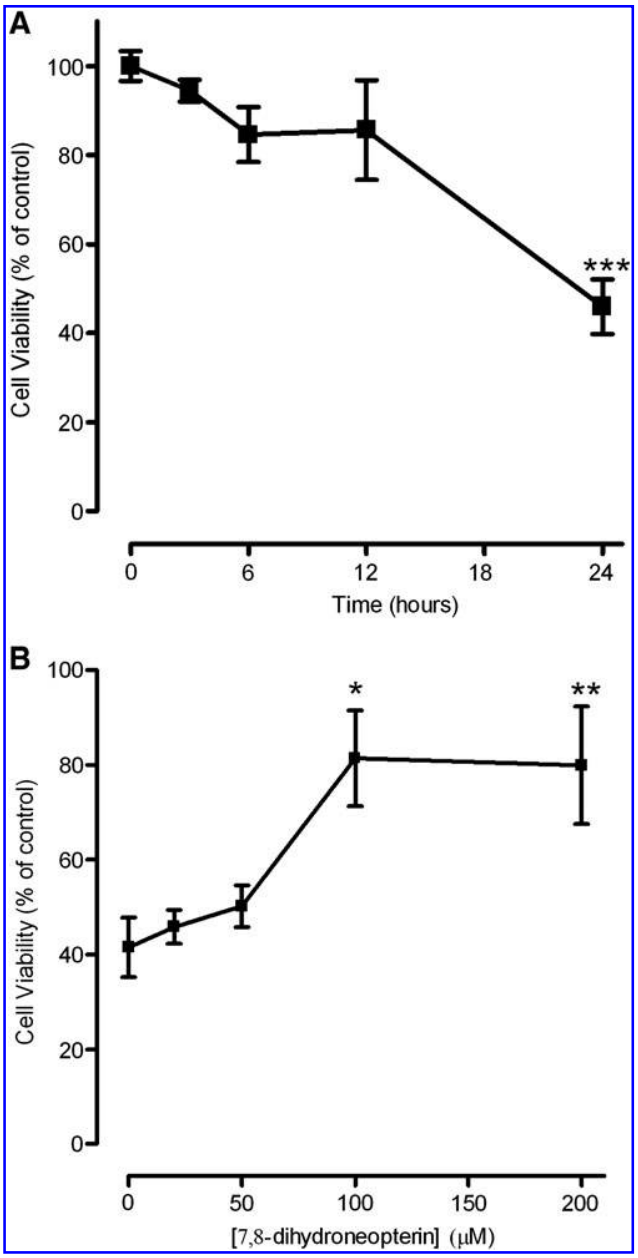

FIG. 1. OxLDL loss of HMDM cell viability is inhibited by 7,8-dihydroneopterin. (**A**) HMDMs were incubated with 1 mg/ml oxLDL in RPMI-1640 supplemented with 10% human serum. At indicated time points, the medium was removed, and the cell viability was determined by measuring MTT reduction. (**B**) Increasing concentrations of 7,8-dihydroneopterin inhibited oxLDL-induced loss of HMDM cell viability during a 24-h incubation with 1 mg/ml oxLDL. The 7,8-dihydroneopterin was added 10 min before the oxLDL. *$p \leq 0.05$; **$p \leq 0.01$; ***$p \leq 0.001$.

Like the caspases, the glycolytic enzyme glyceraldehyde 3-phosphate dehydrogenase (GAPDH) has a critical thiol within its active site that, when oxidized, results in the loss of

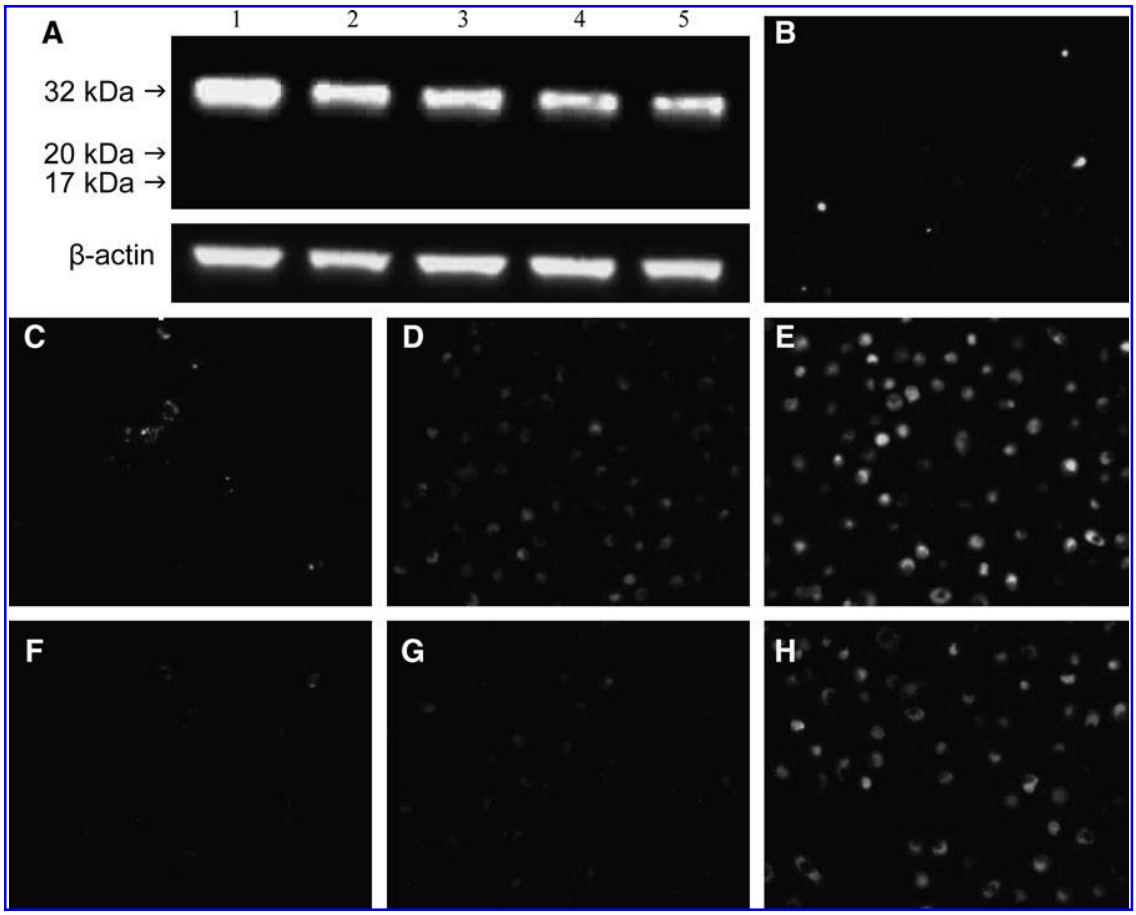

FIG. 2. OxLDL does not activate HMDM cell caspase-3 but causes phosphatidylserine translocation to the plasma membrane, which is inhibited by 7,8-dihydroneopterin. (**A**) HMDMs were incubated under various conditions before washing, and cell lysates were collected for immunoblot staining for caspase-3 activation and β-actin as a loading control. Lane 1: control cells at zero time; lane 2: with 1 mg/ml oxLDL for 12 h; lane 3: with 2 mg/ml oxLDL for 12 h; lane 4: with 1 mg/ml oxLDL for 24 h; lane 5: with 2 mg/ml oxLDL for 24 h. Cells were grown on coverslips before exposure to 1 mg/ml oxLDL for 0 h. (**B**) 3 h (**C, F**), 6 h (**D, G**), and 12 h (**E–H**) with (**F–H**) or without 200 μM 7,8-dihydroneopterin (**C–E**). Phosphatidylserine exposure on the cells surface was visualized by staining with annexin-V under fluorescence microscopy.

enzymatic activity. In HMDMs, oxLDL was observed to cause a rapid reduction of GAPDH activity, which paralleled the loss of glutathione (Fig. 5A). Within 6 h of oxLDL addition, the GAPDH activity had been reduced to 50% of the control. No loss in GAPDH activity was observed in the absence of oxLDL or in the presence of only 7,8-dihydroneopterin. At 50 μM 7,8-dihydroneopterin, a small but statistically significant protection of the GAPDH activity steadily increased with 7,8-dihydroneopterin concentration. 7,8-Dihydroneopterin at 200 μM completely prevented the oxLDL-induced loss of GAPDH activity (Fig. 5B).

The data strongly suggest that 7,8-dihydroneopterin may be scavenging oxidants generated by the cell in response to the oxLDL binding or internalization. Such a mode of activity would require 7,8-dihydroneopterin to enter the cells. This was examined by incubating HMDMs with 7,8-dihydroneopterin and analyzing cell lysates at various time points. A gradual loss of 7,8-dihydroneopterin was observed in the media, with the concentration decreasing by 50% over a 24-h period (Fig. 6). This loss is due to oxidation of the 7,8-dihydroneopterin to 7,8-dihydroxanthopterin and neopterin (13, 18). Intracellularly, the 7,8-dihydroneopterin level increased rapidly, with half the maximum concentration reached within 4 h and maximum at 12 h (Fig. 6). No significant loss of intracellular 7,8-dihydroneopterin was noted over the following 12-h period, even though the media concentration dropped by 25%. As the cells were not stimulated with γ-interferon, the intracellular generation was negligible.

Although intracellular oxidant scavenging by 7,8-dihydroneopterin appeared to explain the cellular protection from oxLDL, reduced uptake of oxLDL into the cells was also explored. By using DiI-labeled oxLDL, we measured oxLDL uptake by HMDMs and found that 7,8-dihydroneopterin reduced the uptake, but only by a third when compared with cells without 7,8-dihydroneopterin (Fig. 7A). The concentration of oxLDL used was below the cytotoxic concentration, thus removing the compounding factor of cell death and lysis from the analysis. A simple explanation for this decrease in oxLDL uptake is downregulation in the levels of the main scavenger receptors of oxLDL, scavenger receptor-A (SR-A)

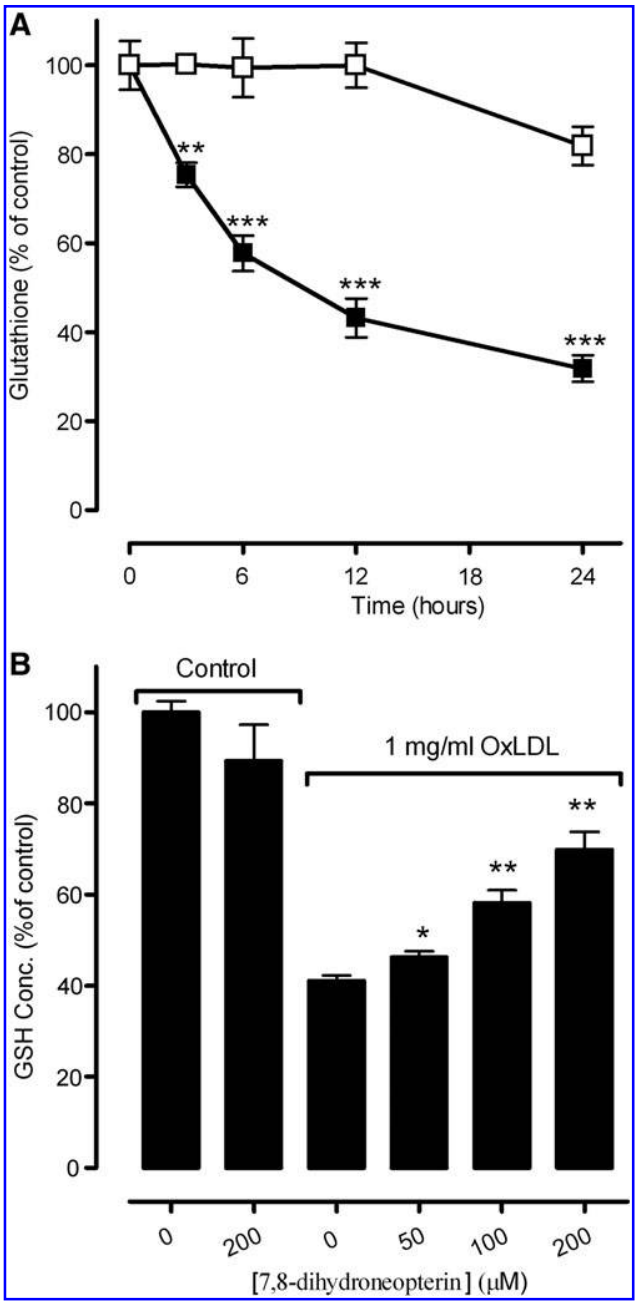

FIG. 3. OxLDL causes a rapid loss of intracellular glutathione, which is inhibited by 7,8-dihydroneopterin. (**A**) Cells in RPMI1640 supplemented with 10% human serum were incubated with (■) and without (□) oxLDL before cell GSH levels were measured with HPLC analysis at indicated time points. (**B**) HMDMs were incubated for 24 h in the indicated 7,8-dihydroneopterin concentrations, without (control) or with 1 mg/ml oxLDL, before the intracellular GSH concentration was determined by HPLC analysis. $^{*}p \leq 0.05$; $^{**}p \leq 0.01$; $^{***}p \leq 0.001$.

and CD36. Immunoblot analysis of HMDMs treated with 7,8-dihydroneopterin showed no significant change in SR-A levels (data not shown), but a significant concentration-dependent loss of the CD36 was observed with both the 83- and 100-kDa bands (Fig. 7B). The greatest loss appears with the 100-kDa plasma membrane form, in which 200 μM 7,8-dihydroneopterin almost completely inhibited the appearance of this isoform.

Discussion

OxLDL induces a large oxidative stress in the HMDMs, causing cellular death, similar to that with U937 cells (4). This study shows that the oxidant release, detected as DHE fluorescence, is associated with rapid loss of glutathione, inactivation of GAPDH, and possible loss of caspase activity. The oxidative stress develops rapidly with >25% of the glutathione and GAPDH activity lost within 3 h of oxLDL addition (Figs. 3 and 5). It is not until 12 h later that this intracellular damage appears as a significant loss of cell viability (Fig. 1). Also similar to the U937 cells (5) is that the presence of 7,8-dihydroneopterin effectively inhibits oxLDL-induced oxidant production and cell death in HMDMs, as shown by decrease in DHE staining, and maintenance of glutathione levels and GAPDH enzyme activity. The presence of 7,8-dihydroneopterin within the cells and the known radical-scavenging properties of 7,8-dihydroneopterin (19, 24, 41) strongly support an intracellular scavenging mechanism for the observed protection.

The heavily oxidized oxLDL used in this study is relatively inert chemically, because most of the LDL components have been oxidized and can no longer sustain any significant oxidant production (16, 51). Treatment of oxLDL with antioxidant before addition to cells does not reduce the oxLDL cytotoxicity (5, 51). It is, therefore, reasonable to assume that the oxLDL-induced intracellular oxidant production is a cellular response to oxLDL. In the case of HMDMs, we have shown that this response is large enough to be cytotoxic.

A number of mechanisms responsible for oxLDL-induced intracellular oxidant production have been reported. Mitochondrial dysfunction (3), NADPH-oxidase activation (33), and lipoxygenase activity (51) have all been demonstrated to occur in response to oxLDL. Our DHE data suggest that superoxide may be the primary reactive oxygen species generated within the cells, possibly due to NADPH-oxidase activation, as has been reported in U937 cells (40, 48). However, DHE is not sufficiently discriminative between superoxide and other ROS, so it is likely that a range of reactive oxygen species is generated.

A strong experimental link exists between CD36 binding of oxLDL and superoxide/oxidant generation. Cell experiments in which CD36 binding of oxLDL is inhibited by anti-CD36 antibodies, or in which the receptor is absent, still take up oxLDL, (likely through SR-A), yet have significantly reduced levels of reactive oxygen species (ROS) production, caspase activation, and cell death (51, 53). OxLDL binding to CD36 of HMDMs has been reported to generate large amounts of hydrogen peroxide (37), which would have originated as superoxide. 7,8-Dihydroneopterin is an effective scavenger of superoxide and also appears to be able to inhibit NADPH-oxidase (32). Both mechanisms may operate within the HMDMs. In addition to radical scavenging, 7,8-dihydroneopterin induced downregulation of the 100-kDa plasma membrane glycoform of CD36 on the HMDMs may also reduce the level of superoxide production. The superoxide generated is then scavenged by the 7,8-dihydroneopterin that has collected within the HMDM cells.

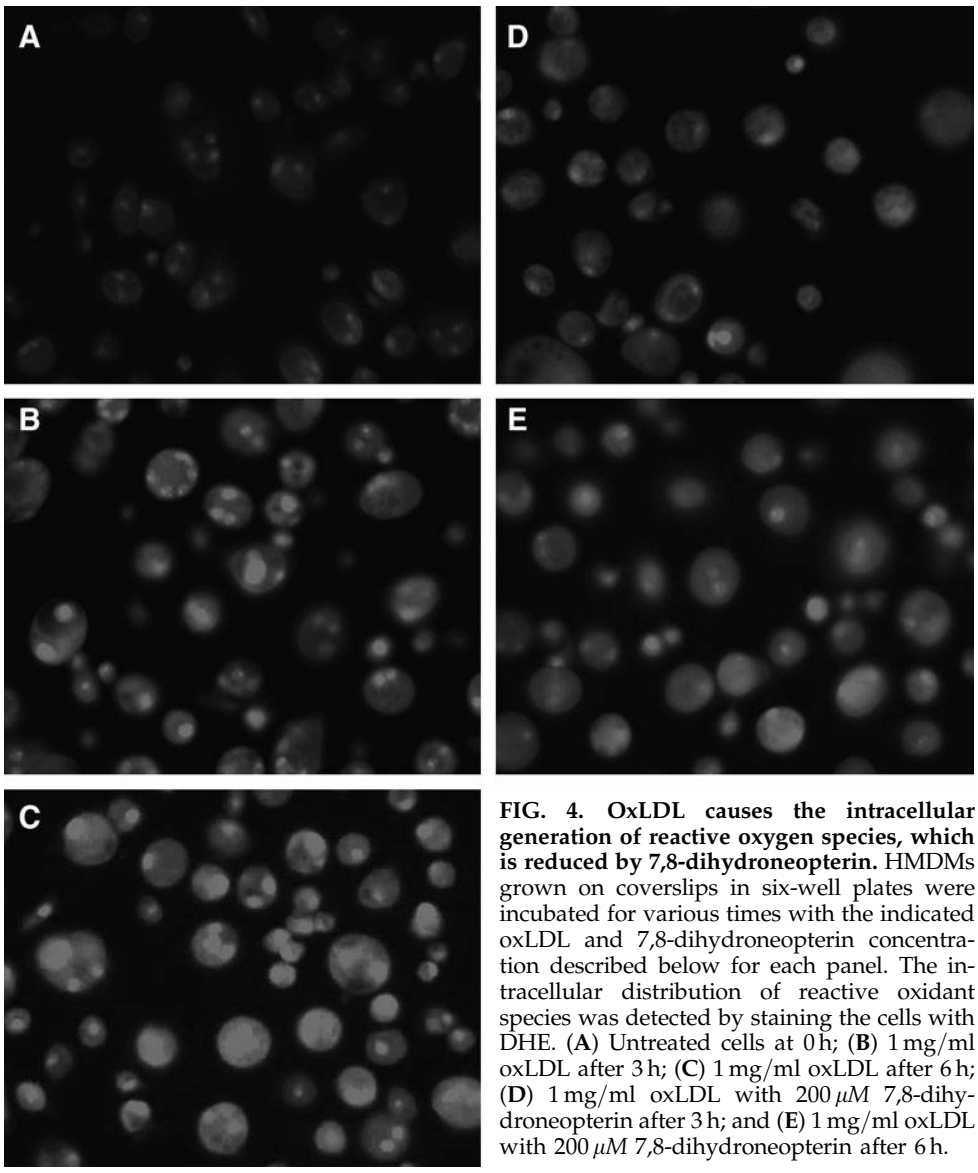

FIG. 4. OxLDL causes the intracellular generation of reactive oxygen species, which is reduced by 7,8-dihydroneopterin. HMDMs grown on coverslips in six-well plates were incubated for various times with the indicated oxLDL and 7,8-dihydroneopterin concentration described below for each panel. The intracellular distribution of reactive oxidant species was detected by staining the cells with DHE. (**A**) Untreated cells at 0 h; (**B**) 1 mg/ml oxLDL after 3 h; (**C**) 1 mg/ml oxLDL after 6 h; (**D**) 1 mg/ml oxLDL with 200 μM 7,8-dihydroneopterin after 3 h; and (**E**) 1 mg/ml oxLDL with 200 μM 7,8-dihydroneopterin after 6 h.

7,8-Dihydroneopterin only decreased DiI-oxLDL uptake by 30% over a 24-h period, suggesting that oxLDL was still entering the cell through another receptor(s), possibly SR-A. This is similar to the effect reported when CD36 was blocked by using an antibody, causing a decrease but not inhibition of oxLDL uptake (53). Increased SR-A activity has been reported to decrease oxLDL cytotoxicity to THP-1 cells, suggesting that SR-A is responsible for uptake and foam cell formation (35) but not for the toxic effects after oxLDL binding and internalization. This suggests that the CD36 downregulation in the HMDMs has an important contribution to the observed protection against oxLDL.

The combination of these arguments led us to advocate that with HMDMs and U937 cells, oxLDL triggers an excessive respiratory-burst response, which is effectively inhibited or quenched by 7,8-dihydroneopterin. This response is not seen with THP-1 cells (4) or cells treated with 7-ketocholesterol, in which changes in the key intracellular kinases and lipid raft–associated calcium channels results in cytochrome *c* release, caspase activation, and apoptosis (6). In the apoptotic mechanism, the oxidative stress is much reduced, and the glutathione levels are reasonably well maintained during the first 12 h of the response (4, 46). Monocyte-like THP-1 cells have significantly lower levels of CD36 expression on the plasma membrane compared with U937 cells (2). This may explain the much lower oxidative-stress levels observed in THP-1 cells exposed to oxLDL. The reason the mechanism triggered in THP-1 cells is not activated in our HMDMs treated with 7,8-dihydroneopterin is uncertain. The oxLDL preparations used in these experiments were rich in oxysterols and therefore should have triggered the caspase-mediated mechanism seen in THP-1 and other cell types. The mechanism we have proposed for 7,8-dihydroneopterin action should only have changed the HMDM death mechanism from necrosis to apoptosis by protecting the caspase activity. Ascorbate has been reported to do just that with HMDMs and, as a result, increased the strength of the apoptotic response to oxLDL (27). The exact mechanism by which oxLDL causes deactivation

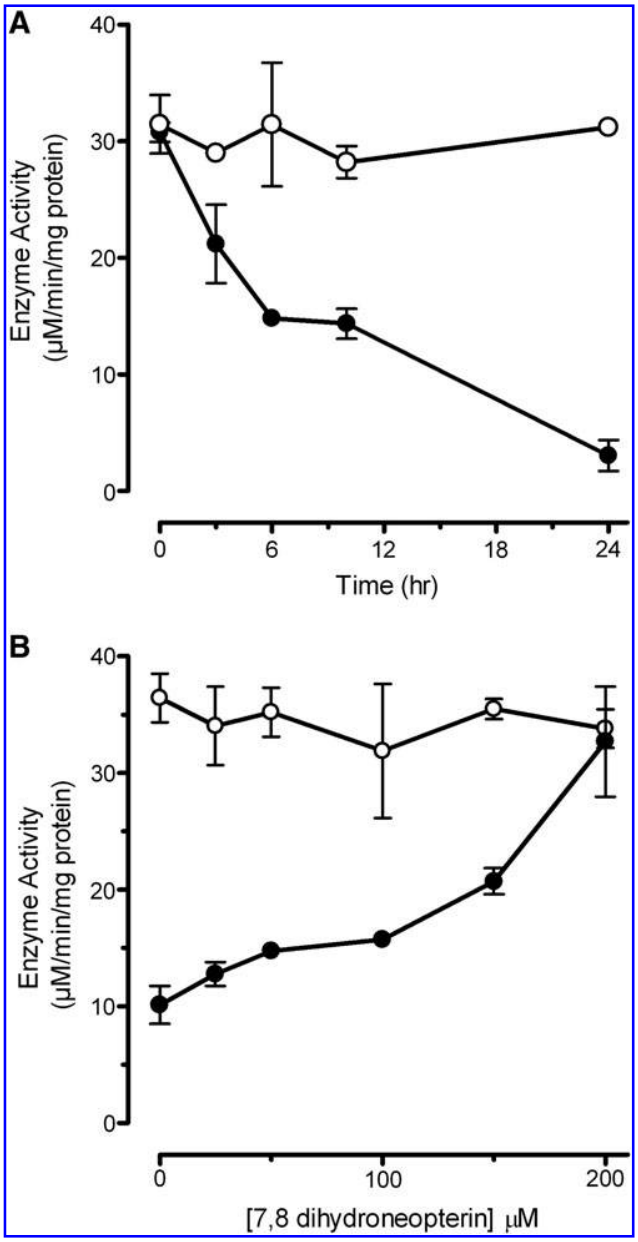

FIG. 5. OxLDL loss of macrophage GAPDH enzyme activity is inhibited by 7,8-dihydroneopterin. (**A**) Monocyte-derived macrophages in RPMI1640 supplemented with heat-inactivated human serum were incubated with 2 mg/ml oxLDL for ≤24 h (●), or 200 μM 7,8-dihydroneopterin was added to the medium before the oxLDL (○). At indicated time points, the cells were collected, and the GAPDH activity was measured. (**B**) Level of GAPDH protection from oxLDL is related to 7,8-dihydroneopterin concentration. Cells were incubated for 24 h with increasing concentrations of 7,8-dihydroneopterin with 2 mg/ml oxLDL (●) or without (○).

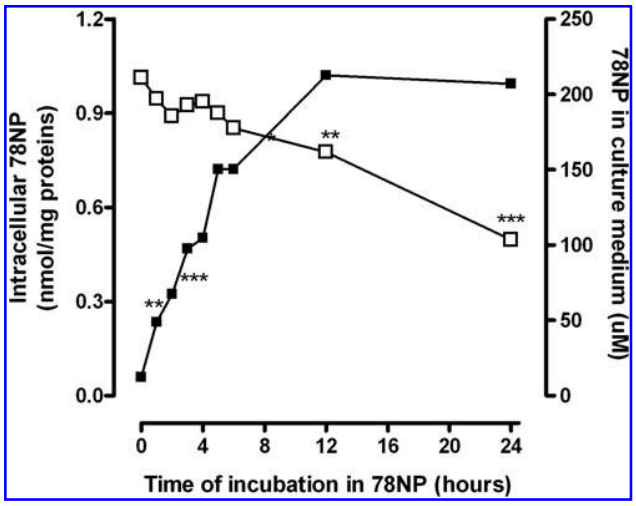

FIG. 6. 7,8-Dihydroneopterin is taken up by HMDMs. HMDMs were incubated with 200 μM 7,8-dihydroneopterin in RPMI-1640 with 10% human serum. At indicated time points, the cells were washed and lysed, and the intracellular 7,8-dihydroneopterin concentration (■) was determined with HPLC analysis. The incubation medium (□) was also analyzed by HPLC to measure the oxidative loss of 7,8-dihydroneopterin over time.

of AKT kinase with subsequent cJNK activation and apoptosis is uncertain (9, 45), and from our data, does not appear to occur in U937 or our HMDMs.

How 7,8-dihydroneopterin is downregulating the level of the CD36 protein in HMDMs also is uncertain. Studies on CD36 in THP-1 and U937 cells clearly show that the 100-kDa band is the active plasma membrane form, whereas the 83-kDa form is the less-glycosylated intracellular precursor form, possibly held within the Golgi (2). The 7,8-dihydroneopterin caused the complete disappearance of the 100-kDa form, whereas only a partial decrease in the intracellular 83-kDa form was observed (Fig. 7). The downregulation with 7,8-dihydroneopterin is very different from the inhibition of CD36 transcription induced by another antioxidant, α-tocopherol (44). α-Tocopherol has an antagonistic effect on oxLDL-induced CD36 expression by preventing oxLDL-induced protein kinase B phosphorylation action on the peroxisome proliferator–activated receptor-γ (PPAR-γ) (39). As 7,8-dihydroneopterin downregulation of CD36 still occurs in the absence of oxLDL, we suspect a different mechanism from that reported with α-tocopherol.

The loss of GAPDH activity within the first hours of oxLDL exposure would potentially exacerbate cellular stress. GAPDH inhibition would cause the glycolytic carbohydrate intermediates to be shunted into the pentose phosphate pathway, generating more NADPH (42). Although increased NADPH generation would normally increase the cells' ability to regenerate GSH (42), with HMDMs and U937 cells, it also provides more NADPH for the NADPH-oxidase. The loss of GSH in the HMDMs (Fig. 3) and U937 cells (4) shows that the increase in GSH regenerative capacity was not enough to protect the cells. As MTT reduction is dependent on NADPH reductases (38), this would also explain the high MTT-reducing potential of the HMDMs for the first 12 h, even though GAPDH and general cell metabolism was failing.

Within actual atherosclerotic plaques, total neopterin levels (neopterin plus 7,8-dihydroneopterin) have been measured in the low micromolar range (13), and this concentration varies along the length of the plaque (17), suggesting that a range of pathologies is occurring. These are advanced plaques in which the possible protective mechanisms of 7,8-dihydroneopterin on

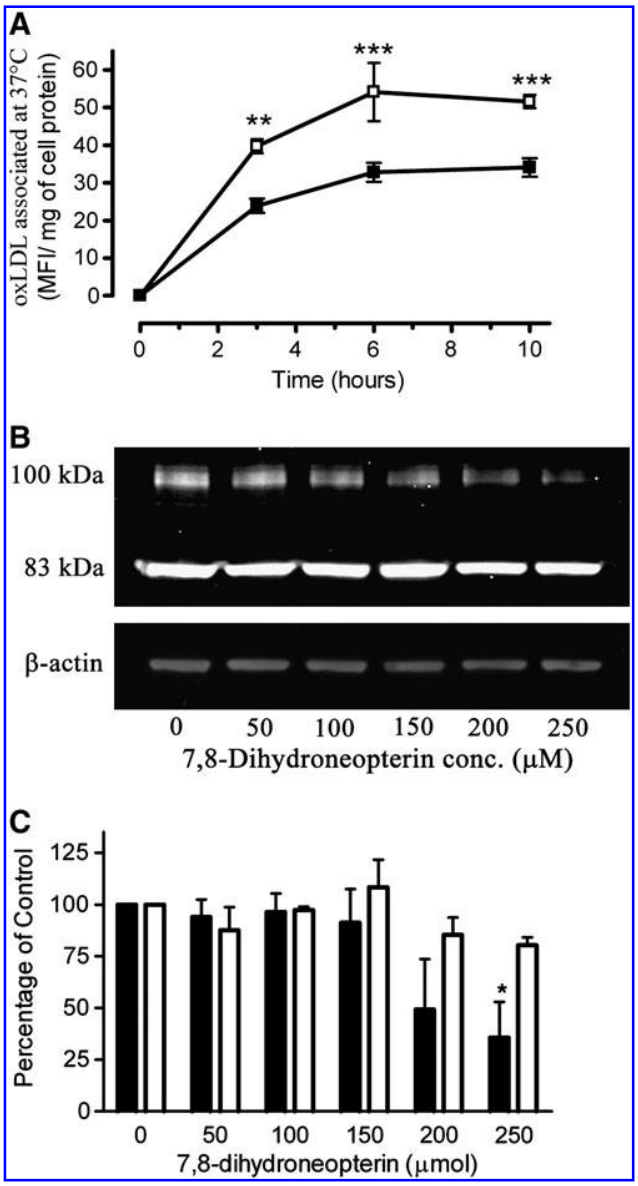

FIG. 7. 7,8-Dihydroneopterin treatment decreases DiI-oxLDL uptake and CD36 levels in HMDMs. (**A**) HMDMs were incubated in RPMI-1640 with 10% human serum and 0.2 mg/ml DiI-labeled oxLDL with (■) and without (□) 200 μM 7,8-dihydroneopterin for ≤ 10 h. Cells were washed with PBS and lysed with isopropanol, and the fluorescence intensity (FI) was measured. Cell protein was recovered from the isopropanol and measured as described in Methods. (**B**) HMDM cells were incubated in RPMI-1640 with 10% human serum containing 200 μM 7,8-dihydroneopterin. At indicated time points, the cells were washed, and the lysates were analyzed with immunoblot analysis for CD36 and β-actin as an internal loading control. (**C**) Graphic display of the CD36 signal of the Western blot in **B**, normalized to the control values with no 7,8-dihydroneopterin. The *black bars* are the 100-kDa isoform, and the *clear bars* are the 83-kDa isoform. $^{*}p \leq 0.05$; $^{**}p \leq 0.01$; $^{***}p \leq 0.001$.

macrophage cell death explored in this research, and the inhibition of oxLDL formation (14, 24), have been overwhelmed. In middle-aged and older subjects with low levels of vascular disease, the action of 7,8-dihydroneopterin may be an important process in slowing or preventing the effects of oxLDL formation.

Acknowledgments

The work was partly funded through a project grant from the National Heart Foundation of New Zealand. Zunika Amit was supported by a Ph.D. Scholarship from the Tunku Abdul Rahman Sarawak Scholarship Foundation and the Universiti Malaysia Sarawak. Anastasia Shchepetkina was supported by a University of Canterbury Postgraduate Scholarship, and Hanadi Katouah, through the Suadi Arabian Postgraduate Scholarship Scheme. We thank our healthy blood donors for our source of blood for lipoprotein preparation and Dr. Jinny Willis for carrying out the blood collection. We also thank the staff and blood donors of Christchurch Blood Service for the blood to prepare the monocytes. This article is dedicated to the memory of Alan M^{c}Curdy, who inspired a love of chemistry in so many students.

Author Disclosure Statement

No competing financial interests exist.

References

1. Adachi T, Naruko T, Itoh A, Komatsu R, Abe Y, Shirai N, Yamashita H, Ehara S, Nakagawa M, Kitabayashi C, Ikura Y, Ohsawa M, Yoshiyama M, Haze K, and Ueda M. Neopterin is associated with plaque inflammation and destabilisation in human coronary atherosclerotic lesions. *Heart* 93: 1537–1541, 2007.
2. Alessio M, Demonte L, Scirea A, Gruarin P, Tandon NN, and Sitia R. Synthesis, processing, and intracellular transport of CD36 during monocytic differentiation. *J Biol Chem* 271: 1770–1775, 1996.
3. Asmis R and Begley JG. Oxidized LDL promotes peroxide-mediated mitochondrial dysfunction and cell death in human macrophages: a caspase-3-independent pathway. *Circ Res* 92: E20–E29, 2003.
4. Baird SK, Hampton M, and Gieseg SP. Oxidised LDL triggers phosphatidylserine exposure in human monocyte cell lines by both caspase-dependent and independent mechanisms. *FEBS Lett* 578: 169–174, 2004.
5. Baird SK, Reid L, Hampton M, and Gieseg SP. OxLDL induced cell death is inhibited by the macrophage synthesised pterin, 7,8-dihydroneopterin, in U937 cells but not THP-1 cells. *Biochim Biophys Act* 1745: 361–369, 2005.
6. Berthier A, Lemaire-Ewing S, Prunet C, Monier S, Athias A, Bessede G, De Barros JPP, Laubriet A, Gambert P, Lizard G, and Neel D. Involvement of a calcium-dependent dephosphorylation of BAD associated with the localization of TRPC-1 within lipid rafts in 7-ketocholesterol-induced THP-1 cell apoptosis. *Cell Death Differ* 11: 897–905, 2004.
7. Brodeur MR, Brissette L, Falstrault L, Ouellet P, and Moreau R. Influence of oxidized low-density lipoproteins (LDL) on the viability of osteoblastic cells. *Free Radic Biol Med* 44: 506–517, 2008.
8. Burnaugh L, Sabeur K, and Ball BA. Generation of superoxide anion by equine spermatozoa as detected by dihydroethidium. *Theriogenology* 67: 580–589, 2007.

9. Choi YK, Kim YS, Choi IY, Kim SW, and Kim WK. 25-Hydroxycholesterol induces mitochondria-dependent apoptosis via activation of glycogen synthase kinase-3 beta in PC12 cells. *Free Radic Res* 42: 544–553, 2008.
10. Chung BH, Segrest JP, Ray MJ, Brunzell JD, Hokanson JE, Krauss RM, Beaudrie K, and Cone JT. Single vertical spin density gradient centrifugation. *Methods Enzymol* 128: 181–209, 1986.
11. Cotgreave IA and Moldeus P. Methodologies for the application of monobromobimane to the simultaneous analysis of soluble and protein thiol components of biological systems. *J Biochem Biophys Methods* 13: 231–249, 1986.
12. Devaraj S, Hugou I, and Jialal I. Alpha-Tocopherol decreases CD36 expression in human monocyte-derived macrophages. *J Lipid Res* 42: 521–527, 2001.
13. Firth CA, Crone EM, Flavall EA, Roake J, and Gieseg SP. Macrophage mediated protein hydroperoxide formation and lipid oxidation in low density lipoprotein is inhibited by the inflammation marker 7,8 dihydroneopterin. *Biochim Biophys Acta* 1783: 1095–1101, 2008.
14. Firth CA, Yang Y, and Gieseg SP. Lipid oxidation predominates over protein hydroperoxide formation in human monocyte-derived macrophages exposed to aqueous peroxyl radicals. *Free Radic Res* 41: 839–848, 2007.
15. Gieseg SP and Cato S. Inhibition of THP-1 cell-mediated low-density lipoprotein oxidation by the macrophage-synthesised pterin, 7,8-dihydroneopterin. *Redox Rep* 8: 113–119, 2003.
16. Gieseg SP, Crone E, and Amit Z. Oxidised low density lipoprotein cytotoxicity and vascular disease. In *Endogenous Toxins: Diet, Genetics, Disease and Treatment*, edited by O'Brien PJ and Bruce WR. Weinheim, Germany: Wiley-VCH 2009, pp. 620–645.
17. Gieseg SP, Crone EM, Flavall EA, and Amit Z. Potential to inhibit growth of atherosclerotic plaque development through modulation of macrophage neopterin/7,8-dihydroneopterin synthesis. *Br J Pharmacol* 153: 627–635, 2008.
18. Gieseg SP, Cruz T, Glubb D, Muzghal D, and Whybrow J. 7,8 Dihydroneopterin can protect cells from free radical mediated damage. *Free Radic Biol Med* 25: 32, 1998.
19. Gieseg SP, Duggan S, Rait C, and Platt A. Protein and thiol oxidation in cells exposed to peroxyl radicals, is inhibited by the macrophage synthesised pterin 7,8-dihydroneopterin. *Biochim Biophys Acta* 1591: 139–145, 2002.
20. Gieseg SP and Esterbauer H. Low density lipoprotein is saturable by pro-oxidant copper. *FEBS Lett* 343: 188–194, 1994.
21. Gieseg SP, Glubb D, and Maghzal G. Protection of erythrocytes by the macrophage synthesized antioxidant 7,8 dihydroneopterin. *Free Radic Res* 34: 123–136, 2001.
22. Gieseg SP, Leake DS, Flavall EM, Amit Z, Reid L, and Yang Y. Macrophage antioxidant protection within atherosclerotic plaques. *Frontiers Biosci* 14: 1230–1246, 2009.
23. Gieseg SP, Pearson J, and Firth CA. Protein hydroperoxides are a major product of low density lipoprotein oxidation during copper, peroxyl radical and macrophage-mediated oxidation. *Free Radic Res* 37: 983–991, 2003.
24. Gieseg SP, Reibnegger G, Wachter H, and Esterbauer H. 7,8-Dihydroneopterin inhibits low density lipoprotein oxidation *in vitro*: evidence that this macrophage secreted pteridine is an antioxidant. *Free Radic Res* 23: 123–136, 1995.
25. Gieseg SP, Whybrow J, Glubb D, and Rait C. Protection of U937 cells from free radical damage by the macrophage synthesized antioxidant 7,8 dihydroneopterin. *Free Radic Res* 35: 311–318, 2001.
26. Greilberger J, Oettl K, Cvirn G, Reibnegger G, and Jurgens G. Modulation of LDL oxidation by 7,8-dihydroneopterin. *Free Radic Res* 38: 9–17, 2004.
27. Harris LK, Mann GE, Ruiz E, Mushtaq S, and Leake DS. Ascorbate does not protect macrophages against apoptosis induced by oxidised low density lipoprotein. *Arch Biochem Biophys* 455: 68–76, 2006.
28. Hutter R, Valdiviezo C, Sauter BV, Savontaus M, Chereshnev I, Carrick FE, Bauriedel G, Luderitz B, Fallon JT, Fuster V, and Badimon JJ. Caspase-3 and tissue factor expression in lipid-rich plaque macrophages - Evidence for apoptosis as link between inflammation and atherothrombosis. *Circulation* 109: 2001–2008, 2004.
29. Kappler M, Gerry AJ, Brown E, Reid L, Leake DS, and Gieseg SP. Aqueous peroxyl radical exposure to THP-1 cells causes glutathione loss followed by protein oxidation and cell death without increased caspase-3 activity. *Biochim Biophys Acta* 1773: 945–953, 2007.
30. Kockx MM, De Meyer GRY, Muhring J, Bult H, Bultinck J, and Herman AG. Distribution of cell replication and apoptosis in atherosclerotic plaques of cholesterol fed rabbits. *Atherosclerosis* 120: 115–124, 1996.
31. Kojima S, Icho T, Kajiwara Y, and Kubota K. Neopterin as an endogenous antioxidant. *FEBS Lett* 304: 163–166, 1992.
32. Kojima S, Nomura T, Icho T, Kajiwara Y, Kitabatake K, and Kubota K. Inhibitory effects of neopterin on NADPH-dependent superoxide-generating oxidase of rat peritoneal macrophages. *FEBS Lett* 329: 125–128, 1993.
33. Leonarduzzi G, Vizio B, Sottero B, Verde V, Gamba P, Mascia C, Chiarpotto E, Poli G, and Biasi F. Early involvement of ROS overproduction in apoptosis induced by 7-ketocholesterol. *Antioxidants Redox Signal* 8: 375–380, 2006.
34. Li W, Yuan XM, and Brunk UT. OxLDL-induced macrophage cytotoxicity is mediated by lysosomal rupture and modified by intralysosomal redox-active iron. *Free Radic Res* 29: 389, 1998.
35. Liao HS, Kodama T, and Geng YJ. Expression of class A scavenger receptor inhibits apoptosis of macrophages triggered by oxidized low density lipoprotein and oxysterol. *Arterioscler Thromb Vasc Biol* 8: 1968–1975, 2000.
36. Libby P, Ridker PM, and Maseri A. Inflammation and atherosclerosis. *Circulation* 105: 1135–1143, 2002.
37. Maxeiner H, Husemann J, Thomas CA, Loike JD, El Khoury J, and Silverstein SC. Complementary roles for scavenger receptor a and CD36 of human monocyte-derived macrophages in adhesion to surfaces coated with oxidized low-density lipoproteins and in secretion of H_2O_2. *J Exp Med* 188: 2257–2265, 1998.
38. Mosmann T. Rapid colorimetric assay for cellular growth and survival: application to proliferation and cytotoxicity assays. *J Immunol Methods* 65: 55–63, 1983.
39. Munteanu A, Taddei M, Tamburini I, Bergamini E, Azzi A, and Zingg JM. Antagonistic effects of oxidized low density lipoprotein and alpha-tocopherol on CD36 scavenger receptor expression in monocytes: involvement of protein kinase B and peroxisome proliferator-activated receptor-gamma. *J Biol Chem* 281: 6489–6497, 2006.
40. Nguyen-Khoa T, Massy ZA, Witko-Sarsat V, Canteloup S, Kebede M, Lacour B, Drueke T, and Descamps-Latscha B. Oxidized low-density lipoprotein induces macrophage respiratory burst via its protein moiety: a novel pathway in atherogenesis? *Biochem Biophys Res Commun* 263: 804–809, 1999.
41. Oettl K, Dikalov S, Freisleben HJ, Mlekusch W, and Reibnegger G. Spin trapping study of antioxidant properties of neopterin and 7,8-dihydroneopterin. *Biochem Biophys Res Commmun* 234: 774–778, 1997.

42. Ralser M, Wamelink MM, Kowald A, Gerisch B, Heeren G, Struys EA, Klipp E, Jakobs C, Breitenbach M, Lehrach H, and Krobitsch S. Dynamic rerouting of the carbohydrate flux is key to counteracting oxidative stress. *J Biol* 6: 10, 2007.
43. Ray KK, Morrow DA, Sabatine MS, Shui A, Rifai N, Cannon CP, and Braunwald E. Long-term prognostic value of neopterin a novel marker of monocyte activation in patients with acute coronary syndrome. *Circulation* 115: 3071–3078, 2007.
44. Ricciarelli R, Zingg JM, and Azzi A. Vitamin E reduces the uptake of oxidized LDL by inhibiting Cd36 scavenger receptor expression in cultured aortic smooth muscle cells. *Circulation* 102: 82–87, 2000.
45. Rusinol AE, Thewke D, Liu J, Freeman N, Panini SR, and Sinensky MS. AKT/Protein kinase B regulation of BCL family members during oxysterol-induced apoptosis. *J Biol Chem* 279: 1392–1399, 2004.
46. Ryan L, O'Callaghan YC, and O'Brien NM. Involvement of calcium in 7 beta-hydroxycholesterol and cholesterol-5 beta, 6 beta-epoxide-induced apoptosis. *Int J Toxicol* 25: 35–39, 2006.
47. Schumacher M, Eder B, Tatzber F, Kaufmann P, Esterbauer H, and Klein W. Neopterin levels in patients with coronary artery disease. *Atherosclerosis* 94: 87–88, 1992.
48. Sellmayer A, Obermeier H, Danesch U, Aepfelbacher M, and Weber P. Arachidonic acid increases activation of NADPH oxidase in monocytic U937 cells by accelerating translocation of p47-phox and Co-stimulation of protein kinase C. *Cell Signal* 8: 397–402, 1996.
49. Steck TL and Kant JA. Preparation of impermeable ghosts and inside out vesicles from human erythrocyte membranes. *Methods Enzymol* 31: 172–180, 1974.
50. Stephan ZF and Yurachek EC. Rapid fluorometric assay of LDL receptor activity by Dil-labeled LDL. *J Lipid Res* 34: 325–330, 1993.
51. Sukhanov S, Higashi Y, Shai SY, Itabe H, Ono K, Parthasarathy S, and Delafontaine P. Novel effect of oxidized low-density lipoprotein: cellular ATP depletion via down-regulation of glyceraldehyde-3-phosphate dehydrogenase. *Circ Res* 99: 191–200, 2006.
52. Wachter H, Fuchs D, Hausen A, Reibnegger G, and Werner ER. Neopterin as marker for activation of cellular immunity: immunologic basis and clinical application. *Adv Clin Chem* 27: 81–141, 1989.
53. Wintergerst ES, Jelk J, Rahner C, and Asmis R. Apoptosis induced by oxidized low density lipoprotein in human monocyte-derived macrophages involves CD36 and activation of caspase-3. *Eur J Biochem* 267: 6050–6058, 2000.

Address correspondence to:
Dr. Steven P. Gieseg
School of Biological Sciences of Canterbury
Private Bag 4800
Christchurch
New Zealand

E-mail: steven.gieseg@canterbury.ac.nz

Date of first submission to ARS Central, December 20, 2009; date of acceptance, March 9, 2010.

Abbreviations Used

DHE = dihydroethidium
GAPDH = glyceradehyde-3-phosphate dehydrogenase
HMDMs = human monocyte–derived macrophages
oxLDL = oxidized low-density lipoprotein
PBS = phosphate-buffered saline
PPAR-γ = peroxisome proliferator–activated receptor-γ
PS = phosphatidylserine
SR-A = scavenger receptor-A

This article has been cited by:

1. Samir Samman . 2010. Antioxidants and Public HealthAntioxidants and Public Health. *Antioxidants & Redox Signaling* **13**:10, 1513-1515. [Citation] [Full Text] [PDF] [PDF Plus]